UNIVERSIDAD DE EXTREMADURA

TESIS DOCTORAL

EVALUACIÓN DE TÉCNICAS DE RECUPERACIÓN DE ZONAS ACARCAVADAS MEDIANTE MODELOS 3D DE ALTA RESOLUCIÓN

ALBERTO ALFONSO TORREÑO

Programa de Doctorado en

Desarrollo Territorial Sostenible

2021

UNIVERSIDAD DE EXTREMADURA

TESIS DOCTORAL

EVALUACIÓN DE TÉCNICAS DE RECUPERACIÓN DE ZONAS ACARCAVADAS MEDIANTE MODELOS 3D DE ALTA RESOLUCIÓN

ALBERTO ALFONSO TORREÑO

Programa de Doctorado en Desarrollo Territorial Sostenible

2021

Con la conformidad del director y de la codirectora de la Tesis Doctoral:

Fdo.: Dr. Álvaro Gómez Gutiérrez Fdo.: Dra. Susanne Schnabel

La conformidad de los directores de la tesis consta en el original en papel de esta Tesis Doctoral

Tesis Doctoral presentada por el doctorando Alberto Alfonso Torreño en el Departamento de Arte y Ciencias del Territorio de la Universidad de Extremadura para la obtención del título de Doctor por la Universidad de Extremadura en el Programa de Doctorado en Desarrollo Territorial Sostenible.

Finalizada en Cáceres el 31 de agosto de 2021.

Título:

Evaluación de técnicas de recuperación de zonas acarcavadas mediante modelos 3D de alta resolución

Doctorando:

Alberto Alfonso Torreño (albertoalfonso@unex.es)

Instituto Universitario de Investigación para el Desarrollo Territorial Sostenible (INTERRA)

Departamento de Arte y Ciencias del Territorio

Universidad de Extremadura

Directores:

Álvaro Gómez Gutiérrez (alvgo@unex.es)

Susanne Schnabel (schnabel@unex.es)

JUNTA DE EXTREMADURA
Consejería de Economía, Ciencia y Agenda Digital

Unión Europea

Esta Tesis Doctoral se ha realizado gracias a la Consejería de Economía, Ciencia y Agenda Digital de la Junta de Extremadura, que ha financiado el contrato predoctoral PD16004, mediante Fondo Social Europeo: "Una manera de hacer Europa", a través de la Ayuda para la Financiación de Contratos Predoctorales para la Formación de Doctores en los Centros Públicos de I+D pertenecientes al Sistema Extremeño de Ciencia, Tecnología e Innovación. La ayuda predoctoral está adscrita al proyecto "Evaluación de técnicas de recuperación de zonas acarcavadas mediante modelos 3D de alta resolución" (CGL2014-54822-R), financiado por el Ministerio de Economía y Competitividad.

Fondo Social Europeo *Una manera de hacer Europa*

ÍNDICE DE CONTENIDOS

LISTADO DE FIGURAS

LISTADO DE TABLAS

AGRADECIMIENTOS

Entiendo el ejercicio de la investigación como una actividad de grupo, siendo esta fundamental para alcanzar los objetivos propuestos. Ortega y Gasset dijo *que somos nosotros y nuestras circunstancias*, sin obviar nuestras colectividades. Con estas palabras quiero expresar mi agradecimiento a todas aquellas personas que de una u otra manera han contribuido en el desarrollo de esta tesis doctoral.

En primer lugar, me gustaría agradecer a la Consejería de Economía, Ciencia y Agenda Digital de la Junta de Extremadura, que ha financiado el contrato predoctoral PD16004, mediante Fondo Social Europeo: "Una manera de hacer Europa", a través de la Ayuda para la Financiación de Contratos Predoctorales para la Formación de Doctores en los Centros Públicos de I+D pertenecientes al Sistema Extremeño de Ciencia, Tecnología e Innovación. La ayuda predoctoral está adscrita al proyecto "Evaluación de técnicas de recuperación de zonas acarcavadas mediante modelos 3D de alta resolución" (CGL2014-54822-R), financiado por el Ministerio de Economía y Competitividad, que ha permitido mi dedicación a tiempo completo durante cuatros años para desarrollar la presente tesis doctoral.

La realización de esta tesis doctoral es fruto de las orientaciones, sugerencias y estímulo del Dr. Álvaro Gómez Gutiérrez y de la Dra. Susanne Schnabel, director y codirectora de esta tesis, respectivamente. Muchas gracias por dedicar vuestro valioso tiempo en ayudarme a crecer como profesional de la docencia y de la investigación. Para mí es un verdadero placer y todo un honor haberos tenido como directores de esta tesis doctoral. No obstante, me gustaría dedicar unas palabras personales a cada uno.

Álvaro, muchísimas gracias por darme la oportunidad de desarrollar el doctorado y formarme como investigador. Hablar de Álvaro es hablar de rigor científico, su calidad como investigador es incuestionable. Desde un principio fui consciente de que tal vez el camino no sería fácil pero sí aprendería mucho de él. Recuerdo mi primera participación en un congreso internacional, a los pocos meses de iniciarme en esta aventura, en el que yo asumía mi participación mediante la presentación de un póster científico y que sus palabras en aquel momento fueran: ¿póster? Presenta una comunicación oral. Esta anécdota resume muy bien todos estos años junto a Álvaro donde te exige lo máximo y quizá no sea la senda más cómoda pero sí la que contribuía a mi crecimiento profesional. Muchas gracias por compartir tus conocimientos conmigo.

Susana, quiero que estas líneas sirvan como agradecimiento no sólo al periodo predoctoral, sino a una etapa que comenzó hace aproximadamente diez años. Durante todo este tiempo y lo que dependiese de mí, siempre tuve claro que Susana tenía que acompañarme en mi proceso de aprendizaje. Ella se ha convertido en un referente para todo el grupo por ser la combinación perfecta de liderazgo, ciencia, sacrificio y bondad. Susana ha sabido enseñarme con total seriedad, generosidad y profesionalidad; y es que en realidad son aspectos que la singularizan y que son claves para guiar exitosamente una investigación. Trabajar con Susana es probablemente uno de los mejores regalos que me ha otorgado todos estos años.

También deseo agradecer profundamente la ayuda incondicional de los compañeros del *Grupo de Investigación GeoAmbiental* que tanto me han ayudado y apoyado a lo largo de estos cuatro años. *Paco (Dr. J. Francisco Lavado Contador)* gracias por estar siempre dispuesto a ayudarme en lo que necesitase. Ya tuve el placer de ser tu alumno en el TFM del Máster en Tecnologías de la Información Geográfica donde pude comprobar tu excelencia como profesor e investigador. Estos cuatro años me han permitido conocerte y tu calidad humana es impresionante. *Manolo*, (Dr. Manuel Pulido Fernández), muchísimas gracias por tus consejos y por involucrarme en trabajos científicos que contribuyen a mi formación. Junto a Manolo he aprendido que la ciencia cobra más sentido si la sociedad se siente partícipe de ella. Gracias *Manolo*, siempre te estaré agradecido por tu amabilidad, cercanía y generosidad. También quisiera dar las gracias a *Silvia* (*Silvia Nadal Chillemi*) por su complicidad conmigo. Silvia siempre está dispuesta a ayudar en momentos difíciles y de agobios. Estaré siempre agradecido por sus palabras y consejos para seguir trabajando con ilusión, optimismo y seguridad en uno mismo. Un agradecimiento especial merece *Jesús* (*Jesús Barrena González*), que la palabra compañero se queda pequeña puesto que se ha convertido en un verdadero amigo. Son muchos los momentos que hemos vivido juntos durante todos estos años. Recuerdo cuando coincidimos los dos por primera vez en un congreso de geografía humana en Villanueva de la Serena (Badajoz), tú hablando de crecimiento urbano y yo de accesibilidad y transporte. *¡Vaya dos personajes!* Curiosamente, ahora, somos doctorandos en geografía física. Ahí radica la versatilidad del geógrafo. Jesús es la alegría del laboratorio de Geografía física y admiro su gran capacidad para proponer ideas interesantes de investigación. Muchas gracias Jesús por visitarme en mis estancias en Italia. Recuerdos que nunca olvidaré. También quisiera agradecer a *Anthony* (*Anthony Gabourel*) por sus correctas y enriquecedoras palabras hacia mí. Estoy seguro que conseguirás todo lo que te propongas y serás el nuevo

doctorando del GIGA. Por supuesto, agradecer también a *Ubaldo* (*Ubaldo Marín Comitre*) y a antiguos doctorandos del grupo, *Javi* (Dr. *Francisco Javier Lozano Parra*), *Judit* (Dr. *Judit Rubio Delgado*), y *Estela* (Dr. *Estela Herguido Sevillano*), por sus consejos y muestras de apoyo.

Quiero dar las gracias también a los compañeros del Laboratorio de SIG por su gran apoyo y ayuda, a *Isabel* (*Isabel Arenas Corraliza*) y en especial a *Ángela* (*Ángela Engelmo Moriche*), mi gran compañera FPI durante estos cuatro años. Cuántas anécdotas tendremos para recordar siempre. Inevitablemente, pensar en Ángela es pensar en mi gran amigo *Juan* (*Juan Carrero Aparicio*). Muchas gracias Ángela y Juan por vuestros consejos y ánimos. Agradecer también a compañeros de carrera como *Isabel Olea*, y a antiguos compañeros del *Campus Virtual* de la Universidad de Extremadura.

Durante este periodo pude disfrutar de experiencias inolvidables como visitar Viena, Barcelona o Mallorca, pero quizá las más especiales son mis dos estancias de investigación realizadas en 2019 y 2020 en Italia. En primer lugar, mostrar mi gratitud al Dr. *Christian Conoscenti* del *Dipartimento Di Scienze Della Terra e Del Mare en la Università Degli Studi di Palermo*, por el tiempo que dedicó para enseñarme sobre técnicas de minería de datos. Siempre agradeceré a Christian su amabilidad y cercanía conmigo. Un gran profesor y una mejor persona. En segundo lugar, quisiera agradecer al Dr. *Marco Cavalli*, al Dr. *Stefano Crema* y a los miembros del *Istituto di Ricerca per la Protezione Idrogeologica del Consiglio Nazionale delle Ricerche* en Padua. Es difícil explicar lo que se siente cuando sabes que vas a trabajar durante un par de meses con dos investigadores que admiras por su extraordinario nivel científico. Siempre recordaré el buen ambiente de trabajo en el instituto, haciéndome sentir uno más del equipo. Dejando a un lado lo profesional y académico, esta estancia fue especial por conocer a personales únicas. Mi agradecimiento a la familia *Caporale del Vento* y en especial a *María Grazia*. Los dos meses que estuve conviviendo con esta familia en Italia fue increíble. Nunca olvidaré la amabilidad, atención, alegría y cariño que tuvieron conmigo y por considerarme uno más de la familia durante ese tiempo. Y es que esta segunda estancia desarrollada entre enero y marzo de 2020 será inolvidable por muchos aspectos, sólo con mencionar norte de Italia, marzo de 2020 y pandemia será suficiente.

Finalmente, agradecer a mis amigos y a lo más importante de mi vida, mi familia. Quiero agradecer a mis padres, a mi hermano, a mi cuñada y a mi chica por su incansable apoyo y fuerza en los momentos de debilidad. Ellos saben mejor que nadie

que el camino no ha sido fácil, quizá por mi personalidad, autoexigencia, y por la manera cuadriculada de entender mi trabajo. Sin embargo, ha merecido la pena todo este proceso porque me estaba dedicando a una profesión muy gratificante como es la investigación, que combinada con la docencia se convierte en la más especial. Sería insuficiente este párrafo para agradecer a mis padres su incansable apoyo y por apostar siempre por mi formación universitaria. Durante todo este tiempo les he hecho partícipes de los conocimientos científicos que progresivamente iba adquiriendo en la universidad. Agradecer infinitamente a mi hermano Carlos y a mi cuñada Carmen su constante apoyo y por confiar siempre en mí. Mi hermano es y será esa persona en la que siempre has tenido y tienes como referente. Un ejemplo para mí. Ellos siempre dicen que están muy orgullosos de todo lo que he conseguido. Si supieran que el orgullo y la admiración es la que yo tengo que hacia ellos. Además ese cariño es todavía mayor por hacerme "tito" hace dos años.

A Luisa, gracias por estar siempre a mi lado, por tus palabras de apoyo, siempre reconfortantes, por aguantar mis bajones y por la paciencia que siempre has tenido conmigo. Ella ha sido mi motor y mi apoyo durante todo este proceso. Solo espero ser capaz de devolverle algún día todo lo que a lo largo de estos años ella me ha brindado.

Y no podría terminar estos agradecimientos sin mencionar a mis abuelos, con especial referencia a mi abuela Eva, "*in memoriam*", destacar su templanza, su bondad y la confianza que siempre depositaba en mí.

A todos, GRACIAS, por contribuir de una u otra manera en una etapa de mi vida inolvidable.

RESUMEN

La erosión hídrica representa un importante proceso de degradación de los ecosistemas terrestres. La zona Mediterránea presenta las tasas de erosión más altas de toda Europa. En el suroeste de la Península Ibérica, la erosión acelerada del suelo ha degradado severamente los sistemas agro-silvo-pastoriles con arbolado disperso, conocidos como dehesas en España. En particular, las cárcavas son importantes fuentes de sedimentos y funcionan como transmisores eficientes de escorrentía y sedimentos en paisajes de dehesa. Existen numerosas consecuencias negativas de los procesos de acarcavamiento, entre ellas, la pérdida de agua en el suelo resulta de especial interés debido al estrés hídrico que experimentan estos ambientes.

Las medidas de restauración, especialmente los diques de corrección hidrológica, sirven para atrapar sedimentos, estabilizar cárcavas, favorecer la revegetación, regular el transporte de sedimentos y reducir la pendiente del cauce. Sin embargo, no se ha evaluado el desempeño y la efectividad de estas medidas en los ambientes de dehesa.

El objetivo de esta tesis es evaluar el funcionamiento de dos experiencias de restauración hidrológica realizadas en dehesas para minimizar las consecuencias negativas de los procesos de erosión por cárcavas. El primer estudio se realizó en seis cuencas restauradas en la Dehesa Boyal de Monroy (DBM) donde se construyeron 160 diques entre 1994 y 2006. El volumen de sedimentos depositados detrás de los diques se determinó utilizando modelos digitales de elevaciones (MDE) de alta resolución y un método topográfico. El segundo estudio se llevó a cabo en la cuenca experimental de Parapuños, concretamente, en una cárcava de fondo de valle parcialmente restaurada en febrero de 2017 mediante diques (gaviones y fajinas) y con la exclusión de ganado por cercado de una de las márgenes más degradadas. Los sedimentos depositados detrás de los diques y los cambios topográficos en la cárcava se estimaron utilizando MDE multi-temporales de alta resolución así como el cálculo de índices de conectividad hidrológica y sedimentológica. Los MDE se produjeron con fotogrametría *Structure-from-motion* (SfM) a partir de imágenes aéreas adquiridas por un vehículo aéreo no tripulado de ala fija.

El estudio de la actuación desarrollada en la DBM mostró una alta variabilidad espacial en la deposición de sedimentos, con mayores volúmenes de material acumulado en las partes bajas de la cuenca, influenciados por la conectividad hidrológica y sedimentológica. El volumen de sedimentos atrapados por dique de manera individual osciló entre 0 y 108,35 m^3, con una tasa de deposición media de

0,141 m^3 ha^{-1} a^{-1}. Además, los diques ubicados en fondos de los valle con muros más largos retuvieron más sedimentos, mientras que los ubicados en vertientes con muros más cortos resultaron ineficaces para capturar sedimento. Con respecto a las variaciones de la deposición dependiendo de la posición topográfica de los diques, la longitud del dique, la pendiente del canal y de la cuenca, la cobertura de árboles y la densidad del camino se correlacionaron significativa y positivamente con la tasa de deposición para los diques ubicados en fondos de valle. Por el contrario, la tasa de deposición se correlacionó negativamente con la conectividad y con la fracción de cabida cubierta en los diques ubicados en laderas.

Los resultados de la segunda experiencia mostraron que el desempeño de las actividades de restauración fue satisfactorio para controlar la erosión y aumentaron notablemente la deposición de sedimentos en el canal. Los diques favorecieron la deposición de sedimentos y redujeron la erosión de las márgenes laterales de la cárcava. La exclusión de ganado promovió la estabilización de las cabeceras laterales existentes y limitó la aparición de nuevas. Además, la producción de sedimentos en suspensión fue considerablemente menor después de la construcción de los diques. Las medidas de restauración produjeron cambios en la conectividad hidrológica y sedimentaria. La conectividad aumentó en las áreas erosionadas, mientras que las áreas de deposición mostraron una disminución de la conectividad. La conectividad también disminuyó en las cabeceras laterales restauradas con fajinas y ubicadas dentro de la zona aislada del ganado.

La presente tesis doctoral sirve de modelo para analizar la evolución de una cárcava de fondo de valle, los procesos geomorfológicos en paisajes de dehesa y para comprender el papel de las medidas de restauración en cárcavas. Además, esta tesis presenta métodos novedosos para la determinación del volumen de sedimentos retenidos en los diques y para el análisis de la efectividad de las medidas de restauración en el ecosistema dehesa a través de MDE de alta resolución. La metodología utilizada puede ayudar en la ubicación estratégica y eficaz de diques de corrección hidrológica. En futuras investigaciones, sería interesante indagar sobre los efectos de las medidas de restauración a largo plazo en el ecosistema de dehesa.

Palabras clave: *Erosión por cárcavas; Producción de sedimentos; Dehesa; Restauración; Fotogrametría SfM; Modelo digital de elevación*.

SUMMARY

Soil erosion by water represents an important process of degradation of terrestrial ecosystems. The Mediterranean area has the highest erosion rates in all of Europe. In the southwest of the Iberian Peninsula, accelerated soil erosion has severely degraded the agro-silvo-pastoral systems with scattered trees, known as dehesas in Spain. In particular, gullies are major sources of sediment and perform as efficient transfers of runoff and sediments in dehesa landscapes. There are numerous negative consequences of gully erosion, e.g., the loss of water in the soil is of special interest due to the water stress experienced by these environments.

Restoration measures, especially check-dams, serve to trap sediments, stabilize gullies, promote revegetation, regulate sediment transport and reduce the slope of the channel. However, the performance and effectiveness of these measures in dehesas have not been evaluated yet.

The objective of this thesis is to evaluate the performance of two hydrological restoration initiatives carried out in dehesas to minimize the negative consequences of gully erosion processes. The first study was conducted in six restored basins in the Dehesa Boyal de Monroy (DBM) where 160 check dams were built from 1994 to 2006. The volume of sediments deposited behind check dams was determined using high-resolution digital elevation models (DEMs) and a topographical method. The second study was carried out in the Parapuños experimental basin, specifically, in a valley-bottom gully partially restored in February 2017 by means of check dams (gabions and fascines) and with livestock exclosure by fencing from one of the most degraded areas. The sediments deposited behind the check dams, topographic changes in the gully and the calculation of hydrological and sedimentological connectivity indices were estimated using multi-temporal high-resolution DEMs. Structure-from-motion (SfM) photogrammetry from aerial images acquired by a fixed-wing unmanned aerial vehicle were used to create the DEMs.

The study of the performance conducted in DBM showed a high spatial variability in sediment deposition, with larger volumes of material accumulated in the lower parts of the catchment influenced by hydrological and sedimentological connectivity. The volume of sediments trapped in the check dams ranged from 0 to 108.35 m^3, with a mean deposition rate of 0.141 $m^3\ ha^{-1}\ y^{-1}$. Furthermore, check dams located in valley-bottoms with longer walls retained the highest amounts of sediments, while those located in hillslopes with shorter walls were ineffective at trapping sediment.

Regarding the variations of the deposition depending on check dams' topographic position, check dam size, slope gradient, tree cover and path density correlated significantly and positively with deposition rate for check dams located in valley bottom. Conversely, deposition rate was negatively correlated with connectivity and with tree cover in hillslope check dams.

The results of the second experience showed that the performance of the restoration activities was satisfactory to control soil erosion and to significantly increase the sediment deposition in the channel. Check dams favored the deposition of sediments and reduced the erosion of the bank headcuts. Livestock exclosure promoted the stabilization of the existing bank headcuts and limited the appearance of new ones. Furthermore, the suspended sediment load registered at the outlet of the catchment was considerably lower after check dam construction. Restoration measures produced changes in hydrological and sediment connectivity. Connectivity increased in eroded areas, while deposition areas showed a decrease in connectivity. Connectivity also decreased in the bank headcuts restored by fascines and located within the isolated area.

The present doctoral thesis serves as a model to analyze the evolution of a valley-bottom gully, the geomorphological processes in dehesa landscapes and to understand the role of restoration measures in gullies. In addition, this thesis presents novel methods for the determination of sediment volume retained in the check dams and the analysis of the effectiveness of the restoration measures in the dehesa ecosystem by means of high-resolutions DEMs. The methodology of the thesis can also help in the strategic and effective location of check dams. In future research, it would be interesting to assess the effects of restoration measures in the long–term implemented in the dehesa ecosystem.

Keywords: *Gully erosion; Sediment load; Dehesa; Restoration; SfM photogrammetry; Digital elevation model*.

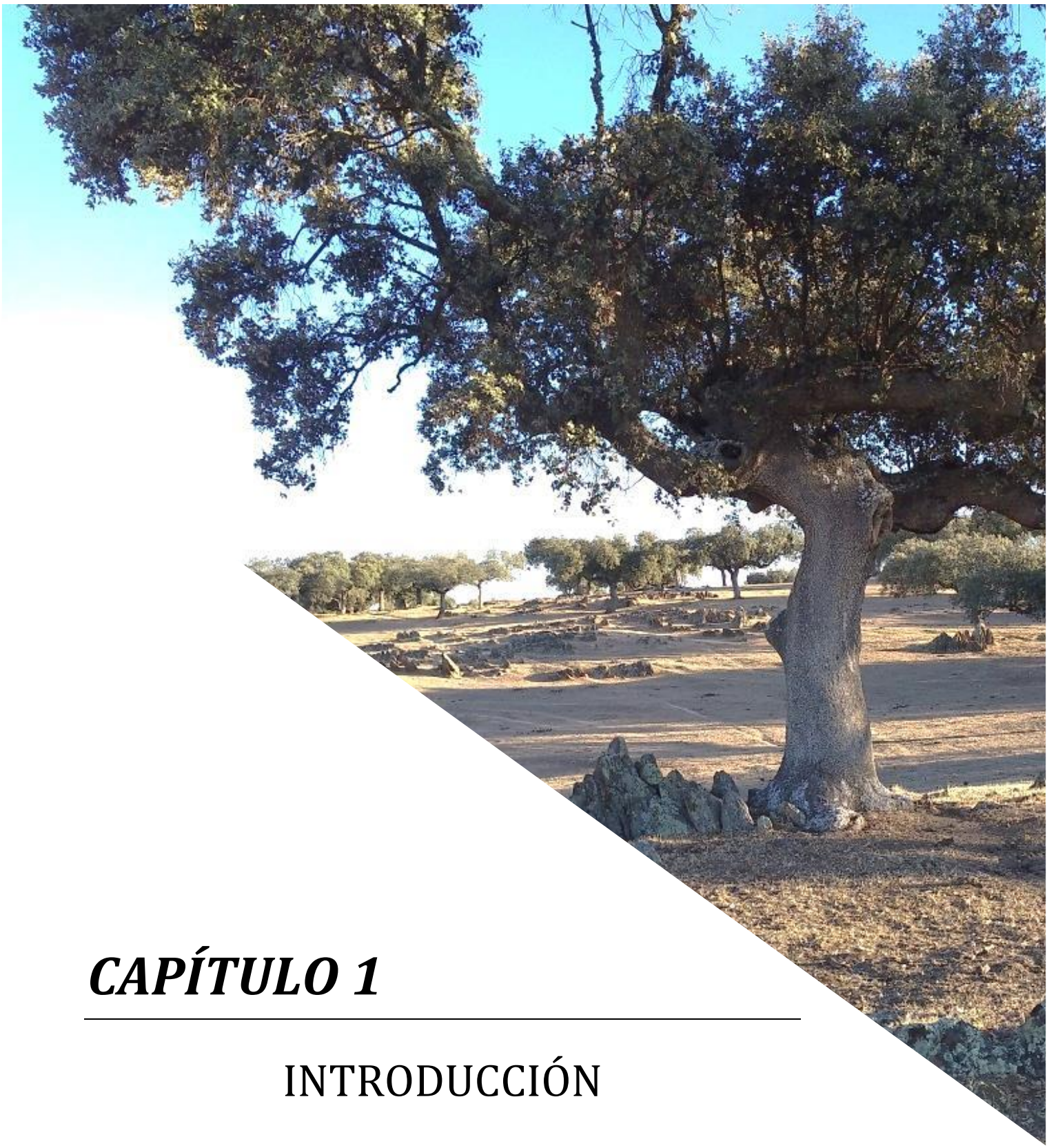

CAPÍTULO 1

INTRODUCCIÓN

CAPÍTULO 1. INTRODUCCIÓN

1.1. Estado de la cuestión

1.1.1. El problema de la erosión hídrica

La erosión del suelo es un proceso de desgaste de la superficie terrestre que consiste en el desprendimiento, el transporte y la sedimentación de las partículas del suelo impulsadas por el agua, el viento, el hielo y la gravedad. La erosión del suelo se considera el proceso dominante de degradación del suelo en todo el mundo (Montanarella et al., 2016; Pennock, 2019; Vanmaercke et al., 2021). El clima, la litología, la topografía, el suelo y la acción humana condicionan los factores que controlan los distintos procesos erosivos (García Ruiz y López Bermúdez, 2009). El proceso de erosión puede abarcar una escala temporal amplia, de tipo geológico. Sin embargo, las tasas de erosión pueden incrementarse por la acción antrópica, denominada *erosión acelerada* (Kirkby y Morgan, 1984) y favorecido por acciones como las señaladas por Porta et al. (2003) e Ibáñez et al. (2003): deforestación, roturación del terreno, incendios forestales, laboreo, sobrepastoreo, quema de restos de cosechas, sobreexplotación de los recursos hídricos, concentración de la actividad económica en zonas costeras, vías de comunicación, edificaciones y su entorno.

La erosión hídrica se produce cuando se desprenden las partículas del suelo de los agregados por la fuerza ejercida por las gotas de lluvia y el flujo de agua. La acción erosiva del agua por el flujo superficial se conoce como *erosión por escorrentía*, mientras que la acción de desprendimiento provocada por el impacto de las gotas de lluvia sobre la superficie del suelo se denomina erosión por salpicadura o *splash*. La erosión como consecuencia de la escorrentía superficial puede clasificarse en laminar (*sheetwash erosion*) o concentrada y cuyos efectos sobre el suelo son distintos. La erosión laminar es causada por el movimiento lento e imperceptible de una película superficial de agua, que provoca la pérdida de una capa fina de partículas del suelo (Foster, 1982; Morgan, 1997). Este tipo de erosión no genera incisiones en el terreno, aunque las pérdidas de suelo que se han registrado son de magnitudes considerables (Cisneros et al., 2012). En la Figura 1 se pueden apreciar los efectos de la erosión laminar y las marcas de acumulación de los sedimentos sobre una vertiente con un uso del suelo silvopastoril.

Figura 1. Evidencias de erosión laminar sobre una vertiente en una finca de Extremadura.

La erosión por flujo concentrado da lugar a estrechas incisiones en el terreno, y se pueden clasificar como regueros (*rills*), cárcavas efímeras (*ephemeral gullies*) o cárcavas permanentes (*permanent gullies*). Los regueros son pequeños surcos efímeros que se generan en las vertientes cuando la escorrentía laminar se concentra (Horton, 1945; Thorne et al., 1986). Algunos estudios han relacionado su génesis con las propias marcas generadas por el laboreo (Haan et al., 1994). En función de la posición topográfica, la erosión laminar y el *splash* se desarrollan generalmente en las zonas más elevadas de las vertientes y los regueros en las partes medias o bajas de las laderas.

La erosión por cárcavas (*gully erosion*) es un proceso de degradación del suelo que tiene lugar bajo diversas condiciones climáticas, geomorfológicas y pedológicas (Billi y Dramis, 2003; Valentin et al., 2005; Zucca et al., 2006). Las cárcavas efímeras se encuentran en las tierras de cultivo y con frecuencia son eliminadas por las labores agrícolas, reapareciendo en el mismo lugar, siendo esta una de las diferencias frente a los regueros, que no reaparecen en las mismas ubicaciones. Por consiguiente, las cárcavas forman parte de la red de drenaje. Las cárcavas permanentes no pueden rellenarse con el laboreo. Las cárcavas también se clasifican en función de su posición topográfica como cárcavas de ladera o cárcavas de vaguada o fondo de valle (Bradford

y Piest, 1980) y pueden ser la consecuencia de procesos de erosión del suelo naturales y/o inducidos por el hombre (Poesen et al., 2003; Valentin et al., 2005). Los factores topográficos, como el área de drenaje y la pendiente, impulsan la formación de cárcavas, destacando la importancia de la escorrentía superficial. En cuanto a las cárcavas de fondo de valle, la saturación del suelo y los flujos subterráneos juegan un papel importante (Gómez-Gutiérrez et al., 2012; Thomas et al., 2004). El acarcavamiento también se ha asociado a cambios en el uso y manejo del suelo o en sistemas de explotación inadecuados (Chaplot et al., 2005; Faulkner, 1995; Gómez-Gutiérrez et al., 2009a; Schnabel, 1997). Los efectos ambientales de la erosión por cárcavas son múltiples: reducción de la calidad del agua (Bartley et al., 2014; Wantzen, 2006), disminución de la productividad de la tierra (Daba et al., 2003; García-Ruiz, 2010) y daños a las infraestructuras (Fox et al., 2016; Jungerius et al., 2002). Además, las cárcavas actúan como enlace entre las partes altas y bajas de una cuenca y aumentan la conectividad hidrológica y de sedimentos (Capra et al., 2005; Poesen et al., 2003). Por otro lado, existen flujos concentrados subsuperficiales que originan formas concretas de erosión, conocidas como erosión en túnel (*piping*) y que frecuentemente están ligadas a altos contenidos de sodio en alguno de los horizontes del suelo (Faulkner et al., 2004). El piping a su vez puede causar el colapso del techo de los conductos tubulares (pipes) produciendo la formación de cárcavas (Romero-Díaz et al., 2007c).

La mayoría de los esfuerzos para comprender y cuantificar la erosión hídrica del suelo se han centrado en la erosión laminar y en regueros a escala grande (por ejemplo: Borrelli et al., 2017; De Vente et al., 2013; Maetens et al., 2012; Montgomery, 2007; Renard, 1997). Poesen et al. (2003) y Sidle et al. (2017), entre otros, argumentan que las tasas de erosión medidas a escala grande no proporcionan una indicación realista de la erosión a escala de cuenca, ni explican adecuadamente la redistribución de sedimentos erosionados en todo el paisaje. No obstante, numerosos estudios han resaltado la preocupación que genera la erosión por cárcavas en muchas regiones del mundo (Poesen et al., 2003; Sidle et al., 2019; Valentin et al., 2005; Vanmaercke et al., 2011).

1.1.2. La erosión hídrica en la zona Mediterránea

Europa presenta una alta variabilidad espacial de la erosión hídrica, considerándose la región mediterránea como la zona más vulnerable (Bakker et al., 2007; Panagos et al., 2015) (Figura 2). La zona mediterránea presenta unas

características favorecedoras para la erosión hídrica como son: lluvias de intensidad elevada, suelos fácilmente erosionables (estructura débil y escasa materia orgánica) y relieves accidentados que promueven diferentes tasas de erosión y producción de sedimentos a lo largo del tiempo y del espacio (García-Ruiz et al., 2013; Peña-Angulo et al., 2019) y las inducidas por la acción antrópica (Ibáñez et al., 2003; Porta et al., 2003). Las tasas más altas de pérdida de suelo se encuentran en áreas con escasa vegetación (Panagos et al., 2015). En este contexto, Vanmaercke et al. (2011) determinaron que más del 50% del área del Mediterráneo supera las 200 t km^{-2} a^{-1} en producción de sedimentos, siendo las tasas más altas de Europa junto con las zonas de montaña.

En España, la erosión es un problema ambiental grave, según las Naciones Unidas es el país europeo con mayor riesgo de desertificación debido a este proceso (Rubio, 2005), con casi un 20% del territorio con riesgo de desertificación alto (Rojo et al., 2009). La erosión del suelo en España ha sido estimada por De Alba (1998) en 23 t ha^{-1} a^{-1}, con una tasa máxima de 48 t ha^{-1} a^{-1} en las cuencas del Sur–Mediterráneo y una tasa mínima de 5 t ha^{-1} a^{-1} en la cuenca norte.

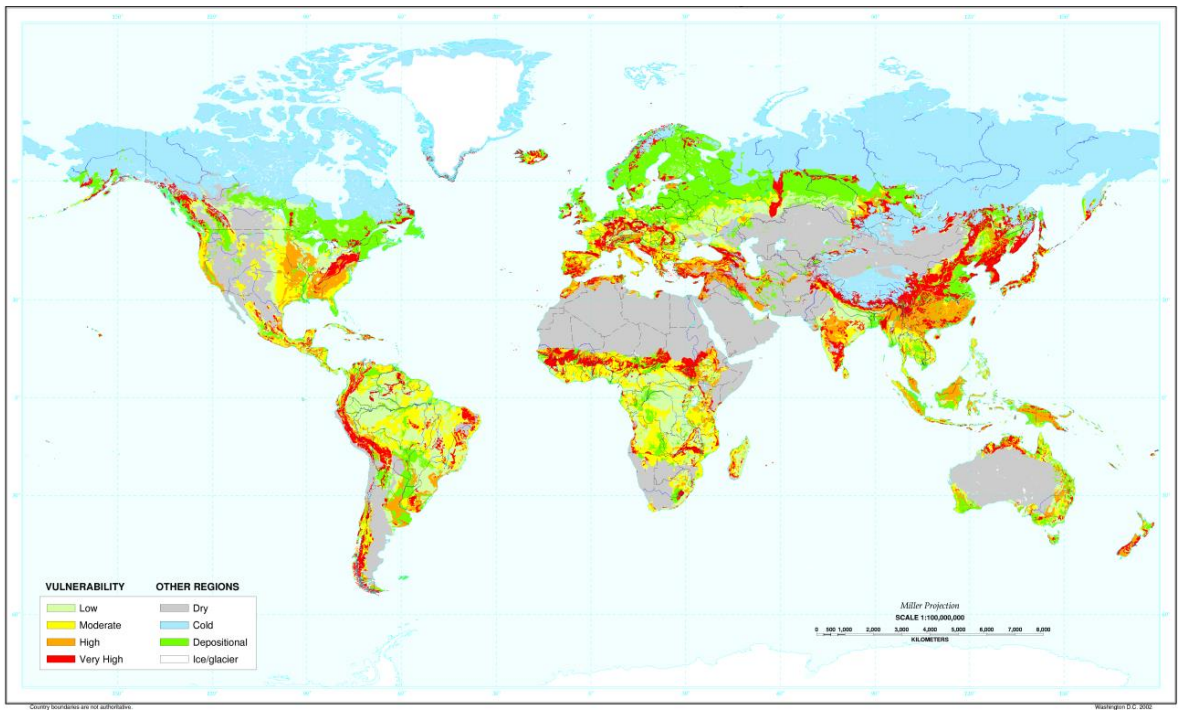

Figura 2. Vulnerabilidad frente a la erosión hídrica. El mapa está basado en una reclasificación del mapa climático global y del mapa global del suelo. Fuente: United States Department of Agriculture – Natural Resources Conservation Service (USDA–NRCS)

La erosión hídrica ha sido un tema de investigación muy estudiado en Europa durante las últimas décadas (Boardman y Poesen, 2007) especialmente en Bélgica,

Reino Unido, Alemania, Italia, Rumania y España. La erosión hídrica se considera una de las principales amenazas para la productividad del suelo (EC, 2002; MEA, 2005). Se pudieron identificar varias líneas de investigación sobre este tipo de erosión hídrica en Europa:

- Seguimiento y cuantificación de la erosión en cárcava mediante el análisis de fotografías aéreas a gran altitud (por ejemplo: Martınez-Casasnovas et al., 2002; Nachtergaele and Poesen, 1999), análisis de fotografías aéreas de alta resolución tomadas por vehículos aéreos no tripulados (Marzolff y Poesen, 2009; Stöcker et al., 2015) y modelado 3D basado en imágenes terrestres (Castillo et al., 2018; Castillo et al., 2012; Frankl et al., 2015).
- Evaluación de la efectividad de medidas de control de la erosión en cárcava, incluidas las geo−membranas (Poesen, 1989), diques de corrección hidrológica (Castillo et al., 2007), estructuras de bioingeniería (Rey y Burylo, 2014) y revegetación (Evrard et al., 2008).
- Cuantificación de las tasas de erosión por cárcavas sobre la producción de sedimentos a escala de cuenca (Bogen et al., 1994; Poesen et al., 2003; Poesen et al., 1996).

Sin embargo, existen lagunas importantes en la investigación del acarcavamiento como por ejemplo las relacionadas con la evaluación de la efectividad de las medidas de control de la erosión por cárcavas a medio y largo plazo, tanto a escala de cauce como de cuenca hidrológica (Bartley et al., 2020; Poesen et al., 2003).

1.1.3. La erosión por cárcavas

La erosión en cárcava es un fenómeno que se produce ante distintas condiciones climáticas (Gómez-Gutiérrez et al., 2011), especialmente en climas semiáridos con acusada estacionalidad. Este tipo de erosión consiste en la formación y posterior expansión de canales erosivos en el suelo como consecuencia del flujo de agua concentrado (Poesen et al., 2003). Las dimensiones de las cárcavas pueden variar en varios órdenes de magnitud (Dube et al., 2020; Vanmaercke et al., 2016) y los tipos más comunes son: (1) cárcavas efímeras en tierras de cultivo (Desmet et al., 1999); (2) cárcavas permanentes en *badlands* (Wilkinson et al., 2018); (3) *bank gullies* que son cárcavas formadas por el colapso de los márgenes de los ríos (Brooks et al., 2009; Poesen y Hooke, 1997; Shellberg et al., 2013) y (4) cárcavas en fondos de valles que

forman parte de la propia red de drenaje (Gómez-Gutiérrez et al., 2009a; Thomas et al., 2004). Morgan (1997) utilizó la posición topográfica para diferenciar dos tipologías: cárcavas de vaguada o fondo de valle y de ladera. También habría que indicar las cárcavas desarrolladas por estructuras construidas o modificadas por el hombre (carreteras, caminos, canalizaciones, etc.) (Imwangana et al., 2015; Poesen, 2018). Las cárcavas presentan unos elementos característicos comunes como son una o varias cabeceras (Figura 3), un canal de desarrollo y una desembocadura.

Figura 3. Cabecera de una cárcava de fondo de valle localizada en una finca de Extremadura.

Los factores que se correlacionan con la extensión y severidad de la erosión en cárcava son el clima semiárido, relieve, alta erosividad pluvial, litología blanda, erosionabilidad y unas condiciones desfavorables para el establecimiento de la vegetación (Castillo y Gómez, 2016). La erosión por cárcavas favorece elevadas tasas de erosión, la producción de sedimentos y reducción en la productividad de la tierra en todo el mundo (Cooke and Reeves, 1976; Poesen et al., 2003; Prosser et al., 2001).

En los últimos tiempos, el estudio de la erosión por cárcavas es de especial interés debido a la creciente preocupación por los impactos *in situ* y también por los de fuera del lugar (*off-site*) a escala de cuenca (Poesen et al., 2003; Valentin et al., 2005). Los impactos *in situ* incluyen la pérdida de tierra, árboles y cultivos, y dificulta el tránsito de personas y animales. En muchas regiones, la erosión en cárcava contribuye a

pérdidas significativas de suelo y reduce la calidad del mismo (Hayas et al., 2017; Ionita, 2006; Poesen et al., 2003; Poesen et al., 1996; Xu et al., 2016). Por ejemplo, la pérdida de suelo y nutrientes en áreas agrícolas y de pastizales puede repercutir en un aumento de los costes de producción al disminuir la fertilidad del suelo y con ello la productividad (Daba et al., 2003; García-Ruiz, 2010).

En España, las tasas de erosión alcanzan valores de entre 32 y 77 t ha^{-1} a^{-1} en las cárcavas de las Bardenas Reales en Navarra (Desir y Marín, 2009) o tasas de entre 16 y 63 t ha^{-1} a^{-1} en las cárcavas del Penedés en Cataluña (Martínez *et al.*, 2009). Las cárcavas son una fuente importante de sedimentos y representan entre el 20 y el 80% de la producción de sedimentos en una cuenca (por ejemplo: Poesen et al., 2003; Poesen et al., 1996; Vanmaercke et al., 2012). El acarcavamiento también puede alterar significativamente la hidrología superficial y subterránea de las laderas. En climas semi-áridos, esto puede contribuir a la desertificación o a la conversión de áreas productivas en tierras baldías (Cánovas et al., 2017; Torri et al., 2018). Dados estos impactos ambientales negativos, se necesitan estrategias de manejo del uso de la tierra y de las cuencas hidrológicas que permitan la prevención y el control de la erosión en cárcava (por ejemplo: Poesen, 2018; Poesen et al., 2003). No obstante, controlar este tipo de erosión hídrica es complejo y costoso y, por lo general, requiere un enfoque integral en toda la cuenca para que sea efectivo (Bartley et al., 2020; Golosov y Belyaev, 2013).

1.1.4. Métodos y técnicas para el seguimiento de cárcavas

La toma de imágenes con cámaras aerotransportadas ha transformado la adquisición de datos topográficos en la última década, reemplazando métodos clásicos para la estimación del cambio topográfico en cárcavas, como por ejemplo la interpolación de secciones transversales (Caraballo-Arias et al., 2016; Ferguson y Ashworth, 1992; Gómez-Gutiérrez et al., 2012). Según Castillo et al. (2012), la interpolación de las áreas transversales para estimar el cambio topográfico en cárcavas genera incertidumbres causadas por la longitud de la cárcava, su sinuosidad y, también por el número de secciones transversales muestreadas. Además, estos métodos tradicionales tienen la desventaja de que generalmente cubren áreas pequeñas y se necesita bastante tiempo para las mediciones. Según Marzolff y Poesen (2009), la fotografía aérea, por el contrario, permite una cobertura espacialmente continua de un

área y con alta resolución y, además favorece un análisis tanto métrico como interpretativo.

El método LiDAR (en inglés, *Light Detection and Ranging*) aerotransportado, por ejemplo, permite cartografiar la morfología y las dimensiones de las cárcavas (por ejemplo: Eustace et al., 2009; Goodwin et al., 2017). Este método, aunque no es barato (Castillo et al., 2012), es relativamente rápido y permite producir modelos digitales de terreno (MDT) con alta resolución espacial. Las técnicas de *Structure–from–Motion* (SfM) (Ullman, 1979) con precisiones muy similares al LiDAR, representan una opción más económica (por ejemplo: Castillo et al., 2012; Clapuyt et al., 2016; Gómez-Gutiérrez et al., 2014; Koci et al., 2017). Las imágenes se pueden capturar tanto desde plataformas aéreas (por ejemplo, a través de vehículos de aeronaves no tripuladas, en inglés *Unmanned Aerial Vehicles* "UAV") como desde tierra (Castillo et al., 2018; Castillo et al., 2012). El uso sincrónico de UAV y SfM junto con MultiView–Stereo (MVS: Seitz et al., 2006) (Figura 4) ha revolucionado la investigación de procesos geomorfológicos. La fotogrametría SfM es fácil de utilizar, económica y útil en estudios a escala grande (Fonstad et al., 2013). El desarrollo de plataformas UAV facilita la adquisición de fotografías aéreas con resolución espacial centimétrica a partir de las cuales se puede utilizar la fotogrametría SfM para producir productos cartográficos 2,5D (modelos digitales de elevaciones o MDE, modelos digitales de superficie o MDS y ortofotografías) y 3D (nubes de punto) (Javernick et al., 2014; Smith and Vericat, 2015; Woodget et al., 2015). Las cárcavas han sido estudiadas por Xiang et al. (2018) y Kaiser et al. (2018) usando fotogrametría SfM y muestreos secuenciales en una misma zona de estudio, siendo útil para la estimación de cambios topográficos en cárcavas (por ejemplo: Castillo et al., 2012; Frankl et al., 2015; Gómez-Gutiérrez et al., 2014).

La identificación y cuantificación de los cambios topográficos resultado de los procesos de erosión-deposición pueden ser estudiados a partir de modelos topográficos multi–temporales. Se pueden restar dos MDE secuenciales para generar un MDE de diferencias (DoD) (Wheaton et al., 2010), proporcionando un modelo espacialmente distribuido del cambio topográfico a través del tiempo (Brasington et al., 2003; Rumsby et al., 2008). Este tipo de técnicas para detectar cambios topográficos se han aplicado en diferentes entornos, como por ejemplo: ribereños (Castillo et al., 2012), agrícolas (Tarolli et al., 2019), montañosos (Cavalli et al., 2017) y tierras baldías (Neugirg et al., 2016). La estimación del cambio topográfico en cárcavas mediante métodos tridimensionales presenta limitaciones de las técnicas de fotogrametría SfM para capturar la topografía en espacios con una cobertura vegetal densa (Cook, 2017;

Niculiță et al., 2020; Westoby et al., 2012) o cubiertos de láminas de agua (Cucchiaro et al., 2018; Gómez-Gutiérrez et al., 2014). El uso de técnicas LiDAR puede ser una alternativa interesante para superar ambas limitaciones (Cavalli et al., 2008; Swetnam et al., 2018).

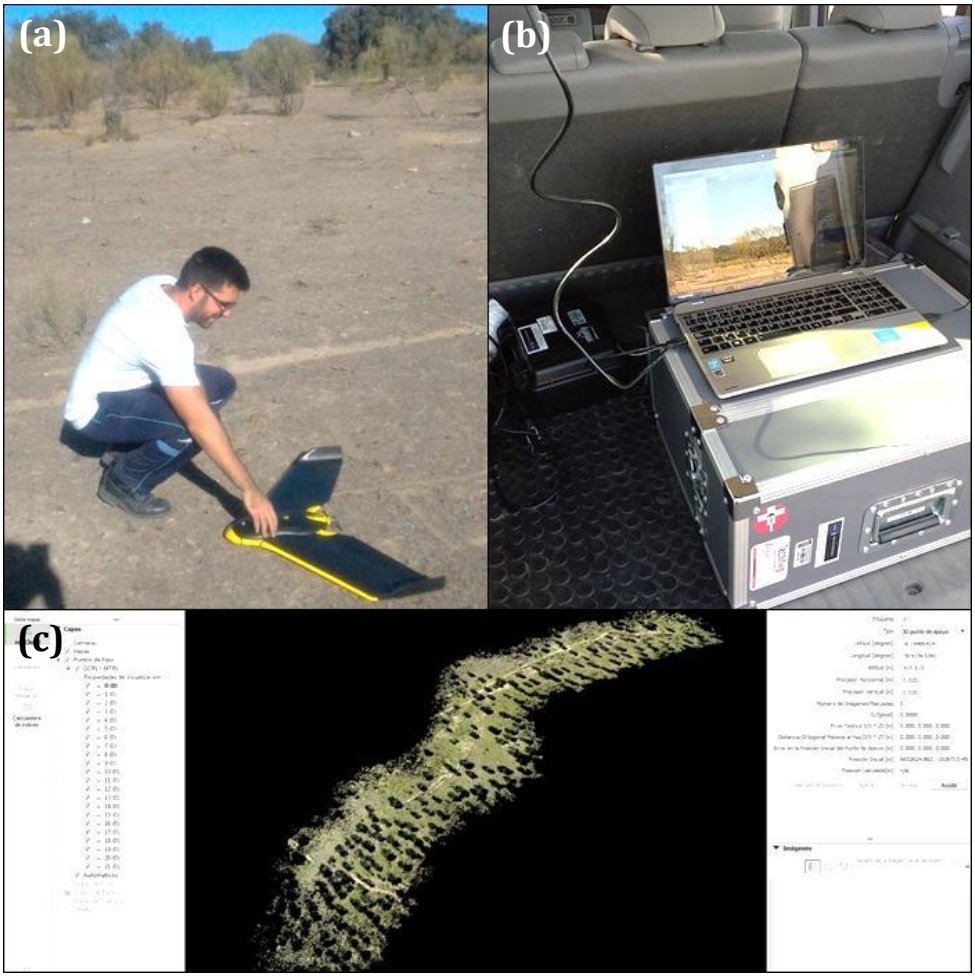

Figura 4. (a) UAV de ala fija en el área de estudio, (b) ordenador externo para el control del UAV mediante un plan de vuelo pre−programado y (c) procesamiento fotogramétrico de imágenes RGB tomadas desde el UAV usando un software de procesamiento de imágenes para obtener nubes de puntos, modelos digitales de elevación (MDE) y ortofotografías.

1.1.5. Medidas de corrección hidrológica y restauración de cárcavas: técnicas y efectividad

El control del acarcavamiento es una tarea difícil y generalmente costosa. La presencia de cárcavas es un reflejo de la degradación de una cuenca. Las cárcavas de fondo de valle son un tema de preocupación para los administradores de tierras y los investigadores, quienes observan que las medidas de restauración implementadas en cárcavas a menudo fracasan o incluso tienen efectos negativos (Boix-Fayos et al., 2008;

Cucchiaro et al., 2019; Polyakov et al., 2014). Pathak et al. (2005) establecieron diferentes enfoques y técnicas para la restauración de cárcavas. En general, se pueden clasificar en tres estrategias generales. La primera se basa en el establecimiento de medidas de restauración en la cuenca de la cárcava mediante el control del ganado, revegetación o desvío de la escorrentía. Esta estrategia es difícil de lograr ya que se debe implementar en grandes superficies de la cuenca (Poesen, 1989). La segunda estrategia se centra en la cárcava en sí, frenando un mayor crecimiento de la cárcava o reduciendo el transporte de sedimentos dentro de la misma. Tales intervenciones pueden ser mediante la construcción de diques (por ejemplo, gaviones o fajinas). Esta estrategia puede requerir menos mano de obra que la primera, pero necesita un diseño minucioso para una implementación eficaz de las medidas de restauración. La tercera estrategia consiste en utilizar una combinación de enfoques que traten tanto la cuenca como la cárcava.

Las principales medidas de restauración y técnicas para el control de cárcavas en zonas acarcavadas se muestran en la Figura 5 y se describen posteriormente. Además, la Figura 5 presenta un modelo conceptual de los factores y procesos clave que controlan la erosión por cárcavas y los flujos de agua y de sedimentos en los sistemas de dehesa.

1) Barreras de vegetación

Las barreras de vegetación ayudan a disminuir la conectividad hidrológica y de sedimentos (Boardman et al., 2019). Estas barreras estrechas de plantas mitigar los efectos negativos de la erosión, impedir el desarrollo de cárcavas y reducen la pérdida rápida de sedimentos. Las barreras ralentizan y extienden la escorrentía superficial y, por tanto, reducen la capacidad erosiva de la escorrentía y favorecen la deposición de sedimentos (Richet et al., 2017).

2) Desvío de la escorrentía

El desvío o la retención de la escorrentía en cabeceras ayudan a reducir la incisión en cárcavas activas y profundas (Sheng y Liao, 1997), pero si el desvío no es controlado puede provocar la formación de nuevas cárcavas (Martins et al., 2019; Smit et al., 2017). Por este motivo, la escorrentía se debe desviar hacia áreas con cobertura herbácea y leñosa donde exista un riesgo mínimo de iniciar nuevas cárcavas. Esta medida de control de cárcavas favorece la deposición de sedimentos y la mejora del crecimiento de la vegetación (Descheemaeker et al., 2009; Guyassa et al., 2017).

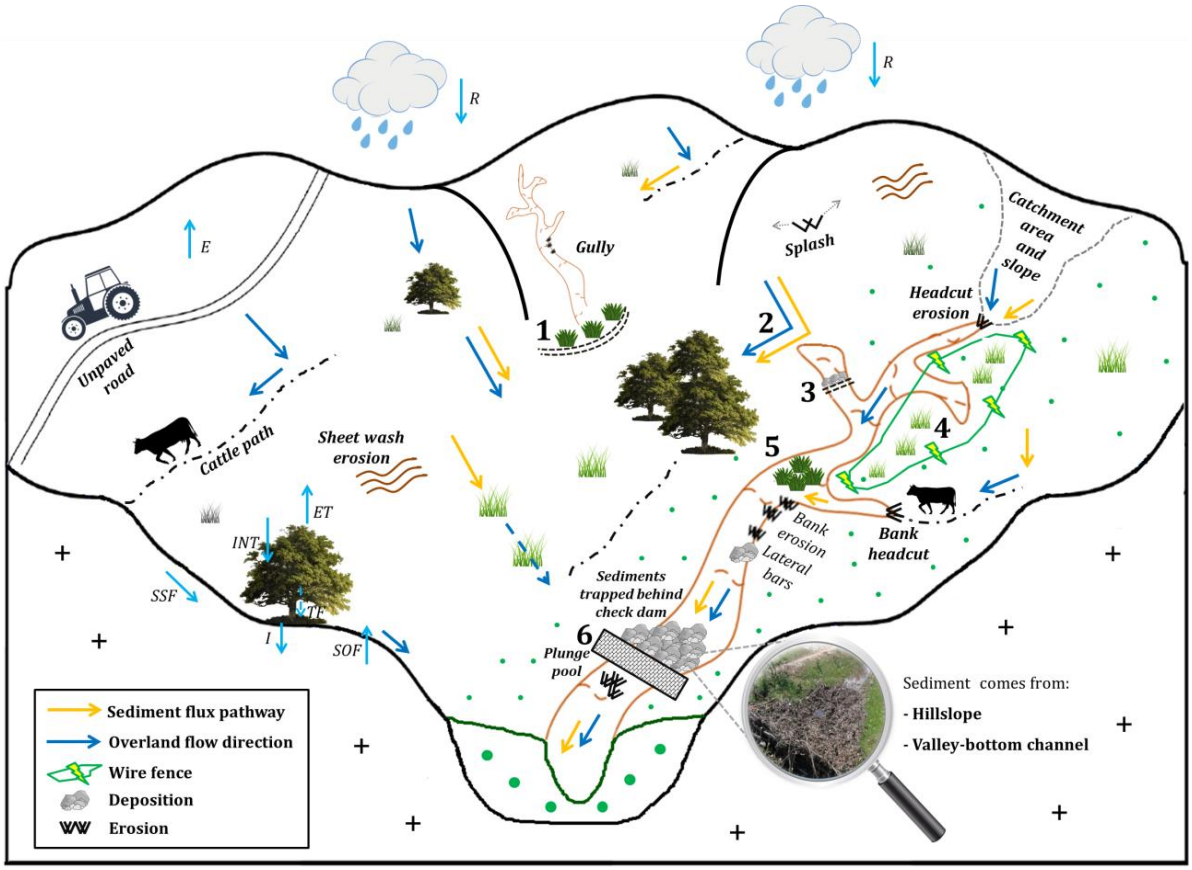

Figura 5. Modelo conceptual de los factores y procesos que controlan la erosión hídrica, y las medidas de prevención y control de cárcavas en un ambiente de dehesa: (1) Barrera de vegetación en áreas acarcavadas; (2) Desviación de la escorrentía hacia zonas altamente vegetadas; (3) Fajinas con escobas extraídas de la zona; (4) Cercado eléctrico para la exclusión del ganado en áreas degradadas; (5) Revegetación en el canal de la cárcava y (6) Gaviones (que muestra la deposición en el canal). Tenga en cuenta que los componentes del modelo conceptual no están a escala. E: evaporación; ET: evapotranspiración; I: infiltración; INT: interceptación; Q: caudal; R: precipitación; SL: carga de sedimentos; SOF: flujo superficial de saturación; SSF: flujo subterráneo; TF: trascolación. Inspirado en Koci (2020).

3) Manejo de la erosión en cárcava mediante el control del acceso del ganado

La pérdida de vegetación en los suelos de los fondos de valle (por ejemplo, debido al sobrepastoreo) ha jugado un papel clave en el desarrollo de cárcavas (Boardman et al., 2017; Gómez-Gutiérrez et al., 2009a; Miller, 2017; Wilkinson et al., 2018). Diversos estudios han demostrado los beneficios de la reducción del pastoreo o la eliminación del mismo para reducir la escorrentía (Descheemaeker et al., 2006), mejorar la calidad del agua de las laderas (Bartley et al., 2006) y de las cuencas (Lusby and Knipe, 1971), y evitar la erosión mecánica del suelo (Gómez-Gutiérrez et al., 2009a). El control del pastoreo puede reducir la escorrentía superficial hasta en un 30% y la producción de

sedimentos en un 40−77% en cuencas experimentales (Hadley, 1974; Wilkinson et al., 2018). La reducción del pastoreo de ganado en áreas extensas y propensas a la erosión, como los sistemas adehesados, no se considera económicamente viable. Según Shellberg et al. (2010), la exclusión temporal de ganado durante periodos en el que el suelo esté saturado de agua reduce la erosión por cárcavas. La combinación de estrategias de reducción o exclusión del ganado en áreas muy degradadas (Figura 7) y otras medidas de restauración, como diques de corrección hidrológica disminuyen la producción de sedimentos (Bartley et al., 2020).

4) Revegetación en el control de cárcavas

Una estrategia clave para controlar el desarrollo de cárcavas es la revegetación, ya que protege el suelo de la escorrentía superficial a la vez que reduce la velocidad del caudal, y por tanto su capacidad erosiva (De Baets et al., 2007). Según Ayele et al. (2016) y Frankl et al. (2019) la vegetación reduciría la erosión por cárcavas en los fondos de los valles (Ayele et al., 2016; Frankl et al., 2019; Miller et al., 2011; Shellberg et al., 2016). No obstante, Navarro-Hevia et al. (2013) señalaron que en áreas de la región mediterránea, con un clima semiárido, esta técnica no ha dado resultados satisfactorios. El establecimiento de la vegetación en la cárcava puede ser mediante la siembra de semillas con fajinas compuesta por material natural de la zona (Díaz-Gutiérrez, 2015) o con técnicas de bioingeniería más reciente como el empleo de geotextiles que ayudan al asentamiento de la vegetación (Navarro-Hevia et al., 1997). Alternativas interesantes dada la escasez de nutrientes y materia orgánica y poca capacidad de retención hídrica para el desarrollo de la vegetación en el lecho de una cárcava.

Hay estudios que sugieren que la restauración de la vegetación en cuencas (que a menudo es una combinación de reforestación y plantación de pastos) puede reducir la escorrentía superficial, la erosión por cárcavas en fondos de valle y también una reducción en la producción de sedimentos en toda una cuenca (Chen y Cai, 2006; Gomez et al., 2003).

5) Diques de corrección hidrológica

Los diques de corrección hidrológica son medida de restauración eficaz para el control de la erosión por cárcavas en regiones áridas y semiáridas (Abbasi et al., 2019; Lucas-Borja et al., 2019). Estas estructuras controlan el transporte de sedimentos (Catella et al., 2005); estabilizan canales activos (Conesa García, 2004; Conesa García

and García Lorenzo, 2007; Romero-Díaz, 2008); recargan acuíferos (Conesa García, 2004; Conesa García and García Lorenzo, 2007); atrapan sedimentos (Belmonte et al., 2005; Conesa García and García Lorenzo, 2007; Martin-Rosales et al., 2003) y reducen la capacidad erosiva del agua (Belmonte et al., 2005; Romero-Díaz, 2008). Sin embargo, la retención de los sedimentos aguas arriba de los diques provoca que el flujo no cargue sedimentos por lo que emplea la energía en el arranque de las partículas del suelo, que ya no la emplea en el transporte de los sedimentos (Puigdefábregas y García-Ruiz, 1985).

Debido a la alta eficiencia de los diques en la reducción de sedimentos y los costes en la construcción son relativamente bajos, este tipo de estructuras son muy comunes en México (Lucas-Borja et al., 2018), España (Castillo et al., 2007; Díaz-Gutiérrez et al., 2019; Quiñonero-Rubio et al., 2016), Italia (Bombino et al., 2009; Catella et al., 2005; Cucchiaro et al., 2019), Irán (Hassanli et al., 2009) y China (Xu et al., 2004). El país con un mayor número de diques es China; donde en la meseta de Loess, por ejemplo, se han construido alrededor de 110.000 diques en los últimos 50 años (Wang et al., 2011).

Los diques pueden ser estructuras permanentes o temporales:

Las estructuras permanentes se utilizan cuando el problema de la erosión en cárcava no puede ser controlado por estructuras temporales. Los materiales son variados (Frankl et al., 2021) y pueden ser: estructuras reticulares de madera, perfiles o jaulas metálicas rellenas de piedra, estructuras de mampostería gavionada, mampostería hidráulica, hormigón armado u otros materiales reciclados. Los diques de mampostería gavionada (Figura 6c) son permeables, por lo cual retienen parte de los sedimentos y permiten el paso del flujo de agua cuando se ven sometidos a grandes avenidas.

Las estructuras temporales sirven para facilitar el crecimiento de la vegetación. Retienen los sedimentos y la humedad (Sharma et al., 1994), y pueden ser: fajinas compuestas de ramas secas, apiladas entre estacas verticales (Figura 5 y 6a-b) o barreras de adobe.

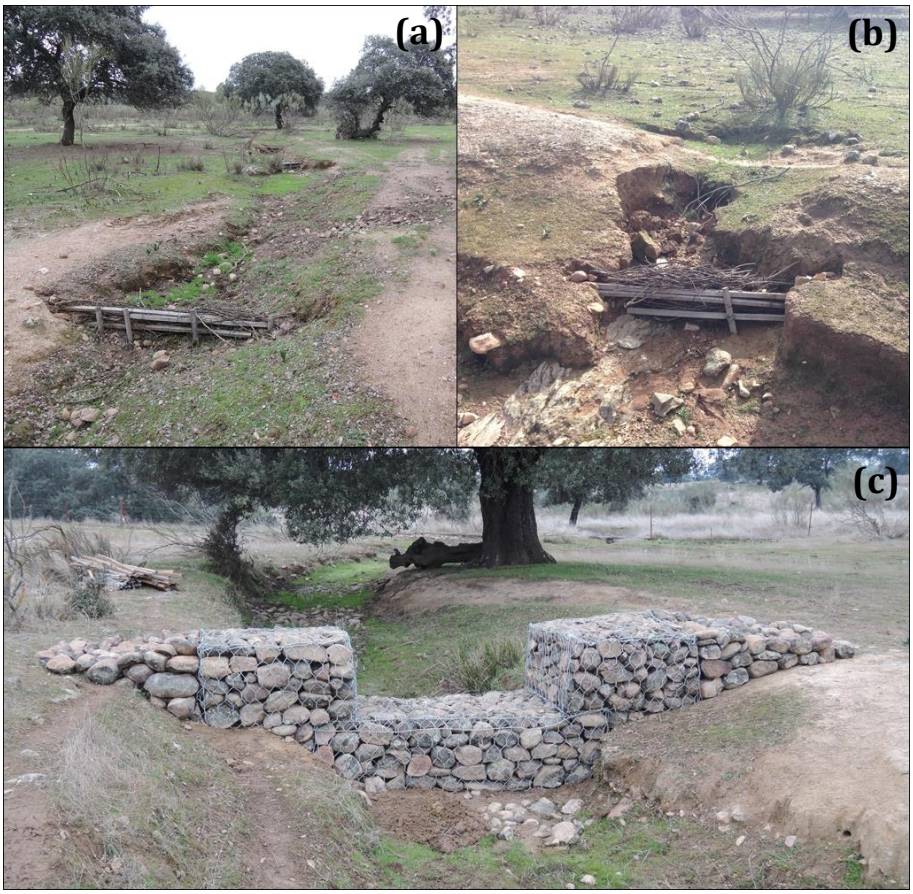

Figura 6. Ejemplos de medidas de corrección y control de cárcavas implementadas en una cuenca de dehesa en Extremadura: (a) una fajina hecha con escobas e implementada perpendicular a la cárcava, (b) una fajina instalada en una cabecera lateral y (c) un gavión formado por cantos y bloques de cuarcita y construido perpendicular a la cárcava.

Figura 7. (a) Vista aérea de la superficie cercada en la que se aprecia las diferencias en la cobertura de plantas herbáceas y (b) fotografía del cercado eléctrico.

1.2. Justificación, objetivos y estructura de la tesis

1.2.1. Justificación y objetivos

La erosión del suelo ha sido reconocida como la principal causa de degradación del suelo en todo el mundo. En particular, la erosión hídrica es un proceso de graves consecuencias en la destrucción y formación de suelo. Según Walling y Fang (2003) alrededor del 15% del suelo a nivel mundial está afectado por la erosión hídrica y aproximadamente 1.094 millones de hectáreas se encuentran amenazadas por procesos de erosión acelerada como consecuencia de la acción antrópica.

La erosión hídrica desempeña un papel preponderante entre los procesos de degradación física del suelo en los ambientes adehesados. En el contexto de cambio climático y globalización del siglo XXI la dehesa, como ecosistema, se enfrenta a diversos retos, entre ellos su pervivencia en el tiempo. Estos sistemas agrosilvopastoriles constituyen pastizales con arbolado disperso, predominantemente encinas (*Quercus ilex*) y alcornoques (*Quercus suber*), y prestan diferentes usos como la ganadería extensiva, el uso agrícola y forestal, o cinegético. Durante las últimas décadas, las subvenciones de la Unión Europea han favorecido un incremento de las cargas ganaderas y al abandono de la explotación de las tierras más improductivas (Lavado-Contador et al., 2004). Todo ello ha desembocado en serios problemas de degradación ambiental, sobre todo importantes pérdidas de suelo (Schnabel et al., 2013) y en una escasa regeneración del arbolado (Herguido Sevillano et al., 2017; Pulido-Fernández et al., 2013). Los principales procesos de erosión hídrica que se han observado y cuantificado en las dehesas son la erosión laminar de las vertientes (Rubio-Delgado et al., 2017; Rubio-Delgado et al., 2018; Schnabel, 1997; Schnabel et al., 2010)en y el acarcavamiento de los fondos de valle (Gómez-Gutiérrez et al., 2012; Gómez-Gutiérrez et al., 2009a). La erosión por cárcavas presenta un especial interés que se debe a varias circunstancias. La primera de ellas es que se trata de un fenómeno bastante frecuente en las cuencas de cabecera de las dehesas. El segundo factor que provoca un interés especial en este proceso es que suele afectar a los fondos de valle o vaguadas. Esta unidad hidro−geomorfológica se caracteriza por presentar un relleno sedimentario con suelos más profundos que en las zonas culminantes y las vertientes y que funcionan como un importante reservorio de recursos hídricos, resultando de especial interés debido al contexto climático en el que se enmarca la Península Ibérica.

En la última década, algunas investigaciones han demostrado el efecto negativo de la existencia de cárcavas de fondo de valle. Cabe destacar el trabajo de Nyssen et al.

(2004) en los *Highlands* de Etiopía, donde demostraron que se extendió la red de drenaje, disminuyó la humedad del suelo y se redujo la producción agrícola. Por otra parte, la canalización de la escorrentía superficial y de la producción de sedimentos en suspensión puede provocar una reducción en la capacidad de transporte de ríos aguas abajo, aumenta el riesgo de inundaciones, obstruye canales de riego y acorta la vida útil de embalses y pantanos. Los efectos negativos del acarcavamiento han sido estudiados en numerosos ambientes y como consecuencia, son ampliamente conocidos (Poesen et al., 2003). En Extremadura, las investigaciones más recientes en este tipo de canales se han centrado en cuantificar las pérdidas de suelo (Gómez-Gutiérrez et al., 2012), en analizar las causas del fenómeno (Gómez-Gutiérrez et al., 2009a) y en modelizar la distribución espacial del proceso (Gómez-Gutiérrez et al., 2009c; Gomez Gutierrez et al., 2009b). Los resultados de estas investigaciones pueden ayudarnos a prevenir la aparición y crecimiento de cárcavas. Sin embargo, poco se ha hecho todavía por la restauración de aquellos fondos de valle afectados por la erosión en cárcava. De hecho, se desconoce qué estrategias de conservación y control de la erosión del suelo resultan idóneas para la tipología de cárcavas que existen en las dehesas.

Como ya se ha mencionado en el apartado sobre métodos y técnicas para el seguimiento de cárcavas, el uso de plataformas UAV y junto con la fotogrametría SfM ha supuesto un gran avance en la adquisición de datos topográficos de alta resolución y en la generación de modelos 3D. Los modelos de elevación digitales repetidos de alta resolución son clave para cuantificar la distribución espacial y la morfología de las cárcavas (Evans y Lindsay, 2010; Sidle et al., 2019), para identificar transferencias de sedimentos y rutas de transporte (Heckmann y Vericat, 2018), para detectar cambios geomorfológicos (Cavalli et al., 2017; Turner et al., 2015; Woodget et al., 2015) y para la estimación del volumen de sedimentos retenido en diques mediante métodos topográficos (Sougnez et al., 2011). Además, frente a la evaluación tradicional de la eficiencia de medidas de restauración basada en la cubicación geométrica y manual de la cuña sedimentaria en diques, la disponibilidad de UAV y técnicas de fotorreconstrucción permiten, en la actualidad, llevar a cabo un seguimiento intensivo desde el punto de vista espacial y temporal.

Atendiendo a lo anteriormente mencionado, los objetivos de este trabajo son:

- Utilizar técnicas novedosas de captura y generación de cartografía de gran detalle para caracterizar tramos de cauce degradado o no degradado con criterios geomorfológicos y en zonas con cárcavas de fondo de valle.

- Desarrollar una metodología que permita cuantificar el volumen de sedimento retenidos en los diques a partir de MDE y mediante el uso de métodos topográficos.
- Estimar el volumen de sedimentos depositado en diques establecidos a una escala temporal media en un sistema de dehesa y estudiar su variabilidad espacial.
- Analizar la efectividad de los diques ubicados en posiciones topográficas diferentes.
- Evaluar la relación del volumen de sedimentos retenido en los diques con diferentes variables físico–ambientales.
- Estudiar la dinámica de erosión y deposición en el cauce acarcavado antes y después de las actividades de restauración mediante MDE de alta resolución.
- Examinar el papel de la geomorfometría en los cambios topográficos observados en la cárcava.
- Analizar el efecto de las medidas de restauración en los cambios topográficos en el canal, la dinámica hidrológica y la producción de sedimentos en suspensión.
- Evaluar el efecto de las actividades de restauración sobre los patrones espaciales de conectividad de sedimentos a escala de cuenca y de canal.
- Estudiar la relación existente entre la situación actual de cauces y vaguadas y la dinámica reciente del uso del suelo y la cubierta vegetal en las áreas con cárcavas en los fondos de valle.

1.2.1. Estructura de la tesis

La presente tesis doctoral es un compendio de 3 publicaciones y está articulada en un total de siete capítulos. Dos han sido publicados en revistas incluidas en el *Journal Citation Report* (JCR) situadas en el primer cuartil (*Science of the Total Environment*), en el segundo cuartil (*Land*), y un tercero está en revisión en la revista *Catena*, también incluida en el JCR y situada en el primer cuartil.

Se detallan, a continuación, las referencias completas de los capítulos 4 y 5 que ya han sido publicados y del capítulo 6 que está en revisión:

- ✓ **Capítulo 4**: Alfonso–Torreño A, Gómez–Gutiérrez Á, Schnabel S, Lavado–Contador JF, de Sanjosé Blasco JJ, Sánchez Fernández M, 2019. sUAS, SfM–MVS photogrammetry and a topographic algorithm method to quantify the

volume of sediments retained in check–dams. *Science of the Total Environment* 678: 369–382. DOI: 10.1016/j.scitotenv.2019.04.332

- ✓ **Capítulo 5**: Alfonso–Torreño A, Gómez–Gutiérrez Á, Schnabel S, 2021. Dynamics of erosion and deposition in a partially restored valley bottom gully. *Land* 10, 62. DOI: 10.3390/land10010062
- ✓ **Capítulo 6**: Alfonso–Torreño A, Schnabel S, Gómez–Gutiérrez Á, Crema S, Cavalli M, 2021. Effects of gully rehabilitation on runoff production and sediment yield. *Catena [In revision]*

El primer capítulo consta de una introducción general en la que se presenta el estado de la cuestión que aborda el problema de la erosión del suelo y los procesos de erosión hídrica con especial énfasis en la erosión en cárcava. Además, se describen los procesos de erosión hídrica y los principales métodos y técnicas de foto–reconstrucción 3D que se utilizan para monitorizar la erosión en cárcava. También se hace referencia a las principales medidas de corrección hidrológica y restauración de cárcavas. Por último, se justifica la coherencia e interés de la tesis y se describen los objetivos, la estructura y los contenidos del documento.

El segundo capítulo se ha centrado en el marco geográfico de la tesis, describiendo la evolución histórica de los usos y manejos del suelo en la dehesa, así como los problemas ambientales que presenta este ecosistema en la actualidad. Además, se ha incluido una descripción detallada de las diferentes áreas que han sido objeto de estudio en este trabajo.

El tercer capítulo recoge los resúmenes en castellano de los capítulos de la investigación de la tesis doctoral escritos en inglés.

El contenido del cuarto capítulo ha sido publicado en la revista *Science of the Total Environment*, en el artículo científico titulado "sUAS, SfM–MVS photogrammetry and a topographic algorithm method to quantify volume of sediments retained in check–dams". En él se presenta la metodología desarrollada para estimar el volumen de sedimentos retenidos en diques de corrección hidrológica mediante MDE de alta resolución. También se describe la variabilidad espacial de los sedimentos retenidos en los diques y su relación con las variables físico–ambientales.

En el quinto capítulo se analiza la efectividad de las actividades de restauración implementadas en una cárcava de fondo de valle en la dehesa a través de MDE multi–temporales y de alta resolución. El contenido de este capítulo ha sido publicado

en la revista *Land*, en el artículo científico titulado "Dynamics of erosion and deposition in a partially restored valley bottom gully".

El sexto capítulo se centra en el análisis de la efectividad de las medidas de restauración en la dinámica hidrológica y la producción de sedimentos en la cuenca. También se presenta una evaluación del efecto de las medidas de corrección hidrológica sobre los patrones espaciales de la conectividad de sedimentos a escala de cuenca y cauce. Este capítulo está sujeto a revisión en la revista *Catena* con el título de "Effects of gully rehabilitation on runoff production and sediment yield".

El séptimo es un capítulo de síntesis en el que se presentan los principales resultados y conclusiones del trabajo. Este capítulo se redactó tanto en castellano como en inglés, dividiéndolo por tanto en dos subapartados.

Finalmente se presenta la lista de referencias bibliográficas citadas en la presente tesis doctoral.

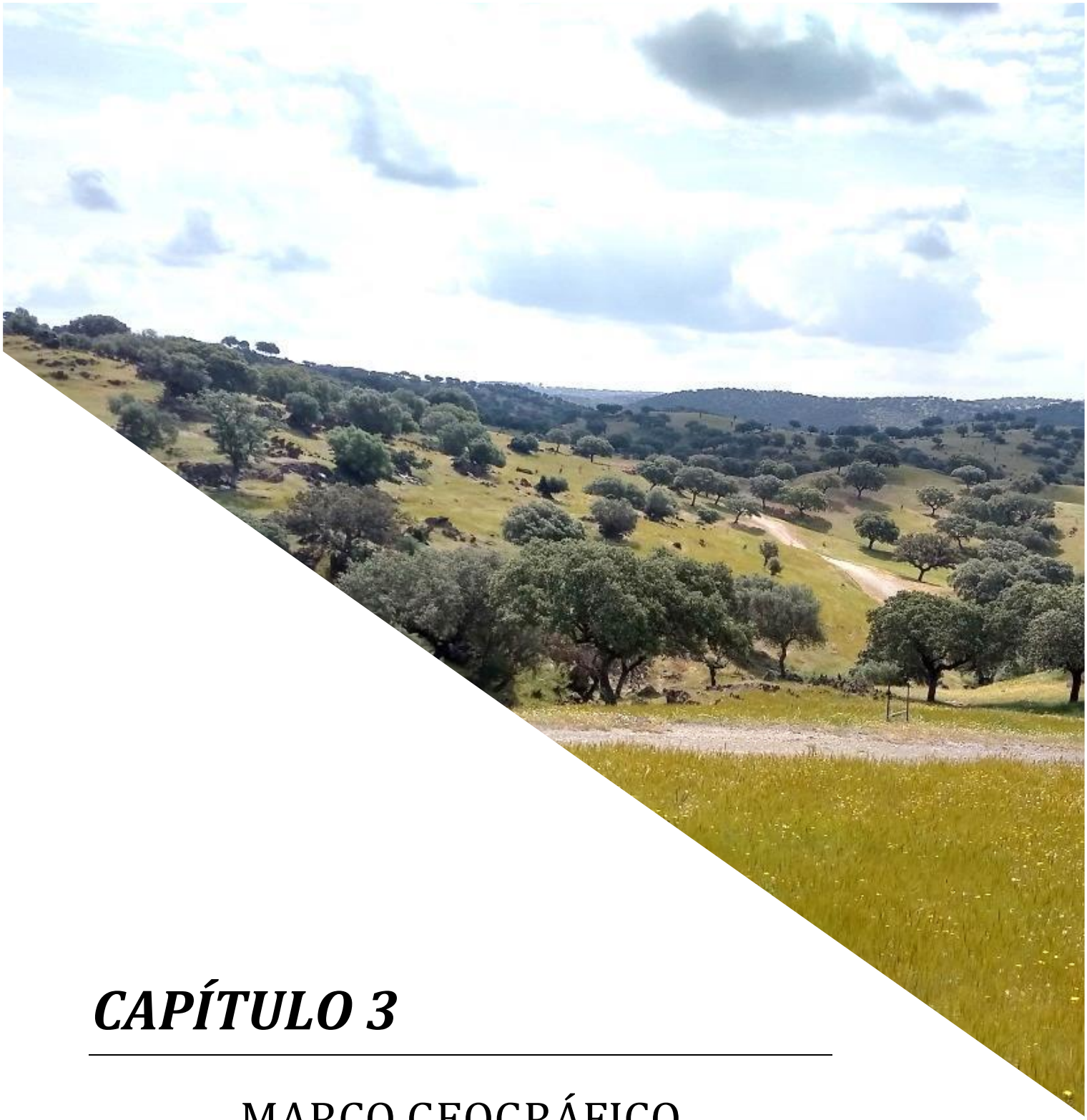

CAPÍTULO 3

MARCO GEOGRÁFICO

CAPÍTULO 2. MARCO GEOGRÁFICO

2.1. El ecosistema de dehesa

La dehesa es el sistema de aprovechamiento agrosilvopastoril más característico y representativo del suroeste de la Península Ibérica. Un ecosistema de aprovechamiento de unos recursos escasos y de carácter estacional asentados sobre suelos pobres. Se ubican por el sur-oeste de España y zonas limítrofes portuguesas, sobre aproximadamente de 4 millones de hectáreas (MAPA, 2008). Las zonas de dehesa en España se desarrollan principalmente en Extremadura y al oeste de Andalucía, y en provincias como Salamanca, Ciudad Real y Toledo (Olea et al., 2011).

En las últimas décadas varios autores han establecido diferentes definiciones de dehesa (Campos, 1992; Fernández y Porras, 1998; Martín Galindo, 1966; Montoya, 1993; Parsons, 1966; Scarascia-Mugnozza et al., 2000), destacar la definición de dehesa ibérica mediterránea establecida por el Ministerio de Agricultura, Pesca y Alimentación (MAPA, 2008): "*sistema antrópico de uso y gestión de la tierra basado principalmente en la explotación ganadera extensiva de una superficie de pastizal y arbolado mediterráneo, en la que más del 20% está ocupada por especies frondosas con una fracción de cabida cubierta arbolada comprendida entre el 5 y el 60%, que da lugar a un ecosistema en el que la conjunción de manejo silvopastoril propicia importantes valores ambientales, el uso sostenible del territorio, un paisaje equilibrado y una adecuada diversidad a distintos niveles de integración*".

El ser humano despejó el bosque primitivo mediterráneo de encinas (*Quercus ilex va. rotundifolia)* y alcornoques (*Quercus suber*) para un aprovechamiento agrícola, ganadero y forestal (González et al., 2012). Los arbustos que pueden aparecer en la dehesa están constituidos principalmente por especies pertenecientes a los géneros *Cistus, Rusmarinus, Lavandulas, Sarothamus*, etc. (Olea et al., 2011).

Estos espacios seminaturales son lugares con una gran riqueza ambiental y territorios con una importante trascendencia histórica, que ha sido crucial para el desarrollo histórico de la dehesa pero también fundamental en la realidad económica y ambiental de este sistema. Según Pardo-Navarro et al. (2003), estos territorios forestales fueron causa de conflictos entre ganaderos tras la aparición de la trashumancia durante la Edad Media. Este contexto propició la delimitación de un territorio forestal que estuviera protegido de la entrada de ganado trashumante: la dehesa (del latín *deffesa*, defendida) (Montero et al., 1998).

En los años cincuenta, el aprovechamiento productivo de los recursos naturales de la dehesa tradicional no suponía un impacto negativo en la estabilidad ecológica de la dehesa arbolada. Sin embargo, a partir de los años ochenta ese equilibrio natural de los recursos comenzaba a ser degradante debido a una mala gestión productiva de la dehesa (Campos, 1983). Según Campos et al. (2010), un 75% de las explotaciones de dehesa son de propiedad privada. El resto pertenecería a las denominada Dehesas Boyales que son de gestión colectiva y de propiedad comunal.

La dehesa destaca, entre otros muchos aspectos, por ser uno de los sistemas silvopastoriles de mayor extensión en la Unión Europea, incluyendo tanto las áreas de dehesa arbolada como los pastizales (Gea-Izquierdo et al., 2006). Los pastos representan un 71% de la superficie geográfica total de la dehesa (González López y Maya Blanca, 2013). Estos son el componente fundamental para el sustento del ganado y se desarrollan principalmente sobre terrenos ondulados con pendientes suaves, suelos ácidos con textura franco-arenosa y franca, elevada densidad aparente, poca profundidad y escasas aptitudes agrológicas (Schnabel et al., 2006).

La producción ganadera es la actividad comercial dominante en estos espacios, aunque depende en gran medida de las subvenciones de la PAC, exceptuando la especie porcina. La dehesa es una explotación donde domina el pastoreo del ganado vacuno y ovino, normalmente de razas rústicas para carne, en fase de cría, coincidiendo ésta en su mayoría con los periodos de crecimiento del pasto (Granda Losada, 1981). Además de actividades ganaderas, en los espacios adehesados se practican actividades cinegéticas y forestales, como la obtención de corcho y leña. En la última década con el desarrollo del turismo rural y natural, las dehesas ofrecen nuevas oportunidades de aprovechamiento, como es el agroturismo. Dada la escasa rentabilidad económica de estos bosques, representa una oferta alternativa la prestación de servicios turísticos con el objetivo de disfrutar del medio ambiente y del patrimonio cultural de los sistemas adehesados. En la actualidad, el manejo de la dehesa permite la conservación de un paisaje cultural en el que intervienen incluso agentes sociales fuera de la explotación silvopastoril (Pulido et al., 2010). Actualmente, existe una nueva "cultura de la dehesa" con un importante y rico patrimonio etnográfico (Campos et al., 2010).

En las dehesas existen una serie de problemas ambientales que afectan a la conservación y mantenimiento de estos espacios tan importantes desde el punto de vista natural y cultural. Si no se analizan y se intentan solucionar o aminorar determinados impactos sobre el medio, puede suponer el fin de este bosque

mediterráneo tan valioso. El mayor problema de este ecosistema es la falta de regeneración natural del arbolado, convirtiendo a la dehesa en un gerontobosque (San Miguel, 1993). Según Hernández-Díaz Ambrona (1996), la pérdida de quercíneas en las dehesas de Extremadura afecta a su economía, a los recursos naturales y a su riqueza paisajística. Desde el punto de vista ecológico, este bosque mediterráneo actúa en el ciclo de nutrientes del suelo, protege la calidad de las aguas de escorrentía, proporciona hábitats a la fauna, suministra alimento al ganado, produce madera y carbón vegetal y favorece el desarrollo de la caza y el turismo rural (Hernández-Díaz Ambrona, 1996). Además, un aspecto actual es que las dehesas aportan o mantienen el *stock* de carbono en el suelo (Pulido-Fernández et al., 2013).

La dehesa arbolada sufre un lento pero continuo proceso de deforestación. En 25 años se ha estimado una pérdida aproximada de 250.000 pies anuales, lo que hace indicar que en 2070 se podría deforestar Extremadura (Elena-Rosselló et al., 1987). Sin embargo, esa proyección de la deforestación en la región no tuvo en cuenta las medidas de conservación aplicadas posteriormente en el sistema de dehesa, como por ejemplo la regulación del corte de encinas y alcornoques. El problema es la falta de regeneración natural, debido al sobrepastoreo en la mayoría de estos espacios. Una de solución para la regeneración natural es gestionar mejor el ganado y/o reducir la carga ganadera, y otras pueden ser siembras, plantaciones, rozas de regeneración y tubos protectores. Herguido Sevillano et al. (2017) desarrollaron modelos espaciales de la dinámica temporal de los árboles en zonas de dehesas para analizar las pérdidas o ganancias de individuos. Los resultados indicaron que, aunque en términos generales hay un aumento de la densidad del arbolado en la mayor parte de las fincas estudiadas, realmente se está produciendo una polarización entre el incremento y una pérdida de arbolado. La regeneración se produce en las áreas menos aprovechadas de las fincas, mientras que la pérdida de arbolado se centra en las áreas donde el pasta el ganado.

Otro problema que amenaza a la dehesa, especialmente al arbolado, es la enfermedad comúnmente llamada «seca». Según Campos et al. (2010), "*la seca es el principal problema fitosanitario del arbolado de las dehesas, además existe una especial preocupación debido a la proliferación de los focos y al aumento de su extensión*". El origen de la seca siempre ha sido una incógnita, y se han barajado distintas posibilidades en función de una serie de condicionantes y peculiaridades físicas de las dehesas. En un principio se atribuía a factores edafoclimáticos, relacionados con suelos con escasa capacidad de retención de agua, de difícil encharcamiento y expuestos a periodos prolongados de sequía. Por otro lado, Brasier (1996) determinó que se

trataba de un origen patógeno, concretamente del hongo *Phytophthora cinnamomi*. Durante las últimas décadas del siglo XX, la alternancia de intensas lluvias y encharcamientos con periodos largos de sequía favorecerían la presencia del hongo *Phytophthora cinnamomi* (De Sampaio e Paiva Camilo-Alves et al., 2013). La sintomatología que manifiesta el arbolado puede ser de dos tipos: debilitamiento progresivo y muerte súbita. A este problema de la seca hay que añadir otros como la excesiva explotación y malas prácticas realizadas con el arbolado, como las podas o descorches inadecuados.

Estos problemas ambientales repercuten en una progresiva degradación del suelo y con ello, en la sostenibilidad de los sistemas adehesados. Según Campos et al. (2010), el árbol en la dehesa mejora y protege el suelo. Se han llevado a cabo estudios en dehesas que han comparado la pérdida de suelo bajo influencia de las copas de los árboles y en espacios abiertos (Schnabel, 1997). En sistemas pastoriles la degradación dominante es la física, así como la biológica, relacionadas con la actividad ganadera. El pisoteo provoca generalmente un incremento de la densidad aparente y una disminución de la porosidad del suelo, reduciendo la capacidad de retención del agua y de infiltración (Gamougoun et al., 1984; Mulholland and Fullen, 1991; Pulido et al., 2018; Schnabel et al., 2006). Por un lado, la cubierta vegetal es importante para proteger el suelo de la erosión hídrica, y por otro lado, como proveedor de materia orgánica para el crecimiento de la vegetación (Dunjó Denti, 2004). Dicho crecimiento de la vegetación puede dificultarse con determinados usos y manejos del suelo. El manejo debe ser técnicamente eficaz y económicamente rentable en el aprovechamiento de la superficie ocupada por el ganado (Olea et al., 2011). Para maximizar el consumo de pasto hay que alcanzar una presión óptima en la carga ganadera y evitando, en cualquier caso, el sobrepastoreo (Hernández-Díaz Ambrona, 1996), pero también, el abandono del pastoreo produce cambios en la vegetación, repercute en la invasión de arbustos y en un aumento del riesgo de incendios forestales (Schnabel et al., 2013). Por tanto, se debe controlar tanto el sobrepastoreo como el subpastoreo para evitar procesos de degradación del suelo.

La reducción de la vegetación y de la cobertura del suelo debido al pastoreo causa una disminución en la interceptación de las precipitaciones, un aumento de suelo desnudo y, como consecuencia, una menor protección frente a la erosión del suelo por salpicadura (Figura 8). Además, una reducción del contenido de materia orgánica del suelo, provoca una degradación física del mismo, disminuyendo la capacidad de retención hídrica e incrementando la cantidad de escorrentía superficial (Imeson y

Sala, 1987; Schnabel et al., 2006). Este aumento de la escorrentía superficial provoca un incremento de la erosión hídrica, especialmente de la erosión laminar y de la erosión en cárcava, los dos procesos erosivos principales en las dehesas (Schnabel et al., 2010). Las mayores pérdidas de suelo se concentran en periodos afectados por sequía, por lluvias intensas o por sobrepastoreo (Schnabel et al., 2010). Los factores de degradación del suelo en las dehesas son mucho más graves si se añade que son suelos duros, de escasa profundidad y poco fértiles (Schnabel, 1997).

A pesar de los problemas ambientales, las dehesas muestran una gran diversidad biológica, fisiográfica y de diferentes formas de uso y manejo (Ibáñez Martí et al., 1997; Martínez et al., 2012). Son sistemas complejos interesantes en términos de sustentabilidad por el equilibrio entre economía y medio ambiente, adaptados a las escasas potencialidades edáficas y climáticas de las áreas en las que se desarrollan.

Figura 8. Vertiente con suelo desnudo en la Dehesa Boyal de Monroy como consecuencia de la ausencia de lluvias y del pastoreo, y los efectos de la erosión hídrica con los afloramientos verticales de pizarra, conocidos como *dientes de perro*.

2.2. Áreas de estudio

Con el objetivo de analizar la efectividad de medidas de restauración en áreas adehesadas con cárcavas de vertiente y de fondos de valle se seleccionaron dos zonas de estudio representativas de dicho ecosistema en el suroeste peninsular. Estas áreas mostraban claras evidencias de erosión hídrica del suelo con la presencia de suelo desnudo y cárcavas. Además fueron restauradas con medidas de corrección hidrológica. Las cuencas y cauces acarcavados objeto de estudio están ubicados en dos fincas de Extremadura (Figura 9), la Dehesa Boyal de Monroy (DBM) (39°37 'N, 6°12' W) y Parapuños de Doña María (39°37‘ N, 6°8‘ W). Las áreas de estudio representan las dos formas predominantes de tenencia de la tierra. Parapuños es un ejemplo típico de una finca privada de gran extensión, mientras que DBM es de aprovechamiento comunal por parte de la población local. La selección de DBM se basa en la existencia de 269 diques de corrección hidrológica establecidos en un periodo de 11 a 23 años que permite analizar la variabilidad espacial de los sedimentos retenidos en los diques. La selección de Parapuños se fundamenta en la presencia de un cárcava de fondo de valle donde se instalaron diques y un cercado de aislamiento del ganado con el objetivo de estudiar la dinámica de erosión y deposición antes y después de las medidas de restauración, y a analizar el efecto de estas medidas en la escorrentía superficial, la conectividad hidrológica y sedimentológica, y la producción de sedimentos a escala de cuenca. Parapuños ha sido objeto de estudio desde hace más de 20 años por el *Grupo de Investigación GeoAmbiental* donde se han desarrollado investigaciones sobre procesos hidrológicos y erosivos.

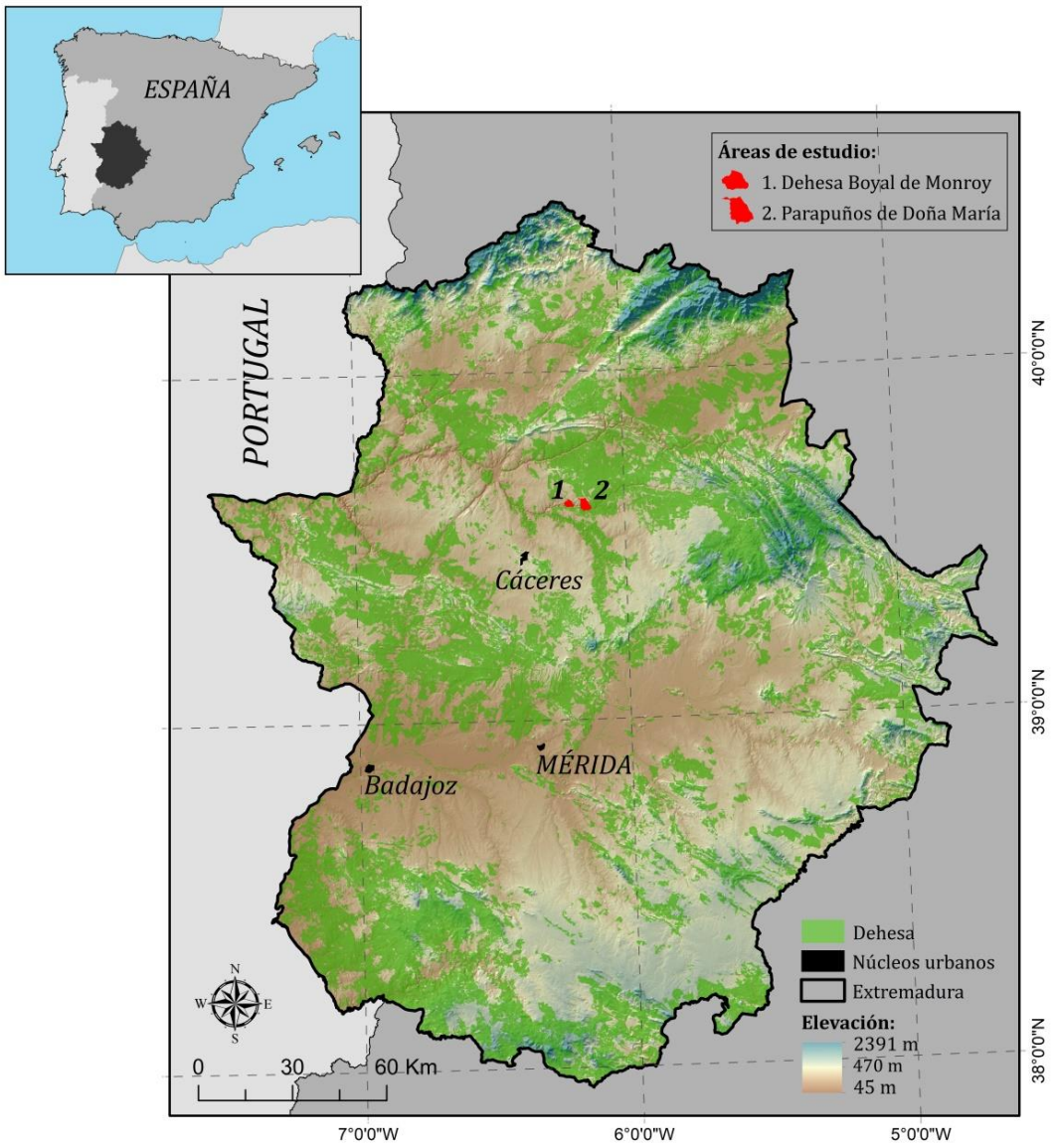

Figura 9. Localización de las áreas de estudio en la región de Extremadura. En verde se muestra la distribución del ecosistema de dehesa en Extremadura en 2014. Fuente: elaboración propia con datos del Sistema de Información sobre Ocupación del Suelo de España (SIOSE).

2.2.1. Dehesa Boyal de Monroy

La dehesa Boyal de Monroy está ubicada en el término municipal de Monroy, en el centro de la Provincia de Cáceres (Extremadura, España). La finca tiene una superficie de 533 ha. El estudio se llevó a cabo en seis cuencas que ocupan una superficie total de 239 ha, ubicadas en la finca comunal (39°37 'N, 6°12' W) (Figura 10). Las cuencas son parte de la extensa Superficie General de Erosión (SGE; Gómez Amelia, 1985) de topografía ondulada formada por pizarras y grauvacas. Las partes más altas de las cuencas presentan una topografía ondulada con pendientes que aumentan hacia el sur.

La altitud media es de 327 m, y la pendiente es del 18,9%. El área de estudio está compuesta por cuencas de bajo orden con una red de drenaje que fluye hacia el sur, donde se unen al río Almonte, un afluente del río Tajo. Los canales principales conducen flujos efímeros y algunos son canales discontinuos. La mayoría de los suelos son poco profundos y se desarrollan en pizarras, predominando *Cambisoles* y *Leptosoles* (Schnabel et al., 2013). Los suelos tienen textura arenosa a limosa, con cantidades muy bajas de materia orgánica (generalmente por debajo del 3% en el horizonte A). El clima pertenece a la clase *Csa Köppen*, es decir, mediterráneo mesotermal con veranos secos, con una temperatura anual media de 16°C y una precipitación anual media de 514 mm. La cubierta de la vegetación se compone de un estrato disperso de encinas y vegetación herbácea en el sotobosque. La densidad arbórea es de aproximadamente 26 árboles ha^{-1}, con una fracción de cabida cubierta inferior al 18%. La producción ganadera es el principal uso del suelo en la dehesa boyal, donde pastan cabras, vacas, cerdos y caballos, con un total de 234 UGM (unidad de ganado mayor), equivalente a una carga ganadera de 0.97 UGM ha^{-1}. Además, se practican otras actividades en la dehesa como la caza, la apicultura y el uso recreativo.

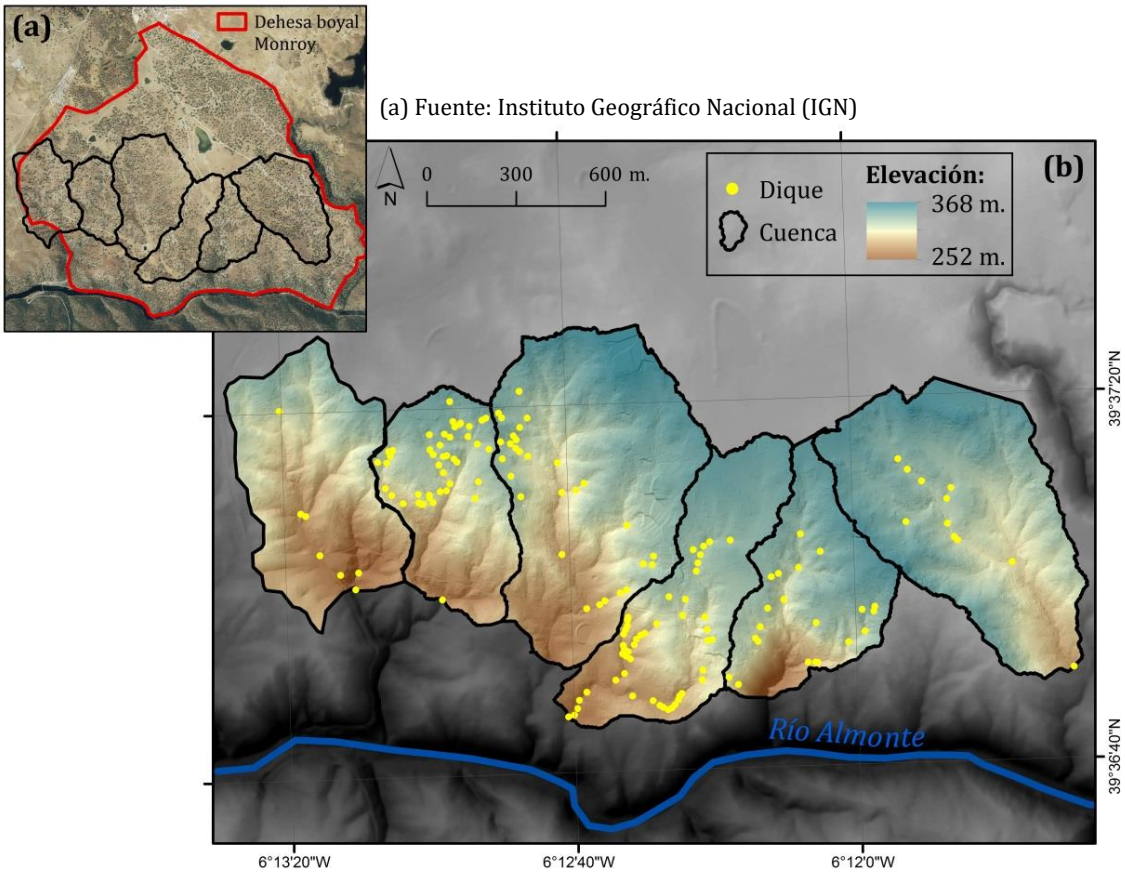

Figura 10. (a) Localización de las cuencas hidrológicas en la dehesa boyal de Monroy, (b) modelo digital de elevaciones y ubicación de los diques en el área de estudio.

2.2.2. Parapuños de Doña María

La finca Parapuños de Doña María también está situada en el término municipal de Monroy, al SO de España, en la comunidad autónoma de Extremadura. El estudio se realizó en una cuenca experimental de Parañuños con 99,5 ha (Figura 11). La cubierta vegetal está compuesta por una cubierta arbórea dispersa de encina, con una densidad arbórea promedio de 22,5 árboles ha^{-1}, con arbustos como la *Retama sphaerocarpa, Cytisus multiflorus y Genista hirsuta*, y vegetación herbácea en el sotobosque. La finca es pastoreada por 1.000 ovejas, 55 vacas y 40 cerdos, con un total de 190 UGM, equivalente a una carga ganadera de 0.18 UGM ha^{-1}. El clima es mediterráneo con una temperatura media anual de 16°C y una precipitación media anual de 513 mm con alta estacionalidad. La cuenca de estudio tiene una elevación promedio de 396 m sobre el nivel del mar, con un rango de 362 a 434 m y una pendiente media del 8%. Existen dos tipos de litología en la cuenca: pizarras del Ediacárico y conglomerados no consolidados del Mioceno, que forman parte de restos de un pedimento que ocupan el 32% de la cuenca. Este pedimento está compuesto por cantos rodados de cuarcita en una matriz arenosa y una capa rica en arcilla a aproximadamente 0,5 m de profundidad. Los fondos de valle, con un relleno de sedimentos aluviales que alcanzan 1,5 metros de máxima, son áreas casi planas y con pendientes inferiores al 5%. Los suelos dentro de la cuenca son poco profundos y se pueden clasificar como *Leptosoles* y *Cambisoles* en las laderas sobre pizarras y *Luvisoles crómicos* en las zonas culminantes del pedimento. Sobre el relleno de sedimentos aluviales donde se ubica la cárcava, encontramos *Regosoles* que presentan un 13% de fragmentos rocosos (>2 mm) y un 87% en tierra fina (<2 mm). La fracción fina del relleno sedimentario presenta una textura franco limosa y está compuesta principalmente por limo (53%), seguida de arena (23%) y un contenido menor de arcilla (11%). Esta composición granulométrica varía según la profundidad, presentando una capa rica en cantos o fragmentos de roca. La cárcava es un cauce discontinuo de segundo orden compuesto por el canal principal y un tributario, con una longitud de 832 m y 163 m, respectivamente. El canal se encuentra en la parte inferior de la cuenca, incidiendo en el relleno de sedimentos aluviales con una profundidad máxima de 1,5 m.

Estudios de Gómez-Gutiérrez et al. (2009a) sitúan el inicio de la cárcava entre 1726 y 1790, mientras que el tramo tributario apareció en 1989. Los periodos de crecimiento de la cárcava se producen por un aumento de la superficie cultivada en la cuenca entre 1945 y 1956, y también por un incremento de la densidad ganadera (Gómez-Gutiérrez et al., 2009a). La cárcava se puede dividir en tres tramos diferentes:

(1) tramo inferior, (2) tributario y (3) tramo superior donde se llevaron a cabo medidas de restauración. Para mitigar las consecuencias de la erosión hídrica, en febrero de 2017 se construyeron 8 gaviones con malla metálica y 25 fajinas en el cauce. Los gaviones con cantos rodados de cuarcita tienen un ancho de 0,5 m con longitudes entre 1 y 3 m con una altura de 1,5 m. Los vertederos de gaviones tienen un aliviadero central. Las fajinas con una longitud de 2 m se construyeron con escobas de la zona y se anclaron a la superficie con postes de acacia. Además, se instaló una valla eléctrica en el margen izquierdo de la cárcava como medida de aislamiento del ganado en un área particularmente degradada con varias cabeceras laterales activas (Figura 11c). La alambrada tiene un perímetro de 117 m y aísla 416 m^2.

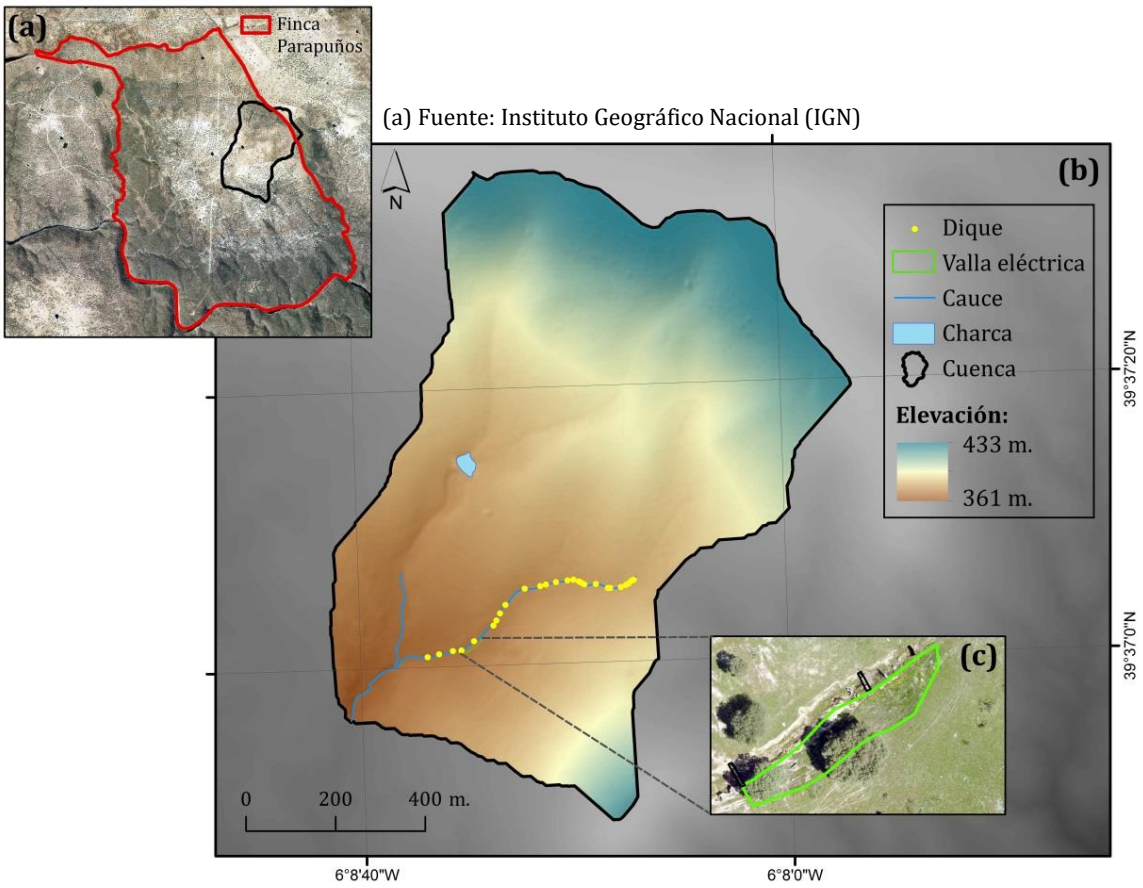

Figura 11. (a) Localización de la cuenca experimental en la finca Parapuños, (b) modelo digital de elevaciones y ubicación de las medidas de restauración en el área de estudio, y (c) zona de exclusión del ganado en la margen izquierda de la cárcava.

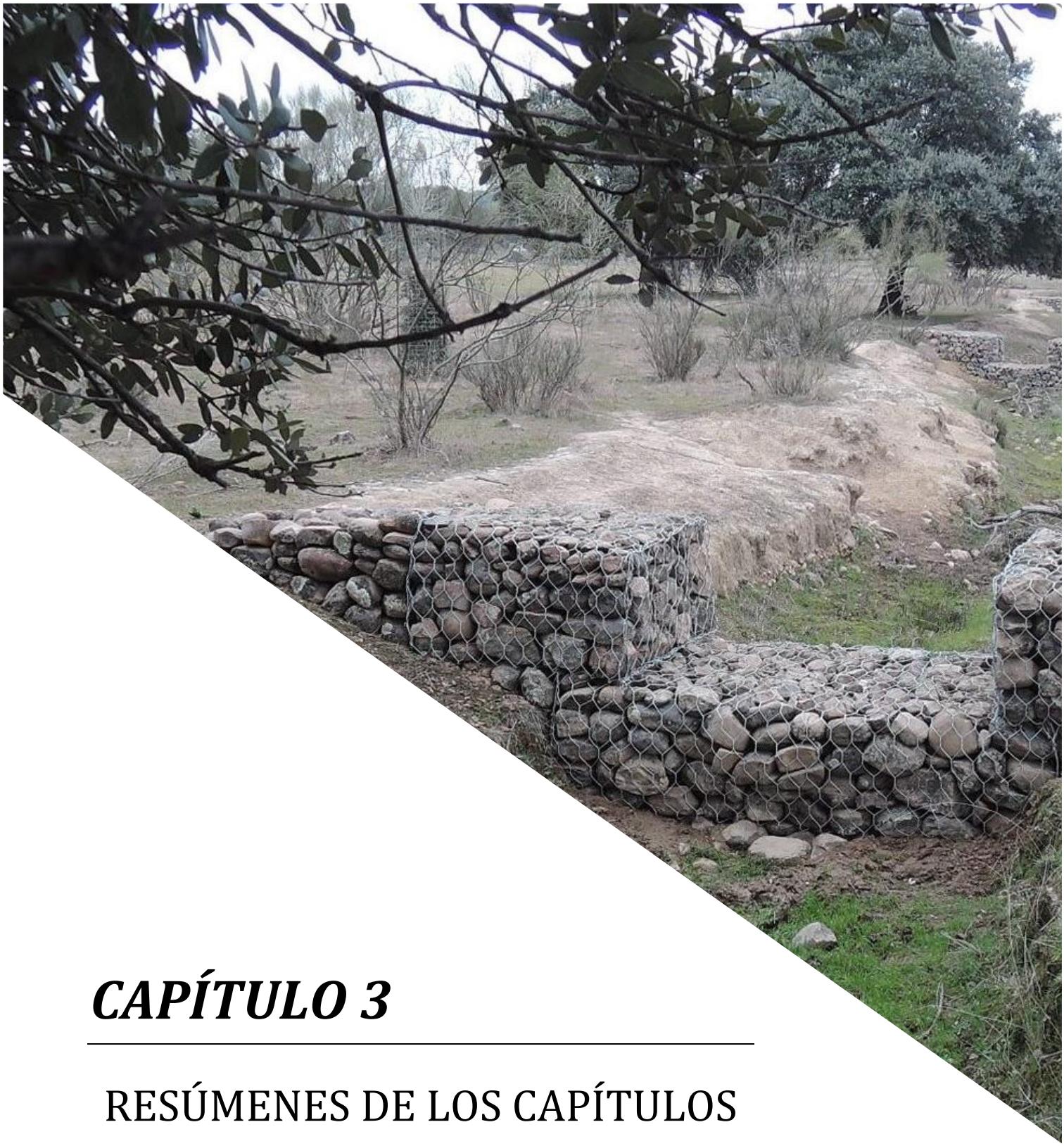

CAPÍTULO 3

RESÚMENES DE LOS CAPÍTULOS 4, 5 Y 6

CAPÍTULO 3. RESÚMENES DE LOS CAPÍTULOS 4, 5 Y 6

3.1. Resumen del capítulo 4: Pequeño sistema aéreo no tripulado, fotogrametría SFM-MVS y un método de algoritmo topográfico para cuantificar el volumen de sedimentos retenidos en los diques

Alfonso-Torreño, Alberto; Gómez-Gutiérrez, Álvaro; Schnabel, Susanne; Lavado Contador, J. Francisco; de Sanjosé Blasco, José Juan; Sánchez-Fernández, Manuel.

Publicado en *Science of the Total Environment* 678 (2019) 369–382

DOI: 10.1016/j.scitotenv.2019.04.332

Los sedimentos retenidos en los diques de corrección hidrológica son una fuente útil de información para comprender las tasas de erosión del suelo y los flujos de sedimentos. Doscientos sesenta y nueve diques distribuidos en un área de 239 ha en el suroeste de España acumularon sedimentos durante un periodo de 11 a 23 años. El objetivo de este trabajo es estimar el volumen de sedimentos depositados en esos diques y estudiar la variabilidad espacial de los sedimentos acumulados y sus relaciones con diferentes variables físico-ambientales. La metodología incluyó cinco pasos: (1) vuelo del área de estudio con un vehículo aéreo no tripulado de ala fija para capturar fotografías aéreas de alta resolución, (2) Fotogrametría *Structure–from–Motion* (SfM), (3) procesamiento de las nubes de puntos obtenidas y los modelos digitales de elevación (MDE) para crear la topografía actual y modelar la superficie del suelo pasada, (4) estimación del volumen de sedimentos detrás de cada dique utilizando una técnica topográfica y (5) análisis de la relación entre los sedimentos y las diferentes variables físico-ambientales. Se identificaron un total de 269 diques, de los cuales 160 fueron adecuados para cuantificar el volumen de sedimentos depositados. El volumen de sedimentos atrapados por dique de manera individual osciló entre 0 y 108,35 m^3, con una tasa de deposición media de 0,141 m^3 ha^{-1} a^{-1}. El 77% de los diques retuvieron menos de 1 m^3 de sedimento. La posición topográfica y la longitud del muro del dique jugaron un papel fundamental para explicar las diferencias en la acumulación total de sedimentos, así como en las tasas de deposición. La tasa de deposición se correlacionó negativamente con el área de drenaje, el índice de conectividad, el índice de potencia del flujo superficial, el índice de humedad topográfica, la longitud del canal aguas arriba y el número de diques aguas arriba. Por el contrario, la tasa de deposición se correlacionó positivamente con la pendiente del canal. Los diques ubicados en fondos de los valle con muros más largos retuvieron más sedimentos, mientras que los ubicados en vertientes con muros más cortos resultaron ineficaces.

3.2. Resumen del capítulo 5: Dinámica de la erosión y deposición en una cárcava parcialmente restaurada

Alfonso-Torreño, Alberto; Gómez-Gutiérrez, Álvaro; Schnabel, Susanne.

Publicado en *Land* (2021) 10, 62

DOI: 10.3390/land10010062

Las cárcavas son fuentes y reservorios de sedimentos y funcionan como transferencias eficientes de escorrentías y sedimentos. En los últimos años, surgieron varias técnicas y tecnologías para facilitar el seguimiento de la dinámica de las cárcavas con resoluciones espaciales y temporales sin precedentes. Aquí presentamos un estudio detallado de una cárcava de fondo de valle en un pastizal mediterráneo con una cubierta vegetal similar a una sabana que fue parcialmente restaurada en 2017. Las actividades de restauración incluyeron diques (vertederos de gaviones y fajinas) y aislamiento del ganado mediante vallas. Los objetivos específicos de este trabajo fueron: (1) analizar la efectividad de las actividades de restauración, (2) estudiar la dinámica de erosión y deposición antes y después de las actividades de restauración utilizando modelos digitales de elevación (MDE), (3) examinar el papel de la geomorfometría en los cambios topográficos observados, y (4) comparar la dinámica actual y reciente del canal con estudios previos realizados en la misma área de estudio a través de diferentes métodos y escalas espacio-temporales, cuantificando los cambios a medio plazo. Los cambios topográficos se estimaron utilizando MDE multi–temporales de alta resolución producidos mediante fotogrametría *Structure–from–Motion* (SfM) e imágenes aéreas adquiridas por un vehículo aéreo no tripulado (UAV) de ala fija. El desempeño de las actividades de restauración fue satisfactorio para controlar la erosión de la cárcava. Los diques fueron efectivos favoreciendo la deposición de sedimentos y reduciendo la erosión de los márgenes laterales de la cárcava. La exclusión de ganado promovió la estabilización de las cabeceras laterales. Las medidas de restauración implementadas aumentaron notablemente la deposición de sedimentos.

3.3. Resumen del capítulo 6: Efectos de la rehabilitación en cárcava en la producción de escorrentía y sedimentos

Alfonso-Torreño, Alberto; Schnabel, Susanne; Gómez-Gutiérrez, Álvaro; Crema, Stefano; Cavalli, Marco.

Enviado a *Catena* (2021)

La rehabilitación de cárcavas se aplica a menudo como parte de la gestión de cuencas con el objetivo de reducir la producción de sedimentos aguas abajo. Sin embargo, rara vez se estudiaron las influencias de las medidas de restauración en los procesos de escorrentía y transporte de sedimentos en los sistemas agroforestales. En este trabajo se realizó un análisis exhaustivo de estos procesos. La evolución de una cárcava se determinó antes y después de diferentes actividades de restauración que incluyeron: gaviones, fajinas y medidas de aislamiento. Los objetivos de este trabajo son (1) analizar el efecto de las medidas de restauración sobre los cambios topográficos en el cauce, la dinámica hidrológica y la producción de sedimentos en suspensión, y (2) evaluar el efecto de las actividades de restauración en los patrones espaciales de conectividad de sedimentos en las escalas de cuenca y canal. Los cambios en la topografía y la conectividad se estimaron utilizando modelos digitales de elevaciones (MDE) secuenciales de alta resolución generados por *Structure–from–Motion* (SfM) a partir de imágenes aéreas adquiridas por un vehículo aéreo no tripulado (UAV). Se monitorearon el caudal y los sedimentos en suspensión en la salida de la cuenca. Los resultados mostraron que la carga total de sedimentos suspendidos fue sustancialmente menor después de la construcción de los diques, mientras que la escorrentía no se redujo. Sin embargo, estos tratamientos tuvieron un efecto menor sobre el limo y las arcillas. El sedimento depositado detrás de las presas de contención contenía fracciones menos finas que otras ubicaciones en la cuenca y el mayor contenido de elementos gruesos. La integración del índice de diferencia de conectividad (DoIC) con las diferencias de los modelos digitales de elevaciones (DoD) destacó el impacto de las medidas de restauración en los cambios en la conectividad de los sedimentos. Se observó una estrecha relación entre la dinámica de la cárcava y la conectividad funcional. El índice de conectividad (IC) aumentó en las áreas erosionadas, mientras que las zonas de deposición mostraron una disminución del IC. La conectividad también disminuyó en las cabeceras laterales ubicadas dentro del área aislada. La implementación de las medidas de restauración en el canal fue exitosa y tuvo efectos beneficiosos a corto plazo, pero los efectos de los diques aún se desconocen a largo plazo.

CAPÍTULO 4

sUAS, SFM-MVS PHOTOGRAMMETRY AND A TOPOGRAPHIC ALGORITHM METHOD TO QUANTIFY VOLUME OF SEDIMENTS RETAINED IN CHECK-DAMS

CAPÍTULO 4. sUAS, SFM-MVS PHOTOGRAMMETRY AND A TOPOGRAPHIC ALGORITHM METHOD TO QUANTIFY VOLUME OF SEDIMENTS RETAINED IN CHECK-DAMS

Alfonso-Torreño, A., Gómez-Gutiérrez, Á., Schnabel, S., Lavado Contador, J.F., de Sanjosé Blasco, J.J., Sánchez Fernández, M., 2019. sUAS, SfM-MVS photogrammetry and a topographic algorithm method to quantify the volume of sediments retained in check-dams. Science of The Total Environment, 678, 369-382.

Abstract

Sediments retained in hydrological correction check dams are a useful source of information to understand soil erosion rates and sediment fluxes. Two hundred sixty nine check dams distributed in an area of 239 ha in SW Spain accumulated sediments over a period of 11 to 23 years. The aim of this work is to estimate the volume of sediments deposited in those check dams and to study the spatial variability of the accumulated sediments and its relationships with different environmental variables. The methodology included five steps: (1) flying the study area with a fixed-wing Unmanned Aerial Vehicle to capture high-resolution aerial photographs, (2) Structure-from-Motion photogrammetry, (3) processing the obtained point clouds and Digital Elevation Models (DEMs) to create the current topography and model the past soil surface, (4) estimating the volume of sediments behind each check dam using a topographic technique and (5) exploring the relationship between sediments and different environmental variables. A total of 269 check dams were identified, from which 160 were suitable to quantify the deposited sediment volume. The volume of sediments trapped by individual check-dams ranged from 0 to 108.35 m^3, with an average deposition rate of 0.141 $m^3\ ha^{-1}\ y^{-1}$. The 77% of the check dams retained <1 m^3 of sediment. The topographic position and the size of the dam wall played a fundamental role in explaining the differences of total sediment accumulation as well as the deposition rates. Deposition rate was negatively correlated with drainage area, connectivity index, stream power index, topographic wetness index, upstream channel length and the number of upstream check dams. Conversely, deposition rate was positively correlated with the slope of the channel. Those dams located in valley bottoms with longer walls retained more sediment, while those of hillslopes with shorter check dam walls were ineffective.

Keywords: Check dam, Structure from Motion photogrammetry (SfM), small Unmanned Aerial System (sUAS), Digital Elevation Model, Sediment volume.

4.1. Introduction

Soil erosion has been recognized as the main cause of land degradation throughout the world (Valentin et al., 2005). In Mediterranean environments, water erosion represents a serious problem with negative consequences in soil resources (Riesco García, 2015). In the Iberian Peninsula, an agro-silvo-pastoral land use system, locally called dehesa in Spain, covers >3 million hectares. It is characterized by the presence of cleared oak woodlands and annual grassland understory and is grazed by different domestic animal species (Eichhorn et al., 2006). Deforestation, overgrazing and land use changes are the factors that encourage erosion, threatening the sustainability of this land use system (Herguido Sevillano et al., 2017; Pulido et al., 2018). The two main erosive processes in this landscape are sheetwash in hillslopes (Rubio-Delgado et al., 2017; Schnabel et al., 2010), and gully erosion due to concentrated flow in valley bottoms (Gómez-Gutiérrez et al., 2012; Schnabel et al., 2013).

Despite suffering land degradation, in many cases, there are no studies about soil conservation and restoration strategies in dehesas. Many types of restoration strategies and control measures for catchments and channels have been developed for different landscapes. The measures applied in gullied channels include: check dams (concrete wall, masonry wall, fascines i.e., wooden poles and planks), rockfills and breakwaters. The establishment of check dams along channels is one of the most widespread methods to trap sediments and mitigate soil erosion effects. Check dams are often used in Mediterranean areas (Bombino et al., 2009; Castillo et al., 2007; Cucchiaro et al., 2019; Quiñonero-Rubio et al., 2016). They control sediment transport (Catella et al., 2005); stabilize slopes and torrential channels (Conesa García, 2004; Conesa García and García Lorenzo, 2007; Romero-Díaz, 2008); recharge aquifers (Conesa García, 2004; Conesa García and García Lorenzo, 2007); retain and decrease the contribution of solid material (Belmonte et al., 2005; Conesa García, 2004; Conesa García and García Lorenzo, 2007; Martin-Rosales et al., 2003); decrease water speed, consequently reducing its erosive capacity and delaying the silting up of reservoirs and lengthen their useful life (Belmonte et al., 2005; Romero-Díaz, 2008). However, some authors consider that check dams are not always effective because they alter the sedimentary dynamics and channel bed stability (Boix-Fayos et al., 2008; Wohl, 2006).

Sediments trapped behind check dams may be used to estimate sediment yields produced by upstream catchments (Baade et al., 2012; Bellin et al., 2011; Verstraeten

and Poesen, 2002; White et al., 1997) and to evaluate the effectiveness of sediment trapping of check dams (Abedini et al., 2012; Sougnez et al., 2011; Wang et al., 2011).

Geometric methods equate the sediment deposit to a geometric shape, such as a prism (Castillo et al., 2007), pyramid (Romero-Diaz et al., 2007a) or trapezoid (Bellin et al., 2011), estimating the volume on the basis of theoretical equations. Topographic methods obtain the volume of sediment accumulated from the estimation of two surfaces, the present soil/channel surface, based on direct measurements of the sediment deposit and its adjacent area, and the soil/channel surface prior to check dam construction. The latter is commonly obtained by extrapolation using the slope of the margins and of zones of the channel not affected by check dam-related deposition because the antecedent topographic surface is not always available. The topographic method was used by Díaz et al. (2014) applying sections and by Sougnez et al. (2011) using Digital Elevation Models (DEMs).

Topographical methods usually require intensive fieldwork and are more accurate in estimating the sediment volume retained behind check dams (Ramos-Diez et al., 2017b). The recent development of small Unmanned Aerial System (sUAS) platforms facilitates the acquisition of high resolution aerial photos from which Structure-from-Motion (SfM) (Ullman, 1979) photogrammetry together with MultiView-Stereo (MVS) algorithms can be applied to obtain point clouds, DEMs and orthophotographs (Javernick et al., 2014; Smith and Vericat, 2015; Woodget et al., 2015). The concurrent use of sUAS platforms and SfM-MVS photogrammetry produces high-resolution and accurate DEMs over relatively large areas.

There is a growing interest in the knowledge and patterns of water, sediment and organic matter fluxes from catchments to major river systems (Baartman et al., 2013). Connectivity can be defined as the probability that a part of a catchment transfers its "sediment contribution" to another part, and is an important environmental parameter determining the magnitude and frequency of sediment transfer. Thus, the easier a particle can move from a specific source to a specific sink, the greater the connectivity will be between those spots (Harvey, 2002; Hooke, 2003). Channels and particularly gullies are effective links to transfer runoff and sediments from the upper parts of a catchment to its outlet so they clearly favor sediment connectivity (Poesen et al., 2003); while soils with a high infiltration capacity, areas with dense vegetation, and cultivated lands, burrowing animals and the construction of dams are factors decreasing connectivity (Keesstra et al., 2018).

The connectivity index (CI) is used to model the transport routes of channelized sediments and has been applied in different fields and watersheds around the world, such as the studies by Heckmann and Schwanghart (2013) in Austria, D'Haen et al. (2013) in Turkey, Vigiak et al. (2012) in Australia and Chartin et al. (2013) in Japan. In Spain, several studies analyzed its ability to map runoff and sediment connectivity (Foerster et al., 2014; López-Vicente et al., 2013).

In the present work, we propose a methodology to estimate the sediment deposited in check dams distributed over large areas using the sUAS+SfM workflow. To our knowledge, this is the first time that this topographic method is used for this purpose. In addition, the large amount of check dams built in the study area provides a valuable data-base for understanding sediment flows on a medium-term temporal scale. The efficiency of these check dams is evaluated in terms of sediment trapped. Finally, we explore the spatial variability of the accumulated sediments and its relationship with different physical-environmental variables, including the CI based on that proposed by Borselli et al. (2008) and modified by Cavalli et al. (2013). The understanding of these relationships may be crucial to guide future restoration activities.

4.2. Study area

The study was carried out in six catchments (239 ha), located in a communal farm (39°37′ N, 6°12′ W) in the SW of the Iberian Peninsula (Figure 12). The catchments are part of an extensive erosion surface of undulating topography characterized by Ediacaran slates and greywackes. The higher parts of the catchments present an undulated topography with slope gradients increasing to the South, approaching a major river channel. The average altitude is 327 m a.s.l., and the mean slope gradient is 17.8%. The study area is composed of low order catchments with the drainage network flowing to the south where they join the Almonte River, a tributary of the Tagus River (Figure 12c). Principal channels drive ephemeral flows and some tributaries are discontinuous channels. Most of the soils are shallow and developed on slates, dominating *Cambisols* and *Leptosols* in the area (Schnabel et al., 2013). Climate is Mediterranean, with an average annual temperature of 16 °C and an average annual rainfall of 514 mm with high seasonality. The area is representative of the dehesa land use system. The vegetation cover is composed of a disperse layer of Mediterranean oak (Quercus ilex) and herbaceous plants in the understory. The tree density is about 26

trees ha^{-1}, canopy cover <18%. Pastoralist livestock rearing is the main land use in the study area, with goats, cattle, pigs and horses, resulting in a total of 234 LU (livestock unit), equivalent to 0.97 LU ha^{-1}. The farm has not been cultivated since 1953. Other activities in the area are hunting, beekeeping and recreational use. A total of 269 check dams were established in the area over a period of 11 to 23 years to trap sediments and prevent erosion. This intervention represents a valuable source of information for soil erosion studies in Mediterranean landscapes, where data on medium-term soil erosion rates are scarce (Rubio-Delgado et al., 2018).

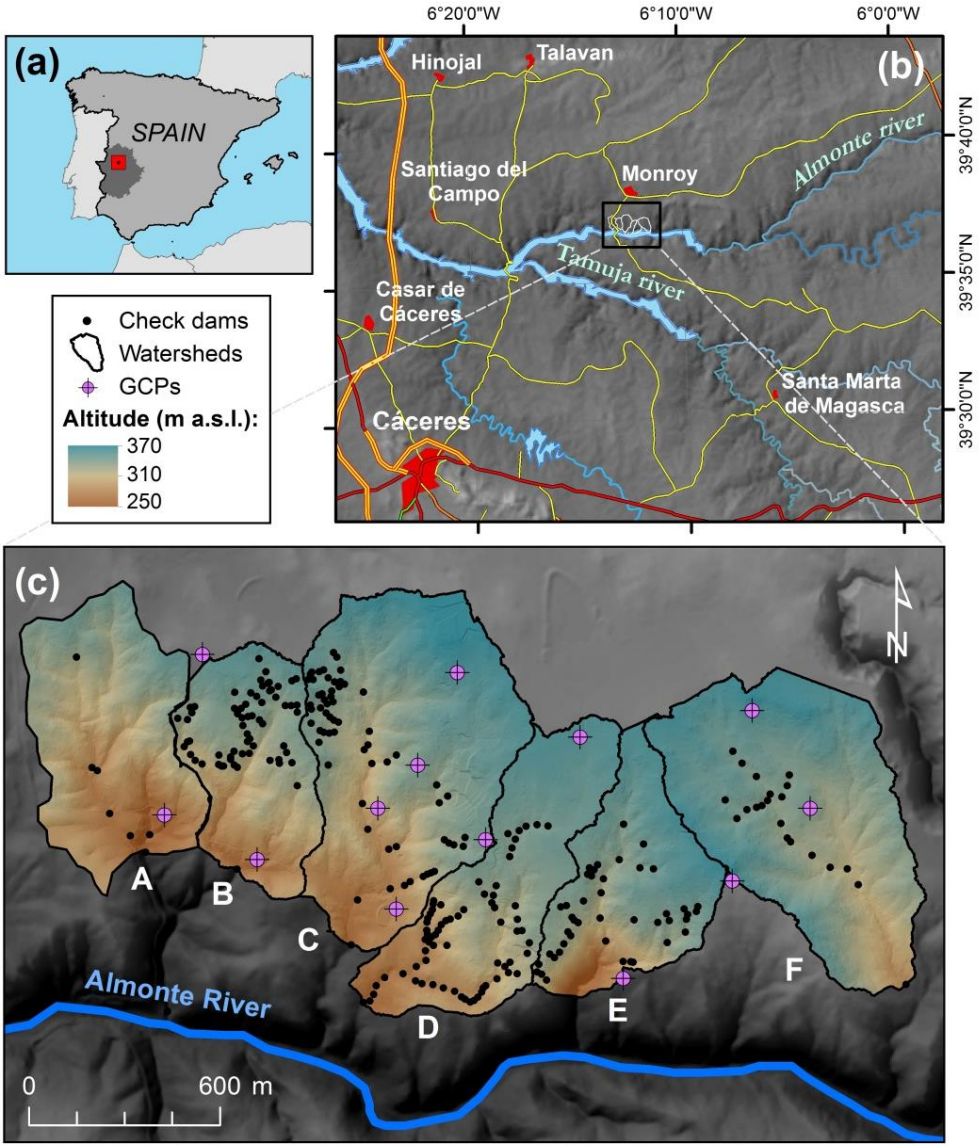

Figure 12. (a) Location of the study area in the Iberian Peninsula, (b) regional setting of the study area and (c) study area including the location of the six catchments (from A to F) and the check-dams. Pink points represent the location of the GCPs. (For interpretation of the references to color in this figure legend, the reader is referred to the web version of this article.)

4.3. Material and methods

4.3.1. Field survey and photogrammetry

The SfM-MVS workflow was fed using aerial photographs acquired by a fixed-wing sUAS (Ebee by Sensefly) carrying on board a Sony WX220 sensor (18 Mpx). Four flights were necessary to cover the study area at an approximate altitude of 60 m and a total of 1257 images were captured. Thirteen GCPs were registered with a Leica GPS 1200 system (with RTK and Post-Processed solutions using GPS + GLONNASS satellites) (Figure 12c) and employed later to scale and georeferenced the resulting 3D model. Pix4D mapperPro software (v. 3.1.18) was used for this purpose and software settings were set to get the maximum point cloud density, resolution and accuracy. The resulting cartographic products included point clouds, DEMs and orthophotographs.

4.3.2. Sediment volume estimation

Two DEMs are necessary to estimate the volume of deposited sediments. The first one represents the current topography and is the SfM-MVS-derived DEM. The second one corresponds to the initial topography, i.e., the surface just before check dam construction and was obtained by the following steps: (1) digitizing the extent of sediment deposit in each check dam (with a nadir viewpoint and using a digital slope model and a hillshade model to support this procedure (Figure 13), (2) clipping points in the cloud within the polygon and (3) interpolating the antecedent surface using the surrounding points and the ANUDEM algorithm (Hutchinson, 1988) in ArcMap Geographical Information System (GIS): *topo to raster* tool. This strategy takes into account the changes in slope between the sedimentary wedge and the inclined slopes, i.e., slope of the hillslope and the slope of the channel.

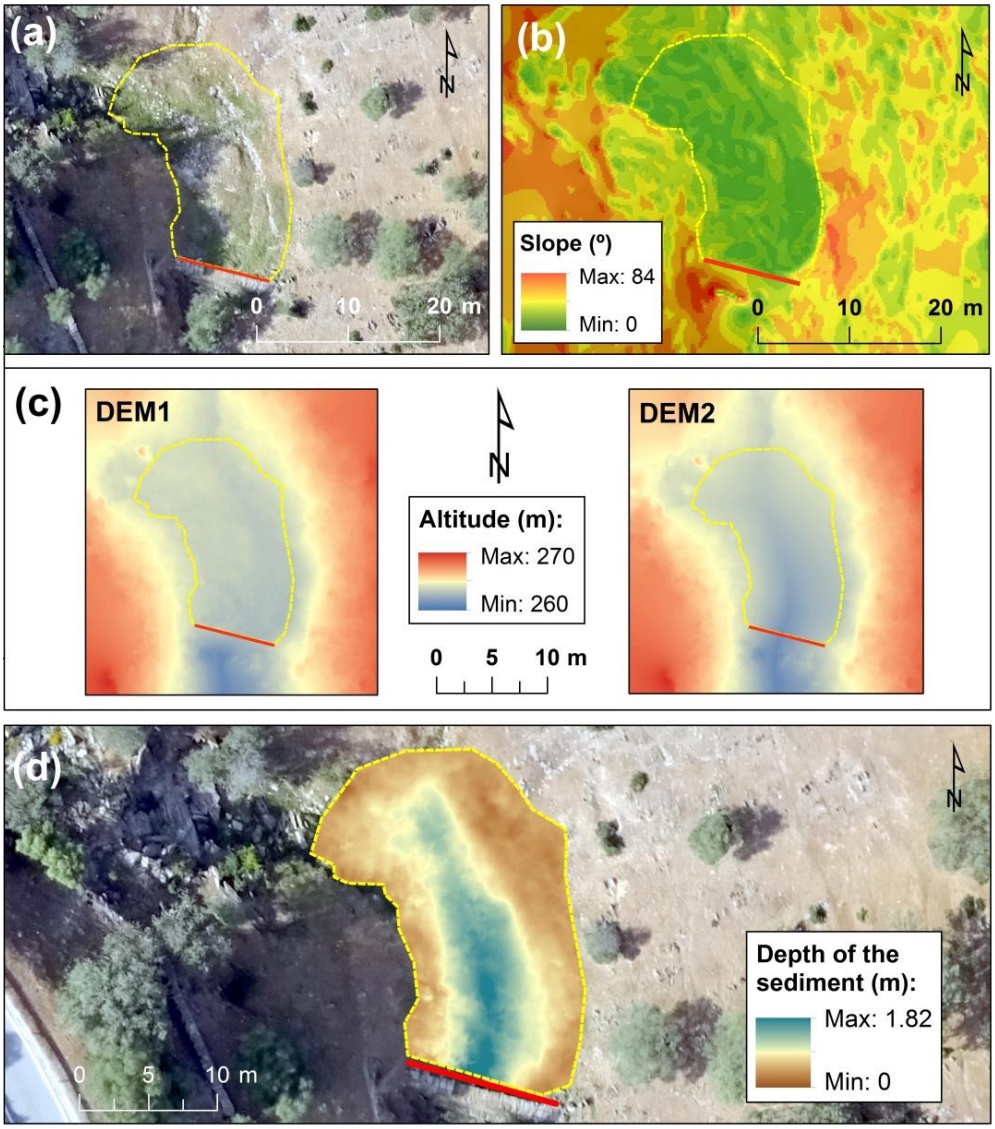

Figure 13. Example of sediment depth estimation: planimetric delineation of the deposit using the (a) orthophotograph and (b) the slope gradient digital model, (c) DEMs used as input for the DoD approach and (d) the result.

A *DEMs of Difference* (DoD) (Wheaton et al., 2010) approach was used to subtract the current DEM from the antecedent DEM. In order to discriminate real geomorphic change, the root-mean-square error (RMSE) of the SfM-MVS workflow and the interpolation errors associated to the antecedent surface were incorporated in the DoD analysis as a minimum level of detection. Individual errors in DEMs can be propagated to the DoD (Brasington et al., 2003) with the following equation:

$$E_{DoD} = \sqrt{(E_{DEM1})^2 + (E_{DEM2})^2} \qquad (1)$$

where E_{DoD} is the error propagated into the DoD, E_{DEM1} is the interpolation error associated to the antecedent DEM (before check dam construction) and the (RMSE) of the SfM-MVS processing and the E_{DEM2} is the RMSE of the SfM-MVS-derived DEM (i.e., the current topography).

The interpolation error associated with the antecedent surface was obtained by simulating virtual check dams and their associated deposits (using dimensions of real check dams and sedimentary wedges) in places without check dams. The points in the point cloud within the polygon that simulates the check dam and the deposit were clipped. Then, we used the ANUDEM algorithm to model the surface and compared the interpolated with the actual DEM. This interpolation error is expected to be variable depending on 1) topographic position of check dams, i.e., valley bottom or hillslope and 2) check dam size. Therefore, check dams were classified in four categories: (1) those located in valley bottoms presenting >8 m in length (n = 55) and (2) <8 m in length (n = 61); (3) check dams located on hillslopes with >6 m in length (n = 23) and (4) <6 m in length (n = 21). Those length values of the check dam wall were selected because they represent the average length of the check dam's wall for each topographic position. Errors were estimated for each category and applied as minimum level of detection for each check dam types.

Additionally, the depth of the sediment deposit estimated by this method (sUAS+SfM+ANUDEM+DoD) was validated using field data. An auger was used to sample the depth of the deposit at 28 different locations within 27 check dams and observed values were tested against the estimated depths (by the DoD approach).

Deposition rates were calculated considering the dates of check dam construction which varied from 1994 to 2006. The check dams of catchment A were built in 1994, those in catchment B in 1995, in catchment C between 1995 and 1997, in catchment D in 1996, in catchment E between 1998 and 2001 and finally those in the catchment F between 2004 and 2006.

4.3.3. Physical-environmental variables and the sediment connectivity index

To explore the relationships between the sediments deposited in check dams and different physical-environmental variables a database was elaborated (Table 1).

Table 1. Physical-environmental variables used for the regression analysis. The sUAS derived orthophtograph and two DEMs were used to produce these variables. For most of the variables, the SfM-MVS derived DEM was used (DEM_02: 0.2 m pixel size) while for those like curvature, representing landforms at a coarser scale a subsampled DEM was used (DEM_5: 5 m pixel size).

Variable	Units	Definition	Source
Drainage area	Ha	Drainage area of a check dam	DEM_02
Slope catchment	%	Average slope over the catchment of each check dam	DEM_02
Slope channel	%	Average slope in the channels of each check dam	DEM_02
Number upstream check dams		Number of upstream check dams	Orthophoto
Upstream sediments accumulated	m^3	Sediments accumulated in the check dams	DEM_02
Stream power index (SPI)	index	SPI = $A_s \tan \beta$; Measure of erosive power of flowing water based on assumption that discharge (q) is proportional to specific catchment area (A_s)	DEM_02
General curvature	1/radius (m)	Curvature of the surface itself (not the curvature of a line formed by the intersection of the surface with a plane)	DEM_5
Plan curvature	1/radius (m)	Curvature of the surface perpendicular to the slope direction	DEM_5
Profile curvature	1/radius (m)	Curvature of the surface in the direction of the steepest slope	DEM_5
Topographic wetness index (TWI)	index	TWI = ln (A_s/tan β); where A_s is the specific catchment area and β is the local slope. This equation assumes steady-state condition sand describes the spatial distribution and extent of zones of saturation (i.e., variable source areas) for runoff generation as a function of upslope contributing area, soil transmissivity, and slope gradient.	DEM_5
Connectivity index	index	Equation 2; The chances that a particle has to reach the nearest sink and it depends on: distance to the sink; characteristics of the rout; water available to transport from upslope; water that is gained/lost along the downslope route (Borselli et al., 2008)	DEM_02
Check dam size	m	The size of the check dam wall	Orthophoto
Bare soil	%	Soil that does not have a superficial layer with vegetation, so it is at risk of being eroded by water	Orthophoto
Paths	km ha^{-1}	Narrow pathways formed by the transit of livestock	Orthophoto
Tree cover	%	Fraction of the catchment occupied by the vertical projection of the treetops	Orthophoto

A version of the CI proposed by Borselli et al. (2008) is used here (Cavalli et al., 2013). Basically, for each cell of the study area, the CI was calculated using Eq. (2) that integrates the upslope component D_{up} (i.e., the features of the upstream drainage area) and the downslope component D_{dn} (i.e., the features of the flow path to the outlet),

$$IC = log_{10}\left(\frac{Dup}{Ddn}\right) = log_{10}\left(\frac{\overline{WS}\sqrt{A}}{\sum_i \frac{di}{\overline{WiSi}}}\right) \quad (2)$$

where $\overline{W}$ is the average weighting factor of the upslope contributing area (dimensionless parameter) that express the impedance to runoff and sediment fluxes, using the roughness index by Cavalli and Marchi (2008), $\overline{S}$ is the average slope gradient of the upslope contributing area (m/m), A is the upslope contributing area (m^2) computed with the D-infinity algorithm (Tarboton, 1997), d_i is the length of the flow path (m) along the *ith* cell according to the steepest downslope direction, and W_i and S_i are the weighting factor and the slope gradient of the *ith* cell.

CI values, defined over a range of [-∞, +∞], may vary from one study to another depending on different factors such as catchment area, DEM resolution, or weighting factor used. In order to estimate the connectivity of each check dam, the immediately downstream pixel of each dam has been selected to avoid any alteration suffered by the construction of the check dams.

4.3.4. Statistical analysis

A visual analysis of the relationships between variables was carried out using scatter plots. In the case of non-linearity, or when the variables were strongly biased, logarithmic transformations were applied to compress the range of variability of that variable. We explored the relationships between the physical-environmental variables (fifteen in total, Table 1) and the independent variable (sediment volume or deposition rates) to calculate the Pearson correlation coefficients.

Due to the correlations and interactions between the physical-environmental variables, correlation coefficients may reveal only a part of the relationship between the volume of sediments retained in the check dams and the physical-environmental variables.

4.4. Results

4.4.1. Photogrammetric results

A point cloud with an average volumetric density of 39.22 points m^{-3} was obtained (a total of 171,757,830 points), from which a DEM and an orthophotograph

with a Ground Sampling Distance (GSD) of 0.04 m were elaborated. The RMSE was 0.7 cm showing centimeter-level accuracies in the resulting cartographic products. Figure 14 shows details of the orthophotograph, the point cloud and the DEM obtained.

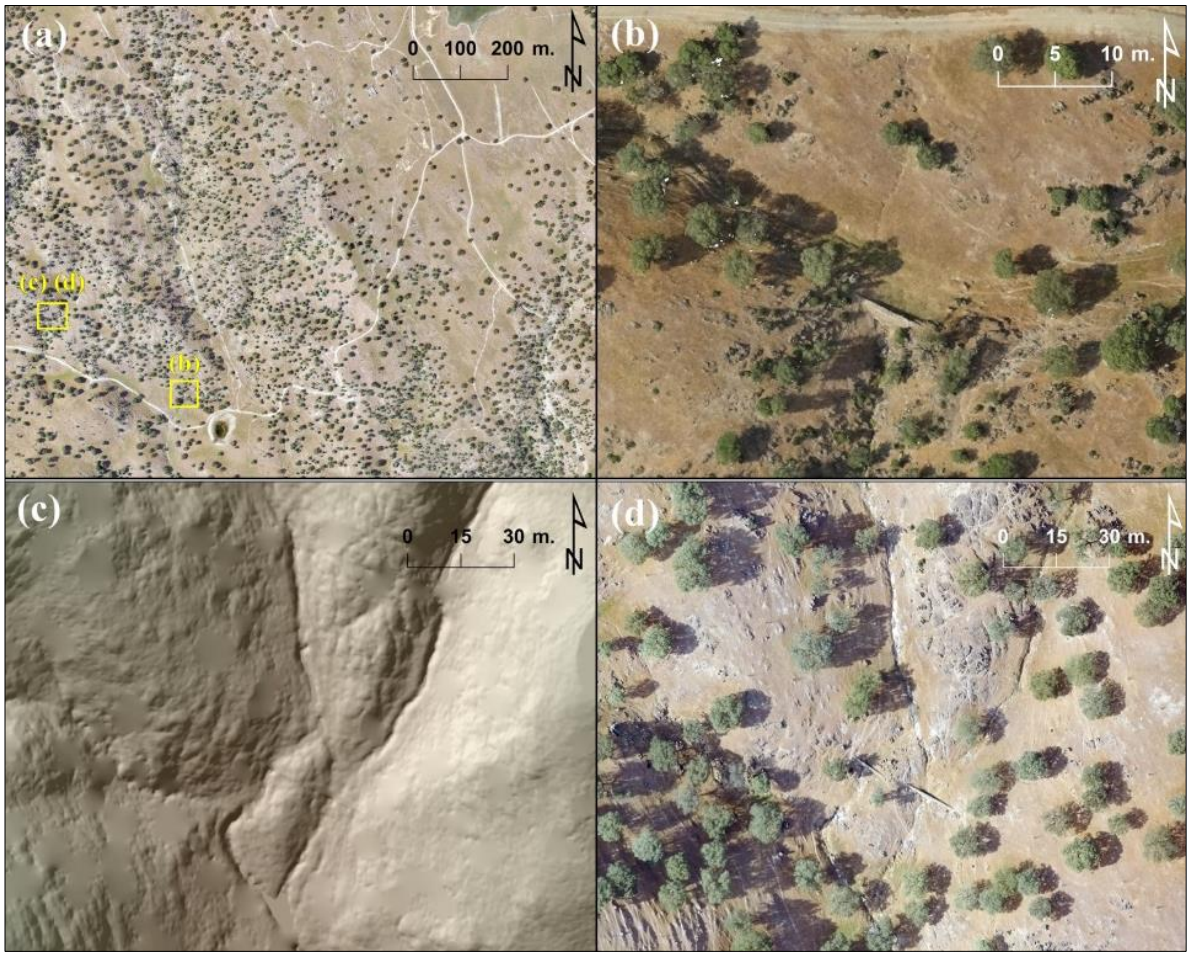

Figure 14. Detail of the cartographic products obtained: (a) tile of the orthophotograph showing the location of (b) and (c, d), (b) three-dimensional view of the resulting point cloud, (c) hillshaded DEM and (d) orthophotograph for the same area displayed in (c) showing several valley bottom check dams.

4.4.2. Sediment volume retained in the check dams

Figure 15a presents the relationship between the estimated sediment depth and the sediment depth measured in the field, indicating a performance of the proposed methodology, with a RMSE of ±3.1 cm.

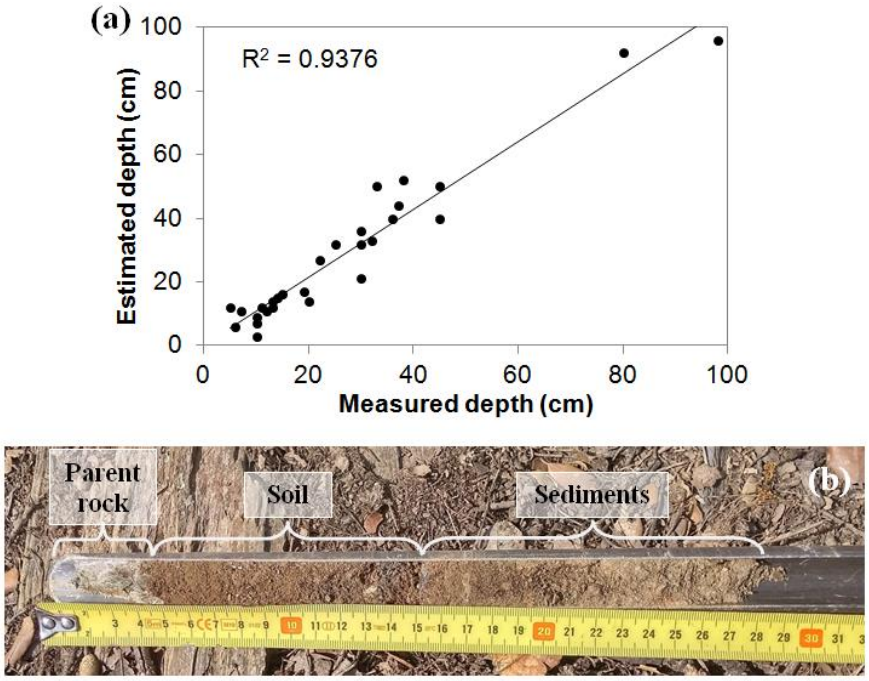

Figure 15. (a) Relationship between the estimated sediment depth and the sediment depth measured in the field and (b) example of a sediment core illustrating the original soil and the sediment deposited.

Two hundred sixty nine check dams were identified and digitized, from which only 160 were suitable for quantifying the deposited sediment volume (i.e., without dense vegetation cover). The total volume of sediments deposited was 424.15 m^3 with an average of 2.65 m^3 in each check dam, ranging from 0 to 108.35 m3. A total of 123 check dams (77%) retained <1 m^3 of sediments, from which 101 retained <0.5 m^3 (Figure 16). On the other hand, a few number of check dams (37) accumulated 23% of the total deposited material.

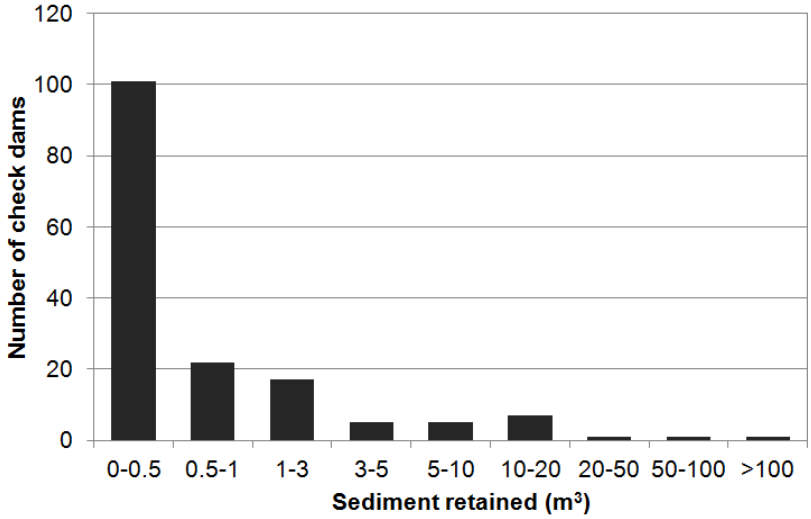

Figure 16. Frequency distribution of sediment volume in check dams.

Table 2 presents descriptive statistics of the sediment volumes retained in check dams located in different catchments. Catchment A presented a higher volume of sediments deposited in the check dams. Check dams in catchment A were the first established (in 1994), however no statistical relationship was observed between the amounts of sediment trapped and the age of the check dams. The three check dams with the largest amount of retained sediments were located in catchment A (≥38.43 m^3). On the contrary, catchments B and D presented fewer check dams with larger volumes than catchments A, C, E and F. The average rate of deposition at each dam site was 0.133 $m^3\ y^{-1}$, resulting in a deposition rate of 0.141 $m^3\ ha^{-1}\ y^{-1}$. In accordance with the information provided by the local government and managers, the check dams have never been emptied.

Table 2. Sediment volume retained by catchment. STD = standard deviation.

Catchment	N	Mean	Median	STD	Minimum	Maximum
		m^3	m^3	m^3	m^3	m^3
A	7	34.34	11.45	40.82	0.00	108.35
B	43	0.76	0.22	3.01	0.00	19.94
C	29	1.35	0.28	3.06	0.00	11.70
D	49	0.56	0.28	0.67	0.00	2.91
E	21	2.00	0.30	3.46	0.00	11.34
F	11	3.85	2.30	4.60	0.44	13.91
All	160	2.65	0.30	10.81	0.00	108.35

According to the location and size of the check dams (Figure 17), those located on valley bottoms accumulated 3.55 m^3 on average. However, check dams situated on hillslopes retained a small amount of sediments, being the average 0.29 m^3 (Table 3). Valley bottom check dams with larger wall (>8 m) retained more sediments than hillslope check dams, with an average of 7.16 m^3. Seven of 160 check dams presented volumes between 10 and 20 m^3, being all of them located in valley bottoms. On the contrary, check dams located on hillslopes with short walls (<6 m) retained smaller amounts of sediment than check dams with long walls, with 0.21 m^3 on average. Check dams located on hillslopes accumulated <1.10 m^3 of sediment.

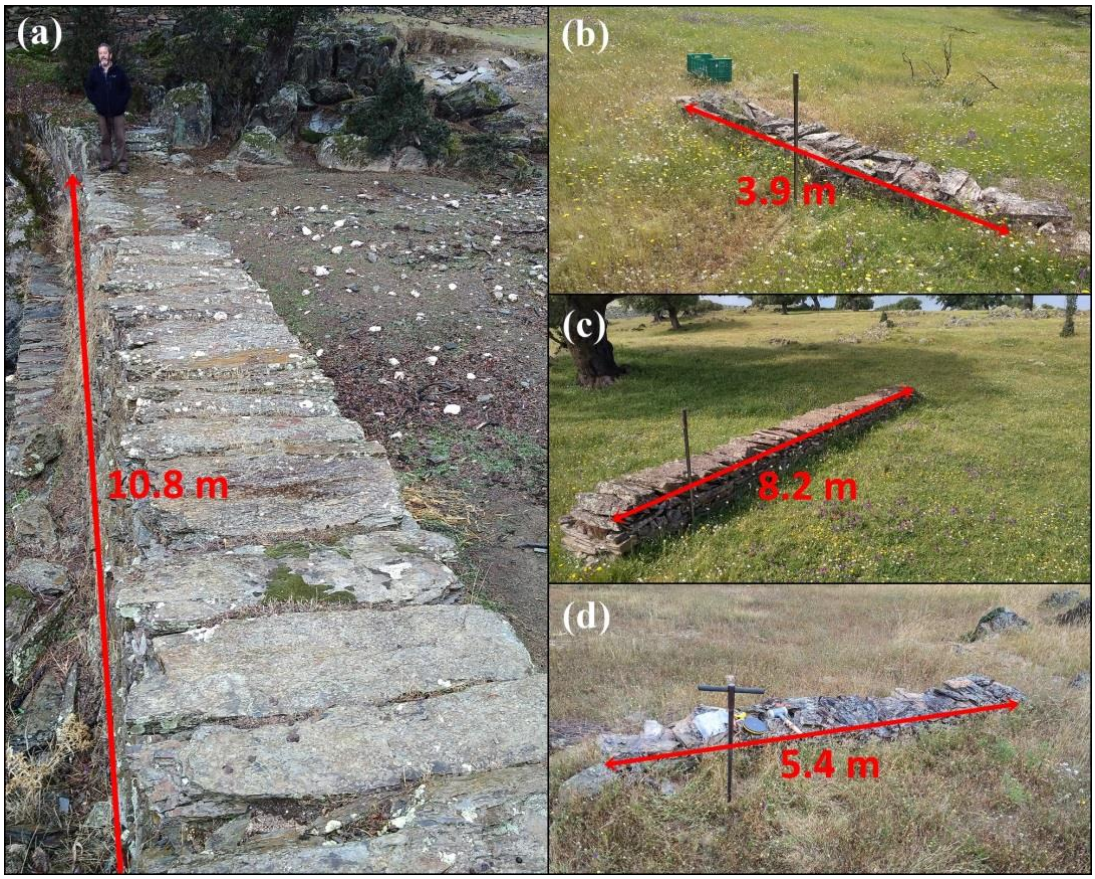

Figure 17. (a) Check dams located in valley bottoms with long wall and (b) short wall. Hillslope check dams with (c) long and (d) short walls. Note that the auger is stuck upstream.

Table 3. Volume of sediment retained in check dams with different topographic location and length of the walls. STD = standard deviation.

Topographic location and wall length	N	Mean	Median	STD	Minimum	Maximum
		m^3	m^3	m^3	m^3	m^3
Hillslope / Long	23	0.36	0.24	0.40	0.00	1.10
Hillslope / Short	21	0.21	0.10	0.30	0.00	1.04
Hillslope / All	44	0.29	0.15	0.36	0.00	1.10
Valley bottom / Long	55	7.16	1.66	17.68	0.00	108.35
Valley bottom / Short	61	0.29	0.23	0.28	0.00	1.09
Valley bottom / All	116	3.55	0.37	12.65	0.00	108.35
All	160	2.65	0.30	10.81	0.00	108.35

4.4.3. Relationships between deposition, catchment characteristics and topographical setting

The physical-environmental characteristics for the individual catchment of every check dam were estimated and grouped according to their topographic location (i.e.,

valley bottom or hillslope). This exercise revealed interesting differences for many physical-environmental variables (Table 4). The CI ($t > 10$), animal paths density, upstream channel lengths, drainage area, stream power index (SPI), curvatures, topographic wetness index (TWI) and number of check dams upstream ($4 > t < 10$) were the most outstanding. Check dam size was also significantly different for check dams settled in different topographic position. On the other hand, catchment and channel slope were not statistically different for check dams located in valley bottoms and hillslopes (t value = 0.85, 0.11, p = 0.39, 0.91, respectively).

Deposition rates observed in valley bottoms were lower than those found at hillslopes and statistically different. The average volume of sediments retained per check dam was 3.55 m^3 (n = 116) in valley bottoms and 0.29 m^3 (n = 44) in hillslopes. The average deposition rate for the whole dataset was 0.14 m^3 ha^{-1} y^{-1}, with 0.07 m^3 ha^{-1} y^{-1} (n = 116) in valley bottoms and 0.32 m^3 ha^{-1} y^{-1} (n = 44) in hillslopes.

Table 4. Mean and standard deviation of sediment volume, deposition, deposition rate and physical-environmental characteristics of the catchments according to check dams location (STD = standard deviation, n = 116 in valley bottom, n = 44 in hillslope). Significant differences of the variables according to check dams' topographic position are shown.

Variable	Valley bottom	Hillslope	Valley bottom	Hillslope	t-value	p
	Mean	Mean	STD	STD		
Sediment volume (m^3)	*3.55	*0.29	12.59	0.36	1.71	0.09
Deposition (m^3 ha^{-1})	**1.25	**7.53	3.50	10.14	-5.77	0.00
Deposition rate (m^3 ha^{-1} y^{-1})	**0.07	**0.32	0.21	0.45	-4.71	0.00
Drainage area (ha)	**8.64	**0.20	11.88	0.43	4.70	0.00
Slope catchment (%)	17.10	16.25	5.57	5.66	0.85	0.39
Slope channel (%)	15.56	15.45	5.84	4.60	0.11	0.91
Number upstream check dams	**10.92	**0.30	16.87	0.73	4.17	0.00
Upstream sediments accumulated (m^3)	**5.53	**0.17	13.95	0.42	2.54	0.01
Upstream channel lengths (km)	**16.01	**0.38	21.89	0.89	4.72	0.00
Stream power index	**132.78	**2.58	193.37	4.87	4.46	0.00
General curvature	**-2.88	**-0.89	1.61	1.13	-7.51	0.00
Plan curvature	**-1.98	**-0.86	1.53	0.84	-4.58	0.00
Profile curvature	**0.95	**0.03	1.26	0.52	4.69	0.00
Topographic wetness index	**11.17	**7.17	4.55	3.99	5.11	0.00
Connectivity index	**-5.47	**-6.73	0.73	0.44	10.68	0.00
Check dam size (m)	**9.04	**6.63	4.54	2.70	3.29	0.00
Bare soil (%)	**14.73	**11.13	8.33	12.32	2.12	0.04
Paths (km ha^{-1})	**0.25	**0.11	0.14	0.19	5.22	0.00
Tree cover (%)	**13.25	**10.99	4.18	7.95	2.33	0.02

The regression analysis showed that the sediment volume retained in the check dams was positively correlated with the amount of sediment accumulated upstream (R = 0.783), followed by the profile curvature (R = 0.553), the SPI (R = 0.501), the CI (R = 0.413), the drainage area (R = 0.389), the upstream channel length (R = 0.335) and check dam size (R = 0.237) (Table 5), being all of them significant at a confidence level of 95%. On the contrary, sediment volume retained in the check dams was negatively correlated with the general curvature (R = −0.504) and the plan curvature (R = −0.454). Deposition rate was negatively correlated with CI (R = −0.269), followed by drainage area (R = −0.219), upstream channel length (R = −0.219), number of upstream check dams (R = −0.213), the SPI (R = −0.198) and TWI (R = −0.187). On the other hand, the general curvature (R = 0.196), the slope of the channel (R = 0.195) and the profile curvature (R = 0.163), presented a positive correlation with deposition rate ($p < 0.05$).

According to the topographic position, the volume of sediments retained in the check dams located in valley bottoms was positively correlated with upstream sediment deposition, followed by profile curvature, SPI, CI, drainage area, upstream channel length and check dam size (Table 5).

The relationships between the physical-environmental variables for all check dams and those located in valley bottoms were similar, which is logical as they represent 73% of the total number of cases. Independent analysis of valley bottom and hillslope check dams were carried out to overcome the prevalence of valley bottom data in the whole dataset. Only the level of relationship of the CI in check dams located in valley bottoms increased with respect to all check dams. The deposition rate for valley bottom check dams was positively correlated with the slope of the channel, followed by the slope of the catchment, the check dam size, paths density and tree cover. On the contrary, the number of upstream check dams and upstream sediment accumulated presented a negative correlation with respect to deposition rate for valley bottom check dams.

In general, check dams located in hillslopes obtained worse correlations with the physical-environmental variables than those located in valley bottoms. The sediment volumes of hillslope check dams were positively correlated with dam size and negatively with catchment slope. The deposition rate of the check dams located on hillslopes was negatively correlated with CI and with tree cover, being all of them significant at a confidence level of 95%.

Table 5. Pearson correlation coefficient (r) between the sediment volumes retained in check dams, the deposition rate and different physical-environmental variables.

Variable	Sediment volume (m^3)			Deposition rate (m^3 ha^{-1} y^{-1})		
	All check dams	Valley bottom	Hillslope	All check dams	Valley bottom	Hillslope
Drainage area (ha)	*0.389	*0.368	0.153	*-0.219	-0.171	-0.266
Slope of the catchment (%)	0.124	0.140	*-0.311	0.132	*0.257	0.069
Channel slope (%)	0.106	0.120	-0.241	*0.195	*0.283	0.154
Upstream check dams (n)	0.062	0.021	-0.116	*-0.213	*-0.185	-0.128
Upstream accumulated sediments (m^3)	*0.783	*0.779	0.022	-0.097	*-0.046	-0.168
Upstream channel length (km)	*0.335	*0.309	0.164	*-0.219	-0.169	-0.202
Stream power index	*0.501	*0.488	0.060	*-0.198	-0.144	-0.300
General curvature	*-0.504	*-0.554	-0.258	*0.196	-0.053	0.162
Plan curvature	*-0.454	*-0.461	-0.271	0.100	-0.103	0.148
Profile curvature	*0.553	*0.562	0.124	*0.163	-0.041	-0.112
Topographic wetness index	0.106	0.069	-0.065	*-0.187	-0.088	-0.043
Connectivity index	*0.413	*0.459	0.074	*-0.269	-0.005	*-0.334
Check dam size (m)	*0.237	*0.223	*0.383	0.065	*0.302	-0.055
Bare soil (%)	-0.018	-0.057	0.105	0.029	0.026	0.137
Paths (km ha^{-1})	0.013	-0.054	-0.045	-0.080	*0.184	-0.090
Tree cover (%)	0.047	0.036	-0.003	-0.114	*0.247	*-0.327

* Statistically significant values ($p < 0.05$).

The regression analysis provided information about the relationship between the volume of sediments retained in check dams and the physical-environmental variables. Sediment volume was positively related with the upstream accumulated sediments (R^2 = 0.878; Figure 18a), log-transformed SPI (drainage area multiplied by slope) and CI (R^2 = 0.258; Figure 18b). Small amounts of sediment were observed in places of variable SPI and CI. Check dams trapping large amounts of sediment were found only in places with high SPI and CI (R^2 = 0.258; Figure 18b). Small amounts of sediment were estimated for check dams with low values for the variables upstream channel length and drainage area, while large sediment volumes correspond to high values of these two parameters.

Check dams located in valley bottoms with large sediment volumes were found in large drainage areas and with a high SPI. Additionally, small amounts of sediments were found both in check dams with short and long walls. However, the largest sediment volumes in the study area were always registered in check dams with long

walls (for both topographic positions: valley bottoms and hillslopes). Check dams located in hillslopes with large amounts of sediments were observed in catchments with low slope gradient, while check dams with small amounts of sediments were located in catchments with high slope gradient. A positive correlation between the sediment volume and the upstream accumulated sediments was observed, being higher in valley bottoms than in hillslopes (R^2 = 0.878; Figure 18a).

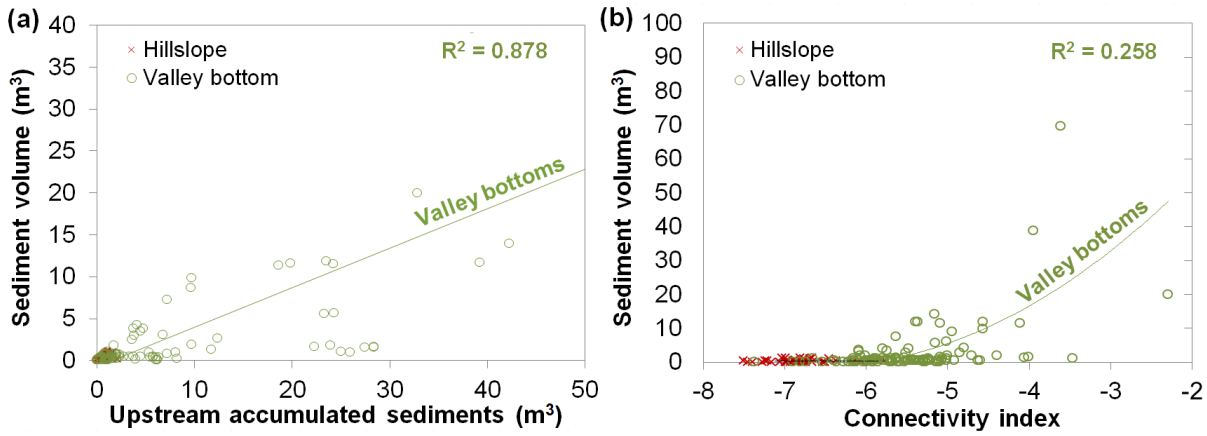

Figure 18. Relationship between the sediment volume in the check dams and a) upstream accumulated sediments and b) CI (at check dam). Equations and regression lines showed in both plots refer exclusively to valley bottom check dams.

Figure 19 presents the relationship between the deposition rate and the physical-environmental variables which are significantly correlated. Low deposition rates were observed equally in check dams with very different values of connectivity and channel slope, while high deposition rates were registered only in check dams with low CI (R^2 = 0.111; Figure 19a) and high channel slopes. Furthermore, check dams with low deposition rates were found in catchments with high SPI (R^2 = 0.274; Figure 19b) and with long upstream channels (R^2 = 0.137; Figure 19c), while check dams with high deposition rates were identified in catchments with low SPI values and short upstream channels.

According to the topographic position, low deposition rates for valley bottom check dams can be found in catchments varying with respect to size of check dam walls, channel slopes, tree cover and animal path density, while high deposition rates only found in long check dam walls, with high channel slopes and in catchments with high tree cover (R^2 = 0.061; Figure 19d) and with high path density. Check dams located in hillslopes with low deposition rates were observed in catchments with different CI and

different tree cover. However, high deposition rates can be found in catchments with low CI (R^2 = 0.111; Figure 19a) and low tree cover (R^2 = 0.107; Figure 19d).

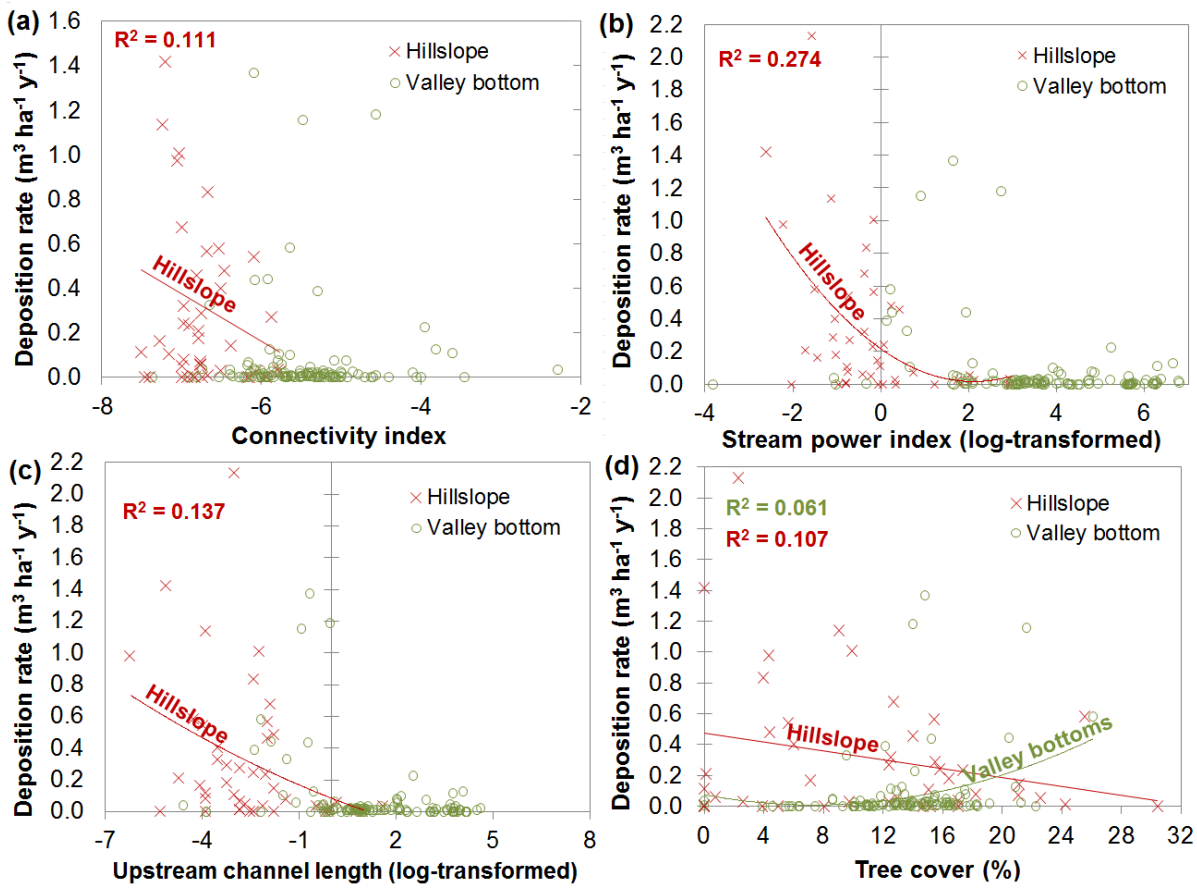

Figure 19. Relationship between the deposition rate in check dams and (a) CI (at check dam), b) stream power index (log transformed), (c) upstream channel length (log transformed) and (d) tree cover (for the catchment of every individual check dam).

4.4.4. Connectivity and sediment deposition in check dams

The CI and the volume of sediment retained by the check dams were mapped together and their spatial distribution was analyzed. Figure 20 shows that the highly connected areas were, obviously, channels and valley bottoms as they route flows and sediments to the outlet of every catchment. Poorly connected areas were observed in hillslopes with low slope gradient. Check dams with the largest amounts of sediments were always located in well-connected places while check dams found in poorly connected areas showed the smallest values. Figure 21 represents box and whisker plots of CI according to catchment and topographic position of check dams, respectively.

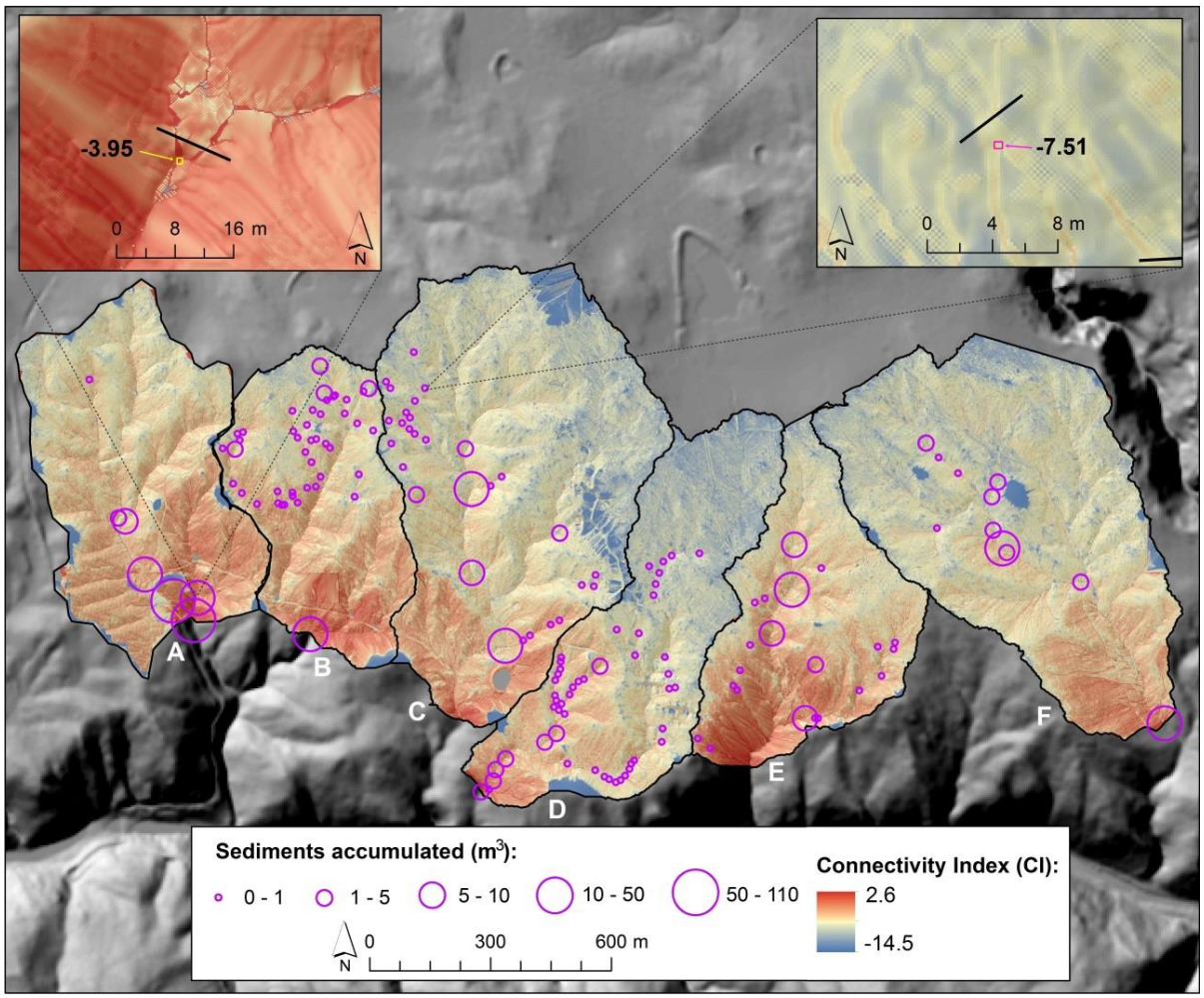

Figure 20. Location of check dams and the amount of sediments retained with CI in the background.

By catchment, A showed the highest average CI per check dam (−4.58, n = 7) and the largest sediment deposits. On the contrary, B and C presented poorly connected check dams, with average values of −6.25 (n = 43, std. dev. 0.86) and −6.30 (n=29, std. dev. 0.77), respectively. The spatial pattern of CI was corroborated by the average figures calculated for check dams located in valley bottoms and those sited in hillslopes with CI values of 5.47 and 6.73, respectively.

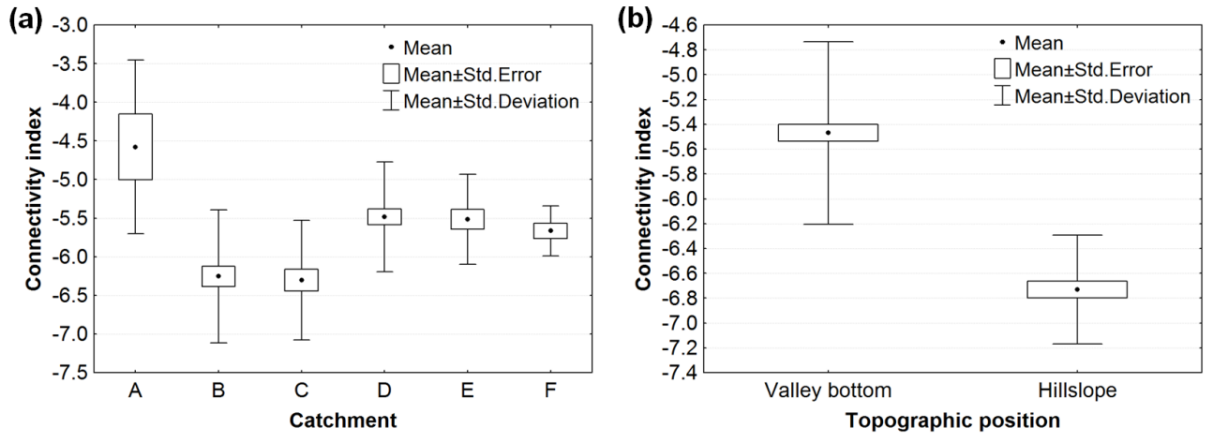

Figure 21. (a) CI values for check dams grouped by catchment and (b) CI values according to the topographic position of the check dams ($p < 0.05$).

4.5. Discussion

In this work we introduce a method to estimate the volume of sediments accumulated in check-dams based on the use of two topographic surfaces. The first one, which represents the current topography, was elaborated using SfM-MVS photogrammetric techniques and aerial photos acquired by means of a fixed-wing sUAS. The error estimated here for this technique was similar to the most accurate topographic methods proposed in the recent literature to model the topography of sediment deposits in check dams (TLS: Ramos-Diez et al., 2017b; and GNSS: Sougnez et al., 2011). With the high-resolution DEM the sedimentation area of each check dam is delimited according to the sudden changes in slope between the sedimentary wedge and the inclined slopes, and the presence or absence of bedrock on the surface (Figure 13). The second surface was obtained by interpolating the topography previous to the check dam establishment (over the extent of the sediment deposit) using the ANUDEM algorithm and the deposit surrounding points. This interpolation procedure takes into account the slope of the hillslopes, the channel and the form of the deposit and show a high performance for ridges as well as valley bottom areas (Arun, 2013). This strategy allows to adapt the analysis for asymmetric deposits (like the one showed in Figure 13) or deposits with complex morphologies. Finally, a DoD approach was carried out using both surfaces and associated errors to produce a map of sediment depth for each check dam. A RMSE of ±0.03 m was calculated for the estimation of sediment depth comparing the DoD results and sediment cores sampled at field, showing the outstanding performance of the proposed methodology in the study area.

The proposed methodology reduces field work to one day by three people (one sUAS pilot and two GNSS operators) covering an area of 239 ha and overcoming other techniques for topographic data acquisition that would use weeks to acquire similar data (172 million of XYZ points with RGB values and a volumetric point density of 39 pts · m^{-3}). The processing time of the photographs and GCPs to obtain the point cloud, the DEM and the orthophotograph was about 13 h (using an Intel Core i7 CPU at 2.50 GHz with 8GB RAM, GPU Intel HD Graphics 4600). An additional time of 50 h was used to filter, clean and edit the point cloud besides the interpolation procedure and the DoD calculation. An average processing time of 24 min per check dam was estimated (including the SfM processing and the subsequent processes of filtering, editing, interpolating and DoD). On the other hand, an important limitation of the proposed methodology is the unsuitability of SfM techniques in areas with dense vegetation cover (Gómez-Gutiérrez et al., 2014; Westoby et al., 2012). In our study, the topography of 100 check dams was not reconstructed because of the occlusion produced by vegetation. Alternatives for these places are: 1) the use of LIDAR sensors on board of medium-size Unmanned Aerial Systems (UAS) platforms, although currently they are not affordable for most researchers or 2) traditional topographic methods such as GNSS (Sougnez et al., 2011) or total stations (Ramos-Diez et al., 2017a; Wei et al., 2017).

Sougnez et al. (2011) also used the DoD approach, and developed the methodology by comparing DEMs and applying a threshold aimed at filtering noises in the DoD that cannot be reliably assumed to be "real". As observed by James et al. (2012), this filtering process can rule out small real changes that are cumulatively important.

Sediment deposition in check dams generally encompasses several discharge events. The DoD approach works with a temporary work scale whose interval is delimited by two moments, the installation of the check dam and the data capture by the sUAS. In this study the dynamic of deposition and erosion of the sediments retained in the check dams inside this time interval is unknown. A continuous and an accurate monitoring of geomorphic processes is required to analyze and understand this aspect (Comiti et al., 2014; Cucchiaro et al., 2019), which would be expensive, due to the large number of dams and access difficulties in areas with steep slopes. The presented methodology may help to easily estimate soil sediment volume deposited in check

dams over large areas and therefore assists land managers and researchers to understand sediment dynamics increasing spatial-temporal observation scales.

Two considerations should be done before discussing the relationships between the sediment deposition rate-volume of sediments and the environmental factors: 1) the prevalence of valley bottom check dams in the dataset (being 73% of the sample) and 2) the total volume of sediments quantified is influenced by the construction date of the check dams (1994–2006) and the deposition rate is considered a more suitable parameter to understand the relationships between the sedimentation process and the environmental factors in this case. To overcome the prevalence of valley bottom data, additional independent correlation analysis for valley bottom and hillslope check dams were carried out (Table 4).

Among the proposed environmental variables, CI and variables influenced by the drainage area contributed significantly to the explanation of the deposition rate (Table 5). Particularly interesting is the role of CI, with a negative relationship for the deposition rate and positive for the volume of sediments retained in check dams. As expected, check dams located in valley bottoms had better CI than those located in hillslopes. Connectivity played an important role in hillslope check dams, where high deposition rates were observed in poorly connected check dams. Drainage channels are effective links to transfer runoff and sediment from the upper parts of a catchment to their outlet (Poesen et al., 2003). Nevertheless, the construction of check dams hampers catchment connectivity factors (Keesstra et al., 2018) and disturbs sediment transfer routes (Cavalli et al., 2013).

Furthermore, a negative correlation was obtained for the relationship between deposition rate and the variables influenced by the area (drainage area of each check dam, SPI and upstream channel length) as in several other studies in Mediterranean environments (e.g., Bellin et al., 2011; Boix-Fayos et al., 2008; De Vente et al., 2007; Díaz et al., 2014; Martin-Rosales et al., 2003; Romero-Díaz et al., 2007b; Sougnez et al., 2011), suggesting that large catchments are usually associated with less sediment deposition within the catchment (Birkinshaw and Bathurst, 2006; Haregeweyn et al., 2008). The negative relationship between drainage area and sediment yield was also found by Nadal-Romero et al. (2011) in badlands with drainage area <10 ha. In catchments with drainage areas larger than 10 ha the number of sinks, where the sediments may be trapped, commonly increase. A negative correlation coefficient for SPI was obtained and supported by the influence of the drainage area on SPI equation.

The highest deposition rates were registered for small and steep catchments with short channels corroborating the results observed by Martínez Lloris et al. (2001) in a Mediterranean catchment. Despite the fact that curvature showed a week and significant relationship with deposition rate, the visual analysis of the plot did not allow a coherent interpretation of the trend. Livestock path density, tree cover and bare soil are indicators of land use pressure while land use may be assumed constant since the establishment of the check dams according to interviews with local managers and examination of historical aerial orthophotographs. There was a positive and significant correlation between the deposition rate and the density of livestock paths in the catchments of check dams located in valley bottoms, but not for those located on hillslopes. A high density of animal paths is an indicator of overgrazing and this causes an increase in the sediment production and bare soil (Prosser et al., 2001; Wasson et al., 1998). Animal paths favor sediment transfer from the hillslopes to the channels and promote the formation of bank headcuts and bank erosion (Gomez-Gutierrez et al., 2018) thus providing available sediments in the channel to be evacuated and trapped in the check dams. High-resolution DEMs and point clouds, like the ones used here (0.2 m pixel size), are suitable products to represent the effect of animal paths (i.e., lineal micro-depressions) and reveal their role increasing connectivity between hillslopes and channels.

It was not possible to confirm a direct relationship between tree density in the moment of the field survey and deposition, in spite of having a significant correlation between both variables for check dams located in valleys and on slopes. The main cause is due to the relationship between the density of trees and the slope of the channel and of the catchment. There was also a relationship between the bare ground and the slope in the study area (note this relationship is not showed in the Table 5). The effect of slope on erosion occurs through an increase in the speed of surface runoff, resulting in an increased capacity of the runoff to disaggregate and transport sediments and promoting bare soil (Bagarello and Ferro, 2010; Fox et al., 1997; Nassif and Wilson, 1975; Truman et al., 2011).

Upstream accumulated sediments, curvature and variables including drainage area (CI, SPI and upstream channel length) were the attributes that best explain the volume of sediments retained in the check dams. A positive correlation between the volume of sediments in the check dams and the upstream sediments accumulated was observed, being higher in valley bottoms than in hillslopes and denoting a relatively

homogeneous functioning of every catchment. General and plan curvature were negatively correlated to the sediment volume, denoting that the check dams located in concave areas accumulated more sediments than those located in convex surface. On the contrary, profile curvature was positively correlated with the sediment volume, revealing that the highest sediment volume was registered for check dams located in concavity (decrease in gradient downslope) encouraging more the deposition of sediments. These results justify those observed by Di Stefano et al. (2000) which determine that the local morphology also influences the deposition of sediments. Sediment volume was negatively correlated with average catchment slope for hillslope check dams indicating that upper parts of the catchments with enough slope gradient export, for a medium-term temporal scale, most of the available sediments that are finally trapped by valley bottom check dams. Higher correlation coefficients were observed for drainage area than for slope angle regarding the volume of sediments retained in check dams.

It is a certain fact that check dams trap an important amount of sediment. Nevertheless, a proportion of the sediment is not trapped by check dams, but passes through the dam as suspended sediment, particularly the fine sediment fraction. Therefore, the sediment trapping efficiency of the dams must be estimated in order to know the sediment production of a given area and for establishing sediment budgets (Mekonnen et al., 2015). The high costs of sediment check dams highlight the need to improve the definition of their location and size (Fox, 2011; Quiñonero-Rubio et al., 2016; Romero-Diaz et al., 2007a). Results obtained here show that CI may be used as surrogate to determine the effectiveness of check dams trapping sediments and the mapped CI proved to be a valuable resource to guide suitable check dam locations. Additionally, the CI is a parameter easy to calculate (only needs as input a DEM) and to interpret. Other authors suggest that check dam locations should be made also taking into account accessibility problems for dam maintenance and cost-benefit concerns (Osti and Egashira, 2008). Other environmental parameters that were related to the amount of accumulated sediments (channel slope, catchment slope, tree density and path density) may be used to support the decision of check dam location. Dehesas are fragile ecosystems from an economic and environmental viewpoint and any decision about fund investment, including restoration activities, should be made carefully and thoughtfully. Approaches like the one presented here may support the sustainability of these ecosystems.

4.6. Conclusions

The concurrent use of a fixed-wing sUAS platform and SfM-MVS photogrammetry allowed to produce an accurate high-resolution dense point cloud, a DEM and an orthophotograph. These cartographic products and several geoprocessing procedures were used to estimate the depth of sediments deposited in check dams and the total volume of accumulated material. Field survey sampling made possible to validate the proposed methodology by measurements of sediment depth at different locations. A quantitative analysis was carried out to understand the relationship between the physical and environmental features of the catchments and the sediments retained in the check dams.

There was a spatial distribution pattern in the sediments deposited, with large volumes of sediment accumulated in the lower areas of the catchment than in the upper parts. Only a few check dams efficiently retained sediments, particularly those located in valley bottoms in contrast to those in hillslopes. Moreover, CI in valley bottom check dams was greater than the one of hillslope check dams, particularly those with larger walls. The check dams with high sediment retention correspond with highly connected areas, measured by a GIS-based index. Variations of the obtained deposition rates were very high depending on check dams' topographic position and the results demonstrated relationships with several physical-environmental parameters. In general terms, the greater the drainage area, the greater SPI and the upstream channel lengths, the lower the deposition rate. CI and channel slope played a fundamental role, with low deposition rates found in sites with very different CI and with different channel slope, while high deposition rates only took place in areas with poor connectivity and with high channel slope. In relation to the topographic position of check dams, deposition rate was positively correlated with the check dam size, followed by slope (channels and catchments), tree cover and path density for in valley bottom check dams. Deposition rate was negatively correlated with CI and with tree cover in hillslope check dams.

In short, we can obtain the precise results of the sediments retained in the check dams in our proposed method, aimed at evaluating the level of intensity of land degradation in Mediterranean landscapes. There are environments, such as the dehesa, where the establishment of check dams is not commonly used to control erosion and sediment retention. Findings obtained in this work could be of interest for regional planners interested in implementing restoration measures in the future. Additionally,

the proposed methodology may assist in the strategic and effective location of check dams.

Aknowledgments

Alfonso-Torreño is a beneficiary of a PhD scholarship (PD16004) of the Regional Government of Extremadura and the study was financed by the Spanish Ministry of Economy and Competitiveness (CGL2014-54822-R).

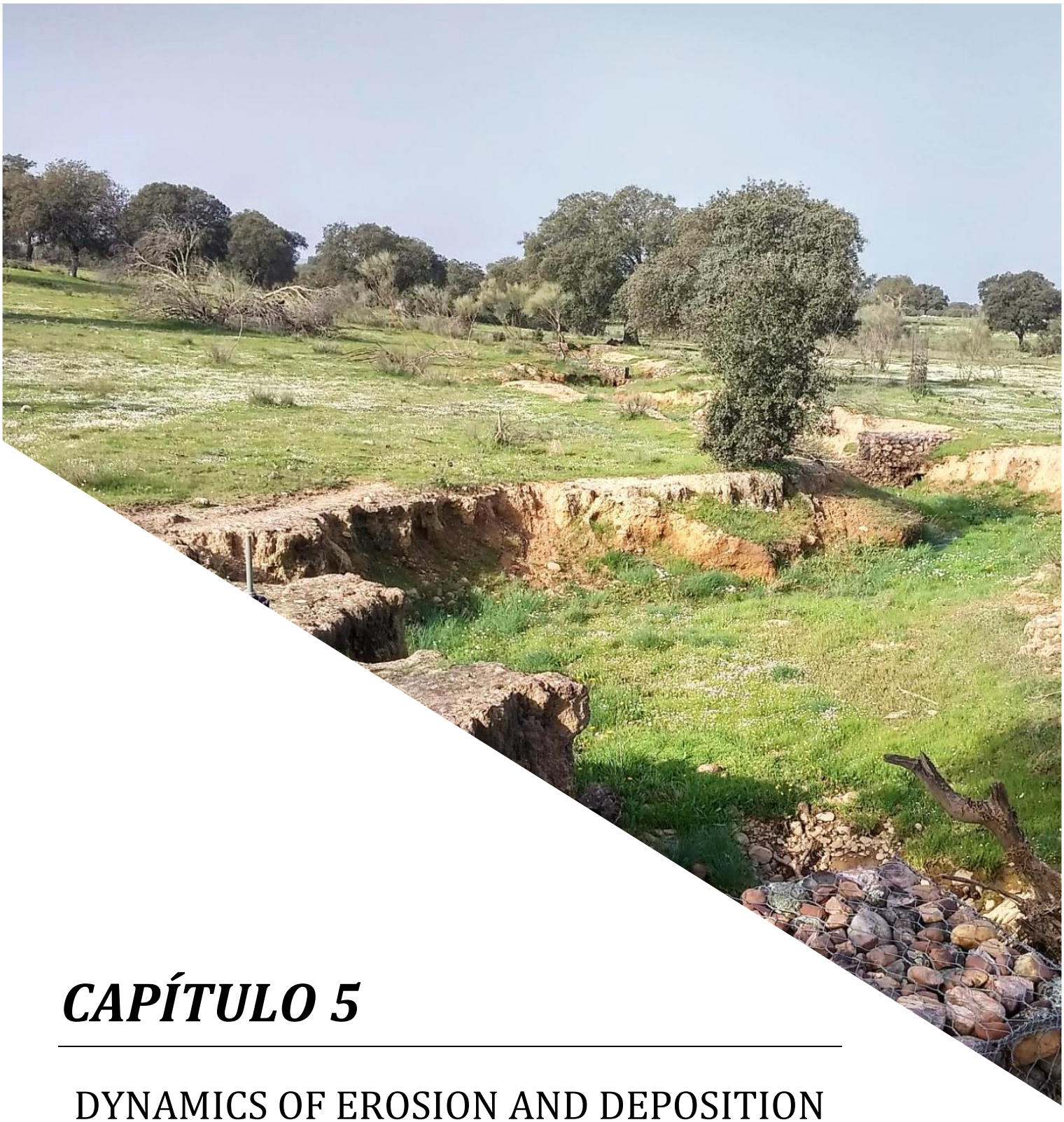

CAPÍTULO 5

DYNAMICS OF EROSION AND DEPOSITION IN A PARTIALLY RESTORED VALLEY BOTTOM GULLY

CAPÍTULO 5. DYNAMICS OF EROSION AND DEPOSITION IN A PARTIALLY RESTORED VALLEY BOTTOM GULLY

Alfonso-Torreño, A., Gómez-Gutiérrez, Á., Schnabel, S., 2021. Dynamics of Erosion and Deposition in a Partially Restored Valley-Bottom Gully. Land, 10, 62.

Abstract

Gullies are sources and reservoirs of sediments and perform as efficient transfers of runoff and sediments. In recent years, several techniques and technologies emerged to facilitate monitoring of gully dynamics at unprecedented spatial and temporal resolutions. Here we present a detailed study of a valley-bottom gully in a Mediterranean rangeland with a savannah-like vegetation cover that was partially restored in 2017. Restoration activities included check dams (gabion weirs and fascines) and livestock exclosure by fencing. The specific objectives of this work were: (1) to analyze the effectiveness of the restoration activities, (2) to study erosion and deposition dynamics before and after the restoration activities using high-resolution digital elevation models (DEMs), (3) to examine the role of micro-morphology on the observed topographic changes, and (4) to compare the current and recent channel dynamics with previous studies conducted in the same study area through different methods and spatio-temporal scales, quantifying medium-term changes. Topographic changes were estimated using multi-temporal, high-resolution DEMs produced using structure-from- motion (SfM) photogrammetry and aerial images acquired by a fixed-wing unmanned aerial vehicle (UAV). The performance of the restoration activities was satisfactory to control gully erosion. Check dams were effective favoring sediment deposition and reducing lateral bank erosion. Livestock exclosure promoted the stabilization of bank headcuts. The implemented restoration measures increased notably sediment deposition.

Keywords: topographic change; restoration; gully dynamics; UAV; SfM photogrammetry; rangeland

5.1. Introduction

Gully erosion is a land degradation process that takes place in a wide range of climatic, geomorphological, and pedological conditions (Billi and Dramis, 2003; Valentin et al., 2005; Zucca et al., 2006). Gullies can be classified as permanent or ephemeral (Poesen et al., 2003). Ephemeral gullies occur in cropland and are frequently filled by farmers and reappear in the same location, while permanent gullies are not filled by common agricultural labors. Gullies are also classified, depending on topographic position, as hillslope gullies or valley-bottom gullies (Bradford and Piest, 1980) and may be the consequence of natural and/or human-induced soil erosion processes (Poesen et al., 2003; Valentin et al., 2005). Topographical factors, such as drainage area and slope gradient, drive the formation of gullies, showing the importance of surface runoff. In the specific case of valley-bottom gullies, saturation and subsurface flows also play a major role (Gómez-Gutiérrez et al., 2012; Thomas et al., 2004). Gully development has also been associated to land use changes, management, and exploitation systems (Chaplot et al., 2005; Faulkner, 1995; Gómez-Gutiérrez et al., 2009a; Schnabel, 1997).

The environmental effects of gully erosion are manifold: reduction of water quality (Bartley et al., 2014; Wantzen, 2006), decrease of land productivity (Daba et al., 2003; García-Ruiz, 2010), and infrastructure damages (Fox et al., 2016; Jungerius et al., 2002). Gullies perform as links between the upper and lower lands of a basin, increasing flow and sediment connectivity, i.e., facilitating rapid transport of water and sediments to lowlands (e.g., Capra et al., 2005; Poesen et al., 2003).

Gully erosion represents one of the most significant types of soil degradation in Mediterranean environments (Faulkner, 1995; Vandekerckhove et al., 1998). In the Iberian Peninsula, a semi-natural landscape with an agrosilvopastoral land use system, named dehesa in Spanish, covers more than 4 million hectares. It is characterized by cleared oak woodlands with an annual grassland understory that is grazed by domestic animal species such as sheep, cows, pigs, and horses (Eichhorn et al., 2006). Soils are commonly shallow in dehesas, except for the valley bottoms where they are deeper. The two main erosive processes in dehesa are sheet wash in hillslopes (Rubio-Delgado et al., 2017; Schnabel et al., 2010) and gully erosion in valley bottoms (Gómez-Gutiérrez et al., 2012; Schnabel et al., 2013). In dehesas, gully erosion was studied in two small experimental basins with similar physical and environmental conditions, called Guadalperalón (Schnabel et al., 2010) and Parapuños (Gómez-Gutiérrez et al., 2014;

Gómez-Gutiérrez et al., 2012; Gómez-Gutiérrez et al., 2009a; Schnabel et al., 2013), with the latter being the study area of the present work. Parapuños serves as a model of dehesa exploitation system for its representativeness. At the same time, the existence of previous research sets the basis for a medium-term analysis of gully dynamics.

Restoration activities may be carried out at different spatial scales (catchment or channel). At the catchment scale, installing ponds or other water-retention measures may reduce surface runoff, slow down water, promote infiltration into the soil (Morgan, 2005), and/or establish better vegetation ground cover or reforestation to increase infiltration. This strategy is difficult to achieve since it must be implemented over a large extension of the entire gully catchment (Poesen, 1989). At the channel scale, measures commonly used include check dams (built with different techniques and materials, e.g., gabion weirs, masonry wall, fascines, i.e., piled wooden poles and planks), rockfills, and breakwaters. Other restoration measures include livestock exclosure from the channel (by fencing) to avoid the mechanical effect of animal movement. Fencing around existing gullies, forcing animals to cross the gullied channel in less degraded areas and excluding the animals from the valley bottoms during the rainiest months may perform well to reduce erosion in gullies and to promote their recovery. Among the different restoration strategies, check dams are often used (with or without other measures) in Mediterranean areas (e.g., Alfonso-Torreño et al., 2019; Castillo et al., 2007; Quiñonero-Rubio et al., 2016). They trap sediments (Belmonte et al., 2005; Conesa García, 2004) and mitigate soil erosion effects. Sediment trapped behind check dams may be used to estimate sediment yield produced by upstream catchments (e.g., Verstraeten and Poesen, 2002; White et al., 1997).

In the last decade, developments in airborne-based surveying technologies transformed the topographic data acquisition, replacing more classic methods like the one based on interpolating cross sections (CSs) to estimate the volumetric change in channels (Caraballo-Arias et al., 2016; Ferguson and Ashworth, 1992; Gómez-Gutiérrez et al., 2012). For instance, the concurrent use of unmanned aerial vehicles (UAV) platforms and structure-from-motion (SfM) photogrammetry together with MultiView-Stereo (MVS) has meant a breakthrough in earth science research. The low-cost photogrammetric method SfM, ideally suited for low-budget research and precise 3D data generation, emerged as a new, efficient monitoring technology (James and Robson, 2014; Westoby et al., 2012). SfM photogrammetry requires little training, is extremely inexpensive, and is effective in detailed scale studies (Fonstad et al., 2013). The development of UAV platforms facilitates the acquisition of high-resolution aerial

photos from which SfM photogrammetry may be used to obtain point clouds, digital elevation models (DEMs), and orthophotographs (Javernick et al., 2014; Smith and Vericat, 2015; Woodget et al., 2015), being particularly useful for the estimation of topographic changes in gullies (e.g., Castillo et al., 2012; Frankl et al., 2015; Gómez-Gutiérrez et al., 2014). Gullies have been monitored using SfM photogrammetry and repeated surveys by Xiang et al. (2018) and Kaiser et al. (2018). Multitemporal topographic models (like DEMs) may help to identify changes due to erosion-deposition processes and to quantify soil losses. Two DEMs of different dates may be subtracted to produce a DEM of differences (DoD) (Wheaton et al., 2010), which is particularly relevant to geomorphic studies because it provides a spatially distributed model of topographic and volumetric change through time (Brasington et al., 2003; Rumsby et al., 2008). UAV platforms have been used to acquire data useful to detect geomorphic changes in different environments: mountainous ranges (Borrelli et al., 2019; Cavalli et al., 2017; Martínez-Casasnovas et al., 2009; Martins et al., 2019), agricultural landscapes (Tarolli et al., 2019; Turner et al., 2015), riverine (Cook, 2017; Woodget et al., 2015), Badlands (Neugirg et al., 2016), and mines (Haas et al., 2016). The most important factor determining the reliability of a DoD is the accuracy of the individual DEMs and their coregistration (Williams, 2012). Uncertainties in the topographic representation of a surface by means of a DEM have implications for forthcoming DEM applications (e.g., geomorphic change detection, hydraulic modelling, etc.). Such uncertainties may be quantitatively assessed by estimating errors (Bangen et al., 2016). In geomorphological studies, errors in DEMs should be considered, as they may lead to overestimation of net erosion or deposition in sediment budgets (Wheaton et al., 2010). There are different strategies to manage errors in the DoD approach, the most simple to consider being the error spatially uniform along every DEM (Brasington et al., 2000; Milan et al., 2007). In the spatial uniform error approach, a minimum level of detection threshold (minLoD) is used to differentiate topographic changes from error (Fuller et al., 2003). The minLoD is typically based on an average error value, which tends to discard more information than necessary in areas where elevation uncertainty is low and to include information in areas where elevation uncertainty is high (Wheaton, 2008). An alternative is to consider the spatial error distribution. Several researchers found a strong relationship between roughness and DEM error (Heritage et al., 2009; Milan et al., 2011). Wheaton et al. (2010) and Prosdocimi et al. (2015) used a fuzzy inference system (FIS) to estimate error from multiple sources that contribute to DEM uncertainty.

The present work aimed to analyze the effectiveness of restoration activities (i.e., gabion weirs, fascines, and isolation measures) carried out in a valley-bottom gully representative of channels that usually take place in dehesa landscapes (SW of the Iberian Peninsula). The specific objectives included: (1) to study the dynamics of erosion and deposition before and after the restoration activities with the help of high-resolution DEMs, (2) to analyze the role of micro-morphology in the topographic changes observed, and (3) to compare the current and recent dynamics of the channel with previous studies carried out in the same study area but with different methods and spatio-temporal scales, quantifying medium-term changes. The geomorphic changes were estimated using five high-resolution DEMs and orthophotographs produced using photogrammetry and images acquired with a UAV between 2016 and 2019. The gully was partially restored with check dams (of different types) and isolation measures in February 2017.

5.2. Material and methods

5.2.1. Study area

The study was conducted in the Parapuños experimental catchment (99.5 ha) located in the SW of the Iberian Peninsula (Figure 22a). Parapuños is representative of the dehesa land use system and is part of an extensive erosion surface characterized by an undulating topography (Figure 22b). The channel is a discontinuous second-order stream with a main channel (832 m in length) and a tributary (163 m). The channel flows in the lower part of the catchment and is incised into an alluvial sediment fill of approximately 1.5 m in depth, reaching the underlying schist. The gully may be divided into three different reaches: (1) lower reach, (2) tributary reach, and (3) upper reach where the restoration measures were carried out in February 2017 (Table 6). The lower reach flows from the outlet of the catchment to the junction between the tributary and the upper reach. Additionally, a recent study explained the development of an incipient auxiliary channel in the upper reach influenced by the existence of cattle paths (Gomez-Gutierrez et al., 2018).

The average altitude of the catchment is 396 m a.s.l. and the mean slope is 8% ranging from almost flat surfaces in the valley bottoms to 12% at the hillslopes. There are two types of bedrocks in the basin: slates and unconsolidated conglomerates, the latter forming part of a pediment and occupying 32% of the catchment. Generally, the soils developed on slates are shallow. The pediment is found in the highest parts of the

catchment, composed of quartzite cobbles, gravelly sand, and loam. The soils can be classified as *Leptosols* and *Cambisols*. The alluvial sediment fill, where the gully is located, can be classified as *Regosol*. Climate is Mediterranean with an average annual temperature of 16°C and a mean annual rainfall of 513 mm with high seasonality.

The vegetation cover is composed of a disperse tree cover of Holm oak (*Quercus ilex va. rotundifolia*), with an average tree density of 22.5 tree ha^{-1} and herbaceous plants in the understory. At steeper slopes shrubs are frequent, mainly composed of *Retama sphaerocarpa*, *Cytisus multiflorus*, and *Genista hirsuta*. Livestock rearing is the main land use in the study area, with 1200 sheep, 38 cows, and 50 pigs.

The study area showed evidences of sheet erosion on the hillslopes (Rubio-Delgado et al., 2017) and the existence of a gully in the valley bottom. To mitigate consequences of soil erosion by water, 8 gabion weirs (GWs) with metal mesh (Figure 22d) and 25 fascines (Fs) (Figure 22e) were built in the channel in February 2017. Five gabion weirs have a dimension of 2 × 0.5 × 1 m (with two fins of 1 × 0.5 × 0.5 m), 2 units of 2 × 0.5 × 1 m, and a one of 3 × 0.5 × 1 m (with two fins of 1 × 0.5 × 0.5 m). The distance between GWs is approximately 27 m. The mesh was manually filled with quartzite cobbles collected in the area. The fascines were made with brooms (i.e., local material), anchored to the surface with acacia posts (rot-proof wood) and tied with hemp material. The fascines have a length of 2 m and an average separation of 12 m. Finally, an electric shepherd was installed close to the gully as an isolation measure in a particularly degraded area that showed several active bank headcuts (Figure 22f). The wired fence had a perimeter of 117 m and it covered 416 m^2. In addition, two parts were clearly differentiated in the restored channel with the main goal of observing differences in the volume of sediments retained in the gabion weirs and fascines, before and after the construction of the restoration measures. The first were the check dams in the lower part of the channel (i.e., between GW-01 and GW-04) and the second were check dams located near the channel head and predominantly fascines (i.e., between F-07 and F-17).

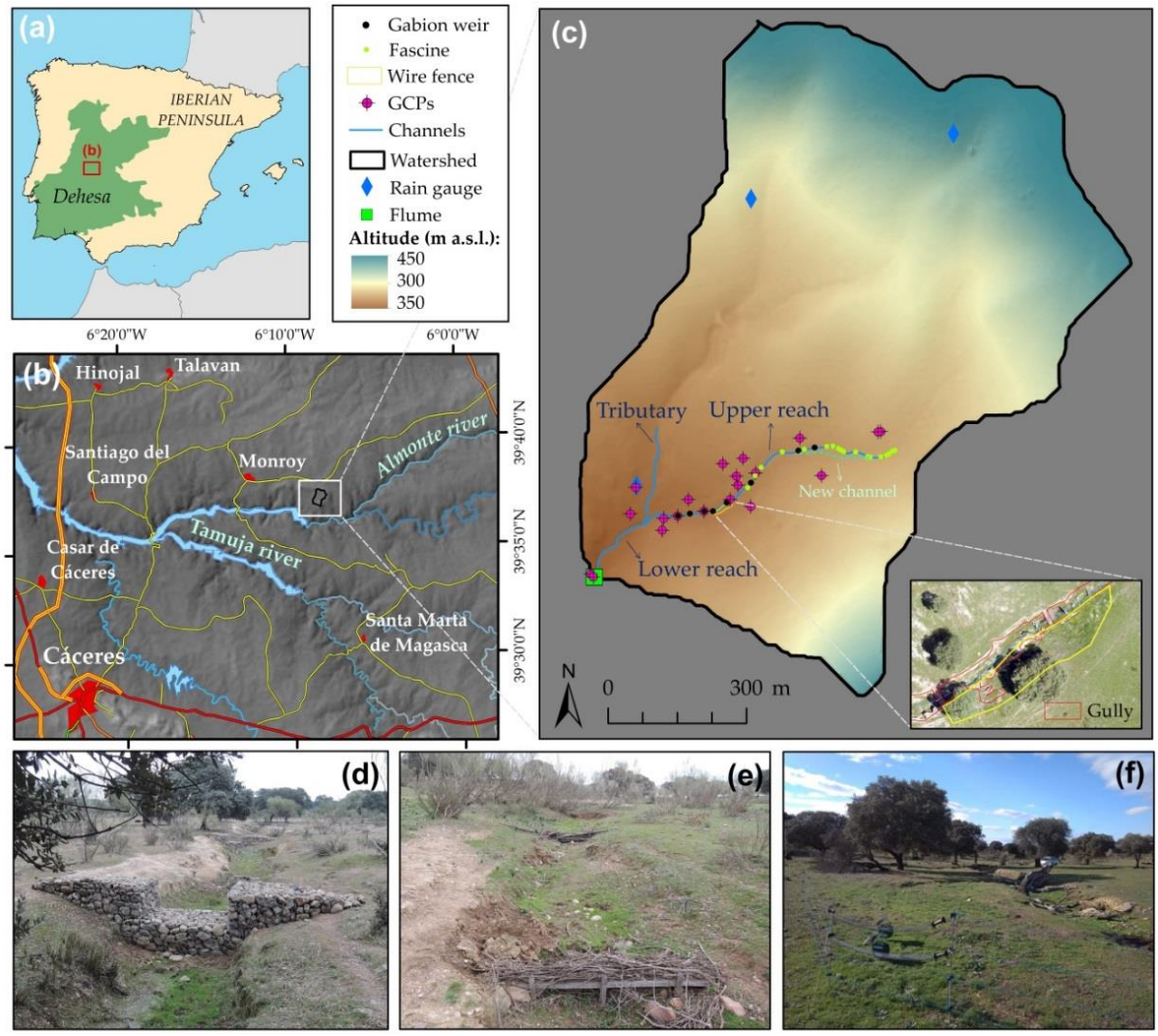

Figure 22. (a) Location of the study area in the Iberian Peninsula where the green area displays where dehesas are frequent and the red rectangle represents the area shown in (b); (b) regional setting of the study area where the main towns, rivers, and roads are shown over the hillshade and the white rectangle of the area shown in (c); (c) Parapuños catchment including the restoration measures carried out and the ground control points (GCPs); examples of gabion weirs (d), a fascine structure (e), and the isolated area in the left bank of the gully (f).

Table 6. Characteristics of the channel reaches belonging to unmanned aerial vehicle (UAV) survey completed in January 2019.

	Lower Reach	Tributary	Upper Reach
Maximum and minimum elevation (m a.s.l.)	436–419	421–419	419–414
Length (m)	174.30	163.10	658.50
Slope (%)	2.60	2.10	2.60
Drainage area (ha)	99.50	45.40	49.90
Mean width (m)	4.40	1.90	2.00
Max width (m)	7.50	3.50	6.00
Min width (m)	2.90	1.00	2.10
Mean depth (m)	0.57	0.56	0.53
Max depth (m)	1.47	1.28	1.27

5.2.2. SfM workflow and digital elevation model generation

The UAV surveys of the gully were completed in March 2016, February 2017, October 2017, March 2018, and January 2019 (Table 7). The SfM photogrammetry workflow was fed with aerial photographs acquired by a fixed-wing UAV (Ebee by Sensefly) carrying a Sony WX220 sensor (18 Mpx) on board. The UAV was operated autonomously by using an external PC with a radio modem and a pre-programmed flight plan. The images (190 images per survey on average) were acquired at an approximate altitude of 60 m above ground. Ground control points (GCPs) were required for both relative and absolute topographic accuracy and to improve the alignment of surveys and, consequently, the detection of topographical changes (Cook, 2017; Lallias-Tacon et al., 2014). Twenty GCPs were registered across the area during the first field survey and surveyed with a Leica GPS 1200 system (with RTK and post-processed solutions with GPS + GLONNASS satellites) (Figure 22c) and used to scale and to georeference the models. GCPs were based on natural, permanent, and clearly identified features in the images such as wall corners and sharp rocks. The Pix4D software (v. 3.1.18) was used to process the UAV-derived photographs together with the GCPs and to produce point clouds, high-resolution DEMs, and orthophotographs.

Table 7. Characteristics of the surveys carried out. GSD: ground sampling distance, GCPs: ground control points, RMSE: root mean square error

Date	24 March 2016	16 February 2017	25 October 2017	03 May 2018	25 January 2019
Area covered (ha)	30.8	22.3	27.5	15.19	17.6
Number of photos	271	263	148	142	155
Number of GCPs	19	20	21	21	20
RMSE (m)	0.016	0.042	0.026	0.013	0.028
GSD (m)	0.018	0.017	0.035	0.023	0.022
Number of points	134,136,325	130,194,090	285,686,716	279,987,096	82,969,351
Point density (points m^{-3})	1383.8	1500.5	881.5	2727.6	1026.6
Processing time (hh:mm:ss)*	04h:11m	03h:22m	03h:51m	06h:56m	02h:44m

(*) Includes time for initial alignment, point cloud densification, orthomosaic, DSM, and DEM generation using an Intel Core i7 CPU at 2.50 GHz with 8 GB RAM, GPU Intel HD Graphics 4600.

5.2.3. DEMs of Difference and error analysis

Geomorphic change analysis was conducted through the DoD approach (Wheaton et al., 2010), using the Geomorphic Change Detection (GCD) v7.1 add-in (Riverscapes-

Consortium, 2018) freely available from https://gcd.riverscapes.xyz/Download, within the ArcGIS Desktop software v10.6. We considered a spatially variable error estimated using rules implemented through a fuzzy inference system in addition to the georeferencing error calculated for every individual DEM during the photogrammetry processing. Two rules, based on slope gradient and vegetation height (obtained subtracting DEM from digital surface model (DSM)), were used in the FIS system. Slope gradient is a common input in FIS DEM error models because it is a reasonable proxy for topographic complexity and can be derived easily from the input DEM (Wheaton et al., 2010). DEM error at steep slopes is commonly larger than at gentle slopes due to lower sampling density, and the uncertainty, therefore, is greater than in areas with gentle slopes (Gómez-Gutiérrez et al., 2020; Milan et al., 2011).

The vegetation cover may lead to increased uncertainties in DEM produced using photogrammetric techniques (Fonstad et al., 2013). Here, vegetation cover was filtered from the DSM using the Pix4D algorithm to produce the DEM. A map of differences between both surfaces (i.e., DSM and DEM) was included as input in the FIS analysis to represent the effect of vegetation cover on DEM error. Major differences correspond to woody vegetation (e.g., trees and shrubs), and, consequently, the uncertainty in topographic change estimation is expected to be larger there than in unvegetated areas. We also considered the effect of grassland, applying a minimum level of detection (minLod) based on the height of grasses in the periods analyzed. A supervised image classification of the multitemporal orthophotographs was conducted in order to detect the grassland cover. The influence of slope and vegetation cover on the final error surface depends on predesigned membership functions (MFs). Every variable is divided into three classes (low, medium, and high) and the MFs result from the combination of these values in another four classes (low, average, high, and extreme). This information is then used to produce a map of elevation uncertainties (δz) for each DEM. The GCD ArcGIS plugin was used to elaborate the FIS, defining the MFs for the input variables.

$$LoD = t\,(\delta z_{DEMnew}^{2} + \delta z_{DEMold}^{2})^{0.5} \quad (1)$$

where the level of detection (LoD) is the critical threshold error in the DoDs for a significant topographic change with a confidence interval of 95%, and δz_{DEMnew} and δz_{DEMold} are the estimated uncertainties of the compared DEMs using the FIS output previously described. Actual geomorphic changes were considered in pixels where topographic change was larger than the LoD calculated using Equation (1).

The SfM-derived DEMs allowed us to estimate the geomorphic change of the gully before (i.e., P1) and after the restoration activities (P2, P3, and P4; see Figure 23).

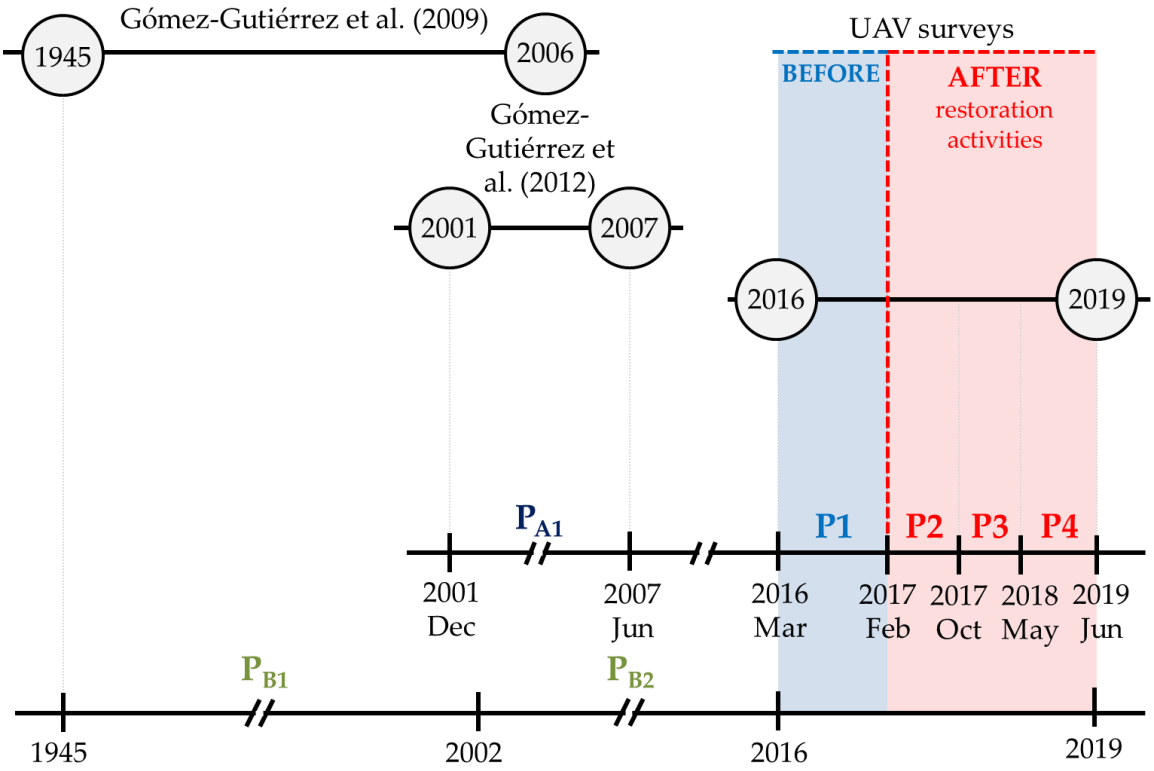

Figure 23. Time periods considered in the study as a result of the availability of topographic data. The vertical red line displays the date of the restoration measure implementation.

5.2.4. Overlapping current topography with older information

The gully in Parapuños has been monitored by different techniques in the past. For example, Gómez-Gutiérrez et al. (2012) used 28 fixed cross-sections (CSs) to study the dynamics of the gully from 2001 to 2007 (P_{A1}; see Figure 23). This data set used an absolute reference frame (i.e., ETRS89 UTM29 North) that facilitates the overlap with our DEMs with the aim of quantifying medium-term changes. Nine out of the 28 original CSs were not suitable for comparison because of the presence of woody vegetation at these locations.

Gómez-Gutiérrez et al. (2009a) mapped the area affected by gullying and the number of headcuts in Parapuños valley bottom using aerial photographs for the period from 1945 to 2006. This data set was completed by mapping the gullied area and the number of headcuts in five orthophotographs (from 2016 to 2019) obtained from the SfM photogrammetry. The resulting database is useful to understand the

dynamics of the gully at medium- and long-term temporal scales, as well as the evolution of land use and vegetation cover in the catchment for that timespan. This database was divided into two periods: P_{B1} (from 1945 to 2002) and P_{B2} (from 2002 to 2016).

5.2.5. Geomorphometry

The geomorphometric characterization of the topography may help to understand the spatial and temporal dynamics of the erosion and deposition processes acting in the channel. Slope gradient and curvature topographic attributes were derived from the February 2017 DEM (that represents channel morphology just after check dam establishment) and were compared with the resulting topographic change experienced at every location (pixel) between February 2017 and January 2019.

5.2.6. Explanatory variables for statistical analysis

A statistical analysis was carried out to assess the influence of different environmental factors on the effectiveness of the check dams to trap sediments. We explored the relationships between a set of 11 environmental variables and the sediment volume retained in the check dams using the linear correlation analysis. The selected explanatory variables were: drainage area (ha), check dam length and height (m), upstream check dams (n), slope of the catchment (◦), upstream accumulated sediments (m^3), channel length (m), stream power index, tree density (trees ha^{-1}), connectivity index (Borselli et al., 2008; Cavalli et al., 2013), and path density (km ha^{-1}).

The independent variables were derived from different data sources: (1) the SfM-derived DEM with 0.02-m pixel size, (2) the SfM-derived orthophotograph with resolution of 0.02 m, and (3) the DEM of the Spanish Geographic National Institute (CNIG, 2010) with a pixel size of 5 m. Procedures and calculations to estimate the different variables were conducted using ArcGIS 10.5 (www.esri.com).

5.3. Results

5.3.1. Channel geometry

A total of five clouds with an average volumetric point density of 1504 pts m^{-3} were obtained. DEMs and orthophotographs with a ground sampling distance (GSD) of

0.02 m resulted from the SfM photogrammetric processing (Table 7). The average root mean square error (RMSE) estimated during the SfM processing was 0.03 m, showing centimeter-level accuracies in the resulting cartographic products and allowing a detailed geometrical description of the gully (Table 6).

The channel presented a length of 995.9 m, from which 658.5 m, 163.1 m, and 174.3 m belong to the upper reach, the tributary, and the lower reach, respectively. The slope gradient was slightly lower in the tributary than in the main channel (upper and lower reaches). Table 6 shows the characteristics of every reach.

5.3.2. Dynamics of the gully

The net change at the channel for the study period (2016–2019) was estimated to be 95.4 m^3 (i.e., a net deposition of 33.6 m^3 y^{-1}). Topographic change showed a high temporal variation, from –12.8 m^3 of net erosion experienced during P2 to 62.8 m^3 of net deposition during P3 (Table 8). The total rainfall registered per period ranged from 159 mm (P2) to 486 mm (P3). The average annual rainfall at the basin was 508.8 mm for the period 2005–2019, showing a high temporal variability (annual, seasonal, and monthly). After the establishment of restoration measures, a rainy and a dry year were registered with 560.5 mm and 350.3 mm, respectively.

Table 8. Summary of the data registered during the study period: erosion or deposition, net volume difference (NVD), and rainfall variables (R-max = maximum event rainfall).

Period	**P1**	**P2**	**P3**	**P4**
Duration	24 March 2016 – 16 February 2017	16 February 2017 – 25 October 2017	25 October 2017 – 3 May 2018	3 May 2018 – 25 January 2019
Erosion (m^3)	–8.0	–14.7	–1.4	–5.9
Deposition (m^3)	50.7	5.7	64.2	4.8
NVD (m^3)	42.7	–9.0	62.8	–1.1
NVD rate (m^3 y^{-1})	48.5	–12.8	120.8	–1.5
Rainfall amount (mm)	543.4	107.4	486.4	335.1
Events (N)	30	1	25	19
R–max (mm)	57.7	20.8	21.8	22.2

A high spatial variability of erosion and deposition was observed at the different reaches with the coexistence of erosional and depositional processes but prevailing in the latter. The total net volume of soil deposited at the lower, the upper, and the tributary reaches was 16.5, 71.6, and 7.3 m^3, respectively.

Period 1 (P1) and P3 were filling periods, while P2 and P4 registered erosion. The maximum accumulation in the lower reach and the tributary took place in P1 with 23.8 and 4.3 $m^3 y^{-1}$ (Figure 24a), respectively. In the upper reach, the maximum deposition was registered during P3 with 108.3 $m^3 y^{-1}$, i.e., the largest amount of sediment deposited during the study took place in the restored reach and after the restoration activities. The maximum erosion in the upper reach took place during P4 with –3.8 $m^3 y^{-1}$, while the maximum erosion in the lower reach and the tributary happened in P2, with –9.6 $m^3 y^{-1}$ and –6.6 $m^3 y^{-1}$, respectively.

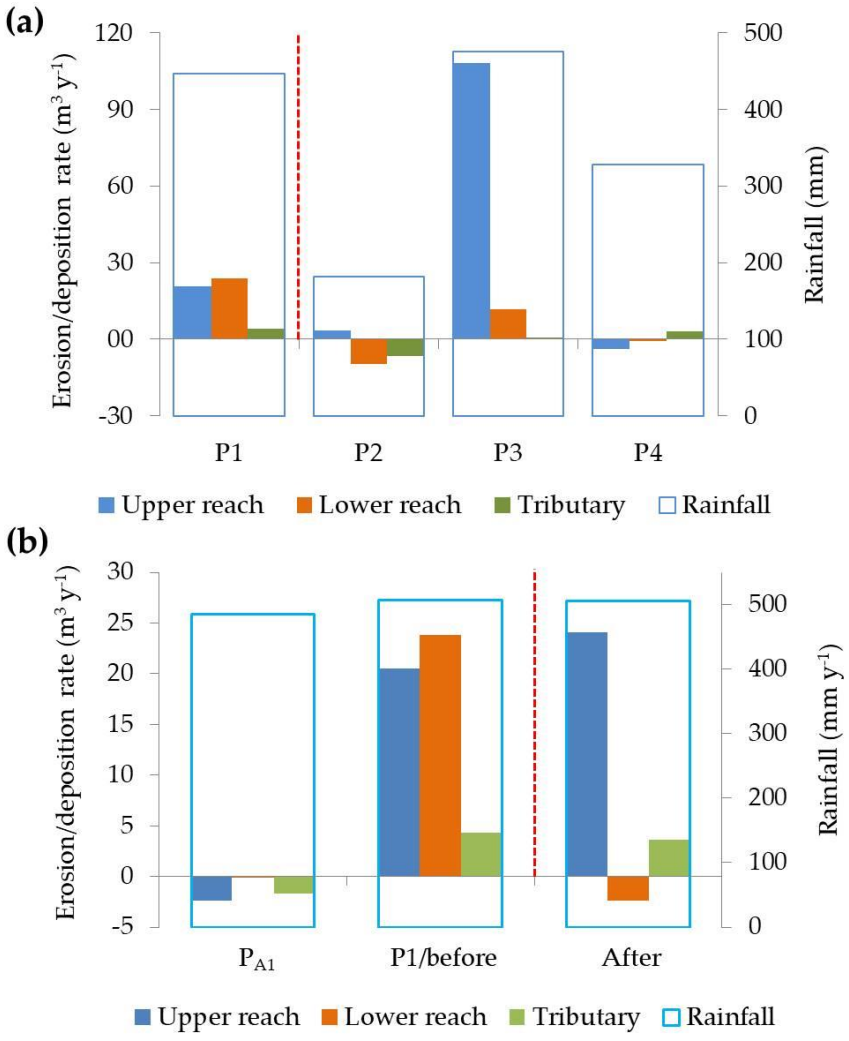

Figure 24. (a) Net erosion/deposition rate registered at the different reaches by period and (b) net erosion/deposition rate recorded before and after the establishment of the restoration measures. Period PA1 (from December 2001 to June 2007) refers to the data obtained by Gómez-Gutiérrez et al. (2012), who surveyed 28 fixed topographic cross sections. The vertical red line indicates the establishment of the restoration measures.

In PA1, the gully erosion rate was estimated at –4.2 m^3 y^{-1}. The largest erosion in the upper reach was registered between 2001 and 2007, with an erosion rate of –2.4 m^3 y^{-1} (Figure 24b). Nevertheless, the lower reach registered the largest amount of accumulation before the establishment of restoration measures. After the restoration of the upper reach, the erosion/deposition rate was 24.1 m^3 y^{-1} against 3.6 m^3 y^{-1} in the tributary and –2.4 m^3 y^{-1} in the lower reach. Of the deposition in the channel, 42% occurred in the restored reach before the construction of the restoration measures, while 86% of the deposition took place in the upper reach (i.e., restored reach) after the restoration.

Different processes were observed in the gully with a general aggradation of the channel according to the estimated topographic changes. Three depositional features were observed: (1) sediments filling the whole channel bed (Figure 25a), (2) sediments forming lateral bars at different locations, and (3) sediment deposits behind check dams.

Several erosion processes were also observed: (1) channel bed erosion, due to the direct action of water flow and transported materials, (2) erosion of previously deposited sediments (both (1) and (2) represented 44% of the total erosion in the channel) (Figure 26a), (3) the widening of the channel at some locations, (4) growth of headcuts at the tributary reach (less than 0.5 m wide and deep) (Figure 25c) and growth in three bank headcuts at the upper reach, representing 39% of the total erosion registered in the channel, and (5) erosion downstream of the check dams forming plunge pools, which represented 17% of the erosion observed in the restored area (Figure 26a). Channel widening usually starts with lateral incision at the base of the bank that leads to reverse slopes. These banks increase their weight during wet periods, promoting the collapse of the upper bank by gravity. Finally, the collapsed material is available at the base of the scarp, to be eroded by the flow (Figure 25b). In four bank headcuts located next to the fenced-isolated area, evidences of revegetation and small blocks of collapsed material were observed (Figure 25d).

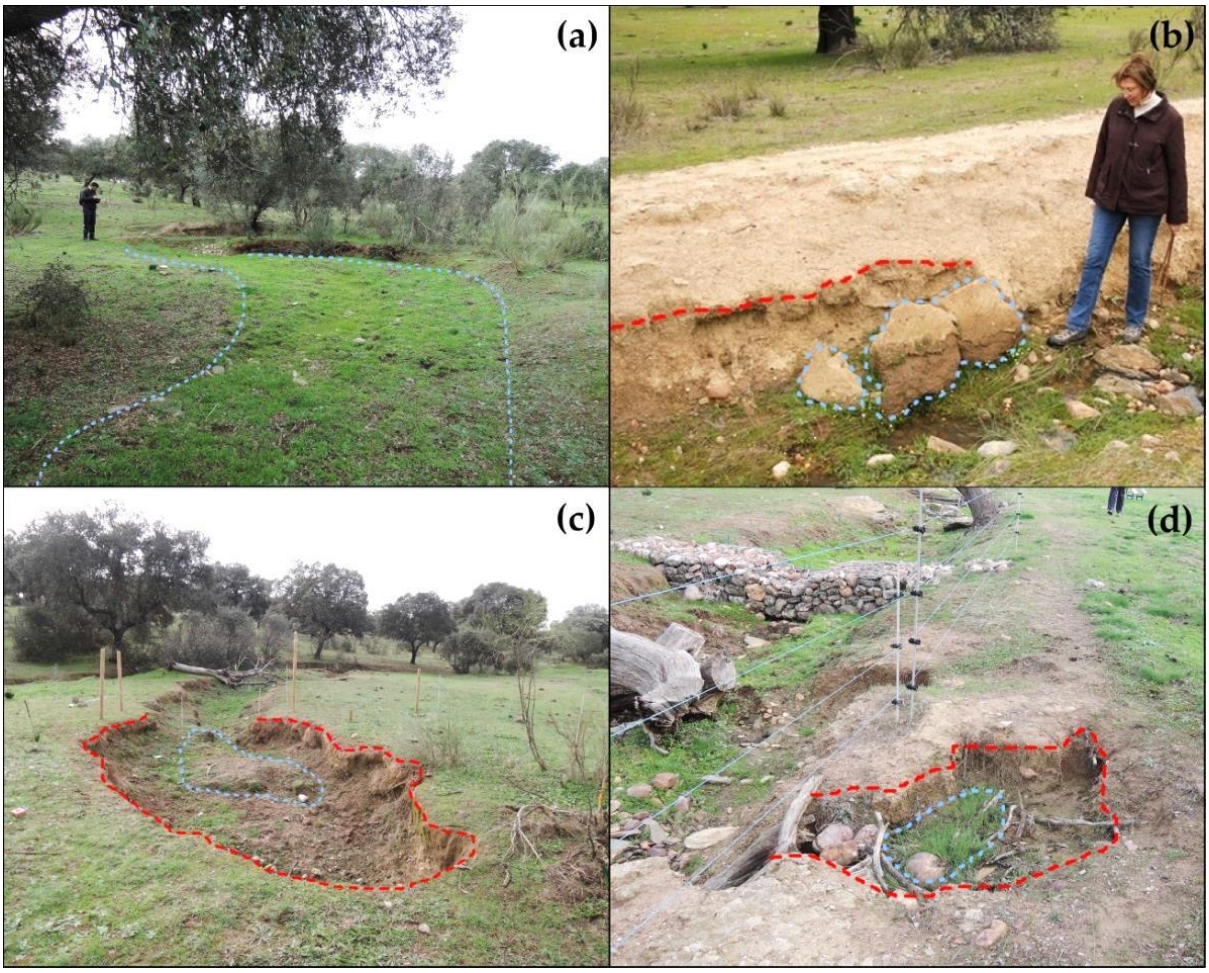

Figure 25. Field observations showing (a) the channel bed filled with sediments and revegetated; (b) lateral bank erosion and bank collapsed materials; (c) evidence of growth in a headcut; and (d) bank headcuts associated with observed cattle paths. Dashed blue and red lines show the extent of depositional and erosional features, respectively.

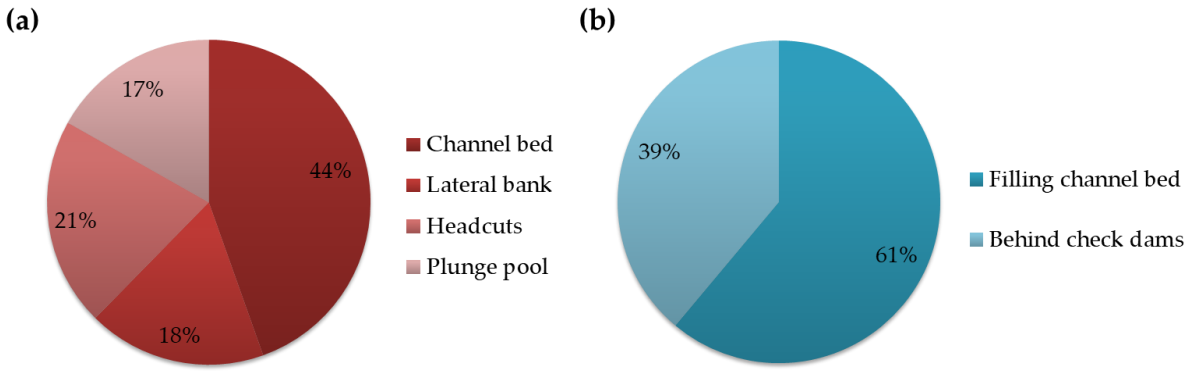

Figure 26. Percentage of the area covered by different erosional (a) and depositional features (only in the restored reach, i.e., the upper reach) (b).

The overlap of our topographic data (i.e., the DEM), through topographic profiles, with the fixed CSs allowed us to detect several geomorphological processes. Figure 27 presents three CSs at different locations for three dates: 2007, 2016, and 2019. Figure 27a represents a CS located 85 m upstream of the outlet of the catchment (i.e., the lower reach). Here, the channel bed was filled by sediments since 2007. Figure 27b presents a CS located in the tributary that shows erosion of the upper banks and filling of the channel bed. Finally, Figure 27c shows a CS located between GW-02 and GW-03 (i.e., the upper reach) that shows erosion at both banks and filling with sediments of the channel bed from 2016 to 2019.

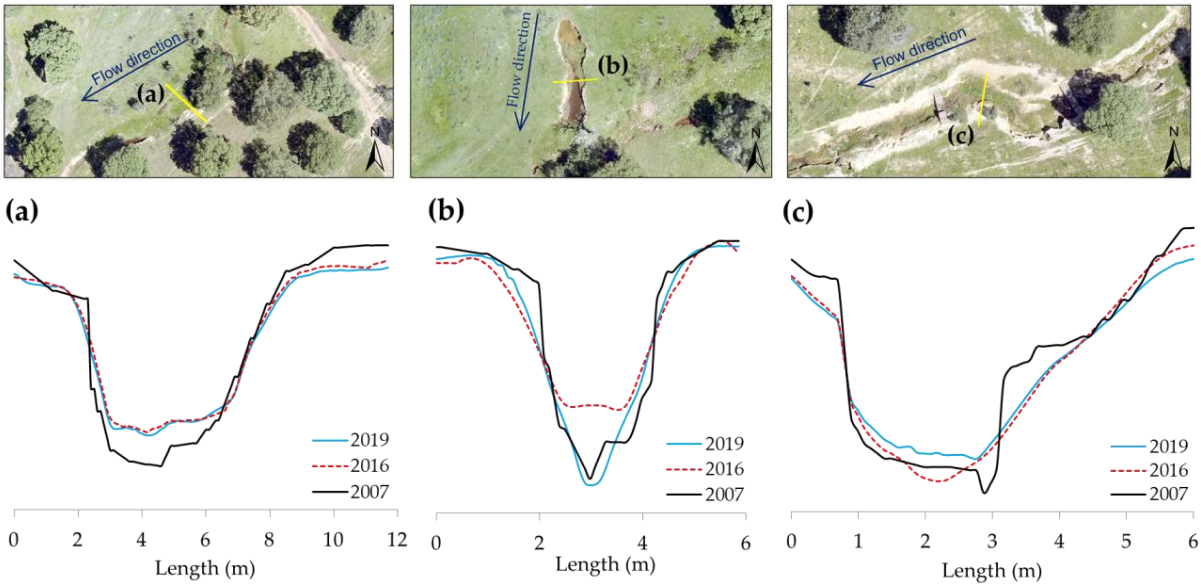

Figure 27. Evolution of three topographic cross sections located at (a) the lower reach, (b) the tributary, and (c) the upper reach from a downstream view, with a spatial resolution of 0.02 m.

The ensemble of our data with Gómez-Gutiérrez et al. (2009a) data set allowed us to describe the area affected by gullying, besides land use and vegetation cover dynamics since 1945. During this period (1945–2019) important changes in vegetation cover and land use took place in Parapuños (Table 9). The main changes can be summarized as follows: (1) a decrease of tree density on 6 trees ha^{-1} from 1956 to 1989, (2) reduction of grasslands with woody vegetation, (3) a strong increase of grasslands with scarce woody vegetation, (4) slight decrease of areas with dense tree cover, (5) a strong reduction of cropland between 1956 and 1989 (Figure 28a), and (6) an important increase on livestock density between 1998 and 2002 (from 0.30 to 2.99 animal unit ha^{-1} (AU ha^{-1}); Figure 28b).

Table 9. Evolution of gullied area, besides land use and vegetation cover in the catchment. Data from 1945 to 2006, taken from Gómez-Gutiérrez et al. (2009a).

	P_{B1}				P_{B2}			AFTER		
Year	**1945**	**1956**	**1989**	**1998**	**2002**	**2006**	**2016**	**2017**	**2018**	**2019**
Grasslands with scarce, woody vegetation (%)	40.7	16.6	68.5	68.5	60.3	60.3	74.0	74.0	74.0	74.0
Grasslands with woody vegetation (%)	47.3	39.5	19.4	19.4	16.9	16.9	19.2	19.2	19.2	19.2
Areas with dense tree cover (%)	12.0	2.1	9.0	9.0	9.0	9.0	6.6	6.6	6.6	6.6
Annual crops (%)	–	41.8	2.9	2.9	13.6	13.6	–	–	–	–
Unproductive (%)	–	–	0.2	0.2	0.2	0.2	0.2	0.2	0.2	0.2
Tree density (trees ha^{-1})	29	31	21	21	21	21	22	22	22	22
Gullied area (m^2)	695	1560	688	605	754	1009	2291	2306	2355	2360
Headcuts (n)	4	4	4	6	11	16	48	48	48	48

The area affected by gullying increased by 1665 m^2 (22 m^3 y^{-1}) from 1945 to 2019 and experienced different trends during that period. The area affected by gullying increased by 865 m^2 (78 m^2 y^{-1}) from 1945 to 1956 and the gully decreased by 955 m^2 (23 m^2 y^{-1}) from 1956 to 1998. The area affected by gullying increased, again, by 1606 m^2 (89 m^2 y^{-1}) from 2001 to 2019, with a surface of 2360 m^2 in 2019. During P_{B2}, the increase of the gully coincided with the heavy increase in livestock density between 2002 until 2017. The channel growth during P_{B2} was produced by the expansion of the gullied reaches and the retreat of the main and bank headcuts.

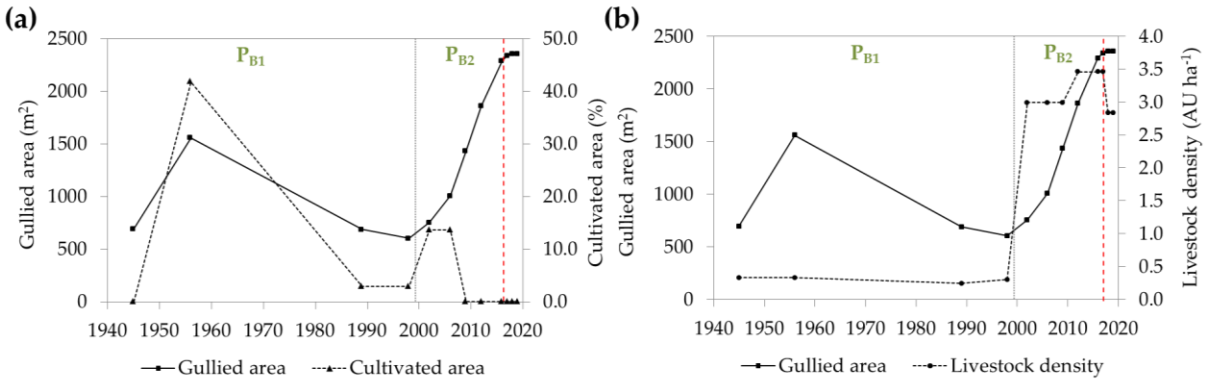

Figure 28. Evolution of the gullied area (m^2): (a) the cultivated area and (b) the livestock density (AU ha^{-1}). The vertical red line indicates the date of the restoration activities. Data from 1945 to 2006, taken from Gómez-Gutiérrez et al. (2009a).

5.3.3. Restoration measures: effectiveness and relationship with other environmental factors

The DoDs for the upper reach, before and after the construction of GW and fascine check dams, are shown in Figure 29. The effect of these measures is clearly visible in Figure 29c-d for GWs and fascines, respectively, with sediments accumulated upstream of these structures. At the same reaches, the amount of sediment accumulated in the same area before check dam construction was significantly less than the deposition observed afterwards.

Table 10 reports the volumes of erosion and deposition for the two selected reaches presented in Figure 29. The net volume difference (NVD) between GW-01 and GW-04 before and after restoration activities was 8.33 m^3 and 33.73 m^3, respectively. The NVD between F-07 and F-17 before and after restoration activities was –6.03 m^3 and 6.02 m^3, respectively. The volume of sediments deposited between GW-01 and GW-04 increased by 404.9% after check dam construction. In the area where fascines predominate, the volume of sediments deposited increased by 209.8% after check dam construction.

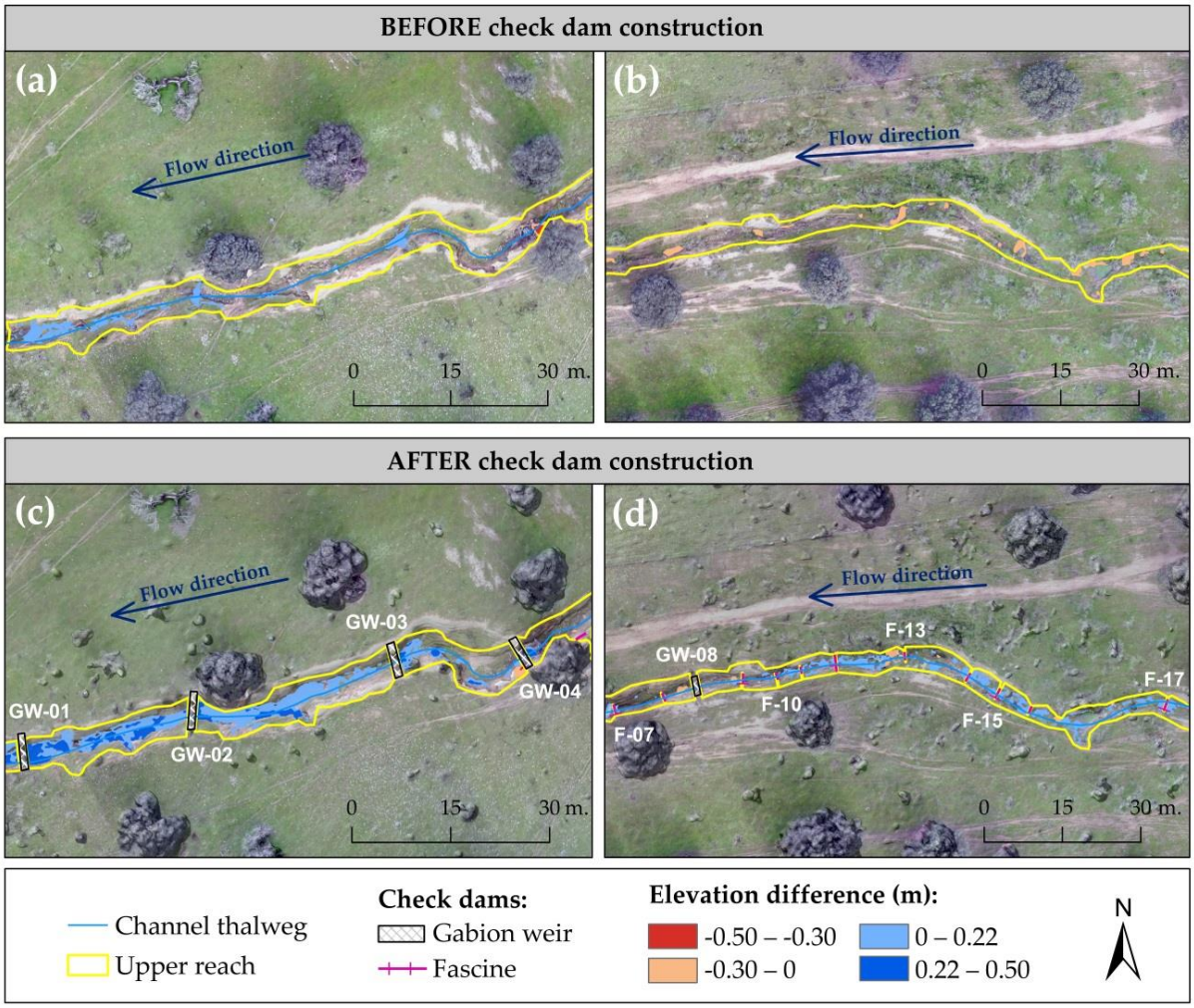

Figure 29. Resulting digital elevation models of differences (DoD) for two reaches at the upper reach (a,b) before check dam construction (DoD 2016–2017) and (c,d) after check dam construction (DoD 2017–2019). Note that (c) shows four gabion weirs (GWs) while (d) presents one GW and 11 fascines (Fs).

Table 10. Total volume of erosion and deposition registered before and after check dam construction for the reaches presented in Figure 29. BEFORE = before check dam construction. AFTER = after check dam construction. NVD = net volume difference.

Channel reaches	BEFORE March 2016 – February 2017			AFTER February 2017 – January 2019		
	Erosion	Deposition	NVD	Erosion	Deposition	NVD
	m^3	m^3	m^3	m^3	m^3	m^3
GW-01 / GW-04	–0.98	9.31	8.33	–0.95	34.68	33.73
F-07 / F-17	–6.15	0.12	–6.03	–1.83	8.45	6.62

A total of 11.7 m^3 of sediments was deposited behind check dams, while 0.9 m^3 were eroded immediately downstream of check dams. The sediments retained behind check dams represent 39% of the total deposition observed in the restored area (Figure 26b). Large amounts of sediment were observed in the check dams located close to the outlet of the catchment (Figure 30). Most of the deposition took place between check dams GW-01 and GW-04 with GW-01 trapping the largest amount of sediment (i.e., 5.37 m^3). Fascines also retained sediments but to a lesser extent than GWs.

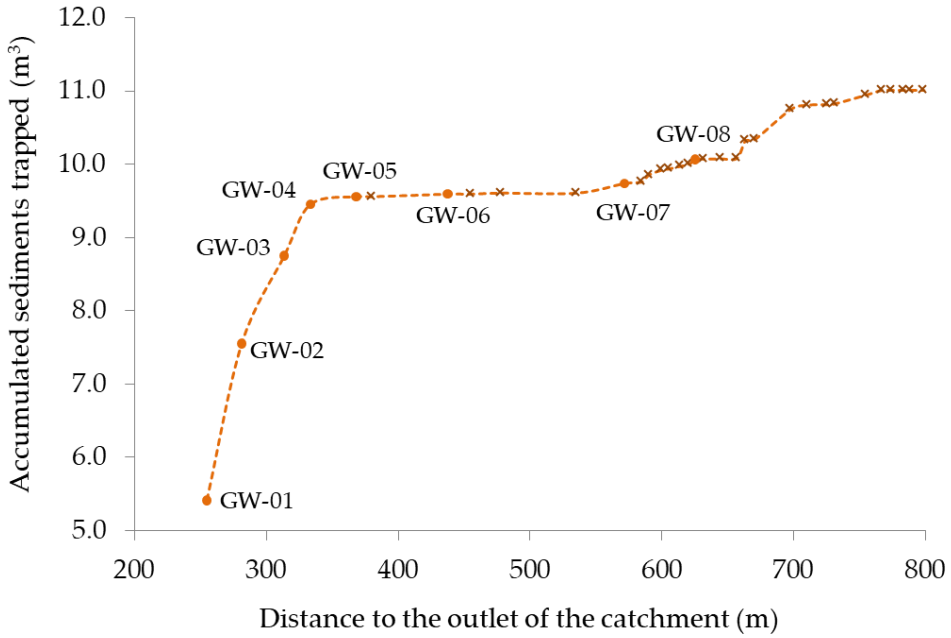

Figure 30. Accumulated sediments trapped at each check dam plotted against the distance to the outlet of the catchment. Note that the line shows the sediments trapped at each check dams plus the sediments trapped downstream of that specific check dam.

The check dams located near the channel head (GW-08, F-09, and F-13) showed erosion in the area immediately downstream of the structure (Figure 29d). Figure 31b presents an example of an eroded plunge pool in GW-08. The volume of material eroded downstream of the wall was higher than the sediment trapped immediately upstream of the structures in three check dams.

During periods P2 and P4 some sediment deposited in the channel were partially removed by stream flow. Erosion of the channel was observed during both periods. Deposition in the check dams took place in P2 and P3 despite erosion prevailing in P2.

Figure 31 shows some detailed examples of the processes observed immediately downstream and upstream of some check dams. For example, Figure 31(a,a.1) shows the sediment deposition experienced at GW-03, while Figure 31(b,b.1) presents the plunge pool erosion that took place at three check dams. At GW-04, F-03, and F-05 the erosion observed immediately downstream was mainly concentrated in the left bank (Figure 31c). The fascines were located in a reach that suffered significant erosion before their installation. F-23 and F-24 stopped this erosive dynamic, but they did not retain any sediment. The effect of a fascine reducing lateral bank erosion with evidences of stabilization is shown in Figure 31d.

Table 11 presents the correlation coefficients for the relationships between the sediment volume retained in check dams and different topographic environmental variables. According to this analysis, the sediment volume retained in the check dams was positively correlated with the amount of sediment accumulated upstream (R = 0.934). We also found a positive correlation, though with lower values for the correlation coefficient, for the stream power index (R = 0.791), the drainage area (R = 0.724), and the check dam length (R = 0.654), with all these relationships being statistically significant at a confidence level of 95%.

The correlation coefficients between topographic environmental variables for all check dams and only GWs were similar (Table 11). The volume of sediments retained in the GWs was positively correlated with sediment accumulated upstream, followed by the stream power index and the connectivity index. On the contrary, the connectivity index presented a negative and weak correlation with respect to sediment volume for fascines.

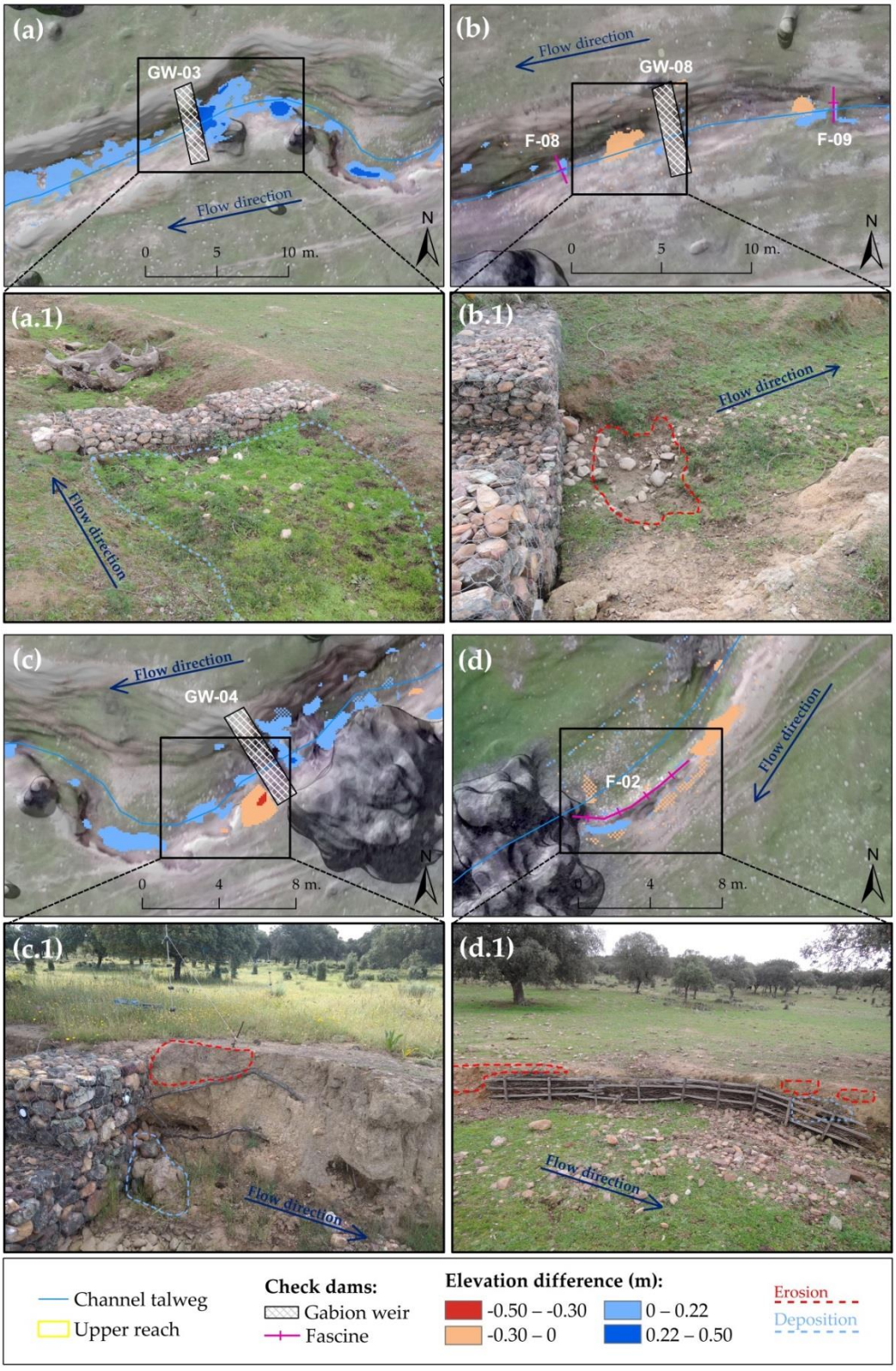

Figure 31. Detailed examples of processes observed close to some check dams through digital elevation model of differences (DoD) from February 2017 to January 2019 and photographs: (a,a.1) sediment deposition behind GW-03 and the corresponding photograph; (b,b.1) channel incision just downstream of GW-08 and the corresponding photograph; (c,c.1) lateral bank erosion downstream of GW-04 and a view of the area; (d,d.1) reduction of lateral bank erosion as result of the implementation of F-02 and the photograph of this geomorphological process. GW = gabion weir and F = fascine.

Table 11. Pearson correlation coefficient (r) between the sediment volume retained in check dams and topographic environmental variables (n = 8 gabion weirs, n = 25 fascines). * Statistically significant values ($p < 0.05$).

	Sediment volume (m^3)		
Variable	**All check dams**	**Gabion weirs**	**Fascines**
Drainage area (ha)	*0.724	*0.774	0.330
Check dam length (m)	*0.654	*0.739	–0.213
Check dam height (m)	0.609	0.311	–0.067
Upstream check dams (n)	0.506	0.691	0.372
Slope of the catchment (◦)	–0.080	0.529	–0.387
Upstream accumulated sediments (m^3)	*0.934	*0.913	0.143
Channel length (m)	*0.648	*0.720	0.263
Stream power index	*0.791	*0.814	0.325
Tree density (trees ha^{-1})	0.637	*0.807	0.192
Connectivity index	0.507	*0.810	*–0.407
Path density (km ha^{-1})	0.242	0.091	0.257

The orthophotograph from 2016 was used to map a total of 82 headcuts, from which 48 were located along the channel and 38 were bank headcuts. Figure 32 displays the growth of some headcuts at different reaches. Four active headcuts were observed in the tributary (Figure 32a) with a mean headcut retreat of 0.87 m^2 (Figure 32d), ranging from 1.33 m^2 to 0.63 m^2 between March 2016 and January 2019.

Figure 32b and 32c presents details of the restored reach; specifically, Figure 11b shows the two types of restoration activities: check dams and isolation by fencing. Eight bank headcuts were isolated within the fenced area in the left bank of a strongly degraded reach (i.e., between GW-04 and GW-05). The mean headcut retreat for these eight headcuts was 0.11 m^2 (Figure 32d). Four of the eight bank headcuts in the isolated area did not grow after the fencing and some evidences of revegetation were observed there. Figure 32c shows the growth of some headcuts, similar to Figure 32b but in an unfenced area of the upper reach. There, the mean headcut retreat was 0.43 m^2 between March 2016 and January 2019. The largest retreat was 0.54 m^2 and was observed in a headcut located in a new channel parallel to the main channel. On the contrary, the smallest retreat was 0.24 m^2, in a headcut of the main channel. Two kinds of bank headcuts were observed in the channel. We observed classic bank headcuts that usually grow perpendicular to the channel and headcuts captured by cattle paths parallel to the gully (Figure 32b) (Gomez-Gutierrez et al., 2018).

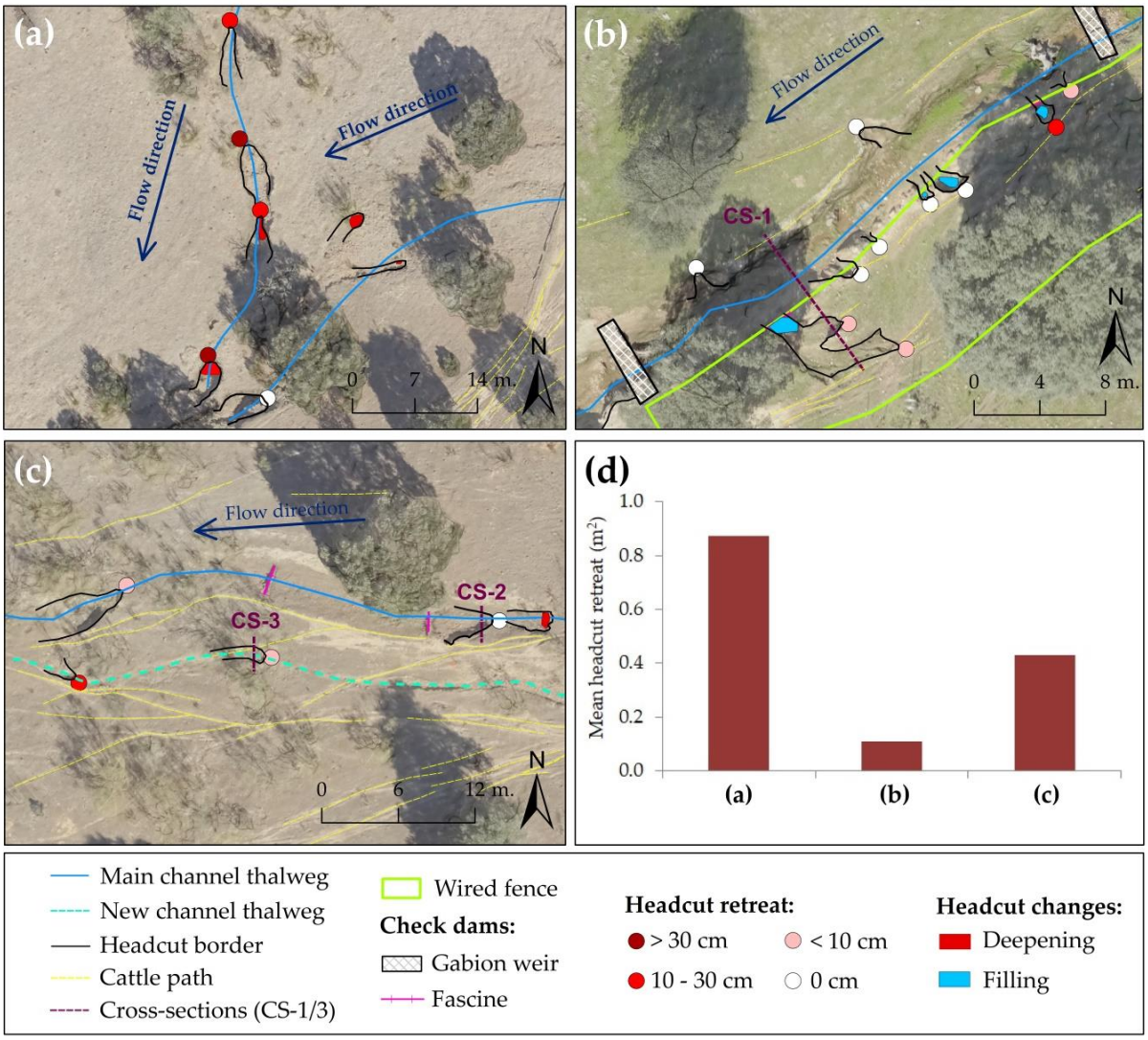

Figure 32. Headcut retreat at different locations: (a) the junction between the tributary and the upper reach forming the main channel; (b) a part of the upper reach with bank headcuts that were fenced to protect against livestock; (c) a part of the upper reach with unfenced headcuts at the left bank of the upper reach; and (d) mean headcut retreat (expressed in m^2) of the reaches shown in this figure during the period with restoration measures (February 2017–January 2019).

Figure 33 presents three CSs of the gully (displayed in Figure 32) before and after the installation of the restoration measures. The bank headcuts and the channel at CS-1 experienced incision before the installation of the restoration measures. However, this erosive dynamic changed to deposition after the restoration activities (Figure 33a). Incision before restoration activities and deposition after the works was also observed at CS-2 (Figure 33b). Finally, the only CS where incision could be observed after the installation of the restoration measures was CS-3 (Figure 33c).

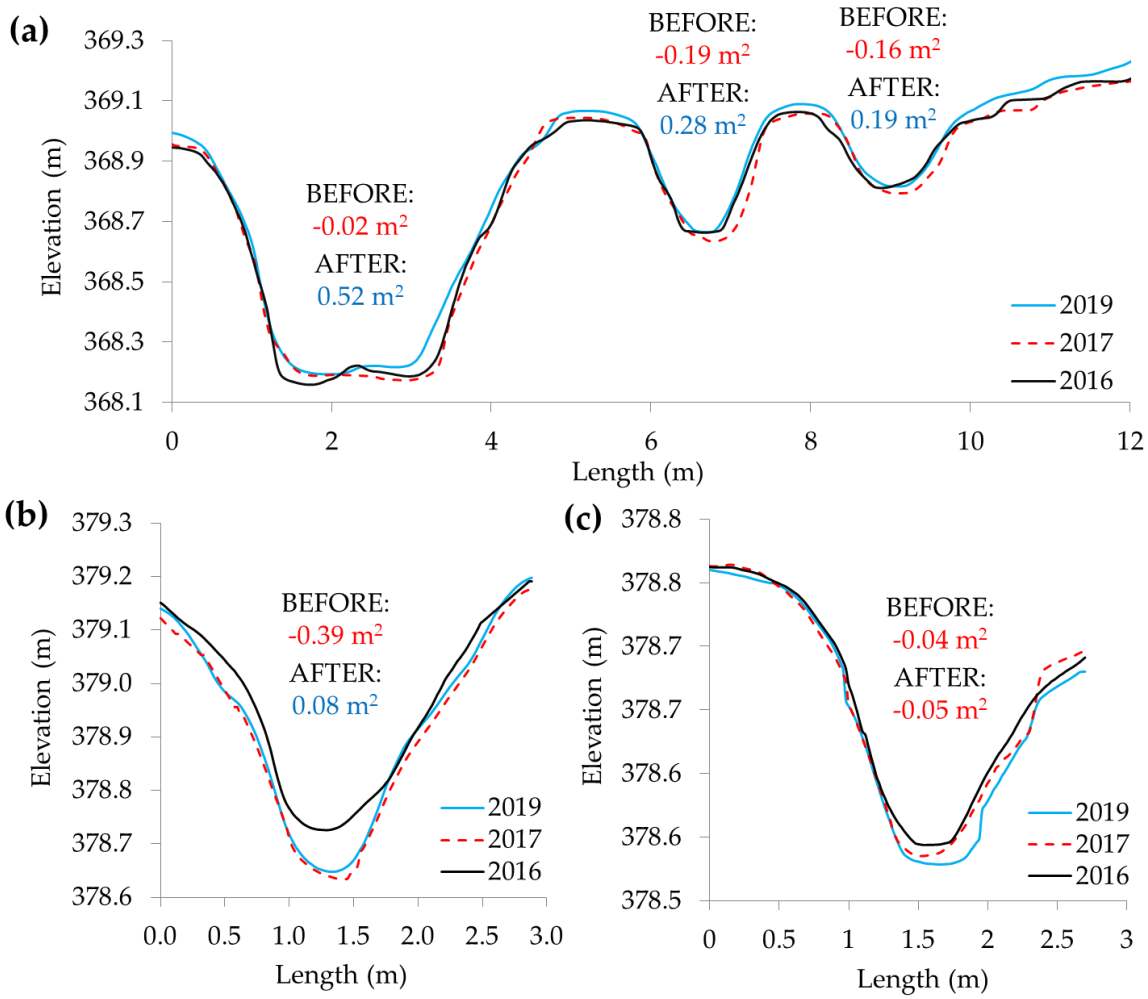

Figure 33. Cross sections (CSs) indicated in Figure 32: (a) CS-1, (b) CS-2, and (c) CS-3, before the installation of the restoration measures (2016) and afterwards (2017–2019).

5.3.4. Micromorphology and topographic change

Planform and profile curvature, computed for the DEM from February 2017, were plotted versus topographic change experienced between 2017 and 2019 (Figure 34). Note that the signs for convexity and concavity in profile curvature are opposite of planform curvature, i.e., negative indicates convexity while positive indicates concavity. Erosion prevailed at convex features in the perpendicular direction to maximum slope for 65.7% of the erosion pixels, while the majority of pixels that experienced deposition correspond to concave features in the 2017 DEM (56.5% of the pixels). A similar pattern is observed for profile curvature (Figure 34b), with the majority of pixels that registered erosion (73.5%) located at convex pixels in the direction of the steepest slope and deposition corresponding mainly to pixels with concave profile curvature (65.9%).

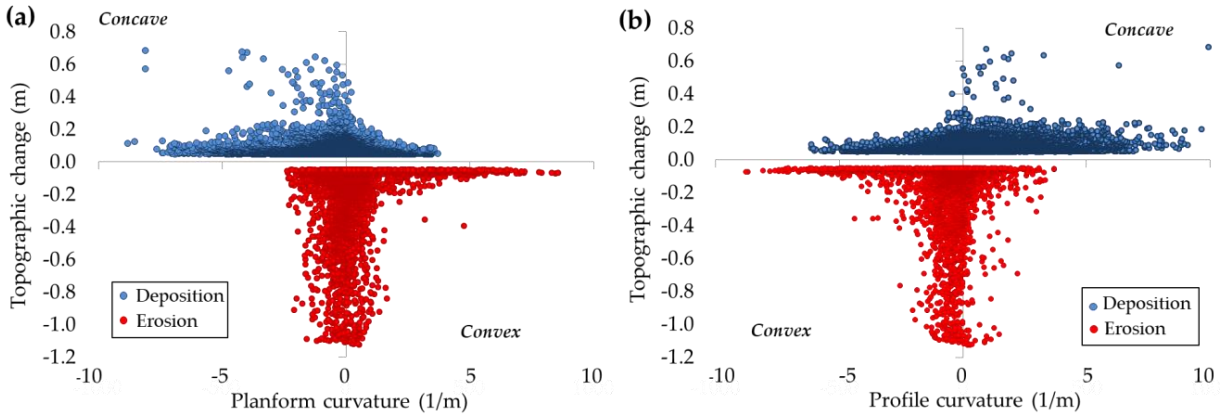

Figure 34. (a) Gully planform curvature and (b) profile curvature derived from 2016 digital elevation model (DEM) and compared to erosion (red) and deposition (blue) for the whole channel during the period 2016–2019.

Figure 35 plots profile curvature and topographic change registered behind the check dams for P2 and P3. The profile curvature was derived from the DEMs from February 2017 and October 2017 and was plotted versus the topographic change experienced behind check dams for P2 and P3, respectively. The results indicate that deposition behind check dams during P2 and P3 mostly took place on concave and flat surfaces, due to the filling of previously concave areas. The deposition during P2 prevailed on concave areas for 44% of the pixels. The deposition during P3 predominated on concave areas for 38% of the pixels. These results indicate an increase of convexity and the transition from concave to plan and/or convex morphology behind the check dams.

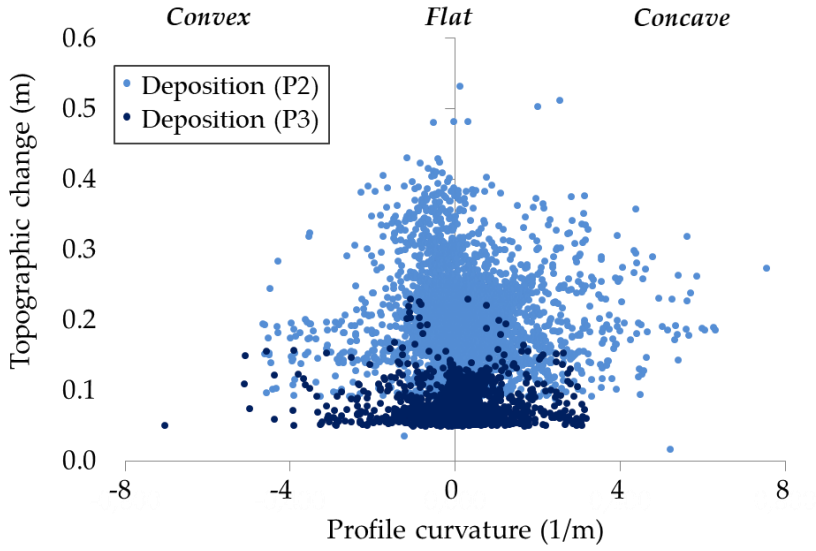

Figure 35. Profile curvature derived from 2017 digital elevation model (DEM) and compared to deposition behind check dams in P2 and in P3 by the DEMs of difference (DoD).

The local slope gradient played an important role in determining whether a pixel will experience erosion or deposition. As expected, the initial slope at pixels that later experienced erosion was significantly higher than those that registered sedimentation (Figure 36), at a confidence level of 95%.

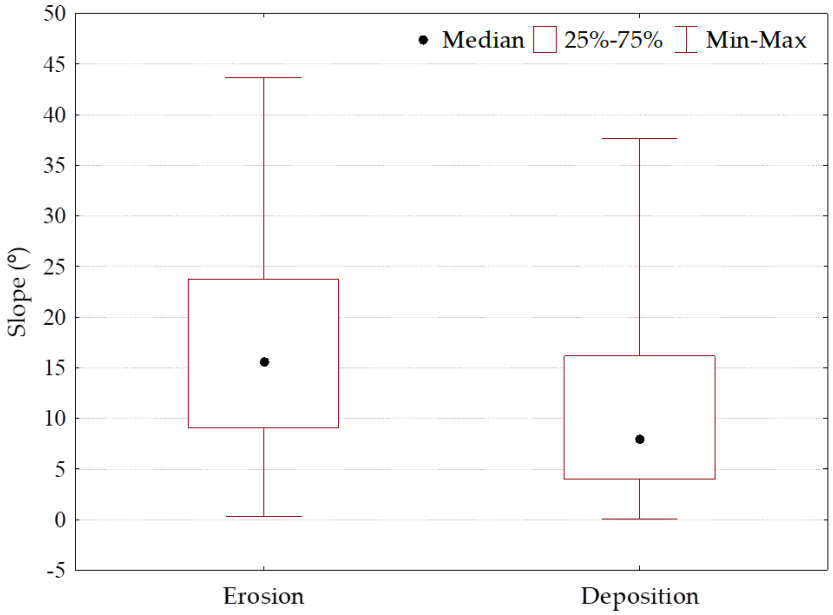

Figure 36. Initial slope gradient (calculated using the DEM from 2016) for pixel that experienced erosion or deposition from 2016 to 2019 ($p < 0.05$).

Regarding channel slope gradient, a slight decrease was observed after the construction of the check dams, mainly at the GWs' location (Figure 37). The average slope gradient of the reach between GW-01 and GW-04 in 2016 and 2019 was 2.9% and 2.3%, respectively. In some places, like the area restored using fascines, the slope of the channel remained stable.

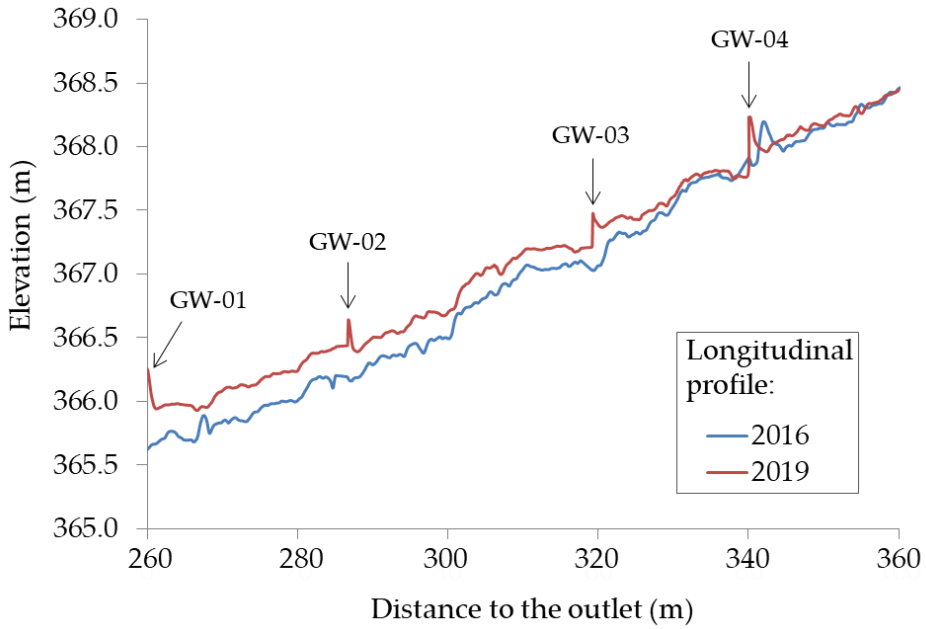

Figure 37. Longitudinal profile of the channel between GW-01 and GW-04. GW = gabion weir.

5.4. Discussion

In this section, we first discuss the uncertainties of the cartographic products acquired using the UAV and the SfM photogrammetry to detect topographic changes in a valley-bottom gully. Afterwards, the spatial pattern of the topographic changes registered before and after restoration activities is discussed. Finally, the effectiveness of the restoration measures (i.e., check dams and livestock exclusion) is also analyzed.

5.4.1. Using SfM photogrammetry to detect topographic changes

Unmanned aerial vehicles and SfM photogrammetry enable detailed quantification and characterization of geomorphic processes in gullies (Gomez-Gutierrez et al., 2018; Kaiser et al., 2014). The combined use of UAV platforms and photogrammetric techniques may be an interesting alternative to classical methods such as the topographic survey of CSs used in previous studies carried out in the same channel (Caraballo-Arias et al., 2016; Gómez-Gutiérrez et al., 2012). In comparison to other topographic techniques, the methodology used here reduced field work to one day for each flight (one UAV pilot and one GNSS operator) covering the whole channel. The fixed-wing UAV provided 30-min flight times on average to cover areas of 23 ha,

acquiring 2-cm resolution images with a longitudinal and lateral overlap of 90%. The processing time of the data sets to produce the point cloud, the DEM, and the orthophotograph was four hours on average (using an Intel Core i7 CPU at 2.50 GHz with 8GB RAM, GPU Intel HD Graphics 4600).

The georeferencing error influences the quality of the resulting DEM and, hence, the estimation of the topographic changes. The number and spatial distribution of GCPs are critical elements that influence the accuracy of the results (e.g., James and Robson, 2014; Midgley and Tonkin, 2017). There are different criteria for establishing the number and distribution of GCPs to minimize georeferencing errors in the evaluation of geomorphological changes: (1) A well-distributed network of GCPs (James et al., 2020; Shahbazi et al., 2015), (2) a densification of GCPs near the areas of interest (i.e., within the channel or close to the banks) (Fonstad et al., 2013; Smith et al., 2014), and (3) a minimum of 15 GCPs in surfaces with more than 18 ha (Agüera-Vega et al., 2017). A combination of the three criteria was considered here to achieve optimal results. The importance of GCPs goes beyond the georeferencing and the coregistration of the DEMs as they are also used for the camera self-calibration procedure (i.e., camera parameters are refined on the basis of GCP accuracy).

Several factors that may add or increase errors in the estimation of topographic changes are the presence of vegetation and water over the surface. An important limitation of the proposed methodology is the unsuitability of SfM techniques to capture topography in areas with dense vegetation cover (Gómez-Gutiérrez et al., 2014; Niculiță et al., 2020; Westoby et al., 2012). In our study, 9% of the channel was not considered for the analysis because of the occlusion produced by vegetation. The use of other sensors and techniques (e.g., LiDAR) may provide solutions that overcome this limitation. UAV-based LiDAR survey to acquire DEMs shows a satisfactory capability to estimate geomorphic changes as vegetation and ground pulse returns can be differentiated (Cavalli et al., 2008; Swetnam et al., 2018). Vegetation prevents direct observation of the ground surface for photogrammetric techniques (Castillo et al., 2012; Cook, 2017; Tonkin et al., 2014). In particular, woody vegetation hides the topography while the herbaceous vegetation may cause an overestimation or underestimation of surface height. We managed to correct the error produced by vegetation cover, besides topography, using the FIS error estimation. Slope gradient was included as a variable that is spatially autocorrelated with the DEM error (Wheaton et al., 2010). The DEM error is usually large at steep slopes due to low point density in these areas (Esposito et al., 2017; Milan et al., 2011). The grassland cover

may produce an overestimation of erosion or deposition (depending on the seasonal growth and sequence of grassland cover). For instance, in the DoD from October 2017 to March 2018 positive values due to grassland cover were identified and removed in very steep slopes or almost vertical banks where only erosion can take place. In this study, the grassland cover was detected through a supervised classification of the orthophotographs. Subsequently, a minimum level of detection (minLod) based on the average height of the grasses was applied. For example, in the DoD from 2017 to 2018, 347.6 m^2 within the channel (i.e., 10.2%) were classified as grassland cover, and this surface would result in an overestimation of 41.7 m^3 of sediments for an average height of 12 cm. The height and extent of grassland cover in dehesas show a high temporal (annual and seasonal) variability governed by rainfall and a high spatial variability influenced by pasture management (Cubera and Moreno, 2007; Pulido et al., 2018).

Regarding the existence of water, ephemeral streams only show water in the channel during and immediately after moderate or important precipitation events. The presence of water in the channel may represent a limitation because reflective, glossy, or transparent objects are not reconstructed in a reliable way (Cucchiaro et al., 2018; Gómez-Gutiérrez et al., 2014). In our study, the submerged surface of the channel was negligible because the gully only drives ephemeral flows, but for channels with permanent flow there are successful applications of SfM photogrammetry to reconstruct these submerged surfaces (e.g., Visser et al., 2019; Woodget et al., 2015).

5.4.2. Gully dynamics before and after the restoration measures

The restoration activities modified, notably, the incision and deposition dynamic. This work focused on short-term or medium-term changes (from 2017 to 2019) and a longer timespan would be necessary to characterize long-term changes induced by the restoration activities. We also exploited data sets produced by Gómez-Gutiérrez et al. (2009a) and Gómez-Gutiérrez et al. (2012), who mapped the area affected by gullying for the period 1945–2006 and analyzed gully dynamics through 28 fixed CSs from 2001 to 2007.

The incision dynamics of the gully in Parapuños were episodic, complex, and deter- mined by extrinsic (climatic, anthropogenic) and/or intrinsic factors (inherent to the gully itself, e.g., changing channel geometry), both performing at the same time. Two incision cycles (1945–1956 and 1998–2016) were observed before the restoration activities in 2016 and attributed to land use and management changes. This

growth of the gullied area in Parapuños was observed by Gómez-Gutiérrez et al. (2009a) and attributed to the increase of the cultivated surface in the catchment between 1945 and 1956. From 1998 to 2016, a new growth episode of the gullied area was observed, coinciding with an important increase in livestock density (from 0.30 to 2.99 AU ha^{-1}) and a slight increase in the cultivated area within the catchment. According to Gómez-Gutiérrez et al. (2009a), the increase of livestock density was influenced by the Common Agricultural Policy (CAP) that promoted excessive stocking rates. Overgrazing has been described as a crucial factor in the development of gullying processes in dehesas (Gómez-Gutiérrez et al., 2009a). Animals provoke mechanical erosion of the soil, causing soil compaction, decreasing soil infiltration capacity, and increasing overland flow. Overgrazing has also played a key role in the development of gullies in Ecuador (Podwojewski et al., 2002), New Zealand (Gomez et al., 2003), Ethiopia (Nyssen et al., 2004), Chile (Mieth and Bork, 2005), and Italy (Zucca et al., 2006). Between the two incision periods, i.e., from 1956 to 1998, the area affected by gullying decreased from 1560 to 605 m^2 due to the abandonment of the agricultural activity and the revegetation of the valley bottom. These results indicate that valley-bottom recovery is plausible without restoration activities, i.e., just relaxing land use intensity, but this situation is improbable in such a lowly profitable exploitation system.

The restoration activities may be considered as an extrinsic anthropogenic force that promoted gully filling and the reduction of bank erosion. The stabilization of the gullied area was related to restoration measures established in the channel in February 2017. Moreover, in the reaches where erosion was observed before the check dam construction, deposition was registered after restoration activities. In the reaches where deposition was observed before the check dam construction, a larger amount of sediment was detected after the check dam construction. The predominance of depositional processes in the channel indicates that the catchment is producing sediments that reach the channel and cannot be evacuated by the concentrated flow. The deposition observed in the channel comes from the sediments eroded at hillslopes by sheet wash and from the gully itself. Former studies confirmed the important supply of sediments from the hillslopes (Rubio-Delgado et al., 2014) to the valley bottoms in the recent history of dehesas.

In this work, the restoration strategy focused on the channel, which is recommended in this type of environment where most of the water resources are stored in the valley bottoms. The existence of gullies in valley bottoms increases

hydrological connectivity and favors the loss of water resources (Avni, 2005; Poesen, 2011). The restoration measures focused on the channel may promote the retention of water and sediments. At the same time, these sediments fill the channel, favoring more revegetation and water retention (Zema et al., 2014). On the other hand, restoration strategies that do not focus only on the channel, and, therefore, include the whole catchment, are commonly more effective at long-term temporal scales (Bartley et al., 2020). The restoration strategies focused on recovering vegetation cover in a catchment reduce runoff and slow the transfer of sediments from hillslopes to valley bottoms. Nevertheless, the application of integral strategies may present limitations in dehesa environments for two reasons: (1) the low profitability or productivity of the economic activities and (2) the difficulty of carrying out a reforestation due to the presence of cattle (Moreno and Pulido, 2009). The results of our work suggest an immediate effect of the restoration activities implemented in the channel but an integral and combined strategy (i.e., considering the whole catchment and the channel) may support the sustainability of the dehesa ecosystem at a long-term temporal scale.

Climatic fluctuations perform as extrinsic factor for gully genesis and development in semi-arid areas (Leopold, 1966; Nogueras et al., 2000). The infilling periods were characterized by a large number of rainfall events (i.e., between 25 and 30 rainfall events) with high amounts of precipitation (i.e., between 480 and 550 mm), while the incision periods registered between 1 and 19 rainfall events with 105 and 340 mm.

After the restoration activities, the deposition in the upper reach was higher than sedimentation registered at the lower reach and the tributary. An interesting finding is that no significant changes in the dynamics of the gully were observed downstream the restored reach. After check dam establishment, aggradation processes were prevalent in the upper reach but incision was also observed in recently filled areas. This removal of recent sediment deposits suggests the occurrence of scour cycles, as already observed by Gómez-Gutiérrez et al. (2009a).

Former studies carried out in Parapuños and similar environments estimated soil erosion rates due to gully erosion, which are presented in Table 12. These studies registered net erosion and described gullies as dynamic erosive forms. In Parapuños catchment, the gully erosion rate between 2001 and 2007 was estimated at –0.04 m^3 ha^{-1} y^{-1}. In a cultivated area located in Alentejo region, the gully erosion rate between 1970 and 1985 was estimated at –3.2 m^3 ha^{-1} y^{-1}. Our results suggest a general

depositional dynamic that was particularly important in the restored reach (i.e., the upper reach) and after the restoration activities. Before the restoration measures were implemented, the sediment deposition rate for the whole channel was 0.48 m^3 ha^{-1} y^{-1} against 0.25 m^3 ha^{-1} y^{-1} after the restoration activities. However, 42% of the deposition in the channel occurred in the restored upper reach before the construction of the check dams, while 86% of the deposition took place in this reach after restoration.

Table 12. Gully erosion rates in Parapuños and other agrosilvopastoral systems.

Source	Location	Period	Gully erosion rate
This work	Parapuños catchment (SW Spain)	2017–2019	0.25 m^3 ha^{-1} y^{-1}
This work	Parapuños catchment (SW Spain)	2016–2017	0.48 m^3 ha^{-1} y^{-1}
(Gómez-Gutiérrez et al., 2012)	Parapuños catchment (SW Spain)	2001–2007	–0.04 m^3 ha^{-1} y^{-1}
(Schnabel, 1997)	Guadalperalón catchment (SW Spain)	1990–1997	–0.15 m^3 ha^{-1} y^{-1}
(Poesen et al., 1996)	Alentejo region (SE Portugal)	1970–1985	–3.2 m^3 ha^{-1} y^{-1}

5.4.3. Effectiveness of the restoration measures

The overall performance of the restoration activities in the channel to control gully erosion was satisfactory. Since their installation, GWs and fascines were effectively reducing lateral bank erosion and favoring sediment deposition. The check dams located near the headwater retained less sediment than those located downstream. For example, the volume of sediments deposited in the reach between GW-01 and GW-04 increased 4-fold after check dam establishment, while the sediments accumulated in the reach between GW-04 and GW-08 increased 3-fold. In contrast, the reaches restored using fascines increased 2-fold the amount of deposited sediments. A similar spatial pattern has been described in the literature (Bussi et al., 2013; Romero-Díaz et al., 2007b) and explained by the reduced flow velocities at the downstream reaches. The accumulation that took place in the check dams reduced channel slope, decreasing flow energy and favoring (in a positive feedback mechanism) again sedimentation, as observed between GW-01 and GW-04. Despite most of the sediments being trapped at downstream check dams, upstream check dams may play an important role stabilizing the channel bed (Zema et al., 2014), laminating floods, and reducing flow velocity. Therefore, the effectiveness of the restoration activities in the

channel should be considered as a whole system of elements working together. The efficiency of restoration activities focused on the channel is limited in time (Zhao et al., 2017) as check dams have a finite capacity to retain sediments. The useful life of a dam is defined as the time from the construction to the complete siltation (Quiñonero-Rubio et al., 2016). For example, GW-01 and GW-04 will be silted in a range of 3.2 to 3.7 years from January 2019 with the current deposition rates.

The Parapuños catchment is a water-limited environment with a mean annual rainfall of 513 mm and high seasonality. The soils, mainly in hillslopes, are shallow with small water retention capacity, and the existence of a valley-bottom gully favors the transfer of water and sediments from the valley bottoms to the outlet. In such a water-limited environment, the role of valley bottom soils collecting and retaining water resources is crucial. The restoration activities implemented in the channel decreased sediment and flow connectivity, trapped sediments, and promoted the retention of water in valley bottoms. The availability of water favors an increase in grass quantity for livestock.

Two main drawbacks were observed as a consequence of the restoration activities: (1) three check dams (GW-08, F-09, and F-13) experienced soil erosion immediately downstream of the wall and (2) the permanent visual impact of GWs in the landscape. The erosive process that takes place immediately downstream of the wall may undermine check dam stability and has been described as a common side effect, besides changes in the hydrological regime and channel morphology (e.g., Boix-Fayos et al., 2007; Castillo et al., 2007; Ramos-Diez et al., 2016). The GWs were designed with a central spillway that allows the evacuation of important floods that result from heavy rains. Every GW generates a small waterfall that may produce channel bed erosion. This process was only observed at check dams where bed materials were mainly fine sediments. In order to minimize soil erosion immediately downstream of the wall, these areas may be protected using coarse rock fragments.

The electric shepherd installed as an isolation measure promoted the recovery of the bank headcuts located within the fence. This measure was already proposed by Gomez-Gutierrez et al. (2018) as pasture management strategy for agrosilvopastoral systems with the goals of isolating degraded areas from livestock, forcing animals to cross the channel at specific places, and excluding them from the valley bottoms, particularly in periods of soil saturation (i.e., high soil moisture content) and rain. This type of restoration measure was also proposed by Shellberg et al. (2013) in alluvial

gullies in Australia. Cattle management through fencing, excluding animals from the most degraded areas, may reduce chronic soil disturbance and increase grass cover, which can protect soils from rainfall and runoff. An interesting strategy would be to prevent livestock access to the valley bottom with saturated soils through effective livestock management from a spatio-temporal viewpoint (e.g., holistic management) and taking into account the seasonal evolution of the vegetation cover (Lozano-Parra et al., 2018). The mechanical effect of animals in the soil is amplified under high soil moisture content. This kind of rehabilitation measure (i.e., livestock exclusion measure) in degraded areas may be useful and cost effective in reducing gully erosion in specific and much degraded hotspots in agrosilvopastoral systems.

In nonfenced areas, cattle can cross the channel and transit through the valley bottom, promoting the development of cattle paths and the formation of bank headcuts. Cattle paths increase the connectivity of flow and sediment coming from the hillslopes, favoring these bank headcuts (Gomez-Gutierrez et al., 2018). The influence of cattle is so strong that the cattle paths influenced the development of a new channel parallel to the main channel in the upper reach, as observed by Gomez-Gutierrez et al. (2018). The diversion of flow from the main channel in this part of the upper reach has promoted its recovery in terms of revegetation and sedimentation.

Channel restoration based on check dams is a common strategy in the region. A recent study carried out in the dehesa boyal of Monroy (DBM) (Alfonso-Torreño et al., 2019) estimated a sediment deposition rate of 0.070 m^3 ha^{-1} y^{-1} at 116 check dams during the period 1994–2017. Our results showed a deposition rate (0.005 m^3 ha^{-1} y^{-1}) that was lower than in DBM. Many factors may support this difference: (1) different length of the study periods with variations of rainfall and flood discharge production producing fluctuations of the sediment deposition rate in time, (2) check dams' characteristics (design, materials, and length), (3) land use intensity, with DBM being a communal farm operated by different managers in time, and (4) topography. Presumably, topography, check dam length, and land use played an important role in the differences observed between deposition rates in Parapuños and DBM. For example, Parapuños showed an average slope of 8% while DBM presented an average slope gradient of 18%. In terms of check dam locations, Parapuños presented check dams with a distance of less than 10 m between them (e.g., between F-06 and F-18) and which retained small amounts of sediment. In DBM, the distance between check dams is slightly greater than Parapuños but the slope gradient is higher. The distances between consecutive check dams have to be considered as a function of slope gradient

and drainage area (Hassanli and Beecham, 2013). A large distance between consecutive check dams will cover a larger, drained area and may lead to higher sediment volume behind check dams. Regarding land use intensity, a total of 12 farmers rented the communal farm (i.e., DBM) for livestock rearing during the last two decades, sometimes carrying out intensive and unsustainable land use. The livestock density experienced a different evolution in Parapuños and DBM in the last decades. In Parapuños, the livestock density grew since 1998 while a decrease was observed in DBM since 2003. The check dams with the highest volume of sediments in DBM were built in a time with very high livestock density (i.e., 1.95 AU ha^{-1}). Nevertheless, the sediment deposition rate in DBM and in Parapuños is of the same order of magnitude (0.01 m^3 ha^{-1} y^{-1} and 0.005 m^3 ha^{-1} y^{-1}, respectively) when only the sediment deposition rate in check dams (n = 33) with similar catchment conditions are considered, i.e., slopes of ~10%, stream power index of ~127, and check dam length of approximately 8 m.

5.5. Conclusions

Multi-temporal topographic surveys using a UAV and SfM photogrammetry allowed us to analyze the effectiveness of restoration activities implemented in a valley-bottom gully in a wooded rangeland catchment. Topographic changes were determined through the DoD approach and the FIS method was used to integrate spatially variable errors. In addition, previous studies conducted in Parapuños allowed us to understand the dynamics of the gully at medium- and long-term temporal scales and to compare with the recent channel dynamics.

The performance of the restoration activities to control gully erosion was satisfactory. The stabilization of the gullied area was related to restoration measures in the channel. GWs and fascines were effective in favoring sediment deposition and reducing lateral bank erosion. A spatial pattern of the stored sediments was observed, with check dams located near the headwater retaining less sediment than those situated downstream. The sediments deposited in the lower part of the restored reach increased 4-fold in comparison with the period before check dam construction. The sediments retained behind check dams reduced the slope of the channel bed and established a positive feedback mechanism for channel revegetation. The fenced-isolated area installed in a strongly degraded area promoted the stabilization of four bank headcuts with evidences of revegetation. Before the restoration activities two incision cycles were observed and were attributed to land use and management changes, with overgrazing playing a key role in the growth of the gully. From 2016 on,

the gully showed general depositional dynamics, being particularly important in the upper reach. Deposition in the upper reach, where check dams were installed, was higher than sedimentation registered at the lower reach and the tributary. Despite deposition prevailing on concave areas, deposition on flat and convex areas increased. The predominance of depositional processes in the channel was attributed to sediments produced by sheet erosion at hillslopes, as well as erosion of the gully itself. Despite the predominance of net deposition in the channel, a high spatial variation of processes was observed. These processes included: channel aggradation along the channel bed and behind the check dams, channel bed incision, lateral bank erosion and bank collapse, deepening and widening in headcuts, and eroded plunge pool. Furthermore, erosion was also observed immediately downstream of three check dams.

A sustainable land management, including adequate cattle grazing practices, is needed to ensure that no new gullies are initiated and to stabilize already existing gullies. The results obtained here are also valuable for analyzing the evolution of a valley-bottom gully and the geomorphological processes in dehesa landscapes and to understand the role of restoration measures in gullies.

Author Contributions: Conceptualization, A.A.-T. and Á.G.-G.; methodology, A.A.-T. and Á.G.-G.; validation, A.A.-T. and Á.G.-G., formal analysis, A.A.-T., Á.G.-G. and S.S.; investigation, A.A.-T., Á.G.-G. and S.S.; resources, Á.G.-G. and S.S.; writing—original draft preparation, A.A.-T.; writing— review and editing, A.A.-T., Á.G.-G. and S.S.; supervision, Á.G.-G. and S.S.; funding acquisition, Á.G.-G. and S.S. All authors have read and agreed to the published version of the manuscript.

Funding: This work was financed by the Spanish Ministry of Economy and Competitiveness (CGL2014-54822-R) and A.A.-T. was supported by a predoctoral fellowship (PD16004) from Junta de Extremadura and European Social Fund.

Institutional Review Board Statement: Not applicable.

Informed Consent Statement: Informed consent was obtained from all subjects involved in the study.

Data Availability Statement: Summarized data are presented and available in tis manuscript and rest of the data used and/or analyzed are available from the corresponding author on reasonable request.

Conflicts of Interest: The authors declare no conflict of interest.

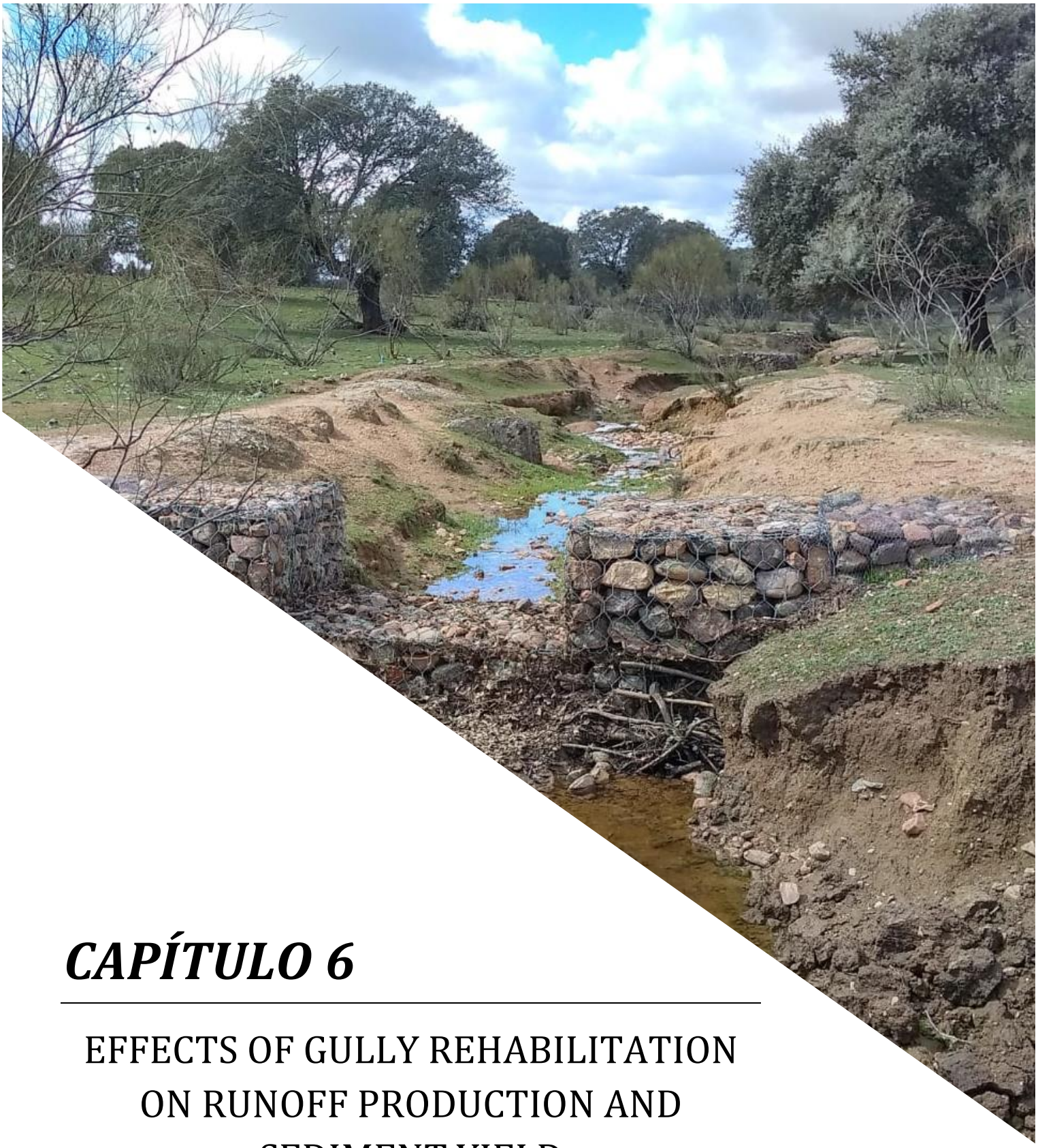

CAPÍTULO 6

EFFECTS OF GULLY REHABILITATION ON RUNOFF PRODUCTION AND SEDIMENT YIELD

CAPÍTULO 6. EFFECTS OF GULLY REHABILITATION ON RUNOFF PRODUCTION AND SEDIMENT YIELD

Alfonso-Torreño, A., Schnabel, S., Gómez-Gutiérrez, Á., Crema, S., Cavalli, M., 2021. Effects of gully rehabilitation on runoff production and sediment yield. Catena *[In revision]*

Abstract

Gully rehabilitation is often applied as part of catchment management aimed at reducing downstream sediment yields. However, the influences of restoration measures on the runoff and sediment transport processes in agroforestry systems were seldom studied. In this paper, a thorough analysis of these processes was carried out. A gully was monitored before and after different restoration activities that included: gabion weirs, fascines and isolation measures. The aims of this work are (1) to analyze the effect of the restoration measures on the geomorphic changes in the channel, the hydrological dynamics and sediment load, and (2) to evaluate the effect of the restoration activities on the spatial patterns of sediment connectivity at the catchment and channel scales. Changes in topography and connectivity were estimated using sequential high–resolution Digital Elevation Models (DEMs) generated by Structure–from–Motion (SfM) photogrammetry from aerial images acquired by an Unmanned Aerial Vehicle (UAV). Discharge and suspended sediment were monitored at the outlet. The results showed that total suspended sediment load was substantially lower after check-dam construction. These treatments, however, had a lesser effect on silt and clays. The sediment deposited behind check dams contained less fine fractions than other locations in the catchment and the highest content of coarse elements. The integration of the difference of connectivity index (DoIC) with DEMs of Difference (DoD) maps highlighted the impact of the restoration measures on changes in sediment connectivity. A strong relationship between gully dynamics and functional connectivity was observed. The connectivity index (IC) increased in eroded areas, while deposition sites showed a decrease of the IC. Connectivity also decreased in the bank headcuts located within the isolated area. The implementation of the restoration measures in the channel was successfully and had beneficial effects in the short–term, but their effects are still unknown in the long–term.

Keywords: sediment load, flood discharge, restoration, sediment connectivity, multi–temporal analysis.

6.1. Introduction

Soil erosion is one of the main factors leading to land degradation worldwide, being water erosion the dominant process (Bakker et al., 2004; Boardman et al., 2003; Zhao et al., 2019). The Mediterranean region is prone to soil erosion by water due to intense rainfall events and long–lasting droughts, steep slopes combined with complex and rough terrain and the human activity reflected in the recurrent use of fire, farming and overgrazing (García-Ruiz et al., 2013). In the southwestern part of the Iberian Peninsula, a semi–natural landscape with an agro–silvopastoral land use system, named dehesa, covers more than 4 million ha. Although the largest extension is found in the southwestern part of the Iberian Peninsula, there are similar agroforestry systems in the whole Mediterranean region. It is formed by cleared oak woodlands with an annual grassland understory that is grazed by cows, sheep, pigs and horses (Eichhorn et al., 2006). The sustainability of the dehesa ecosystem is threatened by deforestation, overgrazing and land use changes (Herguido Sevillano et al., 2017; Pulido et al., 2018) which contribute to the generation of runoff and sediment yield in this landscape (Schnabel et al., 2010). Soils in dehesas are commonly shallow, except for the valley bottoms where they are deeper.

The dominant erosive processes in most of grazed woody grasslands are sheetwash in hillslopes and gully erosion due to concentrated flow in valley bottoms. In dehesas, soil erosion by water was studied in two small experimental catchments with similar topographical and environmental conditions, called Guadalperalón (Schnabel et al., 2010) and Parapuños (Alfonso-Torreño et al., 2021; Gómez-Gutiérrez et al., 2014; Gómez-Gutiérrez et al., 2012; Gómez-Gutiérrez et al., 2009a; Schnabel et al., 2013), being the latter the study area of the present work. Parapuños experimental catchment can be considered a model of the dehesa exploitation system for its representativeness. At the same time, the existence of previous research sets the basis for a medium–term analysis of the hydrological and sedimentological behavior of the catchment and for the investigation of hillslope–to–channel connectivity. These former studies determined an average sheet erosion rate of 0.63 t ha^{-1} y^{-1} at hillslopes (Schnabel, 1997; Schnabel et al., 2010), while gully erosion produced an average loss that varied from 0.07 t ha^{-1} y^{-1} (Gómez-Gutiérrez et al., 2012) to 1.55 t ha^{-1} y^{-1} (Schnabel et al., 2010). More recent studies in dehesas estimated soil erosion rates in the order of 18.5 t ha^{-1} y^{-1} from 1881 to 2014 (Rubio-Delgado et al., 2017; Rubio-Delgado et al., 2018), using exposed tree roots and ^{137}Cs. However, there is a lack of information regarding the relationship between gully erosion and catchment hydrological behavior, mainly due to the

difficulties to carry out a continuous and long term monitoring of topographic channel changes, rainfall and discharge (Gómez-Gutiérrez et al., 2012). Summarizing, previous studies quantified soil erosion rates, studied the causes and factors that encouraged soil erosion and highlighted the problem of soil degradation by water erosion in dehesas.

In order to restore degraded areas affected by gullying different strategies have been applied (Frankl et al., 2021; Heede, 1978; Pathak et al., 2005). According to Frankl et al. (2021), restoration activities may be conducted at different spatial scales, and can be grouped as follows: (1) treating the catchment with measures including livestock control, soil bunds, infiltration ditches, revegetation or water−retention measures such as ponds; (2) installing devices in the gully such as sediment traps, check dams, rockfills or breakwaters; (3) actions taken adjacent to the gully such as livestock exclosure by fencing to avoid the mechanical effect of animal movement; and (4) a combination of all three approaches (Bartley et al., 2020). In Mediterranean areas check dams are often used, sometimes in combination with other measures (Alfonso-Torreño et al., 2019; Castillo et al., 2007; Quiñonero-Rubio et al., 2016). Nevertheless, only few restoration initiatives were implemented in the dehesa ecosystem and evaluation of the effectiveness of those measures is nearly absent. A recent exception is the work by Alfonso-Torreño et al. (2019) who calculated the sediment volume deposited behind 160 check dams in a dehesa in SW Spain. These results showed a high spatial variability in sediment deposition, with larger volumes of material accumulated in the lower areas of the catchment if compared to the upper parts featuring a high hydrological connectivity. In a recent study, Alfonso-Torreño et al. (2021) found that the restoration activities implemented in the Parapuños channel favored stabilization of the gully, favoring sediment deposition and reducing the slope of the channel bed. If on the one hand there is growing attention in the literature in the investigation between hydraulic structure and sediment dynamics and connectivity (e.g., Cucchiaro et al., 2019; Marchi et al., 2019), there are, however, some important gaps of knowledge about the effect of the check dams on the discharge and the suspended sediment in semiarid silvopastoral systems. This research subject has already been studied in other ecosystems. For instance, check dams probed to be suitable to trap sediments (Belmonte et al., 2005; Conesa García, 2004), avoiding transfer of sediments downstream of the check dam (Conesa García, 2004; Martín-Rosales et al., 2003) and reducing bulk sediment yields (Castillo et al., 2007; Heede, 1978; Polyakov et al., 2014). However, it is less well understood whether they effectively reduce fine sediment. For

instance, Mishra et al. (2007) estimated the effects of check dams on sediment transport from a mixed land use basin in India, with an area of 17 km^2, and found that sediment load could be reduced by more than 64%. Boix-Fayos et al. (2007) found a reduction of 77% in sediment yield due to check dams in a catchment located in SE Spain with an area of 53 km^2. In the southwest of the United States, a strong decrease in livestock density combined check dams implemented in gullies lessened sediment yield by a 90% in a decade (Heede, 1978). Xu et al. (2013) evaluated the hydrological and sediment effect of check–dams in a semiarid catchment located in the Chinese Loess Plateau and also found that runoff and suspended sediment load were reduced in the rainy season by 29 and 86%, respectively. It is well documented that check dams typically have a limited life span and their effectiveness generally decreases over time (Gifford et al., 1977; Taye et al., 2015). However, Tang et al. (2020) demonstrated in a small catchment (4.26 km^2) in the Loess Plateau that filled check dams were still able to reduce flood peaks by 31% to 93%.

In the last decades, improvements in remote sensing techniques (e.g., LiDAR and SfM–MVS) and platforms (e.g., UAVs) have greatly improved our capacity to model and understand factors and processes driving gully erosion (Koci et al., 2020; Sidle et al., 2019). These advances have also opened up hopeful opportunities for the study of geomorphological processes focused on hydrological and sediment connectivity (e.g., Cavalli et al., 2019; Heckmann et al., 2018). The concurrent use of UAV platforms and SfM–MVS has meant a breakthrough in acquiring very high resolution (centimeter) topographic data and in 3D model generation. Repeated high–resolution digital elevation models are key to identify overland flow and sediment pathways (Heckmann and Vericat, 2018), to detect geomorphic changes (Alfonso-Torreño et al., 2021; Cavalli et al., 2017; Turner et al., 2015; Woodget et al., 2015) and to analyze the structural and functional connectivity changes (Cucchiaro et al., 2019).

The term of sediment and hydrological ‘connectivity' supplies a valuable tool for the analysis of the linkage between pathways and overland flow in hillslopes and the dynamics of erosion and deposition in valley–bottom gullies. In general terms, hydrological and sediment connectivity describes the degree of dynamism between the elements of a system (e.g., hillslopes to channels) and the associated transfer of water and sediment (Bracken and Croke, 2007; Heckmann and Vericat, 2018; Koci et al., 2020; Sidle et al., 2017). According to Lehotský et al. (2018), there is a large gap between studies undertaken on hillslope processes and those in channel environments.

Gullies are influenced by hillslope and channel processes, which provide an outstanding chance to link and study both topographic positions.

Erosion and deposition dynamics in a channel reflect, in a certain extent, the capacity of that channel (or reach) to retain or export sediment (i.e., sediment 'connectivity') (Wohl et al., 2017). Studies focused on this subject point out that connectivity can fluctuate in a system (Heckmann and Vericat, 2018). This variability may be related to the spatial pattern of hydrological and sediment pathways and shows the capacity of the different landscape features to be linked (i.e., structural connectivity) (Cavalli et al., 2013). The concept of 'connectivity' may also be related to the actual sediment transfer between the components of a geomorphological system at a specific location and time (i.e., functional connectivity) (Bracken et al., 2015). In this context, the volume of sediments entrained along a channel or retained behind a check–dam can be considered a measure of functional sediment connectivity and, at the same time, plays an important role in disconnectivity acting as a barrier (Bracken et al., 2015; Fryirs et al., 2007). The potential of a landscape to be connected has been widely analyzed applying sediment connectivity indices (Borselli et al., 2008; Cavalli et al., 2013; Heckmann and Vericat, 2018; Quiñonero-Rubio et al., 2013). The topographically based index of sediment connectivity (IC) was originally proposed by Borselli et al. (2008) for application in cropland catchments. IC was later modified by Cavalli et al. (2013) for better exploiting high–resolution DEMs. The IC has been widely used, for example by López-Vicente et al. (2013) and López-Vicente et al. (2017) who analyzed the effects of land uses and land abandonment on sediment connectivity changes in Mediterranean mountain catchments. Quiñonero-Rubio et al. (2013) identified in the landscape where check dams had a huge impact on sediment (dis)connectivity in a Mediterranean catchment applying the Catchment Connectivity Index (CCI). Although the IC by Cavalli et al. (2013) was developed in mountainous environments, it could potentially be used to analyze the spatial connectivity patterns in lower slope gradient catchments and thus determine the degree of connection between different locations in a watershed to receive and export flow and sediments. In addition, the connectivity between hillslopes and valley–bottoms allows the identification of intersection points between hydrological and sedimentological flow pathways and the filled areas in a gully.

The present work aims to analyze the effect of restoration activities in a small semiarid rangeland catchment. The restoration activities implemented in the valley bottom gully were gabion weirs, fascines and isolation measures. Furthermore, the

following secondary objectives are included: (1) to analyze the effect of the restoration measures on the geomorphic changes in the channel, the hydrological dynamics and suspended sediment production, and (2) to evaluate the effect of the restoration activities on the spatial patterns of sediment connectivity at the catchment and channel scales.

6.2. Study area

The present work focused in the Parapuños experimental catchment that shows a surface of 99.5 ha and is located in the SW of Spain (Figure 38a). Parapuños is a typical Mediterranean rangeland with dehesa land use system. This landscape is formed of a dispersed tree cover of Holm oak (*Quercus ilex va. rotundifolia*), with an average tree density of 22.5 trees ha^{-1}, and herbaceous plants in the understory. At steeper slopes shrubs are frequent, mainly composed of *Retama sphaerocarpa*, *Cytisus multiflorus* and *Genista hirsuta*. The farm is grazed by 1,000 sheep, 55 cows and 40 pigs. Climate is Mediterranean with an average annual temperature of 16ºC and a mean annual rainfall of 513 mm with high seasonality.

The study basin has an average elevation of 396 m above sea–level, ranging from 362 to 434 m and an average slope of 8%. SSW is the dominant aspect within the catchment. There are two types of bedrock in the basin: Ediacarian slates and unconsolidated conglomerates (Miocene), forming part of remnants of a pediment that occupy 32% of the catchment. This pediment is composed of quartzite cobbles, gravelly sand– and a clay–rich layer at approximately 0.5 m depth. The major portion of the pediment is located in the northern part of the basin and a small remnant is found in the SE, forming a hill. The main pediment can be divided into a flat upper surface and a slope with gradients reaching 25% (Figure 38). The valley–bottom (i.e., the alluvial sediment fill) is an undulating area with a slope below 5%.

The soils within the catchment are commonly shallow and they can be classified as Leptosols and Cambisols at hillslopes and Regosols at valley bottoms. The alluvial sediment fill, where the gully is located, can be classified as Regosol and present a highly variable content of coarse material (> 2 mm) which are usually confined in a layer located at different depths. The fine fraction of the sediment fill (< 2 mm), shows a silt loam texture and is composed mainly of silt (56%), followed by sand (29%), and a minor content of clay (15%). In addition, soils in the valley bottom are acid, with a pH

ranging between 4.7 and 6.4, a low organic matter content (1.4%) and a low cationic exchange capacity (< 6 meq 100 g^{-1}).

The channel is a discontinuous second–order stream composed of the main channel and a tributary, with a length of 832 m and 163 m, respectively (Figure 38c). The channel is situated in the lower part of the basin and is incised into the alluvial sediment fill with an approximate depth of 1.5 m, reaching even the underlying schist at some sites. This channel has been previously defined as a valley bottom gully (Gómez-Gutiérrez et al., 2009a). The gully may be divided into three different reaches: (1) lower reach, (2) tributary reach and (3) upper reach where the restoration measures were carried out in February 2017 (Figure 38c). The lower reach connects the junction between the tributary and the upper reach with the outlet of the catchment.

In addition to the gully erosion by concentrated flow, the study area shows pieces of evidence of sheet erosion on the hillslopes (Rubio-Delgado et al., 2017). Eight gabion weirs (GWs) with metal mesh and 25 fascines (Fs) were built in the channel in February 2017 (Figure 39a) with the aim of reducing negative gullying effects. The GWs have a width of 0.5 m with lengths between 1 and 3 m and most of them a height of 1.5 m. The gabion weirs have a central spillway (Figure 39b). The distance between consecutive GWs is on average 27 m. The mesh was manually filled with quartzite cobbles collected in the area. The fascines were made with brooms growing in the area, anchored to the surface with acacia posts, a rot–proof wood, and tied with hemp material (Figure 39d). The fascines have a length of 2 m and a mean separation of 12 m. The fascines were also installed at three bank headcuts (Figure 39c). Finally, a wire fence was installed adjacent to the gully as an isolation measure in a particularly degraded area that showed several active bank headcuts. The wire fence has a perimeter of 117 m and isolates 416 m^2 (Figure 39e).

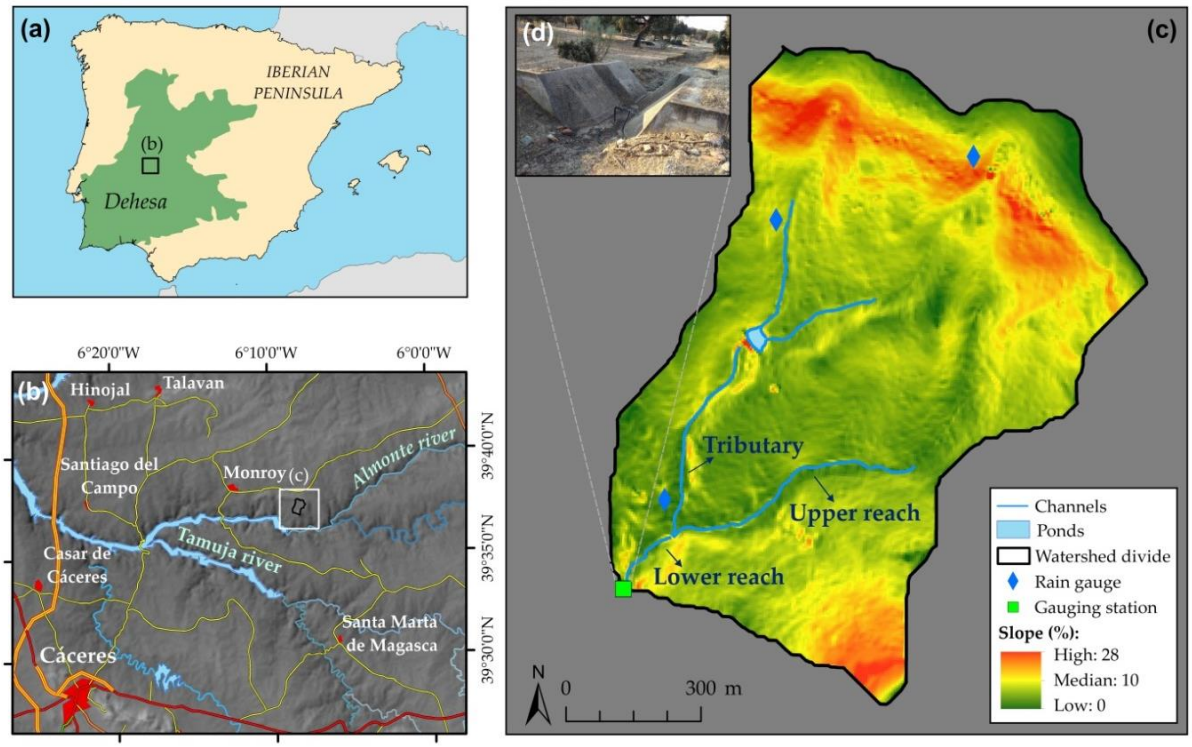

Figure 38. (a) Spatial distribution of dehesa landscapes in the SW of the Iberian Peninsula, (b) regional setting of the studied catchment, (c) Parapuños catchment including slope gradient, the equipment, and the channel reaches and (d) a gauging station at the catchment outlet.

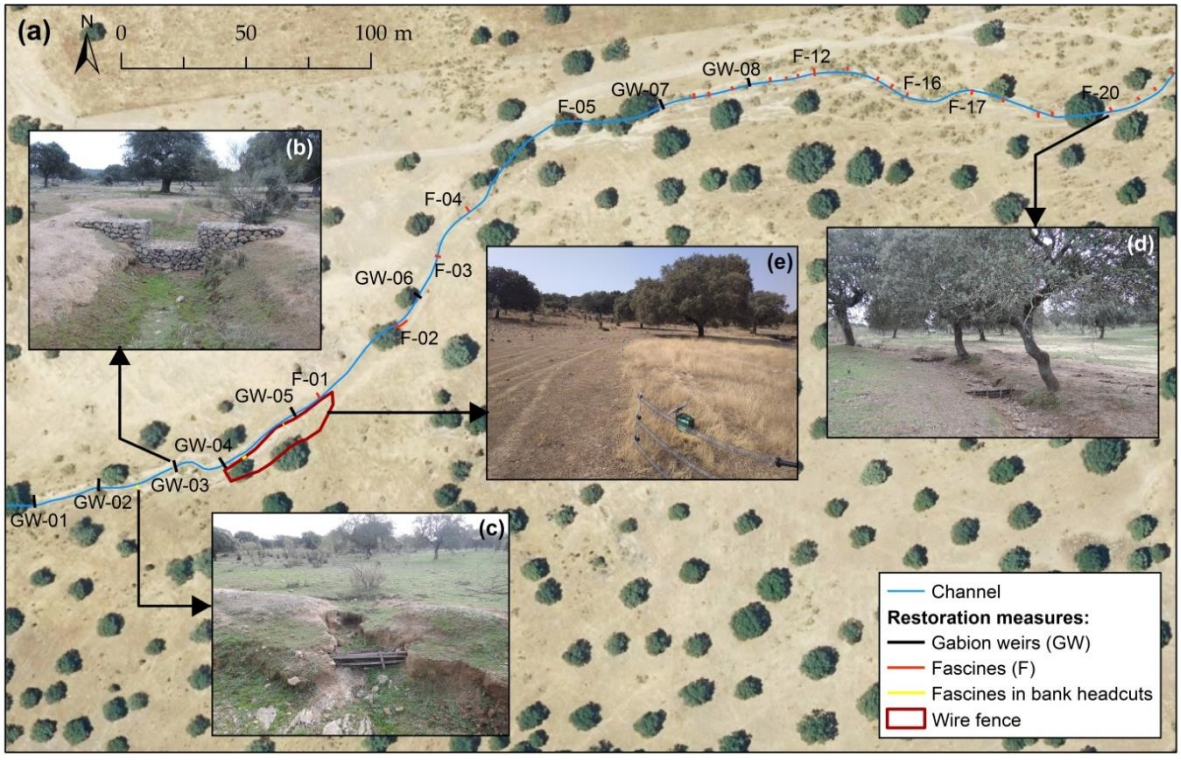

Figure 39. (a) Location of the restoration measures (i.e., gabion weirs (GW), fascines (F) and a wire fence) and (b–e) examples of restoration activities implemented in the upper reach: (b) a gabion weir, (c) a fascine in a bank headcut, (d) a fascine in the channel, and (e) the isolated area by a fence in the left bank of the gully.

6.3. Material and methods

6.3.1. Rainfall, discharge and suspended sediment measurements and soil sampling

The catchment is equipped with three tipping bucket rain gauges (model RG3, Onset Hobo) that record with a resolution of 0.2 mm and collect in an interval of 5–minute. Discharge and suspended sediment were measured at the outlet of the catchment in a weir formed by a V–notched section and a trapezoidal approximation reach (Figure 38d). A capacitive sensor (Unidata 6521 L) was used to obtain water depth data with a range of discharge of 1–4000 l s^{-1} (Schnabel et al., 2013). Suspended sediment concentration was determined using a turbidity meter (OBS–3A). The water depth probe and the turbidimeter were connected to a datalogger (Datataker DT50) registering in 5–minute intervals. Furthermore, suspended sediment concentration was also obtained from water samples taken with an automatic sampler (model Isco 3700C) with 24 bottles of 0.5 l volume, installed in the gauging station and controlled by the datalogger. Water sampling takes place when water level exceeds 0.15 m, corresponding to a discharge of 10.4 l s^{-1}. The turbidity sensor was previously calibrated with a range of concentrations and is, as well, controlled by concentrations obtained from the ISCO samples.

Grain size distribution of soils and sediment deposited behind check dams was determined. For this, a total of 21 surface soil (0–10 cm) samples were taken randomly in five topographic positions (pediment surfaces and slopes, low slopes, valley–bottom and channel bank). Sediment behind check dams was sampled in 6 locations. Soil samples were taken randomly at each study site with an auger (Eijkelkamp). The samples were located using an irregular grid pattern in order to avoid samples below trees. Samples were air dried and disaggregated. The coarse fraction was determined by sieving and the grain size distribution of the fine fraction was carried out using a laser particle analyser (Beckman coulter) applying the USDA classification (USDA, 2004).

6.3.2. Hydrological data processing and analysis

Three different temporal scales were used: rainfall event, month and hydrological year. A database composed of events that produced runoff from September 2013 to 2019 was created. The events were differentiated in time using a minimum interval between two consecutive events of one hour without precipitation. This interval is

appropriate for the temporal distribution of events in the study area. The same value was also used by Lana-Renault et al. (2008) for another small Mediterranean catchment. In order to separate base flow from direct runoff (flood discharge) two methods were applied and compared: the straight line method with inclination (Chow et al., 1988) and the straight line method with a fixed gradient. Best results were obtained with the straight line method with inclination. The criteria used for defining the start of flood discharge was 1.5 times the amount of base flow (Lana-Renault et al., 2008). The technique of the normal depletion curve was applied for identifying the point that establishes the end of direct runoff in a hydrograph (Horton, 1933). Usually the recession curves take the form of an exponential decay function (eq. 1):

$$Q(t) = Q_0 e^{-(t-t_0)/k} \qquad (1)$$

Where Q_0 is the flow at time t_0 and k is the exponential decay constant with time dimensions (Singh and Stall, 1971). The above equation is linearized by plotting the logarithm of Q(t) against time on a linear scale.

A total of 24 variables were derived from rainfall, discharge and sediment records at the event scale for carrying out the statistical analysis and defining relevant relationships amongst them (Table 13).

The rainfall events were grouped into three types (dry, intermediate and humid) based on results obtained from correlation analysis considering antecedent rainfall and base flow as soil moisture indicators. A strong relationship between antecedent soil moisture and discharge production was found by Schnabel et al. (2013). In that study grouping of rainfall events was also carried out, though with discharge data, not flood data. The objectives of the grouping are to fill the gaps of some missing data and to characterize the rainfall–runoff relationships.

The values of hydrological and sedimentological variables did not follow a normal frequency distribution and generally are positively skewed. The nonparametric Kolmogorov–Smirnov and Mann–Whitney test were used to test the significance of differences of rainfall, discharge and sediment variables grouped according to period, i.e., before and after check dam construction. In addition, Spearman's rho test was also used for detecting monotonic trends in the data. All the tests were two–tailed, applying significance p–levels of 0.05 and 0.10. Statistical analysis were conducted using STATISTICA© software.

Table 13. Rainfall, discharge and suspended sediment variables, showing the corresponding abbreviations and measuring units.

Type of variable	Abbreviation	Units	Description
Rainfall	*R*	mm	Total amount of event rainfall
	I5, I10, I30 and I60	mm h^{-1}	Rainfall intensities in 5, 10, 30 and 60 minutes
	R-I60	mm	Difference between total precipitation of the event and the maximum intensity of precipitation in 60 min
	RAnt	mm	Accumulated antecedent rainfall since September 1st of each year
	M_RAnt	mm	Mean daily rainfall since September 1st of each year
	D1, D5, D10, D20 and D40	mm	Amount of rainfall recorded 1, 5, 10, 20 and 40 days prior to the event
Discharge	*Q_max*	l s^{-1}	maximum peak flow
	Discharge	m^3	Total discharge
	Flood discharge	m^3	Total amount of event runoff
	Q base flow	l s^{-1}	Specific base flow just before runoff
	Discharge base flow	m^3	Total amount of base flow during the flood runoff
	Duration of the flood	min	The time interval between the start and the end of the flood
	Flood increase response time	min	The time interval between the start of the flood and Q_max
	Flood descent response time	min	The time interval between Q_max and the end of the flood
	Runoff coefficient	%	A dimensionless coefficient relating the amount of runoff to the amount of rainfall received
Sediment transport	*Suspended sediment load*	t	Amount of suspended sediments at the outlet of the catchment
	Max concentration	g l^{-1}	Maximum suspended sediment concentration
	Mean concentration	g l^{-1}	Mean suspended sediment concentration

6.3.3. 3D models acquisition, DoD elaboration and computation of hydrological connectivity

The database with the geomorphic changes and the DEMs that will be used to estimate the connectivity indices was elaborated for the previous work by Alfonso-Torreño et al. (2021) and hence only a brief description of the production of this dataset is presented here. For more details the reader can refer to the work by Alfonso-Torreño et al. (2021). These authors estimated the geomorphic changes in the valley–bottom gully in the 2016–2019 time window, by using high–resolution DEMs produced through aerial images and SfM-MVS photogrammetric techniques. The dataset was taken in five different surveys using a fixed–wing UAV (Ebee classic by Sensefly) carrying a Sony WX220 sensor on board (18 Mpx). The images were acquired

at an approximate altitude of 60 m above ground resulting in a Ground Sampling Distance of 2 cm. An average number of 190 images were captured per survey. The models were scaled and georeferenced using twenty Ground Control Points (GCPs) which were registered across the area and surveyed with the help of a Global Navigation Satellite system working in Real Time kinematic mode. The Pix4Dmapper Pro software (v. 3.1.18) was fed with the images and the GCPs in order used for the photogrammetric processing to produce 2.5D (Digital Surface Model or DSM, Digital Elevation Model or DEM and orthophotographs) and 3D cartographic products (point cloud). During the processing, a mean Root Mean Square Error of 0.03 m was estimated.

The topographic changes were estimated comparing the DEMs produced for each UAV survey and using the classical DoD (Wheaton et al., 2010). To do this, the Geomorphic Change Detection (GCD) v7.1 add−in (Riverscapes-Consortium, 2018) freely available from http://gcd.joewheaton.org/downloads, within the ArcGIS Desktop software v10.6 was used. We considered a spatially variable error estimated using rules implemented through a fuzzy inference system (FIS) in addition to the georeferencing error calculated for every individual DEM during the photogrammetric processing. Two rules, based on slope gradient and vegetation height (i.e., wood vegetation and grasses), were used in the FIS system. The SfM−derived DEMs allowed the estimation of the geomorphic change at the gully before (BEF) and after the restoration activities (AFT).

The IC formulated by Borselli et al. (2008), with the changes proposed by Cavalli et al. (2013), was used to evaluate the potential connectivity between the watershed slopes and the valley−bottom channel. This index consists of an estimation of the upslope contributing area besides the downstream pathway to the outlet of the catchment (i.e. a pre-defined target) considering a roughness index as the impedance to runoff and sediment fluxes. More details on the formula and the calculation can be found in Cavalli et al. (2013).

The IC was computed for the study basin by using SedInConnect 2.3 software (Crema and Cavalli, 2018), which includes the modifications proposed by Cavalli et al. (2013). The IC was calculated for each date (i.e., each UAV survey) using two DEMs that were merged. For the valley−bottom area, the SfM−derived DEM acquired at each date (0.1 m) was used while for the rest of the catchment a 5 m resolution DEM (Spanish National Geographic Institute) produced by LIDAR techniques was applied. Both DEMs

were merged to a resampled DEM of 0.5 m pixel size and a moving window of 3x3 pixels was set for roughness computation. The input DEM was hydrologically corrected using the Pit remove tool of the TauDEM 5.3.7 add–in (Tarboton et al., 2015) freely available from https://hydrology.usu.edu/taudem/taudem5/, within the ArcGIS Desktop software v10.5.

The Differences, or changes, of IC (DoIC) experienced during the study period were calculated by subtracting the 2019 IC map from the 2016 IC to investigate the influence of the restoration measures on sediment connectivity dynamics. Finally, we compared DoIC maps with the erosion and deposition patterns derived from the DoDs.

The sediment retention and transport were considered as measures of connectivity in the gully. Channel sediment disconnectivity may be defined as the ability of a certain channel reach to retain or deposit sediments (Hooke, 2003). Therefore, the amount of sediments deposited or retained along a channel reach (e.g., with the implementation of restoration measures) is an estimation of sediment connectivity (or dis-connectivity) (Bracken et al., 2015; Fryirs, 2013; Wester et al., 2014; Wohl et al., 2017). Following this definition, a connectivity value for a defined channel reach or strip (Cv–strip) is calculated as the ratio of eroded material to the deposited sediments for a specific period (eq. 2):

$$C_{v-strip} = \frac{Erosion}{Deposition} \quad (2)$$

This ratio involves more channel connectivity at eroded reaches with values of Cv-strip>1. On the other hand, reaches that experienced deposition present Cv-strip<1 and show, by definition less connectivity. The channel was divided into reaches of 5 m of length (i.e., less than the minimum distance between check dams), resulting in 88 strips.

6.4. Results

6.4.1. Characteristics of rainfall, discharge and sediment load

The average annual rainfall in the basin was 512.7 mm for the period 2000 to 2019, showing a high temporal variability. Figure 40 shows annual rainfall and specific discharge (runoff) for this period, being the rainiest years 2000–01 and 2009–10 with 801.8 mm and 794.4 mm, respectively. The lowest annual rainfall was 292.3 mm. Annual discharges ranged from 3329 m^3 to 201,394 m^3, which corresponds to a specific

runoff of 3.3 mm and 202.4 mm. After the implementation of the restoration measures a rainy and a dry year were registered (560.5 mm and 350.3 mm). The high temporal variability of annual discharge is also expressed by its coefficient of variation of 111%. The relationship between annual rainfall and discharge was exponential, although similar rainfall amounts produced varying amounts of discharge. For example, the hydrological years 2015–16 and 2017–18 with approximately 550 mm of rainfall recorded discharges of 17496 m^3 and 56744 m^3, respectively. The mean annual runoff coefficient was 0.09 and ranged from 0.07 to 0.26. Generally, high runoff coefficients (>0.20) corresponded to exceptionally humid years with rainfall above 680 mm. Contrary, dry years with less than 450 mm of rainfall registered runoff coefficients <0.08.

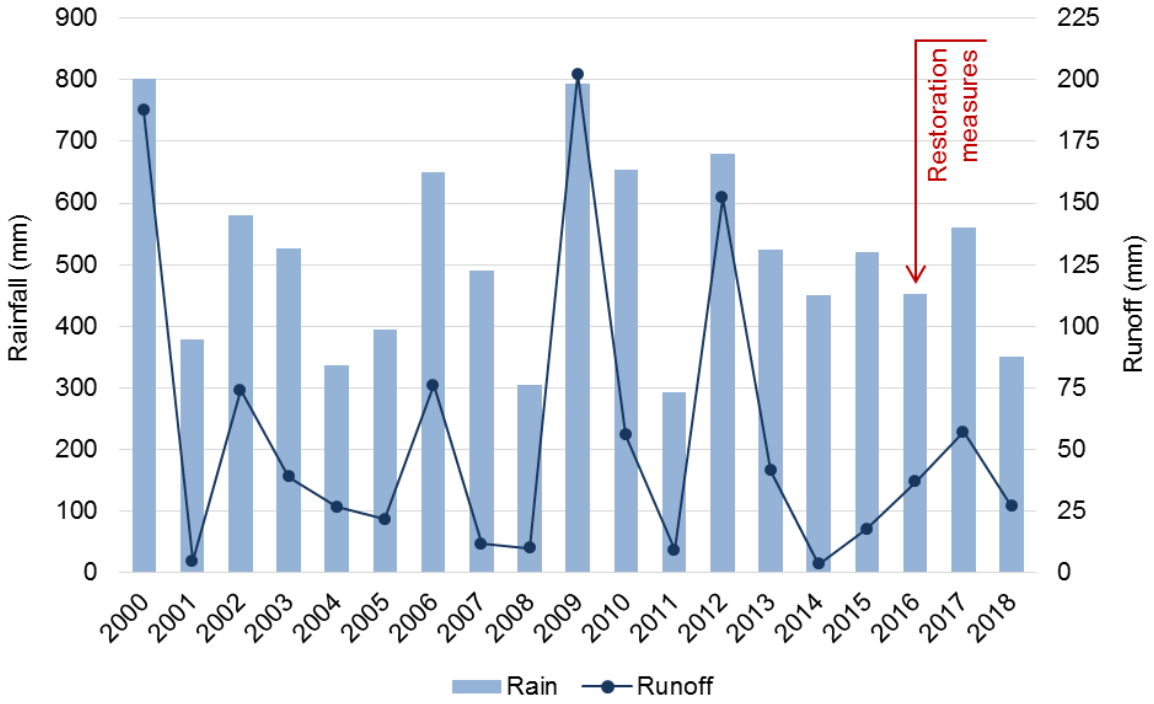

Figure 40. Annual rainfall and runoff in the experimental catchment (2000–2019). The vertical red marks the implementation of the restoration measures.

The rainy season ranges from October until April, being October the rainiest month with 83.0 mm on average. The summers are hot and dry, with July and August registering very low amounts of rainfall (Table 14). Monthly rainfall was strongly variable and exceptional amounts can be expected in nearly every month, except for July and August, as highlighted by the maximum monthly amounts shown in Table 14 and the coefficients of variation with values above 50%. December presented the

maximum monthly value with 211.1 mm, corresponding to the year 2000. Similarly, the absence or very low amounts of rainfall can also be expected in any of the months. Maximum mean monthly discharge corresponds to February with 12132.7 m^3, followed by March (Table 14). Discharge, on average, was low between May and September and no discharge was observed in July. The variability of discharge is higher than that of rainfall.

Table 14. Monthly rainfall and discharge in Parapuños from 2000 to 2019. Mean, maximum (max) and minimum (min). R: rainfall; Q: discharge.

Month	Rainfall (mm)	Discharge (m^3)	Runoff coef. (%)	Min R	Max R	Min Q	Max Q
January	50.7	9023.0	17.9	0.0	164.4	0.0	59539.5
February	53.3	12132.7	22.9	0.2	168.7	0.0	81476.3
March	57.4	11600.3	20.3	0.1	202.0	0.0	95725.4
April	49.3	2669.8	5.4	4.2	113.5	0.0	13546.8
May	36.5	1093.3	3.0	0.7	95.7	0.0	12503.3
June	12.8	28.4	0.2	0.2	64.6	0.0	538.1
July	1.9	0.0	0.0	0.0	13.6	0.0	0.0
August	6.9	1.4	0.0	0.0	24.2	0.0	25.8
September	28.8	153.8	0.5	0.0	121.0	0.0	1869.1
October	83.0	3837.8	4.6	5.7	193.5	0.0	22788.1
November	72.0	6359.2	8.9	2.6	170.8	0.0	65940.6
December	60.1	7547.7	12.6	12.3	211.1	0.0	50030.8

The annual sediment load was 73.8 tons on average, equivalent to 0.72 t ha^{-1} y^{-1}. The interannual variation was very high, ranging from 0.07 in 2018–19 to 1.86 t ha^{-1} y^{-1} in 2009–10, with a standard deviation of 0.748 t ha^{-1} y^{-1} (Figure 41). Suspended sediment load greater than 1 t ha^{-1} only took place when rainfall greater than 450 mm was recorded. However, large discharge may also produce small amounts of sediment load.

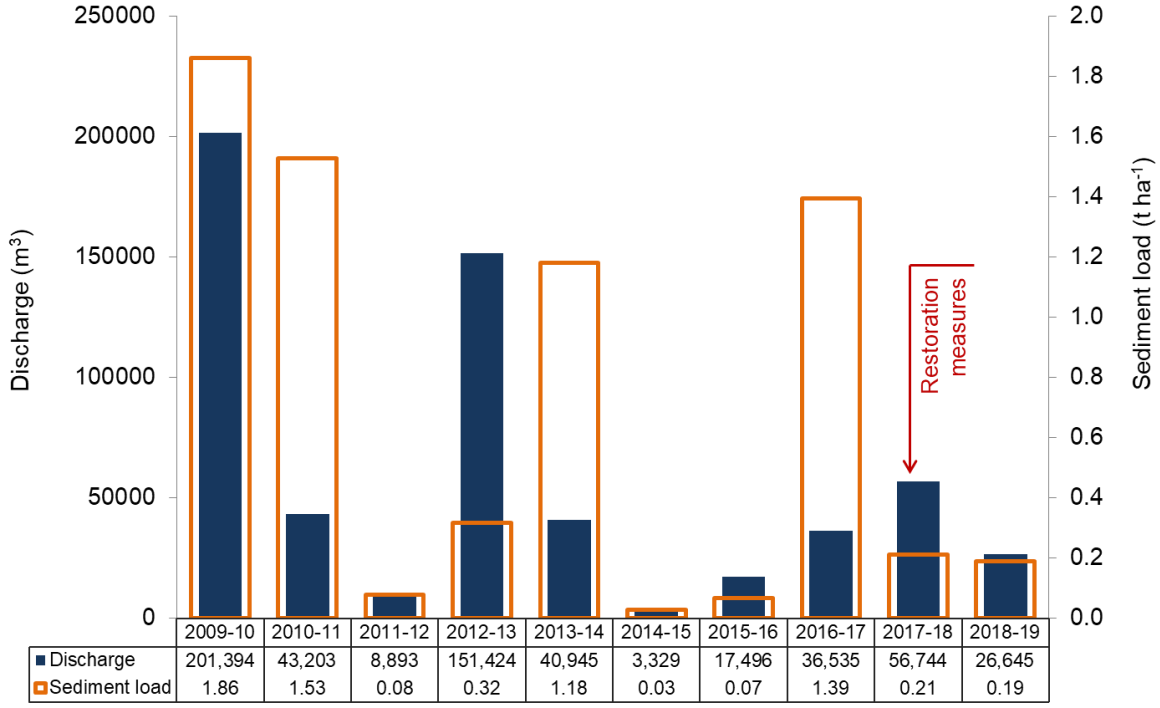

Figure 41. Annual discharge (m^3) and suspended sediment load (t ha^{-1}) from 2009 to 2019. The vertical red arrow marks the implementation of the restoration measures.

As far as the event time scale is concerned, a total of 111 rainfall events were included in the data base which produced a median flood discharge of 118.4 m^3. Table 15 presents basic statistics of variables related to discharge, rainfall and suspended sediment. Discharge and sediment variables were not normally distributed being positively skewed. Flood discharge ranged from 1.2 m^3 to 18136.7 m^3, being the lower and the upper quartile 29.5 m^3 and 796.3 m^3, respectively. Maximum peak flood discharge was 1237.2 l s^{-1}. Runoff coefficients and maximum discharges were also characterized by a high variability. In the set of 111 events analyzed, only 80 events produced suspended sediment load, of which 53 were registered before check dam construction and 27 afterward. The median suspended sediment load was 0.1 t, being the lower and the upper quartile 0.0 t and 0.7 t. The median value of the mean suspended sediment concentration was 0.2 g l^{-1} ranging from 0 to 3.4 g l^{-1}. Rainfall events that generated suspended sediment load only took place between September and April. The highest mean and maximum sediment concentrations were registered in winter (i.e., from December to February). Conversely, the lowest values of sediment concentration corresponded to spring events (i.e., from March to May) despite being the season when rainfall events generated the largest flood discharges.

Median event rainfall was 10.3 mm, with lower and upper quartiles of 5.0 and 15.0 mm, respectively. A total of 48% of the rainfall events were of small magnitude (<10 mm) and did not present a clear seasonal pattern, i.e., they are equally frequent at any time of the year, except for July and August. Only 5 events lasted more than fourteen hours and occurred in winter and autumn. The duration of rainfall events was almost 5 hours on average and 90% of the rainfall events were shorter than 10 hours. The rainfall intensity in 5 minutes had a median of 10.5 mm h^{-1} and 25% of the events registered less than 7.2 mm h^{-1}. The rainfall intensity in 60 minutes ranged between 1 mm h^{-1} and 19.0 mm h^{-1}, with only 10% of the sample above 9.6 mm h^{-1}. Concerning antecedent rainfall conditions (RAnt) the median was 277.2 mm, ranging from 21.8 to 504.8 mm. Table 15 also includes the statistical descriptors for other variables used as indicators for antecedent catchment conditions.

Table 15. Descriptive statistics of event discharge, rainfall and suspended sediment (n = 111). LQ and PQ: lower and upper quartile; P10 and P90: 10 and 90% percentile.

Variable	Mean	Median	Min	Max	LQ	UQ	P10	P90
R (mm)	11.6	10.3	1.0	57.7	5.0	15.0	3.4	21.1
I5 (mm h^{-1})	16.6	10.5	2.4	87.1	7.2	20.5	5.1	36.6
I10 (mm h^{-1})	13.1	9.1	2.4	64.1	5.2	15.4	3.8	29.5
I30 (mm h^{-1})	7.6	5.7	1.6	29.9	4.0	9.4	2.6	15.4
I60 (mm h^{-1})	5.2	4.1	1.0	19.0	2.8	6.8	2.1	9.6
R-I60 (mm)	6.8	5.1	0.0	51.8	1.5	8.8	0.4	13.3
RAnt (mm)	280.6	277.2	21.8	504.8	204.4	372.9	104.8	451.7
M_RAnt (mm)	2.0	2.0	0.5	4.2	1.7	2.2	1.5	2.7
D24h (mm)	10.5	8.1	0.0	38.4	4.5	14.1	2.8	21.1
D5 (mm)	29.4	23.5	0.0	114.2	10.0	42.9	4.7	58.7
D10 (mm)	42.7	33.6	0.1	135.4	19.7	63.1	9.4	84.8
D20 (mm)	64.0	55.2	1.3	198.3	36.3	88.0	19.3	108.1
D40 (mm)	107.6	106.2	14.9	231.2	69.7	143.4	36.6	162.2
RAnt - D40	173.0	169.8	0.0	414.1	111.2	252.0	2.9	317.6
Q_max (l s^{-1})	116.3	23.7	1.3	1237.2	4.5	108.6	2.2	248.3
Discharge (m^3)	1203.0	222.9	4.8	20624.6	50.9	1072.9	9.9	3155.9
Flood discharge (m^3)	904.9	118.4	1.2	18136.7	29.5	796.3	4.0	2094.7
Flood duration (hours)	5.6	4.8	0.5	21.4	2.6	7.5	1.0	10.6
Q base flow (l s^{-1})	3.9	0.3	0.0	49.8	0.0	2.8	0.0	13.9
Discharge base flow (m^3)	198.5	37.5	1.0	1947.5	8.3	229.1	2.2	542.3
Runoff coefficient (%)	5.5	1.8	0.0	40.9	0.4	7.4	0.1	16.8
Suspended sed. load (t)	3.1	0.1	0.0	99.2	0.0	0.7	0.0	4.9
Max. conc.	2.6	1.5	0.1	9.5	0.7	3.9	0.4	6.5
Mean conc.	0.6	0.2	0.0	3.4	0.0	0.7	0.1	2.1

The non−parametric Spearman rank correlation coefficient was calculated for flood discharge, sediment load and the rainfall variables (Table 16). Although the

relationship between rainfall and flood discharge of the events is significant, the correlation coefficient R is low. Similarly, flood discharge and maximum flood discharge correlated significantly with rainfall intensity in 60 minutes, amount of rainfall recorded 10, 20 and 40 days before the event and Q_max.

Sediment load correlated significantly and positively with Q_max, flood discharge and mean suspended sediment concentration. Sediment load was also positively correlated with the specific base flow at the start of runoff. Conversely, suspended sediment load showed worse correlations with the rainfall intensity variables. Mean sediment concentration was positively correlated with Q_max but no relationship could be detected with the rainfall variables.

Table 16. Correlation coefficients between selected event features (** – p < 0.05, * – p < 0.10, n=111).

	Rainfall (mm)	**Flood Q (m^3)**	**Q_max ($l\ s^{-1}$)**	**Mean sediment concentration**	**Sediment load (t)**
I5 ($mm\ h^{-1}$)	**0.523	0.198	*0.326	0.109	0.107
I60 ($mm\ h^{-1}$)	**0.751	*0.381	*0.495	0.140	0.264
RAnt ($mm\ h^{-1}$)	-0.198	0.162	0.093	-0.019	0.245
M_RAnt ($mm\ h^{-1}$)	-0.156	0.059	0.060	0.228	0.152
D10 (mm)	-0.001	**0.488	*0.458	-0.095	*0.403
D20 (mm)	-0.089	**0.454	*0.418	-0.151	*0.378
D40 (mm)	-0.141	*0.370	*0.325	-0.197	*0.297
RAnt - D40	-0.195	0.019	-0.038	0.112	0.169
Q_max ($l\ s^{-1}$)	**0.526	**0.952		*0.306	**0.859
Flood discharge (m^3)	**0.517		**0.952	0.191	**0.821
Flood duration (min)	0.346	**0.686	*0.486	-0.101	*0.407
Q base flow ($l\ s^{-1}$)	-0.224	**0.532	*0.497	0.179	*0.567
Sediment load (t)	*0.374	**0.821	**0.859	**0.619	
Max. concentration	0.133	0.096	0.205	**0.763	*0.500
Mean concentration	0.045	0.191	*0.306		**0.619

The relationship between rainfall and runoff improved by grouping the rainfall events, resulting in three groups that express different antecedent catchment soil moisture conditions: Dry, Intermediate and Humid. All events with a base flow > 0.07 $l\ s^{-1}$ and with 150 mm of antecedent rain (RAnt) or mean accumulated rainfall (M_RAnt) > 2.0 mm were classified as Humid. Intermediate events are those with a base flow > 0.07 $l\ s^{-1}$, RAnt > 150 mm and M_RAnt < 2.0 mm. Dry events are those with RAnt < 150 mm. The non–parametric Kolmogorov–Smirnov test showed that group Dry was

significantly different from group Humid and Intermediate ($p < 0.05$), although the humid events were not significantly different from the intermediate ones.

Regression analysis was conducted in order to clarify the rainfall–flood relationships. Nonlinear regression models were used to establish correlations and the Levenberg–Marquardt algorithm was applied for estimating the parameters. Table 17 shows the regression equations for the three groups and the corresponding statistical parameters.

The best relationship for Dry includes rainfall (R) and rain fallen 5 days before the event (D5), accounting for 0.244 of the variance and a RMSE of 93 m^3. For Humid the best results were obtained considering the event rainfall subtracting the rainfall intensity in 60 minutes (R-I60) and I60, representing 0.870 of the sample variance. Finally Intermediate discharge events correlated best with rainfall and 10 day antecedent rainfall (D10), with a variance accounted of 0.602 and a RMSE of 438 m^3. The regression equations were used to estimate missing flood discharge data, which represented 2.5% of the total discharge amount.

With dry antecedent conditions and low values of base flow only 35% of the events generated flood discharge above 100 m^3, whereas this percentage increased to 69% in humid events. This difference was also noticeable for the maximum flood discharge, with 402 and 18137 m^3, for Dry and Humid, respectively. Regarding the intermediate events, 52% of them generated flood discharges greater than 100 m^3, but never exceeding 5000 m^3. Finally, a total of 17 events (30%) with humid antecedent conditions were registered that exceeded 1000 m^3 of discharge, being 5 events > 5000 m^3.

Table 17. Equations and statistics of regression analysis by group ($p < 0.05$).

Group	N	Regression	Variance accounted for	R	RMSE
Dry	35	$Q = 4.071 \cdot R^{0.983} \cdot D5^{0.216}$	0.244	0.494	93
Intermediate	21	$Q = 21.498 \cdot D10^{0.632} \cdot R^{0.463}$	0.602	0.776	438
Humid	55	$Q = 37.809 \cdot R\text{-}I60^{1.031} \cdot I60^{1.063}$	0.870	0.932	1097

6.4.2. Flood discharge and sediment production before and after check dam construction

In order to study the influence of check dams on discharge and sediment load, event data were used and grouped according to the time of check dam construction, i.e.,

the period before (BEF) or afterward (AFT). Table 18 presents the median values for various rainfall, discharge and sediment variables for each of the two groups. The maximum peak discharge, flood discharge, runoff coefficient and rainfall variables observed of the events BEF were significantly lower than those AFT. The median event value of flood discharge was 104.9 m^3 BEF and 474.9 m^3 AFT. Therefore, the flood discharge was not reduced after the check dam installation. Suspended sediment load was not statistically different for events according to the time of check dam construction ($p = 0.64$). However mean suspended sediment concentration was significantly higher in BEF than AFT with 0.31 g l^{-1} and 0.11 g l^{-1}, respectively.

Table 18. Median, lower and upper quartile of rainfall, discharge and suspended sediment variables for the events according to the time of check dam construction: Before (BEF) or after (AFT). Significant differences of the variables are indicated (** – $p < 0.05$, * – $p < 0.10$).

Variable	BEF Median	AFT Median	BEF Lower	AFT Lower	BEF Upper	AFT Upper	p–level
Rainfall (mm)	**8.98	**13.03	4.70	7.48	13.88	16.66	0.04
I5 (mm h^{-1})	10.45	12.82	5.23	7.69	19.20	20.51	0.18
I10 (mm h^{-1})	8.77	10.25	5.13	6.41	15.38	15.38	0.25
I30 (mm h^{-1})	5.82	5.55	3.77	4.70	9.83	9.40	0.40
I60 (mm h^{-1})	3.92	4.27	2.56	3.42	6.84	6.62	0.21
R-I60 (mm)	**3.76	**8.12	1.28	3.42	7.40	10.04	0.03
RAnt (mm)	269.25	324.54	179.70	220.10	355.50	399.90	0.13
M_RAnt (mm)	**2.00	**1.80	1.80	1.40	2.20	1.90	0.00
D24h (mm)	8.12	10.04	4.27	5.55	14.31	13.67	0.56
D5 (mm)	23.10	31.50	9.80	13.20	37.20	47.30	0.11
D10 (mm)	**30.10	**47.30	19.20	33.50	46.10	90.50	0.01
D20 (mm)	**53.00	**75.30	36.20	40.20	78.90	137.70	0.01
D40 (mm)	**101.00	**138.40	67.20	92.60	134.80	199.10	0.00
RAnt - D40	175.70	150.30	14.40	142.70	255.30	190.50	0.34
Q_max (l s^{-1})	*22.54	*87.18	3.52	5.53	83.99	216.70	0.06
Discharge (m^3)	**190.34	**716.84	36.40	69.19	801.33	2820.56	0.03
Flood discharge (m^3)	**104.98	**474.99	24.80	42.70	402.31	2072.69	0.03
Flood duration (h)	**265.00	**410.00	140.00	335.00	380.00	575.00	0.00
Q base flow (l s^{-1})	**0.19	**1.05	0.03	0.22	1.14	4.72	0.01
Discharge base flow (m^3)	*34.96	*63.13	7.72	15.72	153.68	520.51	0.05
Runoff coefficient (%)	*1.32	*3.98	0.25	0.56	5.64	13.15	0.06
Sediment load (t)	0.07	0.32	0.01	0.01	0.48	0.75	0.64
Max. concentration (g l^{-1})	*1.82	*0.98	0.83	0.56	4.17	3.05	0.07
Mean concentration (g l^{-1})	**0.31	**0.11	0.12	0.08	1.26	0.42	0.01

The first year after check dam construction 561 mm of rainfall were recorded, generating a total of 56744 m^3 of flood discharge with a runoff coefficient of 10.2%. Taking into account the ten years with information on suspended sediment load, this year was the third highest value of discharge, being sediment production only ranked in position 7 (Figure 41). The relationship between event suspended sediment load and flood discharge, grouped according to BEF and AFT, is presented in Figure 42a, showing significant correlations. Similarly, event suspended sediment and maximum peak discharge (Figure 42b) are significantly correlated when grouped accordingly. The lower gradients of the regression lines of the events registered during AFT, for both variables (flood discharge and maximum peak discharge), indicate the effect of check dams on reducing suspended sediment load.

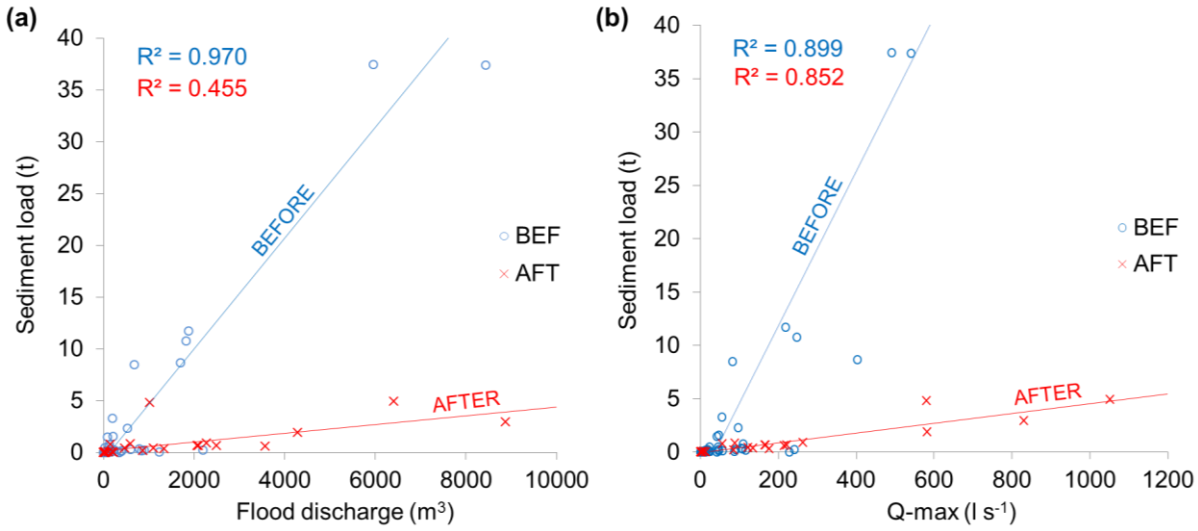

Figure 42. Relationship between the event suspended sediment load and (a) flood discharge and (b) maximum peak discharge before and after check dam construction.

6.4.3. Comparison of gully dynamics with sediment production

Net channel volume change for the study period (2016–2019) was estimated to be 95.4 m3, corresponding to a net deposition rate of 33.6 $m^3\ y^{-1}$. The net change before and after check dam construction was 42.7 m^3 and 52.7 m^3, respectively (Table 19). Considering an average bulk density of 1.5 g cm^{-3} (Gómez-Gutiérrez, 2009) the annual change rate expressed in tons per year for BEF and AFT was 71.2 and 40.7. Suspended sediment load at the outlet of the catchment for the entire study period was 160.8 t, which represented a suspended sediment yield of 56.9 t $km^{-2}\ y^{-1}$. Before check dam construction, net deposition was lower than total sediment load at the outlet of the catchment. Contrary, after check dam construction net deposition was higher than

sediment load at the outlet. Comparing total sediment yield, BEF registered a much higher value than AFT, with 153.0 t km^{-2} y^{-1} and 12.3 t km^{-2} y^{-1}, respectively. It has to be taken into account that sediment load was lower in AFT despite registering potentially more erosive discharge events, as expressed by a greater number of peak floods > 100 l s^{-1} or catchment runoff coefficients. Furthermore, as presented in the previous section, rainfall events with similar flood discharge produced different amounts of suspended sediment load. For example, during BEF an exceptional rainfall event occurred (February 13, 2017), which recorded a precipitation of 49.3 mm, a maximum peak discharge of 1237.2 l s^{-1}, a flood discharge of 18136.7 m^3 and a suspended sediment load of 999.2 t. Previous amounts of discharge and sediment load represented 47.7% and 72.4% of the total flood discharge and sediment load before check dam construction. It was the event with the highest maximum peak discharge since monitoring started in 2000. During AFT, the highest peak discharge was 1052.3 l s^{-1} representing 17.2% and 23.8% of the total flood discharge and suspended sediment load for AFT period.

Table 19. Hydrological and sediment load data and topographic changes registered during the study period: erosion or deposition, net volume difference (NVD), maximum event rainfall (R_max), total flood discharge (Q), maximum peak discharge (Q_max), the number of times discharge exceeded 100 l s^{-1} (Q > 100 l s^{-1}), maximum rainfall intensity in 60 minutes (I60−max).

Period	**BEFORE**	**AFTER**
Duration	24/03/2016 – 10/02/2017	10/02/2017 – 25/01/2019
Erosion (m^3)	-8.0	-22.0
Deposition (m^3)	50.7	74.7
Net volumen difference (m^3)	42.7	52.7
NVD (t)	64.1	79.0
NVD rate (t y^{-1})	71.2	40.7
Rainfall amount (mm)	543.4	928.9
Events (N)	30	45
R_max (mm)	57.7	22.2
Q (m^3)	38334.1	40948.8
Q_max (l s^{-1})	1237.2	1052.3
Q > 100 l s^{-1} (N)	3	7
I60−max (mm h^{-1})	13.0	15.1
Runoff coefficient (%)	4.7	8.7
Sediment load (t)	137.0	23.8
Sediment yield (t km^{-2} y^{-1})	153.0	12.3

6.4.4. Hydrological and sediment connectivity and gully geomorphic change

The hydrological and sedimentological connectivity map shows the potential connection of water and sediment between the hillslope and the valley–bottom gully. Figure 43a presents the IC map calculated for the 2016 DTM of the catchment. The IC is higher along the slope of the main pediment, as well as the slope of the small pediment in the south–eastern part of the basin. The western part of the main pediment slope is poorly connected with the main channel due to the location of a water pond. In contrast, the small pediment is highly connected to the main channel and the eastern part of the main pediment is also connected to the main channel with gentle slopes. The uppermost part of the catchment has low connectivity and corresponds to the upper part of the main pediment with low slope gradients. As expected, connectivity is generally highest close to the main channel and progressively decreases upslope (particularly at the right bank of the upper reach) although some parts with low connectivity close to the main channel can be highlighted. Across the right bank of the main channel, lines of high IC values are clearly aligned with cattle paths, which drive the flow and possibly capture a large proportion of sediment toward the gully (Figure 43b). In addition, an unpaved road crosses the lower reach increasing connectivity towards the valley–bottom gully. This area shows pieces of evidence of soil erosion by water, scarce vegetation cover and patches of bare soil, constituting potential source areas of sediments. In the upper reach, a new channel parallel to the main one developed influenced by a cattle path which caused the diversion of flow (Figure 43c). In fact, the connectivity of the new channel was higher than that of the main channel before check dam construction. The left bank of the upper reach, particularly from GW–01 to GW–05, is an area strongly connected to the channel where eleven bank headcuts were formed. For instance, Figure 43d displays the spatial relationship between the bank headcuts located between GW–01 and GW–03 and the flow pathways. Flow pathways with high values of connectivity are strongly connected to the gully, influencing the growth of bank headcuts.

A positive relationship between linear headcut retreat and the maximum IC value (calculated in the contributing area of each bank headcut) is indicated by a correlation coefficient of 0.821 ($p<0.05$) (Figure 44a). The volume of sediments trapped behind gabion weirs was positively and significantly correlated with the maximum IC value (calculated in the contributing area of each gabion weir) (Figure 44b).

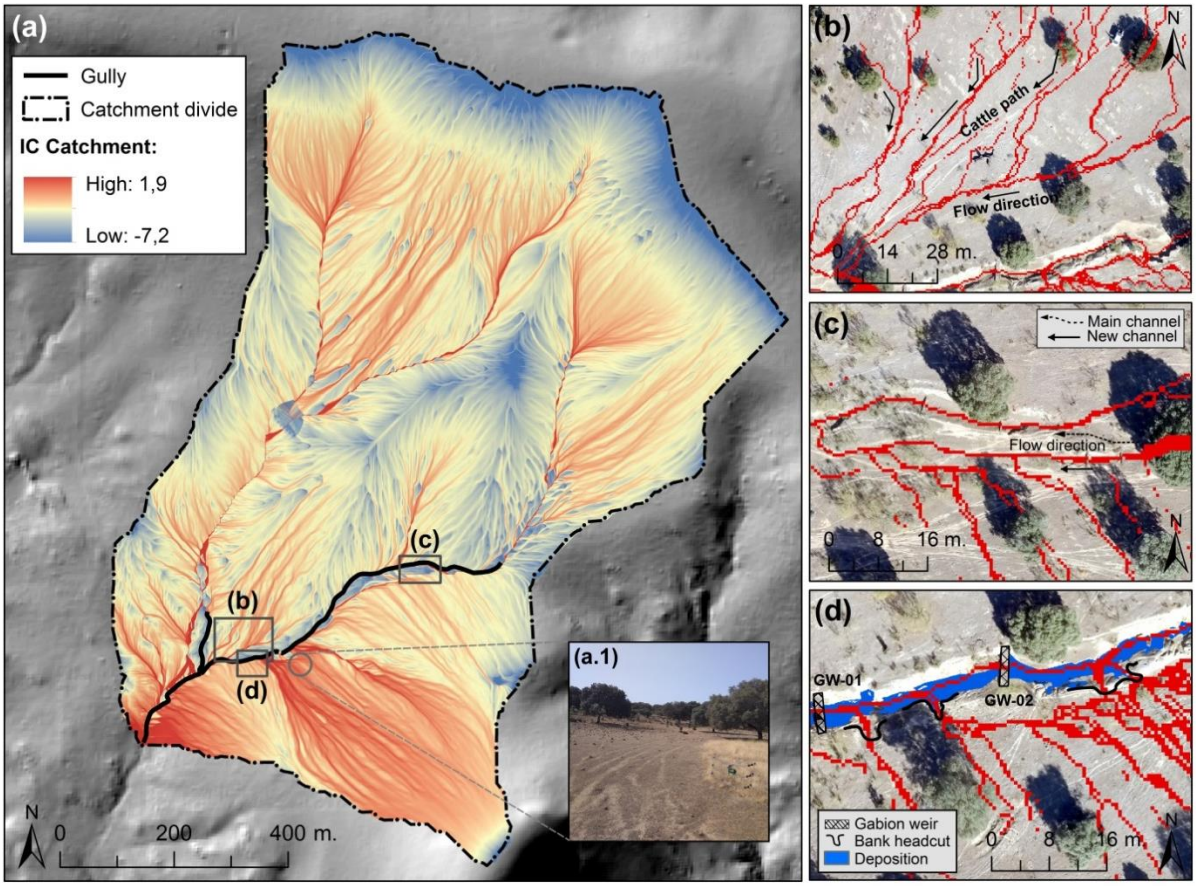

Figure 43. (a) Connectivity index map calculated for the 2016 DTM of the Parapuños catchment and (a.1.) a photograph of the left bank hillslope, (b) cattle paths collecting and driving overland flow, (c) diversion of flow (coming from the left bank hillslope) from the main channel due to a depression originated by a cattle path and (d) detail of the left bank of the reach between GW–01 and GW–03 showing the spatial co–occurrence of bank headcuts and flow pathways draining the left hillslope. Red pixels in (b–d) are locations with contributing area>100 m^2.

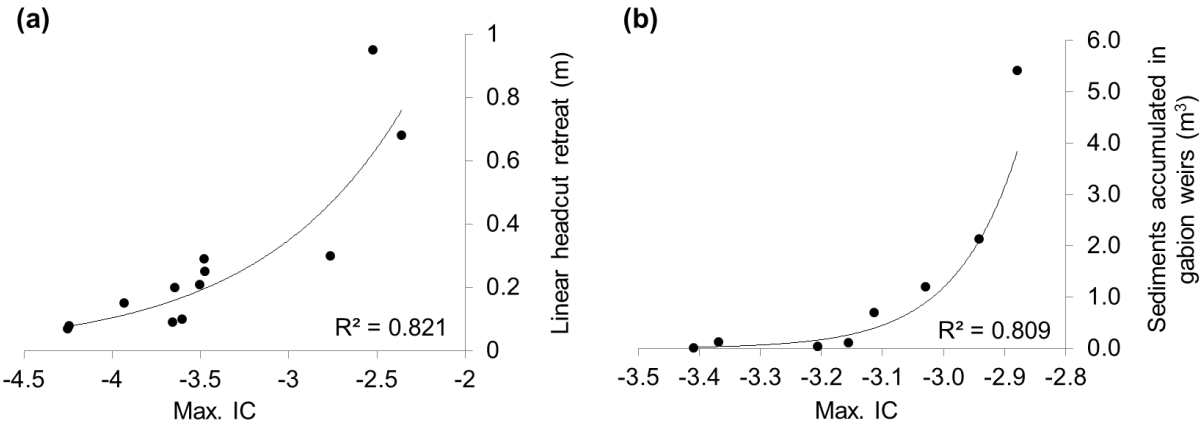

Figure 44. Relationship between maximum IC values of contributing area and: (a) linear headcut retreat (mapped from SfM–derived orthophotographs for every survey) and (b) volume of sediments trapped behind gabion weirs (estimated from SfM–derived DEMs of difference analysis between 2017 and 2019 survey).

The functional connectivity decreased in the upper reach after the implementation of the restoration measures. After the implementation of the restoration measures, an increase of connectivity was only observed downstream of five check dams (i.e., GW–02, GW–05, GW–08, F–09 and F–13) and in the junction between the tributary and the upper reach. Before the implementation of the restoration measures, connectivity increased in the headwater, in the new channel parallel to the main one (i.e., between F–16 and F–19, Figure 45c) and in the left bank of a strongly degraded area where the wire fence was implemented later as a restoration measure. In addition, the values of connectivity experienced a decrease from 2017 between GW–01 and GW–04. Figure 45 shows the spatial co–occurrence of connectivity with net volumes before and after check dam construction per strip. Lower values of connectivity (< 1) highlight the areas where deposition dominated, which implied a decrease in connectivity due to reduced slope gradient and this decreases in the ability to export sediments further down. For example, the section between F–07 and F–17 evolved from being a connected section to one with considerably reduced connectivity. Conversely, high values of connectivity were observed in the strips where erosion processes dominated.

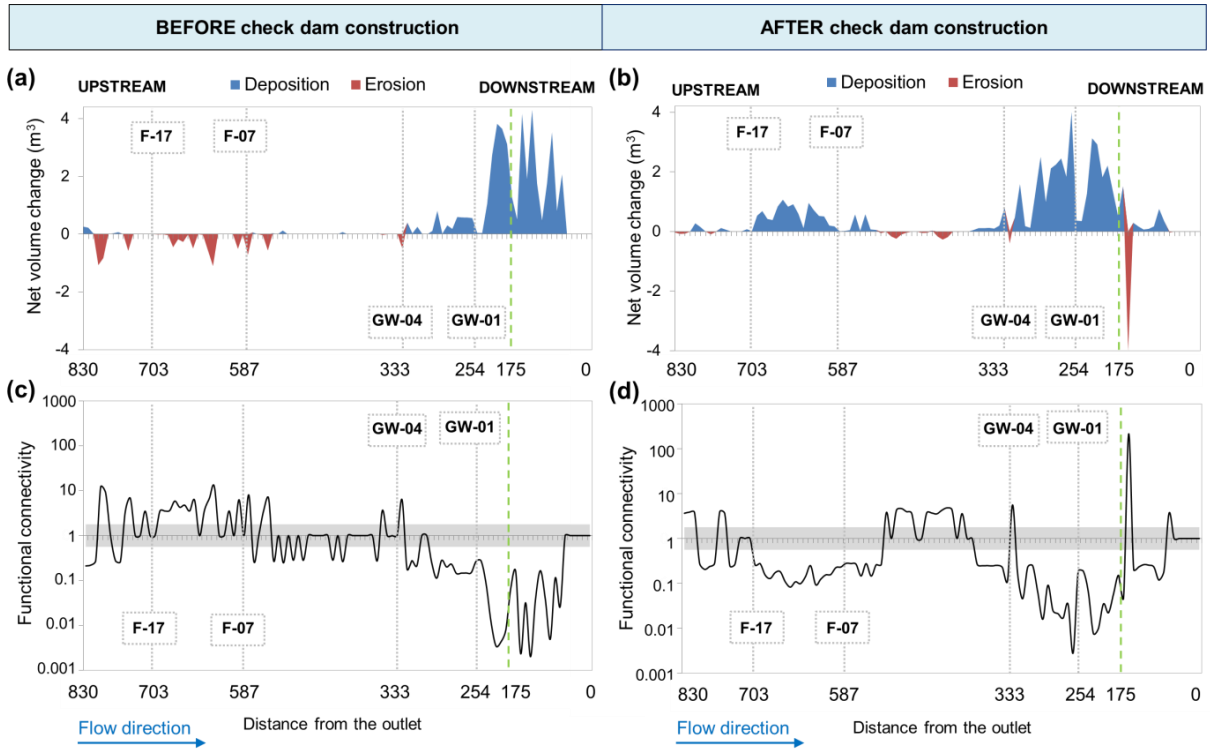

Figure 45. Net volume change (a) before and (b) after check dam construction, (c) functional connectivity (Cv–strip) along the main channel before check dam construction and (d) after check dam construction. Dotted grey lines indicate the location of GW–01, GW–04, F–07 and F–17 and the dotted green line displays the beginning of the lower reach.

The overlap of DoD and DoIC map highlights the close relationship between deposition pattern and areas that experienced a decrease of IC. This tendency is supported by the cross–frequency analysis of DoD and DoIC values (Figure 46d) calculated for the whole gully. Erosion prevailed slightly where IC increased, whereas deposition (78% of the total) was strongly associated with a decrease of IC. Figure 46 presents some detailed examples overlapping DoDs and DoIC maps from 2016 to 2019 in the restored upper reach. For example, Figure 46a shows how the values of connectivity decreased in the bank headcuts, particularly in those where livestock was excluded by a fence and fascines were implemented. Connectivity not only decreased in the bank headcuts but also in large part of the isolated area. After check dam construction, the connectivity values decreased in the area upstream of the structures. This sharp decrease was due to the large sediment deposition experienced between GW–01 and GW–02 (Figure 46c) and the sediments deposited behind GW–06 (Figure 46b). Nevertheless, a slight connectivity increase downstream GW–02 and GW–06 was observed. The values of connectivity also increased in two bank headcuts located between GW–01 and GW–03 (Figure 46c).

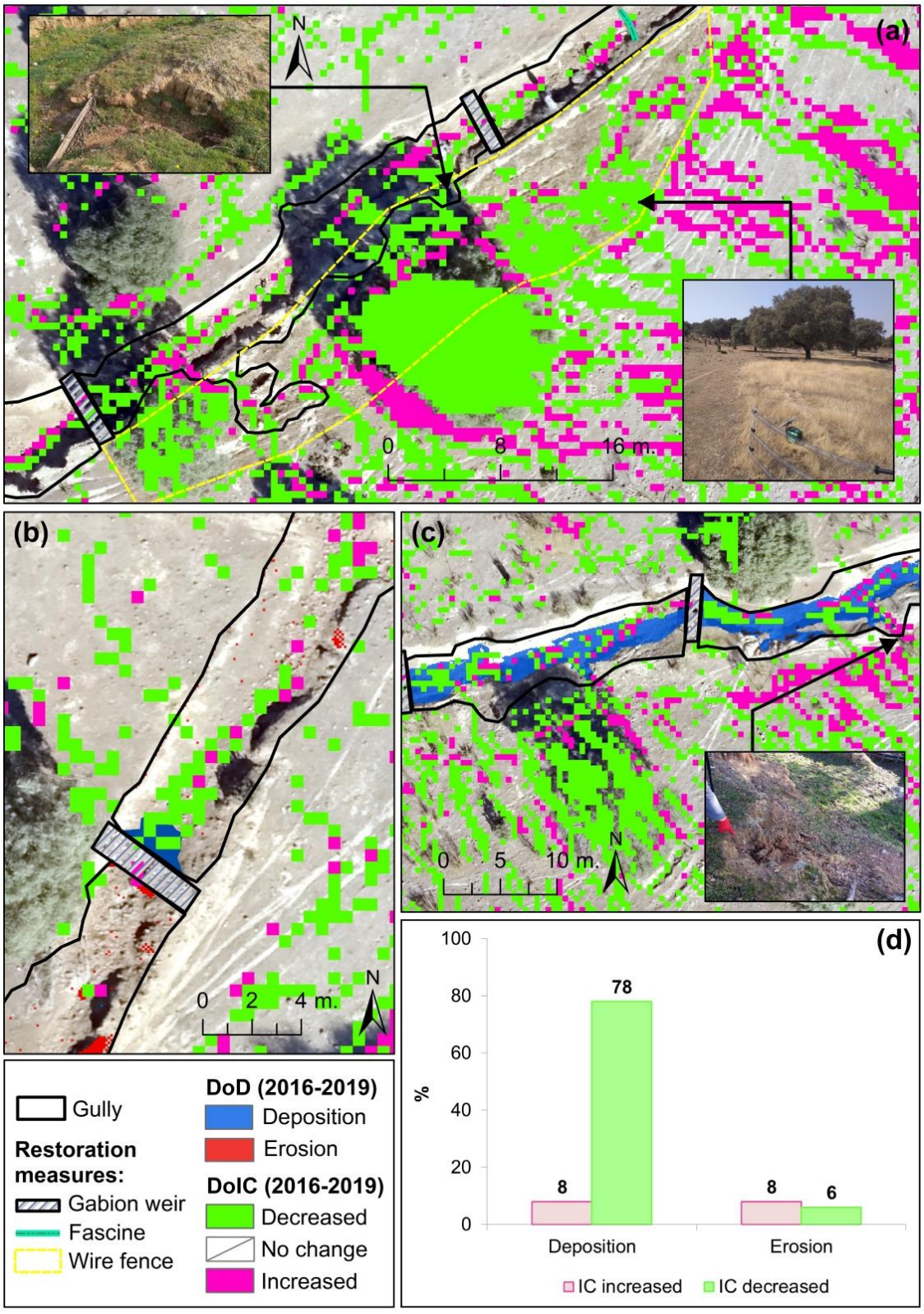

Figure 46. Difference of connectivity index (DoIC) maps and superposed DoD from 2016 and 2019 at three different locations: (a) detail of the upper reach with bank headcuts that were fenced to exclude livestock, (b) GW–06, (c) GW–01 and GW–02 area and (d) IC increase and decrease for the whole channel of areas with either cross–frequency of erosion or deposition (DoD 2017–2019; i.e., geomorphic changes after restoration activities).

6.4.5. Grain size distribution of soils and sediments

Mean grain size distributions of soils and sediments for different topographic positions are displayed in Figure 47. The pediment surface and slope had a high content of rock fragments (31.5%), whereas silt and sand were the dominant fractions of soils on the lower slopes developed on slates. Valley bottom soils, which are also formed on slates, showed the highest silt and clay content, with 53.1 and 11.2%, respectively, and the lowest proportion of sand. In contrast to the valley bottoms, the channel banks had a higher content of sand and coarse elements. Finally, sediment trapped behind check dams had the highest content of coarse elements with 39.2%, and it was also the location with the lowest silt and clay percentages. In summary, the grain size distribution of soils of pediment surface and slopes, as well as of the lower slopes, are dominated by their parent material, whereas in the valley bottoms, apart from the influence of the parent material (slates), these areas seem to be enriched in fine fractions (silt and clays) as a result of deposition of sediments from upslope. In contrast, sediments from the channel bank, with much less fine fractions, are more likely to be of alluvial nature. Sediments trapped behind check dams have even lower contents of clay, silt and sand, as compared to the channel banks, which indicates impoverishment of these fractions and hence, would represent sediment leaving the catchment as suspended load.

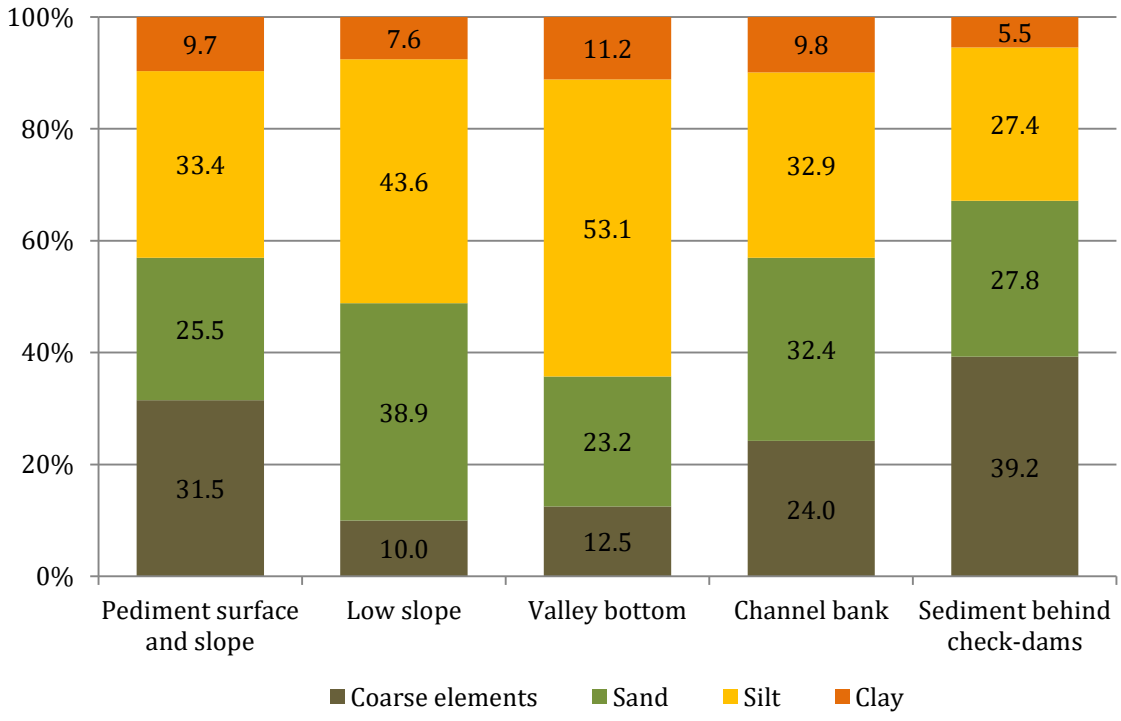

Figure 47. Grain size distribution of soils and sediments depending on topographic position.

6.5. Discussion

6.5.1. The role of restoration measures on runoff production and sediment yield

The restoration activities notably reduced the suspended sediment load at the outlet of the catchment. Check dams did not affect discharge, but did reduce sediment concentration and sediment load. Similar flood discharges resulted in different sediment load with a lower suspended sediment concentration after check dam construction. Previous works has found also that check dams capture, mainly coarse sediments (Hassanli et al., 2009; Nichols et al., 2016; Vaezi et al., 2017). Additionally, in Parapuños check dams reduced the fine fraction of sediments compared to other studies where silt and clay were not reduced by check dams (Koci et al., 2021) or only in reaches of the gully with very low slope gradients (Abedini et al., 2012; Hassanli et al., 2009). Our findings agree with the results of studies that analyzed the impact of check dams on sediment load (Borja et al., 2018; Li et al., 2017; Polyakov et al., 2014). For example, Ran et al. (2008) analyzed a dataset of available figures previously published, concluding that in the watershed of the Kuye River, the establishment of check dams caused a decrease in sediment load of 37% in a period of 26 years. Zhang et al. (2021) found in the same watershed that check dams reduced sediment output by 54% in 2006 and 31% in 2016. Similar reductions were observed by Fortugno et al. (2017) in a watershed located in the southeast of Italy where check dams reduced the sediment yield by 30–35%. A remarkable effectiveness of check dams on reducing sediment yield was also found by Mishra et al. (2007), Boix-Fayos et al. (2007), Xu et al. (2013) and Borja et al. (2018), check dams reduced the sediment yield by 64–85%. This reduction in sediment concentration may be favored by the combination of different restoration measures implemented in a catchment (i.e., check dams, grassed waterway and reduction in livestock grazing pressure), for example Evrard et al. (2008) and Heede (1978) reduced the catchment sediment yield by more than 90%.

Regarding the gully dynamics and sediment production, net deposition registered in the channel was lower than total sediment load measured at the outlet of the catchment before check dam construction. The gully, therefore, facilitated a rapid transport of water and sediments downstream. According to Poesen et al. (2003) and Capra et al. (2005), gullies perform as effective links between the upper and lower lands of a basin, increasing flow and sediment connectivity. Contrary, after check dam construction net deposition in the channel was higher than the sediment load at the outlet, hence the effect of check dams on retaining sediments was remarkable. The

sediment load at the outlet was lower after check dam construction despite more potentially erosive discharge events were registered in this period, as expressed by a greater number of peak floods > 100 l s^{-1} or catchment runoff coefficients. A total of 3 and 7 rainfall events with a peak floods > 100 l s^{-1} was registered before and after check dam construction, respectively.

In similar environments, gully erosion represents the dominant source of sediments registered at the outlet of the catchments (Koci et al., 2017; Waterhouse et al., 2017; Wilkinson et al., 2018). In our study site, the predominance of net deposition in the gully and the high amount of sediment exported at the outlet before check dam construction suggest and important sediment production by sheet wash at hillslopes.

The grain size distributions of soils of valley bottom are dominated by silt and clays as a result of deposition of sediments from upslope. In contrast, sediments from the channel bank have a lower content of fine fractions and are more likely to be of alluvial nature. Sediments trapped behind check dams have the lowest contents of clay, silt and sand, as compared to the channel banks, which indicates impoverishment of these fractions, which presumably corresponds to sediment leaving the catchment as suspended load.

Studies about sheet wash erosion carried out in the same catchment by Rubio-Delgado et al. (2018) using botanical evidences of holm oaks obtained a mean erosion rate of 18.5 t ha^{-1} y^{-1} from 1881 onwards. Schnabel (1997) and Schnabel et al. (2010) measured hillslope erosion using open plots in a similar environmental setting and observed in slightly lower erosion rates (0.63 t ha^{-1} y^{-1}) than sediment yield in Parapuños before check dam construction (2.25 t ha^{-1} y^{-1}). Nevertheless, the erosion rates registered by Schnabel et al. (2010) were similar to those presented in this study for periods when hillslopes had a reduced degree of vegetation cover (<50%) with soil loss of 1.34 t ha^{-1} y^{-1}, due, in part, to high stocking density. Kosmas et al. (2015) highlighted the relation between livestock density and soil erosion rates in a region with overgrazing in southern Europe (Crete Island, Greece) and Gómez-Gutiérrez et al. (2009a) found a relationship between gully erosion and livestock density.

The sediment yield at Parapuños catchment before check dam construction was similar to the sediment yield in other Mediterranean catchments (Vanmaercke et al., 2011). According to Vanmaercke et al.'s work, in the Mediterranean more than 50% of catchments have sediment yields higher than 2 t ha^{-1} y^{-1}. Nevertheless, the temperate and relatively gentle slope catchments of Western, Northern and Central Europe

generally have relatively low sediment yield (with approximately 50% of the catchments lower than 0.4 t ha^{-1} y^{-1}). Vanmaercke et al. (2011) demonstrated the high variability of sediment yield in Europe, also for Mediterranean catchments with sizes similar to our study area. Climatic dynamics are highly variable in the Mediterranean because of several atmospheric and geographical factors. Rainfall seasonality determines sediment transport as rainfall regimes control primarily runoff production and soil erosion by water (García-Ruiz et al., 2013). It is typical in the Mediterranean region that few rainfall events may contribute to most of the soil eroded by water (González-Hidalgo et al., 2007).

6.5.2. The effect of restoration measures and grazing on sediment connectivity

The connectivity analysis, carried out using IC, highlighted how cattle livestock grazing determines preferential sediment pathways in the studied area: cattle livestock paths drive sediment fluxes toward the gully suggesting that this activity plays an important role in increasing sediment connectivity at the catchment scale. Grazing and trampling by sheep and cattle reduces vegetation cover and enhances runoff and erosion in dehesa catchments (Gómez-Gutiérrez et al., 2012; Gómez-Gutiérrez et al., 2009a; Schnabel, 1997). Unpaved roads and cattle paths increased the routing of water in the catchment, limiting water infiltration and concentrating flows. Previous research has highlighted the critical role that unpaved roads and trails play in generating runoff on woodland–grassland ecosystem (Croke et al., 2005; Sidle et al., 2004). Commonly, trails and roads show low hydraulic conductivity (Koci et al., 2020), which capture overland flow from adjacent areas and hillslopes, driving the water effectively to the channel or gully (Sidle and Ziegler, 2010; Sidle et al., 2006). Livestock tracks not only contribute to divert runoff along well-defined pathways, they also increase channel–hillslope connectivity. According to (van der Waal and Rowntree, 2018), cattle paths can notably increase the drainage density. In this example, in a small catchment situated in the Southeast of South África the drainage density was increased by 159%. In Parapuños, flow pathways with high values of connectivity in the catchment were strongly connected to the gully that influenced the growth of channel headcuts and bank headcuts (Gómez-Gutiérrez et al., 2009a; Gomez-Gutierrez et al., 2018). For instance, the bank headcuts located upstream GW–02 and displayed in the Figure 43d is likely to split in two different directions follow the flow pathway.

The effect of human activities on sediment connectivity is recently gaining particular attention in the literature (Llena et al., 2019; Persichillo et al., 2018). In a Pyrenean mountain catchment Llena et al. (2019) found although the presence of agricultural terraces generally reduced connectivity due to the reduction of slope in steep hillslopes, it also induced localized hot spots of high connectivity due to the modification of sediment pathways that caused topographic convergence in certain points. Similar results were found by Calsamiglia et al. (2018) who observed that terraces collapsed in correspondence of the highest IC values mainly concentrated along preferential pathways where erosional processes are most likely to occur. In the same work, check dams also showed relevant decoupling effects along the thalwegs. In fact, the widespread implementation of this type of control measures, on the one hand, is mainly intended to locally retain sediment and reduce erosion along channels (Alfonso-Torreño et al., 2021), on the other hand, these restoration measures considerably reduced values of IC in the channel (i.e., longitudinal connectivity). Similar effects were found by Fryirs (2013) and Marchi et al. (2019), who observed that the restoration measures disconnect the hydrological and sedimentological dynamics in the channel. Nevertheless, other studies (e.g., Cucchiaro et al., 2019; Heckmann et al., 2018; Poeppl et al., 2017; Wohl et al., 2017) highlighted the effect of check dams on reducing lateral (i.e., hillslope–to–channel) connectivity.

In this work an integrated approach encompassing multitemporal analyses of topographic changes (DoD) and sediment connectivity (DoIC) has been applied in order to fully address the issue related to the impact of check dams on sediment dynamics in the study catchment. This kind of approach has been already applied in other contexts and geographical areas (e.g., Cucchiaro et al., 2019; Martini et al., 2019) to analyze natural and anthropic disturbances and the findings of our study seems to confirm its validity stressing the need of such a tool for better sediment management and restoration planning. In particular, we found a notable correspondence between DoD and DoIC patterns. This outcome suggests that DoIC could be used as a predictive variable of future sediment transfer processes: areas featuring an increase of sediment connectivity through time should be carefully monitored because they are potential areas that may feature erosion in the short–term. In general, after the implementation of the restoration measures we observed that functional connectivity decreased in the upper reach and increased only downstream of two check dams and in bank headcuts without the influence of the exclusion measure. The wire fence not only helped to reduce erosion in bank headcuts (Alfonso-Torreño et al., 2021), but also reduced the

values of IC in bank headcuts within the isolated area from sheep and cattle. According to Kirkby and Bracken (2009) and (Wilkinson et al., 2018), the implementation of livestock exclusion (by fencing) measures in the intersection points between hydrological flow pathways and the channel favors the revegetation and the reduction of overland flow concentration in the specific contributing area. In other places, revegetation of hillslopes reduced the erosive effect of runoff, controlling gullying and sediment yields (e.g., Chen and Cai, 2006; Talema et al., 2019). Restoration measures implemented perpendicular to the gully (i.e., check dams), combined with livestock exclusion fencing adjacent to the channel or in hillslopes, facilitated the reduction in sediment transport as also observed Bartley et al. (2020).

6. Conclusions

The combination of rainfall, discharge and suspended sediment data at the event scale with multi−temporal topographic surveys using an UAV and SfM photogrammetry allowed the comparison of gully dynamics with sediment production at the outlet of the catchment. The integration of DoIC and DoD maps allowed the assessment of the restoration measure effects on sediment connectivity variation related to the gully dynamics.

The implementation of check dams in the channel substantially reduced the suspended sediment load at the outlet but no effect was detected on flood discharge. They were particularly effective trapping the coarser sediments. However, they were unsuitable at trapping the fine sediment fractions. The mean sediment concentration was positively correlated with maximum peak flow but no relationship was detected with the rainfall variables. The effect of restoration measures on changes in the gully dynamics and sediment production was also remarkable. Net deposition in the channel was lower than total sediment load at the outlet of the catchment before check dam construction. Contrary, after check dam construction net deposition in the channel was higher than sediment load at the outlet.

The hydrological and sedimentological connectivity map showed the potential link of water and sediment between the hillslope and the channel. As it was expected, connectivity was generally higher close to the main channel. Flow pathways with high values of connectivity are strongly connected to the gully, influencing the growth of bank headcuts and the deposition behind check dams. In addition, lines of high IC values are clearly aligned with cattle paths. The effect of restoration activities (i.e.,

check dams and livestock exclosure by fencing) on longitudinal connectivity was remarkable. The values of connectivity decreased in the upper reach after the implementation of the restoration measures. This decrease took place in areas where deposition dominated and also in the bank headcuts restored by fascines and excluded from livestock by fencing. The isolated area from livestock favored revegetation, and in consequence of this, promoted a decrease of sediment connectivity and a potential reduction of sediment supply to the channel. Conversely, the IC increased in the strips where erosion processes dominated, e.g., downstream of two check dams and in bank headcuts without the influence of the exclusion measure. These critical areas should be the target for the effective implementation of restoration measures for a total to control gully erosion. This study demonstrated that the connectivity framework is an effective tool for assessing the changes on longitudinal and lateral connectivity produced by the implementation of restoration measures.

Declaration of Competing Interest

The authors declare that there is no conflict of interest.

Acknowledgments

The present study was financed by the Spanish Ministry of Economy and Competitiveness (file number CGL2014–54822–R) and Alberto Alfonso-Torreño was the beneficiary of a PhD fellowship from the regional government, i.e. Junta de Extremadura (PD16004).

CAPÍTULO 7

CONCLUSIONES GENERALES

CAPÍTULO 7. CONCLUSIONES GENERALES

7.1. Resumen de los resultados principales y conclusiones

Esta tesis evalúa dos experiencias de restauración realizadas en dehesas con el objetivo de estimar el volumen de sedimentos depositados en diques y controlar la erosión por cárcavas. La primera se realizó en seis cuencas ubicadas en una finca comunal (DBM) y el segundo estudio se llevó a cabo en la cuenca experimental de Parapuños, ubicada en una finca privada.

El uso simultáneo de una plataforma UAV de ala fija y fotogrametría SfM ha permitido la generación de nubes de puntos, MDE y ortofotografías de alta resolución, es decir, resultados fotogramétricos útiles para estudiar los efectos de las medidas de restauración. Se ha desarrollado una metodología basada en el MDE derivado de la fotogrametría SfM y un algoritmo topográfico para estimar el volumen de sedimento atrapado detrás de 160 diques construidos entre 1994 y 2006 en DBM. El trabajo de campo nos permitió validar la metodología novedosa mediante mediciones de la profundidad del sedimento utilizando una barrena en diferentes ubicaciones.

Los MDE secuenciales de alta resolución generados por fotogrametría SfM también hicieron posible evaluar los cambios en la topografía y la conectividad de los sedimentos en una cárcava de fondo del valle. Los MDE de alta resolución se utilizaron para analizar la efectividad de las actividades de restauración implementadas en el canal en febrero de 2017 mediante diques (gaviones y fajinas) y con aislamiento del ganado mediante vallado. Los cambios topográficos en la cárcava se determinaron mediante el método *MDE de diferencias* (DoD) y la *lógica difusa* (*Fuzzy Inference System* en inglés) para integrar los errores espacialmente variables. Además, estudios previos de erosión en cárcava desarrollados en Parapuños permitieron comparar la dinámica reciente del canal y ayudaron a comprender la evolución de la cárcava a escalas temporales de mediano y largo plazo.

La combinación de datos de precipitación, caudal y sedimento en suspensión a escala de evento, junto con los levantamientos topográficos multi-temporales, permitió comparar la dinámica de la cárcava con la producción de sedimentos en la salida de la cuenca. El mapa de conectividad hidrológica y de sedimentos identificó las vías de flujo entre las vertientes y la cárcava de fondo del valle. Además, la integración del mapa de cambios de conectividad con el mapa de cambios topográficos permitió evaluar los

efectos de las medidas de restauración sobre la variación hidrológica y de conectividad de sedimentos relacionada con la dinámica de la cárcava.

Se observó una gran variabilidad espacial de los sedimentos atrapados en los diques de DBM, con grandes volúmenes de sedimentos depositados en las áreas inferiores de la cuenca en contraposición a las partes superiores. Los diques ubicados en los fondos de valle con muros largos retuvieron la mayor cantidad de sedimentos, mientras que los ubicados en laderas con muros cortos fueron ineficaces para atrapar sedimentos. Además, los diques con grandes cantidades de sedimentos retenidos se ubicaron en áreas altamente conectadas.

También se analizó la relación entre la tasa de deposición y diferentes parámetros físico-ambientales. Este estudio reveló que cuanto mayor es el área de drenaje, mayor es el índice de potencia del flujo superficial y la longitud de los canales aguas arriba, menor es la tasa de deposición. La conectividad y la pendiente del canal jugaron un papel fundamental, con bajas tasas de deposición encontradas en sitios con diferente conectividad y pendiente del canal. Por otro lado, las altas tasas de deposición solo ocurrieron en áreas con poca conectividad y alta pendiente del canal. Dependiendo de la posición topográfica de los diques, la tasa de deposición se correlacionó significativa y positivamente con la longitud del muro del dique, la pendiente, la cobertura arbórea y la densidad de veredas en los diques de fondo de valle. Por el contrario, la tasa de deposición se correlacionó negativamente con la conectividad y la cobertura arbórea en los diques ubicados en las vertientes.

Los resultados en Parapuños mostraron que el funcionamiento de las actividades de restauración fue satisfactorio para estabilizar la cárcava y aumentar significativamente la deposición de sedimentos en el canal. La estabilización de la cárcava estuvo relacionada con las medidas de restauración implementadas en el cauce. Los diques, particularmente los gaviones y las fajinas, atraparon eficazmente los sedimentos y redujeron la erosión en las cabeceras laterales. Se observó un patrón espacial de sedimentación, los diques ubicados cerca de la cabecera retuvieron menos sedimentos que los situados aguas abajo. Los sedimentos depositados en el canal después de la construcción de los diques aumentaron 4 y 2 veces en la parte inferior y superior del tramo restaurado, respectivamente. Los sedimentos retenidos detrás de los diques redujeron la pendiente del lecho del canal y favorecieron la revegetación. La exclusión del ganado mediante una valla instalada en un área fuertemente degradada promovió la estabilización de las cabeceras laterales existentes, mostrando evidencias

de revegetación y limitando la formación de nuevas cabeceras. Estudios anteriores demostraron dos ciclos de incisión en la cárcava antes de la presente investigación. Estos ciclos se atribuyeron a cambios en el uso y manejo del suelo, en particular al sobrepastoreo. A partir de 2016, la cárcava mostró una dinámica de deposición en todo el canal y, particularmente, en el tramo superior después de la construcción de los diques. La deposición tuvo lugar principalmente en áreas cóncavas. El predominio de la deposición en el canal se atribuyó a los sedimentos producidos por la erosión laminar en las laderas, así como a la erosión en cárcava en el fondo del valle. A pesar de la deposición neta, también se observaron otros procesos puntuales como: incisión en el lecho del canal, erosión lateral y colapso de los márgenes de la cárcava, profundización y ensanchamiento en las cabeceras y erosión inmediatamente aguas abajo de tres diques.

Con respecto a los efectos de la rehabilitación en la cárcava sobre la producción de escorrentía y sedimentos, la carga de sedimentos suspendidos registrada en la salida de la cuenca fue considerablemente menor después de la construcción de los diques. La concentración de sedimentos en suspensión se correlacionó positivamente con el pico máximo de flujo, pero no se pudo detectar ninguna relación con las variables de precipitación. El efecto de las medidas de restauración sobre los cambios en la dinámica de la cárcava y la producción de sedimentos fue notable. La deposición neta en el canal fue menor que la carga total de sedimentos en la salida de la cuenca antes de la construcción de los diques. Por el contrario, después de la construcción de los diques, la deposición neta en el canal fue mayor que la carga de sedimentos en la salida. Esto indica que parte del sedimento en suspensión se depositó en el canal. Además, las medidas de restauración fueron más efectivas para atrapar sedimentos gruesos que sedimentos finos (limo y arcilla).

El mapa de conectividad mostró que el flujo se concentra en las veredas que posteriormente terminan en la cárcava, lo que influye en el crecimiento de las cabeceras laterales y también en la cantidad de sedimentos depositados en los diques. Además, las veredas favorecieron la concentración del flujo antes de llegar a la cárcava. El efecto de las actividades de restauración sobre la conectividad longitudinal fue notable. Los valores de conectividad longitudinal disminuyeron en el tramo superior tras la implementación de las medidas de restauración. Se observó una fuerte relación entre la dinámica de la cárcava y la conectividad funcional. La conectividad funcional aumentó en las áreas erosionadas, mientras que los sitios de deposición mostraron una

disminución de la conectividad. La conectividad también disminuyó en las cabeceras ubicadas dentro del área aislada debido a la revegetación y al relleno de sedimentos.

En general, esta tesis contribuye al conocimiento de un nuevo método topográfico para determinar el volumen de sedimentos atrapados en diques a partir de MDE de alta resolución, siendo los métodos topográficos más precisos que los métodos geométricos. Esta investigación también ofrece nuevos resultados sobre el efecto de las medidas de restauración sobre la dinámica de la erosión y la deposición, la producción de escorrentía y de sedimentos en una cárcava de fondo de valle ubicada en una cuenca con un uso del suelo agroforestal. Esta tesis podría ayudar a diseñar e implementar medidas de restauración en paisajes agroforestales degradados con el objetivo de controlar la erosión por cárcavas y perseverar la productividad de estos ecosistemas. Además de estas estrategias de restauración, se necesita una gestión eficaz de la tierra con prácticas sostenibles de pastoreo para evitar la formación de nuevas cárcavas y estabilizar las ya existentes en el entorno de la dehesa.

7.2. Summary of the main results and conclusions

This thesis evaluates the performance of two restoration experiences conducted in dehesas aimed to estimate the volume of sediments deposited in check dams and to control gully erosion. The first one was carried out in six catchments located in a communal farm (DBM) and the second study was conducted in the Parapuños experimental catchment, located in a private farm.

The concurrent use of a fixed-wing UAV platform and SfM photogrammetry has enabled the generation of accurate high-resolution point clouds, DEMs and orthophotographs, i.e., useful photogrammetric outcomes to study the effects of restoration measures. A methodology based on the SfM-derived DEM and a topographical algorithm has been developed to estimate the volume of sediment trapped behind 160 check dams built from 1994 to 2006 in DBM. Field survey sampling allowed us to validate the innovative methodology by measurements of sediment depth using an auger at different locations.

Sequential high−resolution DEMs generated by SfM photogrammetry also made possible to evaluate changes in topography and sediment connectivity in a valley-bottom gully. The high-resolution DEMs were used to analyze the effectiveness of restoration activities implemented partially in the channel in February 2017 by means

of check dams (gabions and fascines) and with livestock exclosure by fencing. Topographic changes in the gully were determined through the DoD approach and the FIS method in order to integrate spatially variable errors. In addition, former studies conducted in Parapuños allowed the comparison with the recent channel dynamics and helped understanding the evolution of the gully at medium- and long-term temporal scales.

The combination of rainfall, discharge and suspended sediment data at the event scale together with the multi-temporal topographic surveys enabled the comparison of gully dynamics with sediment production at the outlet of the catchment. The hydrological and sediment connectivity map identified flow pathways between the hillslope and the valley-bottom channel. Furthermore, the integration of the connectivity changes map with the topographic changes map enabled the assessment of the restoration measure effects on hydrological and sediment connectivity variation related to the gully dynamics.

A large spatial variability of sediments trapped in the check dams in DBM was observed, with large volumes of sediment accumulated in the lower areas of the catchment as opposed to the upper parts. Check dams located in valley-bottoms with long walls retained the highest amounts of sediments, while those located in hillslopes with short walls were ineffective at trapping sediment. Moreover, check dams with large amounts of sediment deposited were located in highly connected areas.

The relationship between the deposition rate and different physical-environmental parameters was also analyzed. This study revealed that the greater the drainage area, the greater stream power index and the upstream channel lengths, the lower the deposition rate. Connectivity and channel slope played a fundamental role, with low deposition rates found in sites with varying connectivity and channel slope. On the other hand, high deposition rates only took place in areas with poor connectivity and high channel slope. Depending on check dams' topographic position, deposition rate was significantly and positively correlated with check dam size, slope gradient, tree cover and path density at valley bottom check dams. Conversely, the deposition rate was negatively correlated with connectivity and tree cover at hillslope check dams.

The results at Parapuños showed that the performance of the restoration activities was satisfactory to stabilize the gully and to significantly increase the sediment deposition in the channel. The stabilization of the gullied area was related to

restoration measures implemented in the channel. Check dams, specifically gabion weirs and fascines, were effectively trapping sediment and reducing the erosion of the bank headcuts. A spatial pattern of sedimentation was observed, with check dams located near the headwater retaining less sediments than those situated downstream. The sediments deposited in the channel after check dam construction increased 4-fold and 2-fold in the lower and the upper part of the restored reach, respectively. The sediments retained behind check dams reduced the slope of the channel bed and favored channel revegetation. Livestock exclosure by means of a fence installed in a strongly degraded area promoted the stabilization of the existing bank headcuts, showing evidences of revegetation and limiting the formation of new headcuts. Previous studies reported two incision cycles before the present research. These cycles were attributed to land use and management changes, particularly overgrazing. From 2016 onwards, the gully showed a general depositional dynamic in the whole channel and, particularly, in the upper reach after check dam construction. Deposition mainly took place on concave areas. The predominance of deposition in the channel was attributed to sediments produced by sheet erosion at hillslopes, as well as gully erosion in the valley-bottom. Despite the net deposition, other specific processes were also observed such as: channel bed incision, lateral bank erosion and bank collapse, deepening and widening in headcuts and erosion immediately downstream of three check dams.

Regarding the effects of gully rehabilitation on runoff production and sediment yield, the suspended sediment load registered at the outlet of the catchment was considerable lower after check dam construction. Suspended sediment concentration was positively correlated with maximum peak flow but no relationship could be detected with the rainfall variables. The effect of restoration measures on changes in the gully dynamics and sediment production was remarkable. The net deposition in the channel was lower than total sediment load at the outlet of the catchment before check dam construction. Contrary, after check dam construction the net deposition in the channel was higher than the sediment load at the outlet. This indicates that part of the suspended sediment is deposited in the channel. Furthermore, the restoration measures were more effective in trapping coarse sediments than fine sediments (silt and clays).

The IC map showed that the flow is concentrated in livestock pathways that end up in the gully later, influencing the growth of bank headcuts and the deposition behind check dams too. In addition, cattle paths favored the concentration of the flow before

reaching the gully. The effect of restoration activities on longitudinal connectivity was remarkable. The values of longitudinal connectivity decreased in the upper reach after the implementation of the restoration measures. A strong relationship was observed between gully dynamics and functional connectivity. The functional connectivity increased in eroded areas, while deposition sites showed a decrease of the IC. Connectivity also decreased in the bank headcuts located within the isolated area due to revegetation and filling.

In general, this thesis contributes to the knowledge about a new topographic method to determine the volume of sediments trapped in check dams from high-resolution DEMs, being topographic methods more accurate than geometric methods. This research also delivers new outcomes about the effect of restoration measures on dynamics of erosion and deposition, runoff production and sediment yield in a valley-bottom gully located in a catchment under agroforestry land use. It could help in designing and implementing restoration measures in degraded agroforestry landscapes aiming to control gully erosion and persevere the productivity of these ecosystems. Besides these remediation strategies, an effective land management with sustainable livestock grazing practices is needed to avoid the formation of new gullies and to stabilize already existing gullies in the dehesa environment.

REFERENCES

Abbasi, N.A., Xu, X., Lucas-Borja, M.E., Dang, W., Liu, B., 2019. The use of check dams in watershed management projects: Examples from around the world. Science of the total environment, 676, 683-691.

Abedini, M., Said, M.A.M., Ahmad, F., 2012. Effectiveness of check dam to control soil erosion in a tropical catchment (The Ulu Kinta Basin). Catena, 97, 63-70.

Agüera-Vega, F., Carvajal-Ramírez, F., Martínez-Carricondo, P., 2017. Assessment of photogrammetric mapping accuracy based on variation ground control points number using unmanned aerial vehicle. Measurement, 98, 221-227.

Alfonso-Torreño, A., Gómez-Gutiérrez, Á., Schnabel, S., 2021. Dynamics of Erosion and Deposition in a Partially Restored Valley-Bottom Gully. Land, 10, 62.

Alfonso-Torreño, A., Gómez-Gutiérrez, Á., Schnabel, S., Lavado Contador, J.F., de Sanjosé Blasco, J.J., Sánchez Fernández, M., 2019. sUAS, SfM-MVS photogrammetry and a topographic algorithm method to quantify the volume of sediments retained in check-dams. Science of The Total Environment, 678, 369-382.

Arun, P.V., 2013. A comparative analysis of different DEM interpolation methods. The Egyptian Journal of Remote Sensing and Space Science, 16, 133-139.

Avni, Y., 2005. Gully incision as a key factor in desertification in an arid environment, the Negev highlands, Israel. Catena, 63, 185-220.

Ayele, G.K., Gesses, A.A., Tilahun, S.A., Tebebu, T.Y., Tenessa, D.B., Langendoen, E.J., Nicholson, C.F., Steenhuis, T.S., 2016. A biophysical and economic assessment of a community-based rehabilitated gully in the Ethiopian highlands. Land Degradation & Development, 27, 270-280.

Baade, J., Franz, S., Reichel, A., 2012. Reservoir siltation and sediment yield in the Kruger National Park, South Africa: a first assessment. Land Degradation & Development, 23, 586-600.

Baartman, J.E., Masselink, R., Keesstra, S.D., Temme, A.J., 2013. Linking landscape morphological complexity and sediment connectivity. Earth Surface Processes and Landforms, 38, 1457-1471.

Bagarello, V., Ferro, V., 2010. Analysis of soil loss data from plots of differing length for the Sparacia experimental area, Sicily, Italy. Biosystems Engineering, 105, 411-422.

Bakker, M.M., Govers, G., Jones, R.A., Rounsevell, M.D., 2007. The effect of soil erosion on Europe's crop yields. Ecosystems, 10, 1209-1219.

Bakker, M.M., Govers, G., Rounsevell, M.D., 2004. The crop productivity–erosion relationship: an analysis based on experimental work. Catena, 57, 55-76.

Bangen, S., Hensleigh, J., McHugh, P., Wheaton, J., 2016. Error modeling of DEMs from topographic surveys of rivers using fuzzy inference systems. Water Resources Research, 52, 1176-1193.

Bartley, R., Bainbridge, Z.T., Lewis, S.E., Kroon, F.J., Wilkinson, S.N., Brodie, J.E., Silburn, D.M., 2014. Relating sediment impacts on coral reefs to watershed sources, processes and management: A review. Science of the Total Environment, 468, 1138-1153.

Bartley, R., Poesen, J., Wilkinson, S., Vanmaercke, M., 2020. A review of the magnitude and response times for sediment yield reductions following the rehabilitation of gullied landscapes. Earth Surface Processes and Landforms, 45, 3250-3279.

Bartley, R., Roth, C.H., Ludwig, J., McJannet, D., Liedloff, A., Corfield, J., Hawdon, A., Abbott, B., 2006. Runoff and erosion from Australia's tropical semi-arid rangelands: Influence of ground cover for differing space and time scales. Hydrological Processes: An International Journal, 20, 3317-3333.

Belmonte, F., Romero Díaz, A., Martínez Lloris, M., 2005. Erosión en cauces afectados por obras de corrección hidrológica (Cuenca del Río Quípar, Murcia). Papeles de Geografía, 71-83.

Bellin, N., Vanacker, V., van Wesemael, B., Solé-Benet, A., Bakker, M., 2011. Natural and anthropogenic controls on soil erosion in the Internal Betic Cordillera (southeast Spain). Catena, 87, 190-200.

Billi, P., Dramis, F., 2003. Geomorphological investigation on gully erosion in the Rift Valley and the northern highlands of Ethiopia. Catena, 50, 353-368.

Birkinshaw, S., Bathurst, J., 2006. Model study of the relationship between sediment yield and river basin area. Earth Surface Processes and Landforms, 31, 750-761.

Boardman, J., Foster, I.D., Rownstree, K.M., Favis-Mortlock, D.T., Mol, L., Suich, H., Gaynor, D., 2017. Long-term studies of land degradation in the Sneeuberg uplands, eastern Karoo, South Africa: a synthesis. Geomorphology, 285, 106-120.

Boardman, J., Poesen, J., 2007. Soil erosion in Europe. John Wiley & Sons Ltd., Chichester, United Kingdom.

Boardman, J., Poesen, J., Evans, R., 2003. Socio-economic factors in soil erosion and conservation. Environmental Science & Policy, 6, 1-6.

Boardman, J., Vandaele, K., Evans, R., Foster, I.D., 2019. Off-site impacts of soil erosion and runoff: Why connectivity is more important than erosion rates. Soil Use and Management, 35, 245-256.

Bogen, J., Berg, H., Sandersen, F., 1994. The contribution of gully erosion to the sediment budget of the River Leira. IAHS Publications-Series of Proceedings and Reports-Intern Assoc Hydrological Sciences, 224, 307-316.

Boix-Fayos, C., Barberá, G., López-Bermúdez, F., Castillo, V., 2007. Effects of check dams, reforestation and land-use changes on river channel morphology: Case study of the Rogativa catchment (Murcia, Spain). Geomorphology, 91, 103-123.

Boix-Fayos, C., de Vente, J., Martínez-Mena, M., Barberá, G.G., Castillo, V., 2008. The impact of land use change and check-dams on catchment sediment yield. Hydrological Processes: An International Journal, 22, 4922-4935.

Bombino, G., Gurnell, A., Tamburino, V., Zema, D., Zimbone, S., 2009. Adjustments in channel form, sediment calibre and vegetation around check-dams in the headwater reaches of mountain torrents, Calabria, Italy. Earth Surface Processes and Landforms, 34, 1011-1021.

Borja, P., Molina, A., Govers, G., Vanacker, V., 2018. Check dams and afforestation reducing sediment mobilization in active gully systems in the Andean mountains. Catena, 165, 42-53.

Borrelli, L., Conforti, M., Mercuri, M., 2019. Lidar and UAV system data to analyse recent morphological changes of a small drainage basin. ISPRS International Journal of Geo-Information, 8, 536.

Borrelli, P., Robinson, D.A., Fleischer, L.R., Lugato, E., Ballabio, C., Alewell, C., Meusburger, K., Modugno, S., Schütt, B., Ferro, V., 2017. An assessment of the global impact of 21st century land use change on soil erosion. Nature communications, 8, 1-13.

Borselli, L., Cassi, P., Torri, D., 2008. Prolegomena to sediment and flow connectivity in the landscape: a GIS and field numerical assessment. Catena, 75, 268-277.

Bracken, L.J., Croke, J., 2007. The concept of hydrological connectivity and its contribution to understanding runoff-dominated geomorphic systems. Hydrological Processes: An International Journal, 21, 1749-1763.

Bracken, L.J., Turnbull, L., Wainwright, J., Bogaart, P., 2015. Sediment connectivity: a framework for understanding sediment transfer at multiple scales. Earth Surface Processes and Landforms, 40, 177-188.

Bradford, J.M., Piest, R.F., 1980. Erosional development of valley-bottom gullies in the upper midwestern United States. in: Coates, D.R., Vitak, J.D. (Ed.), Thresholds in geomorphology. Routledge, pp. 75-101.

Brasier, C.M., 1996. Phytophthora cinnamomi and oak decline in southern Europe. Environmental constraints including climate change, Annales des Sciences Forestieres. EDP Sciences, pp. 347-358.

Brasington, J., Langham, J., Rumsby, B., 2003. Methodological sensitivity of morphometric estimates of coarse fluvial sediment transport. Geomorphology, 53, 299-316.

Brasington, J., Rumsby, B., McVey, R., 2000. Monitoring and modelling morphological change in a braided gravel-bed river using high resolution GPS-based survey. Earth Surface Processes and Landforms: The Journal of the British Geomorphological Research Group, 25, 973-990.

Brooks, A., Shellberg, J., Knight, J., Spencer, J., 2009. Alluvial gully erosion: an example from the Mitchell fluvial megafan, Queensland, Australia. Earth Surface Processes and Landforms: The Journal of the British Geomorphological Research Group, 34, 1951-1969.

Bussi, G., Rodríguez-Lloveras, X., Francés, F., Benito, G., Sánchez-Moya, Y., Sopeña, A., 2013. Sediment yield model implementation based on check dam infill stratigraphy in a semiarid Mediterranean catchment. Hydrology and Earth System Science, 17, 3339-3354.

Calsamiglia, A., Fortesa, J., García-Comendador, J., Lucas-Borja, M.E., Calvo-Cases, A., Estrany, J., 2018. Spatial patterns of sediment connectivity in terraced lands: Anthropogenic controls of catchment sensitivity. Land Degradation & Development, 29, 1198-1210.

Campos, P., 1983. La degradación de los recursos naturales de la dehesa: Análisis de un modelo de dehesa tradicional. Agricultura y sociedad, 26, 289-380.

Campos, P., 1992. Reunión Internacional sobre sistemas agroforestales de dehesas y montados. Agricultura y sociedad, 62, 197-202.

Campos, P. et al., 2010. Libro verde de la dehesa. Universidad de Extremadura: Plasencia, Spain, 1-48.

Cánovas, J.B., Stoffel, M., Martín-Duque, J.F., Corona, C., Lucía, A., Bodoque, J.M., Montgomery, D.R., 2017. Gully evolution and geomorphic adjustments of badlands to reforestation. Scientific reports, 7, 1-8.

Capra, A., Mazzara, L., Scicolone, B., 2005. Application of the EGEM model to predict ephemeral gully erosion in Sicily, Italy. Catena, 59, 133-146.

Caraballo-Arias, N., Conoscenti, C., Di Stefano, C., Ferro, V., Gómez-Gutiérrez, A., 2016. Morphometric and hydraulic geometry assessment of a gully in SW Spain. Geomorphology, 274, 143-151.

Castillo, C., Gómez, J., 2016. A century of gully erosion research: Urgency, complexity and study approaches. Earth-Science Reviews, 160, 300-319.

Castillo, C., Marín-Moreno, V., Pérez, R., Muñoz-Salinas, R., Taguas, E., 2018. Accurate automated assessment of gully cross-section geometry using the photogrammetric interface FreeXSapp. Earth Surface Processes and Landforms, 43, 1726-1736.

Castillo, C., Pérez, R., James, M.R., Quinton, J.N., Taguas, E.V., Gómez, J.A., 2012. Comparing the accuracy of several field methods for measuring gully erosion. Soil Science Society of America Journal, 76, 1319-1332.

Castillo, V.M., Mosch, W.M., Conesa-García, C., Barberá, G.G., Navarro-Cano, J.A., López-Bermúdez, F., 2007. Effectiveness and geomorphological impacts of check dams for soil erosion control in a semiarid Mediterranean catchment: El Cárcavo (Murcia, Spain). Catena, 70, 416-427.

Catella, M., Paris, E., Solari, L., 2005. Case study: efficiency of slit-check dams in the mountain region of Versilia basin. Journal of Hydraulic Engineering, 131, 145-152.

Cavalli, M., Goldin, B., Comiti, F., Brardinoni, F., Marchi, L., 2017. Assessment of erosion and deposition in steep mountain basins by differencing sequential digital terrain models. Geomorphology, 291, 4-16.

Cavalli, M., Marchi, L., 2008. Characterisation of the surface morphology of an alpine alluvial fan using airborne LiDAR. Natural Hazards and Earth System Sciences, 8, 323-333.

Cavalli, M., Tarolli, P., Marchi, L., Dalla Fontana, G., 2008. The effectiveness of airborne LiDAR data in the recognition of channel-bed morphology. Catena, 73, 249-260.

Cavalli, M., Trevisani, S., Comiti, F., Marchi, L., 2013. Geomorphometric assessment of spatial sediment connectivity in small Alpine catchments. Geomorphology, 188, 31-41.

Cavalli, M., Vericat, D., Pereira, P., 2019. Mapping water and sediment connectivity. Science of the Total Environment, 673, 763-767.

Cisneros, J., Cholaky, C., Cantero Gutiérrez, A., González, J., Reynero, M., Diez, A., Bergesio, L., Cantero, J.J., Nuñez, C., Amuchastegui, A., 2012. Erosión hídrica. Principios y técnicas de manejo. Río Cuarto, Córdoba, Argentina. UniRío Editora.

Clapuyt, F., Vanacker, V., Van Oost, K., 2016. Reproducibility of UAV-based earth topography reconstructions based on Structure-from-Motion algorithms. Geomorphology, 260, 4-15.

Comiti, F., Marchi, L., Macconi, P., Arattano, M., Bertoldi, G., Borga, M., Brardinoni, F., Cavalli, M., D'agostino, V., Penna, D., 2014. A new monitoring station for debris flows in the European Alps: first observations in the Gadria basin. Natural hazards, 73, 1175-1198.

Conesa García, C., 2004. Los diques de retención en cuencas de régimen torrencial: diseño, tipos y funciones. Nimbus: Revista de climatología, meteorología y paisaje, 13-15, 125-142.

Conesa García, C., García Lorenzo, R., 2007. Litofacies de relleno y modelo de sedimentación de los diques de retención en el tramo inferior de la Rambla del Cárcavo (Cuenca del Segura). Cuaternario y Geomorfología, 21, 77-100.

Cook, K.L., 2017. An evaluation of the effectiveness of low-cost UAVs and structure from motion for geomorphic change detection. Geomorphology, 278, 195-208.

Cooke, R.U., Reeves, R.W., 1976. Arroyos and environmental change in the American South-West. Clarendon Press.

Crema, S., Cavalli, M., 2018. SedInConnect: a stand-alone, free and open source tool for the assessment of sediment connectivity. Computers & Geosciences, 111, 39-45.

Croke, J., Mockler, S., Fogarty, P., Takken, I., 2005. Sediment concentration changes in runoff pathways from a forest road network and the resultant spatial pattern of catchment connectivity. Geomorphology, 68, 257-268.

Cubera, E., Moreno, G., 2007. Effect of land-use on soil water dynamic in dehesas of Central–Western Spain. Catena, 71, 298-308.

Cucchiaro, S., Cavalli, M., Vericat, D., Crema, S., Llena, M., Beinat, A., Marchi, L., Cazorzi, F., 2018. Monitoring topographic changes through 4D-structure-from-motion photogrammetry: application to a debris-flow channel. Environmental Earth Sciences, 77, 632.

Cucchiaro, S., Cavalli, M., Vericat, D., Crema, S., Llena, M., Beinat, A., Marchi, L., Cazorzi, F., 2019. Geomorphic effectiveness of check dams in a debris-flow catchment using multi-temporal topographic surveys. Catena, 174, 73-83.

Chaplot, V., Le Brozec, E.C., Silvera, N., Valentin, C., 2005. Spatial and temporal assessment of linear erosion in catchments under sloping lands of northern Laos. Catena, 63, 167-184.

Chartin, C., Evrard, O., Onda, Y., Patin, J., Lefèvre, I., Ottlé, C., Ayrault, S., Lepage, H., Bonté, P., 2013. Tracking the early dispersion of contaminated sediment along rivers draining the Fukushima radioactive pollution plume. Anthropocene, 1, 23-34.

Chen, H., Cai, Q., 2006. Impact of hillslope vegetation restoration on gully erosion induced sediment yield. Science in China Series D, 49, 176-192.

Chow, V., Maidment, D., Mays, L., 1988. Applyed Hydrology. New York.

D'Haen, K., Dusar, B., Verstraeten, G., Degryse, P., De Brue, H., 2013. A sediment fingerprinting approach to understand the geomorphic coupling in an eastern Mediterranean mountainous river catchment. Geomorphology, 197, 64-75.

Daba, S., Rieger, W., Strauss, P., 2003. Assessment of gully erosion in eastern Ethiopia using photogrammetric techniques. Catena, 50, 273-291.

De Alba, S., 1998. Procesos de degradación del suelo por erosión en ecosistemas agrícolas de condiciones ambientales mediterráneas en la región central de España. Unpublished PhD thesis, Universidad Autónoma de Madrid.

De Baets, S., Poesen, J., Knapen, A., Barberá, G.G., Navarro, J., 2007. Root characteristics of representative Mediterranean plant species and their erosion-reducing potential during concentrated runoff. Plant and Soil, 294, 169-183.

De Sampaio e Paiva Camilo-Alves, C., Esteves da Clara, M.I., Cabral De Almeida Ribeiro, N.M., 2013. Decline of Mediterranean oak trees and its association with Phytophthora cinnamomi: a review. European Journal of Forest Research, 132, 411-432.

De Vente, J., Poesen, J., Arabkhedri, M., Verstraeten, G., 2007. The sediment delivery problem revisited. Progress in physical geography, 31, 155-178.

De Vente, J., Poesen, J., Verstraeten, G., Govers, G., Vanmaercke, M., Van Rompaey, A., Arabkhedri, M., Boix-Fayos, C., 2013. Predicting soil erosion and sediment yield at regional scales: where do we stand? Earth-Science Reviews, 127, 16-29.

Descheemaeker, K., Nyssen, J., Poesen, J., Raes, D., Haile, M., Muys, B., Deckers, S., 2006. Runoff on slopes with restoring vegetation: a case study from the Tigray highlands, Ethiopia. Journal of hydrology, 331, 219-241.

Descheemaeker, K., Raes, D., Nyssen, J., Poesen, J., Haile, M., Deckers, J., 2009. Changes in water flows and water productivity upon vegetation regeneration on degraded hillslopes in northern Ethiopia: a water balance modelling exercise. The Rangeland Journal, 31, 237-249.

Desir, G., Marín, C., 2009. Erosion characteristics in badlands on the Fm. Tudela (Bárdenas Reales, Navarra). Cuadernos de Investigación Geográfica, 35, 195-213.

Desmet, P., Poesen, J., Govers, G., Vandaele, K., 1999. Importance of slope gradient and contributing area for optimal prediction of the initiation and trajectory of ephemeral gullies. Catena, 37, 377-392.

Di Stefano, C., Ferro, V., Porto, P., Tusa, G., 2000. Slope curvature influence on soil erosion and deposition processes. Water resources research, 36, 607-617.

Díaz-Gutiérrez, V., 2015. Control de la erosión ejercido por los diques forestales de la restauración hidrológico-forestal de Tórtoles (Avila), Universidad de Valladolid.

Díaz-Gutiérrez, V., Mongil-Manso, J., Navarro-Hevia, J., Ramos-Díez, I., 2019. Check dams and sediment control: final results of a case study in the upper Corneja River (Central Spain). Journal of soils and sediments, 19, 451-466.

Díaz, V., Mongil, J., Navarro, J., 2014. Topographical surveying for improved assessment of sediment retention in check dams applied to a Mediterranean badlands restoration site (Central Spain). Journal of Soils and Sediments, 14, 2045-2056.

Dube, H.B., Mutema, M., Muchaonyerwa, P., Poesen, J., Chaplot, V., 2020. A global analysis of the morphology of linear erosion features. Catena, 190, 104542.

Dunjó Denti, G., 2004. Developing a desertification indicator system for a small Mediterranean catchment: a case study from the Serra de Rodes, Alt Empordà, Catalunya, NE Spain, Universitat de Girona.

EC, 2002. Towards a Thematic Strategy for Soil Protection. Communication from the Commission to the Council, the European Parliament, the Economic and Social Committe and the Committee of Regions, Commission of the European Communities, Brussels, Belgium COM, pp. 35.

Eichhorn, M., Paris, P., Herzog, F., Incoll, L.D., Liagre, F., Mantzanas, K., Mayus, M., Moreno, G., Papanastasis, V.P., Pilbeam, D.J., 2006. Silvoarable systems in Europe–past, present and future prospects. Agroforestry systems, 67, 29-50.

Elena-Rosselló, M., López Márquez, J.A., Casas Martín, M., Sánchez del Corral Jiménez, A., 1987. El carbón de encina y la dehesa. Instituto Nacional de Investigaciones Agrarias. Ministerio de Agricultura, Pesca y Alimentación, Madrid.

Esposito, G., Salvini, R., Matano, F., Sacchi, M., Danzi, M., Somma, R., Trose, C., 2017. Multitemporal monitoring of a coastal landslide through SfM-derived point cloud comparison. The Photogrammetric Record, 32, 459-479.

Eustace, A., Pringle, M., Witte, C., 2009. Give me the dirt: detection of gully extent and volume using high-resolution lidar, Innovations in Remote Sensing and Photogrammetry. Springer, pp. 255-269.

Evans, M., Lindsay, J., 2010. High resolution quantification of gully erosion in upland peatlands at the landscape scale. Earth Surface Processes and Landforms, 35, 876-886.

Evrard, O., Vandaele, K., van Wesemael, B., Bielders, C.L., 2008. A grassed waterway and earthen dams to control muddy floods from a cultivated catchment of the Belgian loess belt. Geomorphology, 100, 419-428.

Faulkner, H., 1995. Gully erosion associated with the expansion of unterraced almond cultivation in the coastal Sierra de Lujar, S. Spain. Land Degradation & Development, 6, 179-200.

Faulkner, H., Alexander, R., Teeuw, R., Zukowskyj, P., 2004. Variations in soil dispersivity across a gully head displaying shallow sub-surface pipes, and the role of shallow pipes in rill initiation. Earth Surface Processes and Landforms: the Journal of the British Geomorphological Research Group, 29, 1143-1160.

Ferguson, R., Ashworth, P., 1992. Spatial patterns of bedload transport and channel change in braided and near-braided rivers. in: Billi, P., Hey, R., Thorne, C., Tacconi, P. (Eds.), Dynamics of Gravel-Bed Rivers. John Wiley & Sons Ltd, pp. 477-492.

Fernández, P., Porras, C., 1998. La Dehesa, algunos aspectos para la regeneración del arbolado.

Foerster, S., Wilczok, C., Brosinsky, A., Segl, K., 2014. Assessment of sediment connectivity from vegetation cover and topography using remotely sensed data in a dryland catchment in the Spanish Pyrenees. Journal of Soils and Sediments, 14, 1982-2000.

Fonstad, M.A., Dietrich, J.T., Courville, B.C., Jensen, J.L., Carbonneau, P.E., 2013. Topographic structure from motion: a new development in photogrammetric measurement. Earth surface processes and Landforms, 38, 421-430.

Fortugno, D., Boix-Fayos, C., Bombino, G., Denisi, P., Quiñonero-Rubio, J.M., Tamburino, V., Zema, D.A., 2017. Adjustments in channel morphology due to land-use changes and check dam installation in mountain torrents of Calabria (southern Italy). Earth Surface Processes and Landforms, 42, 2469-2483.

Foster, G.R., 1982. Modeling the erosion process. in: Haan, C.T. (Ed.), Hydrologic modeling of small wathersheds. ASAE, pp. 297-380.

Fox, D., 2011. Evaluation of the efficiency of some sediment trapping methods after a Mediterranean forest fire. Journal of environmental management, 92, 258-265.

Fox, D., Bryan, R., Price, A., 1997. The influence of slope angle on final infiltration rate for interrill conditions. Geoderma, 80, 181-194.

Fox, G., Sheshukov, A., Cruse, R., Kolar, R.L., Guertault, L., Gesch, K.R., Dutnell, R.C., 2016. Reservoir sedimentation and upstream sediment sources: perspectives and future research needs on streambank and gully erosion. Environmental management, 57, 945-955.

Frankl, A., Nyssen, J., Adgo, E., Wassie, A., Scull, P., 2019. Can woody vegetation in valley bottoms protect from gully erosion? Insights using remote sensing data (1938–2016) from subhumid NW Ethiopia. Regional Environmental Change, 19, 2055-2068.

Frankl, A., Nyssen, J., Vanmaercke, M., Poesen, J., 2021. Gully prevention and control: techniques, failures and effectiveness. Earth Surface Processes and Landforms, 46, 220-238.

Frankl, A., Stal, C., Abraha, A., Nyssen, J., Rieke-Zapp, D., De Wulf, A., Poesen, J., 2015. Detailed recording of gully morphology in 3D through image-based modelling. Catena, 127, 92-101.

Fryirs, K., 2013. (Dis) Connectivity in catchment sediment cascades: a fresh look at the sediment delivery problem. Earth Surface Processes and Landforms, 38, 30-46.

Fryirs, K.A., Brierley, G.J., Preston, N.J., Kasai, M., 2007. Buffers, barriers and blankets: the (dis) connectivity of catchment-scale sediment cascades. Catena, 70, 49-67.

Fuller, I.C., Large, A.R., Charlton, M.E., Heritage, G.L., Milan, D.J., 2003. Reach-scale sediment transfers: an evaluation of two morphological budgeting approaches. Earth Surface Processes and Landforms: The Journal of the British Geomorphological Research Group, 28, 889-903.

Gamougoun, N.D., Smith, R.P., Wood, M.K., Pieper, R.D., 1984. Soil, vegetation, and hydrologic responses to grazing management at Fort Stanton, New Mexico. Journal of Range Management, 37, 538-541.

García-Ruiz, J.M., 2010. The effects of land uses on soil erosion in Spain: a review. Catena, 81, 1-11.

García-Ruiz, J.M., Nadal-Romero, E., Lana-Renault, N., Beguería, S., 2013. Erosion in Mediterranean landscapes: changes and future challenges. Geomorphology, 198, 20-36.

García Ruiz, J.M., López Bermúdez, F., 2009. La erosión del suelo en España. Cuaternario y geomorfología: Revista de la Sociedad Española de Geomorfología y Asociación Española para el Estudio del Cuaternario, 23, 5-6.

Gea-Izquierdo, G., Cañellas, I., Montero, G., 2006. Producción de bellota en las dehesas españolas de encina. Forest Systems, 15, 339-354.

Gifford, G.F., Thomas, D.B., Coltharp, G.B., 1977. Effects of gully plugs and contour furrows on erosion and sedimentation in Cisco Basin, Utah.

Golosov, V., Belyaev, V., 2013. The history and assessment of effectiveness of soil erosion control measures deployed in Russia. International Soil and Water Conservation Research, 1, 26-35.

Gómez-Gutiérrez, Á., Schnabel, S., Berenguer-Sempere, F., Lavado-Contador, F., Rubio-Delgado, J., 2014. Using 3D photo-reconstruction methods to estimate gully headcut erosion. Catena, 120, 91-101.

Gómez-Gutiérrez, Á., Schnabel, S., De Sanjosé, J.J., Contador, F.L., 2012. Exploring the relationships between gully erosion and hydrology in rangelands of SW Spain. Zeitschrift für Geomorphologie, Supplementary Issues, 56, 27-44.

Gómez-Gutiérrez, Á., Schnabel, S., Lavado-Contador, J.F., 2009a. Gully erosion, land use and topographical thresholds during the last 60 years in a small rangeland catchment in SW Spain. Land Degradation & Development, 20, 535-550.

Gómez-Gutiérrez, Á., Schnabel, S., Lavado-Contador, J.F., 2009c. Using and comparing two nonparametric methods (CART and MARS) to model the potential distribution of gullies. Ecological modelling, 220, 3630-3637.

Gómez-Gutiérrez, Á., Schnabel, S., Lavado-Contador, J.F., 2011. Procesos, factores y consecuencias de la erosión por cárcavas; trabajos desarrollados en la Península Ibérica. Boletín de la Asociación de Geógrafos Españoles, 55, 59-80.

Gomez-Gutierrez, Á., Schnabel, S., Lavado-Contador, J.F., de Sanjosé Blasco, J.J., Atkinson Gordo, A.D.J., Pulido-Fernández., Manuel., Sánchez Fernández, M., 2018. Studying the influence of livestock pressure on gully erosion in rangelands of SW Spain by means of the UAV SfM workflow. Boletín de la Asociación de Geógrafos Españoles, 78, 66-68.

Gómez-Gutiérrez, Á., Biggs, T., Gudino-Elizondo, N., Errea, P., Alonso-González, E., Nadal Romero, E., de Sanjosé Blasco, J.J., 2020. Using visibility analysis to improve point density and processing time of SfM-MVS techniques for 3D reconstruction of landforms. Earth Surface Processes and Landforms, 45, 2524-2539.

Gomez, B., Banbury, K., Marden, M., Trustrum, N.A., Peacock, D.H., Hoskin, P.J., 2003. Gully erosion and sediment production: Te Weraroa Stream, New Zealand. Water Resources Research, 39, 1187.

Gomez Gutierrez, A., Schnabel, S., Felicísimo, Á.M., 2009b. Modelling the occurrence of gullies in rangelands of southwest Spain. Earth Surface Processes and Landforms: The Journal of the British Geomorphological Research Group, 34, 1894-1902.

González-Hidalgo, J.C., Peña-Monné, J.L., de Luis, M., 2007. A review of daily soil erosion in Western Mediterranean areas. Catena, 71, 193-199.

González, F., Schanabel, S., Prieto, P., Pulido Fernández, M., Gragera Facundo, J., 2012. Producción de los pastos en la dehesa y su relación con la precipitación y el suelo. in: Canals Tresserras, R.M., San Emeterio Garciandía, L. (Eds.), Nuevos retos de la ganadería extensiva: un agente de conservación en peligro de extinción. 51 Reunion Cientifica de la Sociedad Española para el Estudio de los Pastos (SEEP). Centro de Investigación La Orden Valdesequera y Universidad de Extremadura.

González López, F., Maya Blanca, V., 2013. Los pastos y su importancia en la comunidad de Extremadura. Métodos de mejora. 52 Reunión Científica de la Sociedad Española para el Estudio de los Pastos (SEEP). Centro de Investigación La Orden Valdesequera. Badajoz., 83.

Goodwin, N.R., Armston, J.D., Muir, J., Stiller, I., 2017. Monitoring gully change: A comparison of airborne and terrestrial laser scanning using a case study from Aratula, Queensland. Geomorphology, 282, 195-208.

Granda Losada, M., 1981. Mejora de la dehesa extremeña. Universidad de Extremadura. Cáceres.

Guyassa, E., Frankl, A., Zenebe, A., Poesen, J., Nyssen, J., 2017. Effects of check dams on runoff characteristics along gully reaches, the case of Northern Ethiopia. Journal of hydrology, 545, 299-309.

Haan, C.T., Barfield, B.J., Hayes, J.C., 1994. Design hydrology and sedimentology for small catchments. Elsevier, London.

Haas, F., Hilger, L., Neugirg, F., Umstädter, K., Breitung, C., Fischer, P., Hilger, P., Heckmann, T., Dusik, J., Kaiser, A., 2016. Quantification and analysis of geomorphic processes on a recultivated iron ore mine on the Italian island of Elba using long-term ground-based lidar and photogrammetric SfM data by a UAV. Nat. Hazards Earth Syst. Sci, 16, 1269-1288.

Hadley, R.F., 1974. Sediment yield and land use in southwest United States, Effects of Man on the Interface of the Hydrological Cycle with the Physical Environment (Proceedings of the Paris Symposium). IAHS Publ. 113, pp. 96-98.

Haregeweyn, N., Poesen, J., Nyssen, J., Govers, G., Verstraeten, G., de Vente, J., Deckers, J., Moeyersons, J., Haile, M., 2008. Sediment yield variability in Northern Ethiopia: A quantitative analysis of its controlling factors. Catena, 75, 65-76.

Harvey, A.M., 2002. Effective timescales of coupling within fluvial systems. Geomorphology, 44, 175-201.

Hassanli, A.M., Beecham, S., 2013. Criteria for optimizing check dam location and maintenance requirements. in: García, C.C., Lenzi, M.A. (Eds.), Check Dams, Morphological Adjustments. Nova Science Publishers, pp. 1-22.

Hassanli, A.M., Nameghi, A.E., Beecham, S., 2009. Evaluation of the effect of porous check dam location on fine sediment retention (a case study). Environmental monitoring and assessment, 152, 319-326.

Hayas, A., Vanwalleghem, T., Laguna, A., Peña, A., Giráldez, J.V., 2017. Reconstructing long-term gully dynamics in Mediterranean agricultural areas. Hydrology and Earth System Sciences, 21, 235-249.

Heckmann, T., Cavalli, M., Cerdan, O., Forster, S., Javaux, M., Lode, E., Smetanová, A., Verica, D., Brardinoni, F., 2018. Indices of sediment connectivity: opportunities, challenges and limitations. Earth-Science Reviews, 187, 77-108.

Heckmann, T., Schwanghart, W., 2013. Geomorphic coupling and sediment connectivity in an alpine catchment—Exploring sediment cascades using graph theory. Geomorphology, 182, 89-103.

Heckmann, T., Vericat, D., 2018. Computing spatially distributed sediment delivery ratios: inferring functional sediment connectivity from repeat high-resolution digital elevation models. Earth Surface Processes and Landforms, 43, 1547-1554.

Heede, B.H., 1978. Designing gully control systems for eroding watersheds. Environmental Management, 2, 509-522.

Herguido Sevillano, E., Lavado Contador, J.F., Pulido, M., Schnabel, S., 2017. Spatial patterns of lost and remaining trees in the Iberian wooded rangelands. Applied Geography, 87, 170-183.

Heritage, G.L., Milan, D.J., Large, A.R., Fuller, I.C., 2009. Influence of survey strategy and interpolation model on DEM quality. Geomorphology, 112, 334-344.

Hernández-Díaz Ambrona, C.G., 1996. Problemas en la dehesa: la falta de regeneración del arbolado. Agricultura: Revista agropecuaria y ganadera, 50-55.

Hooke, J., 2003. Coarse sediment connectivity in river channel systems: a conceptual framework and methodology. Geomorphology, 56, 79-94.

Horton, R.E., 1933. The role of infiltration in the hydrological cycle. Transactions of American Geophysical Union, 14, 446-460.

Horton, R.E., 1945. Erosional development of streams and their drainage basins; hydrophysical approach to quantitative morphology. Geological society of America bulletin, 56, 275-370.

Hutchinson, M.F., 1988. Calculation of hydrologically sound digital elevation models, Proceedings of the Third International Symposium on Spatial Data Handling. Sydney.

Ibáñez, J.J., Jiménez Ballesta, R., Conde, P., 2003. Degradación de suelos per efecto antrópico en la región mediterránea. in: Bienes, R., Marqués, R.J. (Eds.), Perspectivas de la degradación del suelo. Forum Calidad, Madrid.

Ibáñez Martí, J., García-Álvarez, A., González-Rebollar, J., 1997. Desarrollo sostenible y biodiversidad en la agricultura mediterránea tradicional: El uso múltiple en los vergeles adehesados extremeños. Acción humana y desertificación en ambientes mediterráneos, 221-244.

Imeson, A.C., Sala, M., 1987. Geomorphic Processes-In Environments with Strong Seasonal Contrasts.

Imwangana, F.M., Vandecasteele, I., Trefois, P., Ozer, P., Moeyersons, J., 2015. The origin and control of mega-gullies in Kinshasa (DR Congo). Catena, 125, 38-49.

Ionita, I., 2006. Gully development in the Moldavian Plateau of Romania. Catena, 68, 133-140.

James, L.A., Hodgson, M.E., Ghoshal, S., Latiolais, M.M., 2012. Geomorphic change detection using historic maps and DEM differencing: The temporal dimension of geospatial analysis. Geomorphology, 137, 181-198.

James, M.R., Antoniazza, G., Robson, S., Lane, S.N., 2020. Mitigating systematic error in topographic models for geomorphic change detection: Accuracy, precision and considerations beyond off-nadir imagery. Earth Surface Processes and Landforms, 45, 2251– 2271.

James, M.R., Robson, S., 2014. Mitigating systematic error in topographic models derived from UAV and ground-based image networks. Earth Surface Processes and Landforms, 39, 1413-1420.

Javernick, L., Brasington, J., Caruso, B., 2014. Modeling the topography of shallow braided rivers using Structure-from-Motion photogrammetry. Geomorphology, 213, 166-182.

Jungerius, P., Matundura, J., Van De Ancker, J., 2002. Road construction and gully erosion in West Pokot, Kenya. Earth Surface Processes and Landforms, 27, 1237-1247.

Kaiser, A., Erhardt, A., Eltner, A., 2018. Addressing uncertainties in interpreting soil surface changes by multitemporal high-resolution topography data across scales. Land Degradation & Development, 29, 2264-2277.

Kaiser, A., Neugirg, F., Rock, G., Müller, C., Haas, F., Ries, J., Schmidt, J., 2014. Small-scale surface reconstruction and volume calculation of soil erosion in complex Moroccan gully morphology using structure from motion. Remote Sensing, 6, 7050-7080.

Keesstra, S., Nunes, J.P., Saco, P., Parsons, T., Poeppl, R., Masselink, R., Cerdà, A., 2018. The way forward: can connectivity be useful to design better measuring and modelling schemes for water and sediment dynamics? Science of the Total Environment, 644, 1557-1572.

Kirkby, M., Bracken, L., 2009. Gully processes and gully dynamics. Earth Surface Processes and Landforms: The Journal of the British Geomorphological Research Group, 34, 1841-1851.

Kirkby, M., Morgan, C., 1984. Erosión del suelo. México.

Koci, J., 2020. Hillslope gully erosion in savanna rangelands tributary to the Great Barrier Reef: Investigation of hydrogeomorphic processes, sediment and nutrient yields, University of the Sunshine Coast, Qeensland.

Koci, J., Jarihani, B., Leon, J.X., Sidle, R.C., Wilkinson, S.N., Bartley, R., 2017. Assessment of UAV and ground-based structure from motion with multi-view stereo photogrammetry in a gullied savanna catchment. ISPRS International Journal of Geo-Information, 6, 328.

Koci, J., Sidle, R.C., Jarihani, B., Cashman, M.J., 2020. Linking hydrological connectivity to gully erosion in savanna rangelands tributary to the Great Barrier Reef using structure-from-motion photogrammetry. Land Degradation & Development, 31, 20-36.

Koci, J., Wilkinson, S.N., Hawdon, A.A., Kinsey-Henderson, A.E., Bartley, R., Goodwin, N.R., 2021. Rehabilitation effects on gully sediment yields and vegetation in a savanna rangeland. Earth Surface Processes and Landforms, 46, 1007-1025.

Kosmas, C., Detsis, V., Karamesouti, M., Kounalaki, K., Vassilou, P., Salvati, L., 2015. Exploring long-term impact of grazing management on land degradation in the socio-ecological system of Asteroussia Mountains, Greece. Land, 4, 541-559.

Lallias-Tacon, S., Liébault, F., Piégay, H., 2014. Step by step error assessment in braided river sediment budget using airborne LiDAR data. Geomorphology, 214, 307-323.

Lana-Renault, N., Latron, J., Regües, D., Serrano, P., Nadal, E., 2008. Diferencias estacionales en la generación de escorrentía en una pequeña cuenca de campos abandonados en el Pirineo Central. Cuadernos de investigación geográfica, 23-37.

Lavado-Contador, J., Schnabel, S., Trenado-Ordóñez, R., 2004. Comparison of recent land use and land cover changes in two dehesa agrosilvopastoral landuse systems, SW Spain. Agrosilvopastoral systems. Dehesas and montados. advances in geoecology, 37, 55-69.

Lehotský, M., Rusnák, M., Kidová, A., Dudžák J., 2018. Multitemporal assessment of coarse sediment connectivity along a braided-wandering river. Land Degradation & Development, 29, 1249-1261.

Leopold, L.B., 1966. Channel and hillslope processes in a semiarid area, New Mexico. US Government Printing Office.

Li, E., Mu, X., Zhao, G., Gao, P., Sun, W., 2017. Effects of check dams on runoff and sediment load in a semi-arid river basin of the Yellow River. Stochastic Environmental Research and Risk Assessment, 31, 1791-1803.

López-Vicente, M., Poesen, J., Navas, A., Gaspar, L., 2013. Predicting runoff and sediment connectivity and soil erosion by water for different land use scenarios in the Spanish Pre-Pyrenees. Catena, 102, 62-73.

López-Vicente, M., Nadal-Romero, E., Cammeraat, E.L.H.., 2017. Hydrological connectivity does change over 70 years of abandonment and afforestation in the Spanish Pyrenees. Land Degradation & Development, 28, 1298-1310.

Lozano-Parra, J., Schnabel, S., Pulido, M., Gómez-Gutiérrez, Á., Lavado-Contador, F., 2018. Effects of soil moisture and vegetation cover on biomass growth in water-limited environments. Land Degradation & Development, 29, 4405-4414.

Lucas-Borja, M., Piton, G., Nichols, M., Castillo, C., Yang, Y., Zema, D.A., 2019. The use of check dams for soil restoration at watershed level: A century of history and perspectives. Science of the Total Environment, 692, 37-38.

Lucas-Borja, M.E., Zema, D.A., Hinojosa Guzman, M.D., Yang, Y., Cruz Hernández, A., Xiangzhou, X., Carrá, B.G., Nichols, M., Cerdà, A., 2018. Exploring the influence of vegetation cover, sediment storage capacity and channel dimensions on stone check dam conditions and effectiveness in a large regulated river in México. Ecological Engineering, 122, 39-47.

Lusby, G.C., Knipe, O., 1971. Effects of grazing on the hydrology and biology of the Badger Wash Basin in western Colorado, 1953-66, US Govt. Print. Off.

Llena, M., Vericat, D., Cavalli, M., Crema, S., Smith, M., 2019. The effects of land use and topographic changes on sediment connectivity in mountain catchments. Science of the Total Environment, 660, 899-912.

Maetens, W., Vanmaercke, M., Poesen, J., Jankauskas, B., Jankauskiene, G., Ionita, I., 2012. Effects of land use on annual runoff and soil loss in Europe and the Mediterranean: A meta-analysis of plot data. Progress in Physical Geography, 36, 599-653.

MAPA (Ministerio de Agricultura, Pesca y Alimentación), 2008. Diagnóstico de las Dehesas Ibéricas Mediterráneas. Tragsatec.

Marchi, L., Comiti, F., Crema, S., Cavalli, M., 2019. Channel control works and sediment connectivity in the European Alps. Science of the total environment, 668, 389-399.

Martín-Rosales, W., Cerón, J., López-Chicano, M., Fernández, I., 2003. Aspectos ambientales e hidrogeológicos de la Gruta de las Maravillas (Huelva, España). Boletín geológico y minero, 114, 247-254.

Martin-Rosales, W., Pulido-Bosch, A., Gisbert, J., Vallejos, A., 2003. Sediment yield estimation and check dams in a semiarid area (Sierra de Gádor, southern Spain). International Association of Hydrological Sciences, Publication, 51-58.

Martín Galindo, J.L., 1966. La dehesa extremeña como tipo de explotación agraria. Estudios geograficos, 27, 157.

Martınez-Casasnovas, J., Ramos, M., Ribes-Dasi, M., 2002. Soil erosion caused by extreme rainfall events: mapping and quantification in agricultural plots from very detailed digital elevation models. Geoderma, 105, 125-140.

Martínez-Casasnovas, J.A., Ramos, M.C., García-Hernández, D., 2009. Effects of land-use changes in vegetation cover and sidewall erosion in a gully head of the Penedès region (northeast Spain). Earth Surface Processes and Landforms: The Journal of the British Geomorphological Research Group, 34, 1927-1937.

Martínez Lloris, M., Romero Díaz, A., Alonso Sarria, F., 2001. Respuesta erosiva de cuencas, corregidas mediante diques de retención de sedimentos, ante lluvias de alta intensidad. Cuenca del río Quipar, Sureste de España. Papeles de Geografía, 191-203.

Martínez, T., Urquia, J., Tejerina, J., de Miguel, J., 2012. Respuesta de la composición florística y la diversidad biológica de pastizales a las estrategias de manejo en una dehesa de la Sierra de Guadarrama, Madrid. in: Rosa María Canals Tresserras, L.S.E.G.e. (Ed.), Nuevos retos de la ganadería extensiva: un agente de conservación en peligro de extinción. 51 Reunion Cientifica de la SEEP., Pamplona.

Martini, L., Picco, L., Iroumé, A., Cavalli, M., 2019. Sediment connectivity changes in an Andean catchment affected by volcanic eruption. Science of the Total Environment, 692, 1209-1222.

Martins, B., Castro, A.C.M., Ferreira, C., Lourenço, L., Nunes, A., 2019. Gullies mitigation and control measures: A case study of the Seirós gullies (North of Portugal). Physics and Chemistry of the Earth, Parts A/B/C, 109, 26-30.

Marzolff, I., Poesen, J., 2009. The potential of 3D gully monitoring with GIS using high-resolution aerial photography and a digital photogrammetry system. Geomorphology, 111, 48-60.

MEA, 2005. Ecosystems and human well-being: Desertification Synthesis. World Resources Institute, Washington, DC. Island Press Washington, DC.

Mekonnen, M., Keesstra, S., Baartman, J., Ritsema, C., Melesse, A., 2015. Evaluating sediment storage dams: structural off-site sediment trapping measures in northwest Ethiopia. Cuadernos de investigación geográfica, 41, 7-22.

Midgley, N.G., Tonkin, T.N., 2017. Reconstruction of former glacier surface topography from archive oblique aerial images. Geomorphology, 282, 18-26.

Mieth, A., Bork, H.-R., 2005. History, origin and extent of soil erosion on Easter Island (Rapa Nui). Catena, 63, 244-260.

Milan, D.J., Heritage, G.L., Hetherington, D., 2007. Application of a 3D laser scanner in the assessment of erosion and deposition volumes and channel change in a proglacial river. Earth Surface Processes and Landforms: The Journal of the British Geomorphological Research Group, 32, 1657-1674.

Milan, D.J., Heritage, G.L., Large, A.R., Fuller, I.C., 2011. Filtering spatial error from DEMs: Implications for morphological change estimation. Geomorphology, 125, 160-171.

Miller, J.R., 2017. Casualty of historic arroyo incision in the southwestern United States. Anthropocene, 18, 69-75.

Miller, J.R., Lord, M.L., Germanoski, D., 2011. Meadow sensitivity to natural and anthropogenic disturbance [chapter 5]. in: Chambers, J.C., Miller, J.R. (Eds.), Geomorphology, hydrology, and ecology of Great Basin meadow complexes - Implications for Management and Restoration. Department of Agriculture, Forest Service, Rocky Mountain Research Station. p. 68-84., pp. 68-84.

Mishra, A., Froebrich, J., Gassman, P.W., 2007. Evaluation of the SWAT model for assessing sediment control structures in a small watershed in India. Transactions of the ASABE, 50, 469-477.

Montanarella, L., Pennock, D.J., McKenzie, N., Badraoui, M., Chude, V., Baptista, I., Mamo, T., Yemefack, M., Singh Aulakh, M., Yagi, K., 2016. World's soils are under threat. Soil, 2, 79-82.

Montero, G., San Miguel, A., Cañellas, I., 1998. Sistemas de selvicultura mediterránea. La dehesa. in: Jiménez Díaz, R.M., Lamo de Espinosa, J. (Eds.), Agricultura Sostenible. Mundi-Prensa, Madrid, pp. 519-554.

Montgomery, D.R., 2007. Soil erosion and agricultural sustainability. Proceedings of the National Academy of Sciences, 104, 13268-13272.

Montoya, O., 1993. La seca de encinas y alcornoques. Albear. Consejería de Agricultura y Comercio. Junta de Extremadura., 3, 4-11.

Moreno, G., Pulido, F.J., 2009. The functioning, management and persistence of dehesas. in: Rigueiro-Rodróguez, A., McAdam, J., Mosquera-Losada, M.R. (Eds.), Agroforestry in Europe. Springer, pp. 127-160.

Morgan, R., 1997. Erosión del suelo y conservación. Mundi-Prensa, Madrid, 343

Morgan, R., 2005. Soil Erosion and Conservation. Blackwell Publishing: Oxford.

Mulholland, B., Fullen, M., 1991. Cattle trampling and soil compaction on loamy sands. Soil use and management, 7, 189-193.

Nachtergaele, J., Poesen, J., 1999. Assessment of soil losses by ephemeral gully erosion using high-altitude (stereo) aerial photographs. Earth Surface Processes and Landforms: The Journal of the British Geomorphological Research Group, 24, 693-706.

Nadal-Romero, E., Martínez-Murillo, J.F., Vanmaercke, M., Poesen, J., 2011. Scale-dependency of sediment yield from badland areas in Mediterranean environments. Progress in Physical Geography, 35, 297-332.

Nassif, S., Wilson, E., 1975. The influence of slope and rain intensity on runoff and infiltration. Hydrological Sciences Journal, 20, 539-553.

Navarro-Hevia, J., Mongil-Manso, J., Araújo, J.C., 2013. Desertificación secular de las cuestas de Saldaña (Palencia) frente a 80 años de restauración. Cuadernos de la Sociedad Española de Ciencias Forestales, 115-122.

Navarro-Hevia, J., Serrano, C., Ugalde, M., Oria de Rueda, J.A., Jonete, M.A., 1997. Utilización de geotextiles en la corrección de cárcavas del Cristo del Otero (Palencia), I Congreso Forestal Hispano-Luso, Pamplona.

Neugirg, F., Stark, M., Kaiser, A., Vlacilova, M., Della Seta, M., Vergari, F., Schmidt, J., Becht, M., Haas, F., 2016. Erosion processes in calanchi in the Upper Orcia Valley, Southern Tuscany, Italy based on multitemporal high-resolution terrestrial LiDAR and UAV surveys. Geomorphology, 269, 8-22.

Niculiță, M., Mărgărint, M.C., Tarolli, P., 2020. Using UAV and LIDAR data for gully geomorphic changes monitoring. in: Tarolli, P., Mudd, S. (Eds.), Developments in Earth Surface Processes. Elsevier, pp. 271-315.

Nichols, M.H., Polyakov, V.O., Nearing, M.A., Hernandez, M., 2016. Semiarid watershed response to low-tech porous rock check dams. Soil Science, 181, 275-282.

Nogueras, P., Burjachs, F., Gallart, F., Puigdefàbregas, J., 2000. Recent gully erosion in the El Cautivo badlands (Tabernas, SE Spain). Catena, 40, 203-215.

Nyssen, J., Poesen, J., Moeyersons, J., Deckers, J., Haile, M., Lang, A., 2004. Human impact on the environment in the Ethiopian and Eritrean highlands—a state of the art. Earth-science reviews, 64, 273-320.

Olea, L., Paredes, J., Verdasco, P., 2011. Características productivas de los pastos de la dehesa del SO de la Península Ibérica. Pastos, 147-172.

Osti, R., Egashira, S., 2008. Method to improve the mitigative effectiveness of a series of check dams against debris flows. Hydrological Processes: An International Journal, 22, 4986-4996.

Panagos, P., Borrelli, P., Poesen, J., Ballabio, C., Lugato, E., Meusburger, K., Montanarella, L., Alewell, C., 2015. The new assessment of soil loss by water erosion in Europe. Environmental science & policy, 54, 438-447.

Pardo-Navarro, F., Martín-Jiménez, E., Gil-Sánchez, L., 2003. El uso tradicional de la Dehesa Boyal de Puebla de la Sierra (Madrid): efectos sobre la vegetación a corto y largo plazo. Cuadernos de la Sociedad Española de Ciencias Forestales, 173-178.

Parsons, J.D., 1966. La economía de las montaneras en los encinares del suroeste de España. Estudios geograficos, 27, 309.

Pathak, P., Wani, S.P., Sudi, R., 2005. Gully control in SAT watersheds. International Crops Research Institute for the Semi-arid Tropics.

Pennock, D.J., 2019. Soil erosion: The greatest challenge for sustainable soil management. Food and Agriculture Organization of the United Nations.

Peña-Angulo, D., Nadal-Romero, E., González-Hidalgo, J.C., Albaladejo, J., Andreu, V., Bagarello, V., Barhi, H., Batalla, R.J., Bernal, S., Bienes, R., 2019. Spatial variability of the relationships of runoff and sediment yield with weather types throughout the Mediterranean basin. Journal of Hydrology, 571, 390-405.

Persichillo, M.G., Bordoni, M., Cavalli, M., Crema, S., Meisina, C., 2018. The role of human activities on sediment connectivity of shallow landslides. Catena, 160, 261-274.

Podwojewski, P., Poulenard, J., Zambrana, T., Hofstede, R., 2002. Overgrazing effects on vegetation cover and properties of volcanic ash soil in the páramo of Llangahua and La Esperanza (Tungurahua, Ecuador). Soil Use and Management, 18, 45-55.

Poeppl, R.E., Keesstra, S.D., Maroulis, J., 2017. A conceptual connectivity framework for understanding geomorphic change in human-impacted fluvial systems. Geomorphology, 277, 237-250.

Poesen, J., 1989. Conditions for gully formation in the Belgian loam belt and some ways to control them, Soil erosion protection measures in Europe. Proc. EC workshop. Freising, 1988, pp. 39-52.

Poesen, J., 2011. Challenges in gully erosion research. Landform analysis, 17, 5-9.

Poesen, J., 2018. Soil erosion in the Anthropocene: Research needs. Earth Surface Processes and Landforms, 43, 64-84.

Poesen, J., Nachtergaele, J., Verstraeten, G., Valentin, C., 2003. Gully erosion and environmental change: importance and research needs. Catena, 50, 91-133.

Poesen, J., Vandaele, K., Van Wesemael, B., 1996. Contribution of gully erosion to sediment production, Erosion and Sediment Yield: Global and Regional Perspectives: Proceedings of an International Symposium Held at Exeter, UK, from 15 to 19 July 1996. IAHS, pp. 251.

Poesen, J.W., Hooke, J.M., 1997. Erosion, flooding and channel management in Mediterranean environments of southern Europe. Progress in Physical Geography, 21, 157-199.

Polyakov, V., Nichols, M., McClaran, M., Nearing, M., 2014. Effect of check dams on runoff, sediment yield, and retention on small semiarid watersheds. Journal of soil and water conservation, 69, 414-421.

Porta, J., López, M., Roquero, C., 2003. Edafología para la agricultura y el medio ambiente. Ed. Mundi-Prensa. Madrid.

Prosdocimi, M., Calligaro, S., Sofia, G., Dalla Fontana, G., Tarolli, P., 2015. Bank erosion in agricultural drainage networks: new challenges from structure-from-motion photogrammetry for post-event analysis. Earth Surface Processes and Landforms, 40, 1891-1906.

Prosser, I.P., Rutherfurd, I.D., Olley, J.M., Young, W.J., Wallbrink, P.J., Moran, C.J., 2001. Large-scale patterns of erosion and sediment transport in river networks, with examples from Australia. Marine and Freshwater Research, 52, 81-99.

Puigdefábregas, J., García-Ruiz, J.M., 1985. Efectos de la construcción de pequeñas presas en cauces anastomosados del Pirineo Central. Cuadernos de Investigación Geográfica, 11, 91-102.

Pulido-Fernández, M., Schnabel, S., Lavado-Contador, J.F., Mellado, I.M., Pérez, R.O., 2013. Soil organic matter of Iberian open woodland rangelands as influenced by vegetation cover and land management. Catena, 109, 13-24.

Pulido, F., Picardo, A., Campos, P., Carranza, J., Coleto, J., Díaz, M., Diéguez, E., Escudero, A., Ezquerra, F., Fernández, P., Solla, A., 2010. Libro Verde de la Dehesa. Documento para el debate hacia una Estrategia Ibérica de gestión. Consejería de Agricultura y Pesca. 48 pp, pp. 48.

Pulido, M., Schnabel, S., Lavado Contador, J.F., Lozano-Parra, J., González, F., 2018. The impact of heavy grazing on soil quality and pasture production in rangelands of SW Spain. Land Degradation & Development, 29, 219-230.

Quiñonero-Rubio, J., Boix-Fayos, C., de Vente, J., 2013. Desarrollo y aplicación de un índice multifactorial de conectividad de sedimentos a escala de Cuenca. Cuadernos de investigación geográfica/Geographical Research Letters, 203-223.

Quiñonero-Rubio, J.M., Nadeu, E., Boix-Fayos, C., de Vente, J., 2016. Evaluation of the effectiveness of forest restoration and check-dams to reduce catchment sediment yield. Land Degradation & Development, 27, 1018-1031.

Ramos-Diez, I., Navarro-Hevia, J., Fernández, R.S.M., Díaz-Gutiérrez, V., Mongil-Manso, J., 2016. Analysis of methods to determine the sediment retained by check dams and to estimate erosion rates in badlands. Environmental monitoring and assessment, 188, 405.

Ramos-Diez, I., Navarro-Hevia, J., Fernández, R.S.M., Díaz-Gutiérrez, V., Mongil-Manso, J., 2017a. Evaluating methods to quantify sediment volumes trapped behind check dams, Saldaña badlands (Spain). International Journal of Sediment Research, 32, 1-11.

Ramos-Diez, I., Navarro-Hevia, J., San Martín Fernández, R., Mongil-Manso, J., 2017b. Final analysis of the accuracy and precision of methods to calculate the sediment retained by check dams. Land Degradation & Development, 28, 2446-2456.

Ran, D.-C., Luo, Q.-H., Zhou, Z.-H., Wang, G.-Q., Zhang, X.-H., 2008. Sediment retention by check dams in the Hekouzhen-Longmen Section of the Yellow River. International Journal of Sediment Research, 23, 159-166.

Renard, K.G., 1997. Predicting soil erosion by water: a guide to conservation planning with the Revised Universal Soil Loss Equation (RUSLE). United States Government Printing.

Rey, F., Burylo, M., 2014. Can bioengineering structures made of willow cuttings trap sediment in eroded marly gullies in a Mediterranean mountainous climate? Geomorphology, 204, 564-572.

Richet, J.-B., Ouvry, J.-F., Saunier, M., 2017. The role of vegetative barriers such as fascines and dense shrub hedges in catchment management to reduce runoff and erosion effects: Experimental evidence of efficiency, and conditions of use. Ecological Engineering, 103, 455-469.

Riesco García, J.A., 2015. Análisis comparativo de la estimación de la erosión hídrica con la metodología USLE y las técnicas RS SIG. Aplicación al entorno del tramo medio de la cuenca del río Jarama (Guadalajara), Universidad Politécnica de Madrid.

Riverscapes-Consortium, 2018. Geomorphic Change Detection Software. Available online: http://gcd.riverscapes.xyz/Download/ (accesssed on 26 July 2021)

Rojo, L., Martínez, A., Torre, S., García, M., 2009. Inventario y difusión de tecnologías disponbiles en España para la lucha contra la desertificación. Actas 5º Congreso Forestal Español.

Romero-Díaz, A., Alonso-Sarriá, F., Martínez-Lloris, M., 2007b. Erosion rates obtained from check-dam sedimentation (SE Spain). A multi-method comparison. Catena, 71, 172-178.

Romero-Díaz, A., Marín Sanleandro, P., Sánchez Soriano, A., Belmonte Serrato, F., Faulkner, H., 2007c. The causes of piping in a set of abandoned agricultural terraces in southeast Spain. Catena, 69, 282-293.

Romero-Diaz, A., Martínez LLoris, M., Alonso Sarriá, F., 2007a. Los diques de corrección hidrológica. Servicio de Publicaciones de la Universidad de Murcia: Editum, Murcia.

Romero-Díaz, M.A., 2008. Los diques de corrección hidrológica como instrumentos de cuantificación de la erosión. Cuadernos de investigación geográfica/Geographical Research Letters, 83-99.

Rubio-Delgado, J., Guillén, J., Corbacho, J.A., Gómez-Gutiérrez, Á., Baeza, A., Schnabel, S., 2017. Comparison of two methodologies used to estimate erosion rates in Mediterranean ecosystems: 137Cs and exposed tree roots. Science of the Total Environment, 605, 541-550.

Rubio-Delgado, J., Schnabel, S., Gómez-Gutiérrez, Á., Sánchez-Fernández, M., 2018. Estimation of soil erosion rates in dehesas using the inflection point of holm oaks. Catena, 166, 56-67.

Rubio-Delgado, J., Schnabel, S., Gómez Gutiérrez, Á., Berenguer, F., 2014. Estimación de tasas de erosión históricas en dehesas utilizando raíces arbóreas expuestas y láser escáner terrestre. Cuaternario y Geomorfología, 28, 69-84.

Rubio, J.L., 2005. Desertificación. Ambienta, 47, 26-31.

Rumsby, B.T., Brasington, J., Langham, J.A., McLelland, S.J., Middleton, R., Rollinson, G., 2008. Monitoring and modelling particle and reach-scale morphological change in gravel-bed rivers: Applications and challenges. Geomorphology, 93, 40-54.

San Miguel, A., 1993. Silvopascicultura mediterránea. in: Orozco Bayo, E., López Serrano, F.R. (Eds.), Silvocultura mediterránea. Colección Estudios Nº 14, Cuenca, pp. 51-64.

Scarascia-Mugnozza, G., Oswald, H., Piussi, P., Radoglou, K., 2000. Forests of the Mediterranean region: gaps in knowledge and research needs. Forest Ecology and management, 132, 97-109.

Schnabel, S., 1997. Soil erosion and runoff production in a small watershed under silvo-pastoral landuse (dehesas) in Extremadura, Spain. Geoforma Ediciones.

Schnabel, S., Ceballos Barbancho, A., Gómez-Gutiérrez, Á., 2010. Erosión hídrica en la dehesa extremeña. in: Schnabel, S.L.C., J.F.; Gómez-Gutiérrez A.; García Marín, R (Ed.), Aportaciones a la geografía física de extremadura con especial referencia a las Dehesas, pp. 153-185.

Schnabel, S., Dahlgren, R.A., Moreno-Marcos, G., 2013. Soil and water dynamics. in: Campos, P., Oviedo, J.S., Díaz, M., Montero, G. (Ed.), Mediterranean oak woodland working landscapes. Springer, pp. 91-121.

Schnabel, S., Lavado-Contador, J., Gómez-Gutiérrez, A., Lagar Timón, D., 2006. La degradación del suelo en las dehesas de Extremadura. in: Espejo Díaz, M., Martín Bellido, M., Mateos, C., Mesías Díaz, F.J. (Eds.), Gestión ambiental y económica del ecosistema dehesa en la Península Ibérica. Junta de Extremadura, Mérida, pp. 63-71.

Seitz, S.M., Curless, B., Diebel, J., Scharstein, D., Szeliski, R., 2006. A comparison and evaluation of multi-view stereo reconstruction algorithms, IEEE Conference on Computer Vision and Pattern Recognition. IEEE Computer Society. IEEE, New York, pp. 519-528.

Shahbazi, M., Sohn, G., Théau, J., Menard, P., 2015. Development and evaluation of a UAV-photogrammetry system for precise 3D environmental modeling. Sensors, 15, 27493-27524.

Sharma, P.N., Velásquez, S., Ferrán, F., Quesada, M.E., Collinet, J., Shultz, S., Sharma, P.N., Hilje, L., Solís, H., Rojas, F.F., 1994. Prevención y control de carcavas a nivel de finca por medio de métodos vegetativos y estructurales temporales en Honduras tropical. Proyecto RENARM/manejo de cuencas. CATIE, Turrialba, Costa Rica., CATIE, Turrialba (Costa Rica). Programa Manejo Integrado de Recursos Naturales.

Shellberg, J., Brooks, A., Spencer, J., 2010. Land-use change from indigenous management to cattle grazing initiates the gullying of alluvial soils in northern Australia, 19th World Congress of Soil Science, Soil Solutions for a Changing World. Brisbane, Australia, pp. 59-62.

Shellberg, J., Spencer, J., Brooks, A., Pietsch, T., 2016. Degradation of the Mitchell River fluvial megafan by alluvial gully erosion increased by post-European land use change, Queensland, Australia. Geomorphology, 266, 105-120.

Shellberg, J.G., Brooks, A.P., Rose, C.W., 2013. Sediment production and yield from an alluvial gully in northern Queensland, Australia. Earth Surface Processes and Landforms, 38, 1765-1778.

Sheng, J., Liao, A., 1997. Erosion control in south China. Catena, 29, 211-221.

Sidle, R.C., Gomi, T., Usuga, J.C.L., Jarihani, B., 2017. Hydrogeomorphic processes and scaling issues in the continuum from soil pedons to catchments. Earth-Science Reviews, 175, 75-96.

Sidle, R.C., Jarihani, B., Kaka, S.I., Koci, J., Al-Shaibani, A., 2019. Hydrogeomorphic processes affecting dryland gully erosion: Implications for modelling. Progress in Physical Geography: Earth and Environment, 43, 46-64.

Sidle, R.C., Sasaki, S., Otsuki, M., Noguchi, S., Rahim Nik, A., 2004. Sediment pathways in a tropical forest: effects of logging roads and skid trails. Hydrological Processes, 18, 703-720.

Sidle, R.C., Ziegler, A.D., 2010. Elephant trail runoff and sediment dynamics in northern Thailand. Journal of environmental quality, 39, 871-881.

Sidle, R.C., Ziegler, A.D., Negishi, J.N., Nik, A.R., Siew, R., Turkelboom, F., 2006. Erosion processes in steep terrain—truths, myths, and uncertainties related to forest management in Southeast Asia. Forest ecology and management, 224, 199-225.

Singh, K.P., Stall, J.B., 1971. Derivation of base flow recession curves and parameters. Water Resources Research, 7, 292-303.

Smit, H., Muche, R., Ahlers, R., van der Zaag, P., 2017. The political morphology of drainage—how gully formation links to state formation in the choke mountains of Ethiopia. World Development, 98, 231-244.

Smith, M., Carrivick, J., Hooke, J., Kirkby, M., 2014. Reconstructing flash flood magnitudes using 'Structure-from-Motion': A rapid assessment tool. Journal of Hydrology, 519, 1914-1927.

Smith, M.W., Vericat, D., 2015. From experimental plots to experimental landscapes: topography, erosion and deposition in sub-humid badlands from structure-from-motion photogrammetry. Earth Surface Processes and Landforms, 40, 1656-1671.

Sougnez, N., van Wesemael, B., Vanacker, V., 2011. Low erosion rates measured for steep, sparsely vegetated catchments in southeast Spain. Catena, 84, 1-11.

Stöcker, C., Eltner, A., Karrasch, P., 2015. Measuring gullies by synergetic application of UAV and close range photogrammetry—A case study from Andalusia, Spain. Catena, 132, 1-11.

Swetnam, T.L., Gillan, J.K., Sankey, T.T., McClaran, M.P., Nichols, M.H., Heilman, P., McVay, J., 2018. Considerations for achieving cross-platform point cloud data fusion across different dryland ecosystem structural states. Frontiers in plant science, 8, 2144.

Talema, A., Poesen, J., Muys, B., Padro, R., Dibaba, H., Diels, J., 2019. Survival and growth analysis of multipurpose trees, shrubs, and grasses used to rehabilitate badlands in the subhumid tropics. Land Degradation & Development, 30, 470-480.

Tang, H., Pan, H., Ran., Q., 2020. Impacts of filled check dams with different deployment strategies on the flood and sediment transport processes in a Loess Plateau catchment. Water, 12, 1319.

Tarboton, D.G., 1997. A new method for the determination of flow directions and upslope areas in grid digital elevation models. Water resources research, 33, 309-319.

Tarboton, D.G., Dash, P., Sazib, N., 2015. TauDEM, Terrain analysis using digital elevation models.

Tarolli, P., Cavalli, M., Masin, R., 2019. High-resolution morphologic characterization of conservation agriculture. Catena, 172, 846-856.

Taye, G., Poesen, J., Vanmaercke, M., Van Wesemael, B., Martens, L., Teka, D., Nyssen, J., Deckers, J., Vanacker, V., Haregeweyn, N., 2015. Evolution of the effectiveness of stone bunds and trenches in reducing runoff and soil loss in the semi-arid Ethiopian highlands. Zeitschrift für Geomorphologie, 59, 477-493.

Thomas, J.T., Iverson, N.R., Burkart, M.R., Kramer, L.A., 2004. Long-term growth of a valley-bottom gully, western Iowa. Earth Surface Processes and Landforms: The Journal of the British Geomorphological Research Group, 29, 995-1009.

Thorne, C., Zevenbergen, L.W., Grissinger, E., Murphey, J., 1986. Ephemeral gullies as sources of sediment, Proceedings of the Fourth Federal Interagency Sedimentation Conference March 24-27, 1986, Las Vegas, Nevada.

Tonkin, T.N., Midgley, N.G., Graham, D.J., Labadz, J., 2014. The potential of small unmanned aircraft systems and structure-from-motion for topographic surveys: A test of emerging integrated approaches at Cwm Idwal, North Wales. Geomorphology, 226, 35-43.

Torri, D., Ross, M., Brogi, F., Marignani, M., Bacaro, G., Santi, E., Tordoni, E., Amici, V., Maccherini, S., 2018. Badlands and the dynamics of human history, land use, and vegetation through centuries, Badlands Dynamics in a Context of Global Change. Elsevier, pp. 111-153.

Truman, C., Potter, T., Nuti, R., Franklin, D., Bosch, D., 2011. Antecedent water content effects on runoff and sediment yields from two Coastal Plain Ultisols. Agricultural Water Management, 98, 1189-1196.

Turner, D., Lucieer, A., De Jong, S.M., 2015. Time series analysis of landslide dynamics using an unmanned aerial vehicle (UAV). Remote Sensing, 7, 1736-1757.

Ullman, S., 1979. The interpretation of structure from motion. Proceedings of the Royal Society of London. Series B. Biological Sciences, 203, 405-426.

USDA, 2004. Soil Survey Laboratory Methods Manual, Soil Survey Investigations. Lincoln, USA.

Vaezi, A.R., Abbasi, M., Keesstra, S., Cerdà, A., 2017. Assessment of soil particle erodibility and sediment trapping using check dams in small semi-arid catchments. Catena, 157, 227-240.

Valentin, C., Poesen, J., Li, Y., 2005. Gully erosion: impacts, factors and control. Catena, 63, 132-153.

van der Waal, B., Rowntree, K., 2018. Landscape connectivity in the upper Mzimvubu river catchment: an assessment of anthropogenic influences on sediment connectivity. Land degradation & development, 29, 713-723.

Vandekerckhove, L., Poesen, J., Wijdenes, D.O., De Figueiredo, T., 1998. Topographical thresholds for ephemeral gully initiation in intensively cultivated areas of the Mediterranean. Catena, 33, 271-292.

Vanmaercke, M., Maetens, W., Poesen, J., Jankauskas, B., Jankauskiene, G., Verstraeten, G., de Vente, J., 2012. A comparison of measured catchment sediment yields with measured and predicted hillslope erosion rates in Europe. Journal of Soils and Sediments, 12, 586-602.

Vanmaercke, M., Panagos, P., Vanwalleghem, T., Hayas, A., Foerster, S., Borrelli, P., Rossi, M., Torri, D., Casalí, J., Borselli, L., 2021. Measuring, modelling and managing gully erosion at large scales: A state of the art. Earth-Science Reviews, 103637.

Vanmaercke, M., Poesen, J., Van Mele, B., Demuzere, M., Bruynseels, A., Golosov, V., Rodrigues Bezerra, J.F., Bolysov, S., Dvinskih, A., Frankl, A., 2016. How fast do gully headcuts retreat? Earth-Science Reviews, 154, 336-355.

Vanmaercke, M., Poesen, J., Verstraeten, G., de Vente, J., Ocakoglu, F., 2011. Sediment yield in Europe: Spatial patterns and scale dependency. Geomorphology, 130, 142-161.

Verstraeten, G., Poesen, J., 2002. Regional scale variability in sediment and nutrient delivery from small agricultural watersheds. Journal of environmental quality, 31, 870-879.

Vigiak, O., Borselli, L., Newham, L., McInnes, J., Roberts, A., 2012. Comparison of conceptual landscape metrics to define hillslope-scale sediment delivery ratio. Geomorphology, 138, 74-88.

Visser, F., Woodget, A., Skellern, A., Forsey, J., Warburton, J., Johnson, R., 2019. An evaluation of a low-cost pole aerial photography (PAP) and structure from motion (SfM) approach for topographic surveying of small rivers. International Journal of Remote Sensing, 40, 9321-9351.

Walling, D., Fang, D., 2003. Recent trends in the suspended sediment loads of the world's rivers. Global and planetary change, 39, 111-126.

Wang, Y., Fu, B., Chen, L., Lü, Y., Gao, Y., 2011. Check dam in the Loess Plateau of China: engineering for environmental services and food security. Environmental Science and Technology, 45, 10298-1029.

Wantzen, K.M., 2006. Physical pollution: effects of gully erosion on benthic invertebrates in a tropical clear-water stream. Aquatic conservation: Marine and Freshwater ecosystems, 16, 733-749.

Wasson, R., Mazari, R., Starr, B., Clifton, G., 1998. The recent history of erosion and sedimentation on the Southern Tablelands of southeastern Australia: sediment flux dominated by channel incision. Geomorphology, 24, 291-308.

Waterhouse, J., Schaffelke, B., Bartley, R., Brodie, J., Star, M., Thorburn, P., Rolfe, J., Ronan, M., Taylor, B., 2017. Scientific Consensus Statement: Land Use Impacts on Great Barrier Reef Water Quality and Ecosystem Condition (Queensland Government, 2017). chapter 5: Overview of Key Findings, Management Implications and Knowledge Gaps, 15.

Wei, Y., He, Z., Li, Y., Jiao, J., Zhao, G., Mu, X., 2017. Sediment yield deduction from check–dams deposition in the weathered sandstone watershed on the North Loess Plateau, China. Land degradation & development, 28, 217-231.

Wester, T., Wasklewicz, T., Staley, D., 2014. Functional and structural connectivity within a recently burned drainage basin. Geomorphology, 206, 362-373.

Westoby, M.J., Brasington, J., Glasser, N.F., Hambrey, M.J., Reynolds, J.M., 2012. 'Structure-from-Motion'photogrammetry: A low-cost, effective tool for geoscience applications. Geomorphology, 179, 300-314.

Wheaton, J.M., 2008. Uncertainity in Morphological Sediment Budgeting of Rivers. Doctoral thesis Thesis, University of Southampton, 412 pp.

Wheaton, J.M., Brasington, J., Darby, S.E., Sear, D.A., 2010. Accounting for uncertainty in DEMs from repeat topographic surveys: improved sediment budgets. Earth Surface Processes and Landforms, 35, 136-156.

White, P., Butcher, D., Labadz, J., 1997. Reservoir sedimentation and catchment sediment yield in the Strines catchment, UK. Physics and Chemistry of the Earth, 22, 321-328.

Wilkinson, S.N., Kinsey-Henderson, A.E., Hawdon, A.A., Hairsine, P.B., Bartley, R., Baker, B., 2018. Grazing impacts on gully dynamics indicate approaches for gully erosion control in northeast Australia. Earth Surface Processes and Landforms, 43, 1711-1725.

Williams, R.D., 2012. 2.3. 2. DEMs of Difference. Geomorphological Techniques. British Society for Geomorphology, Chap. 2, Sec. 3.2.

Wohl, E., 2006. Human impacts to mountain streams. Geomorphology, 79, 217-248.

Wohl, E., Magilligan, F.J., Rathburn, S.L., 2017. Introduction to the special issue: Connectivity in Geomorphology. Geomorphology, 277, 1-5.

Woodget, A., Carbonneau, P., Visser, F., Maddock, I.P., 2015. Quantifying submerged fluvial topography using hyperspatial resolution UAS imagery and structure from motion photogrammetry. Earth Surface Processes and Landforms, 40, 47-64.

Xiang, J., Chen, J., Sofia, G., Tian, Y., Tarolli, P., 2018. Open-pit mine geomorphic changes analysis using multi-temporal UAV survey. Environmental earth sciences, 77, 220.

Xu, M., Li, Q., Wilson, G., 2016. Degradation of soil physicochemical quality by ephemeral gully erosion on sloping cropland of the hilly Loess Plateau, China. Soil and Tillage Research, 155, 9-18.

Xu, X., Zhang, H., Zhang, O., 2004. Development of check-dam systems in gullies on the Loess Plateau, China. Environmental Science & Policy, 7, 79-86.

Xu, Y., Fu, B., He, C., 2013. Assessing the hydrological effect of the check dams in the Loess Plateau, China, by model simulations. Hydrology and Earth System Sciences, 17, 2185-2193.

Zema, D.A., Bombino, G., Boix-Fayos, C., Tamburino, V., Zimbone, S.M., Fortugno, D., 2014. Evaluation and modeling of scouring and sedimentation around check dams in a Mediterranean torrent in Calabria, Italy. Journal of Soil and Water Conservation, 69, 316-329.

Zhang, X., She, D., Hou, M., Wang, G., Liu, Y., 2021. Understanding the influencing factors (precipitation variation, land use changes and check dams) and mechanisms controlling changes in the sediment load of a typical Loess watershed, China. Ecological Engineering, 163, 106198.

Zhao, G., Kondolf, G.M., Mu, X., Han, M., He, Z., Rubin, Z., Wang, F., Gao, P., Sun, W., 2017. Sediment yield reduction associated with land use changes and check dams in a catchment of the Loess Plateau, China. Catena, 148, 126-137.

Zhao, Y., Jia, R.L., Wang, J., 2019. Towards stopping land degradation in drylands: Water-saving techniques for cultivating biocrusts in situ. Land Degradation & Development, 30, 2336-2346.

Zucca, C., Canu, A., Della Peruta, R., 2006. Effects of land use and landscape on spatial distribution and morphological features of gullies in an agropastoral area in Sardinia (Italy). Catena, 68, 87-95.